Bridge manual commentary

First edition

WAKA KOTAHI
NZ TRANSPORT AGENCY

New Zealand Government

Bridge manual commentary

www.nzta.govt.nz

First edition, Amendment 1

Effective from May 2022

ISBN 978-1-98-851240-2 (online)

More information

Published October 2018
Amendment 1 effective from May 2022
ISBN 978-1-98-851240-2 (online)

If you have further queries, call our contact centre on 0800 699 000 or write to us:
Waka Kotahi NZ Transport Agency
Private Bag 6995
Wellington 6141

This document is available on the Waka Kotahi NZ Transport Agency website at www.nzta.govt.nz

Document management plan

1) Purpose

This management plan outlines the updating procedures and contact points for the document.

2) Document information

Document name	*Bridge manual commentary*
Document number	-
Document availability	This document is located in electronic form on the Waka Kotahi NZ Transport Agency website at www.nzta.govt.nz.
Document owner	National Structures Manager
Document sponsor	National Manager Network Outcomes
Prepared by	Engineering Standards, Waka Kotahi NZ Transport Agency

3) Amendments and review strategy

All corrective action/improvement requests (CAIRs) suggesting changes will be acknowledged by the document owner.

	Comments	Frequency
Amendments (minor revisions)	Updates to be notified to users by publication of a technical advice note placed on the Waka Kotahi NZ Transport Agency website.	As required.
Review (major revisions)	Periodic updates will be undertaken where amendments fundamentally changing the content or structure of the guide or new technology resulting from research or ongoing refinement have been identified.	As required.
Notification	All users that have registered their interest by email to hip.feedback@nzta.govt.nz will be advised by email of amendments and updates.	Immediately.

4) Distribution of this management plan

Copies of this document management plan are to be included in the Waka Kotahi NZ Transport Agency intranet.

Record of amendments

This document is subject to review and amendment from time to time. Amendments will be recorded in the table below.

Changes since the previous amendment are indicated by a vertical line in the margin. The date of issue or amendment of a page appears in the header on each page. This page will be updated each time a new amendment is released.

Amendment number	Description of change	Effective date	Updated by
1	Commentary for steel fatigue loading and design provisions added with new clauses C3.2.6, C4.3.1(I) and C4.3.5 and worked example in appendix C4A. Corrections and additions made to tables C7.1 to C7.4 and C7.7. Commentary on new evaluation loading added with new clause C7.4.4, figures C7.2 to C7.11 and tables C7.10 to C7.14.	May 2022	Nigel Lloyd
0	*Bridge manual commentary* 1st edition published.	October 2018	Nigel Lloyd

Introduction

This informative commentary provides background to various sections of the Waka Kotahi NZ Transport Agency *Bridge manual*. It will be added to as appropriate.

Contents

C3 Design loading

In this section

Section		Page
C3.2	Traffic loads - gravity effects	C3–2
References for C3		C3–9

C3.2 Traffic loads - gravity effects

C3.2.6 Fatigue

For New Zealand road bridges this clause replaces the fatigue load effects set out in clause 7.9 of AS 5100.2 *Bridge design* part 2 Design loads[1]. The basis of the TT530 fatigue loading model is explained in the Waka Kotahi NZ Transport Agency commissioned research report RR 547 *Fatigue design criteria for road bridges in New Zealand*[2], but the long term vehicle mass growth allowances have been reduced compared with the AS 5100.2[1] allowances recommended in the research report.

a. Fatigue design vehicle (TT530)

   The TT530 fatigue vehicle represents a common 8-axle truck-and-trailer configuration scaled up to approximate the effects of higher mass HPMV truck-and-trailers (HPMV conforming vehicles as defined in *Bridge manual* clause 7.1.2). The cycle count calibrations reflect the expected uptake rates for the HPMV mass limits and longer vehicle types on all road types, assuming that all combination vehicles operating at close to general access mass limits (prior to introduction of HPMV limits) would switch to full HPMV limits, with or without upgrades to the longer configurations.

   Using a vehicle configuration comparable to the most common freight vehicle type on NZ roads enabled a more consistent fit to fatigue effects over a wide range of span lengths than the M1600 vehicle in AS 5100.2[1]. Using a fatigue vehicle weight comparable to common heavy vehicles avoids the discrepancies that can arise from different exponents used in fatigue strength curves.

   Treating this long vehicle as indivisible would lead to underestimation of load effects in structures with short continuous spans (with L<15m). Therefore shorter parts of the TT530 vehicle are required to represent effects of rigid trucks and heavy axle sets (in place of the A160 loading in AS 5100.2[1]). Alternatively, the full TT530 vehicle only may be used in conjunction with software that automatically omits axle loads with relieving effects when calculating envelopes of maximum and minimum load effects for the vehicle traversing the structure.

   The positioning of the fatigue vehicle centrally within design lanes for assessment of main members for global effects is consistent with the Eurocode recommendation to select lane locations expected in normal conditions for fatigue loading models (BS EN 1991-2 *Eurocode 1: Actions on structures* part 2 Traffic loads on bridges[3] clause 4.2.4(3)), but likely future carriageway reconfigurations should also be considered.

b. Fatigue load effect scaling

   The 70% factor on loading specified in AS 5100.2[1] clause 7.9 is not required for the TT530 fatigue vehicle.

   The selection of 1.0 for the TT530 fatigue vehicle scale factor can be compared with $0.7(1+\alpha)$ in AS 5100.2[1], giving a net scale factor of 0.91 for the M1600 vehicle. The increased factor for the NZ loading is necessary to compensate for the less onerous lateral positioning requirement compared with AS 5100.2[1], which requires the most critical lateral position for the design lane, and the associated commentary cites that as a consideration for the 70% stress reduction factor (refer to AS 5100.2 Supp 1 *Bridge design–Design loads–Commentary (Supplement to AS 5100.2-2004)*[4]).

C3.2.6 continued

In effect, the TT530 fatigue vehicle loading retains similar assumptions for general dynamic load allowances and stress range reduction factor as AS 5100.2[1]. The justifications for retaining a stress range reduction include:

- The actual stresses in a component are generally less than the theoretically calculated values because of alternative load paths (such as bridge barriers) and the magnitude of actual components in comparison with line elements used to represent them in analysis (from AS 5100.2 Supp 1[4]).
- The load share per beam in multi-beam structures at service load levels may be generally less than calculated values based on analysis models used for strength design.
- Actual dynamic load allowances may be generally less (on average) than the design value (for fully loaded vehicles), provided bridge surfacings are kept in good condition. Annex B of BS EN 1991-2[3] indicates that 0.2 is appropriate for surfacing with "good" roughness. AASHTO LRFD *Bridge design specifications*[5] fatigue loadings incorporate 0.15 dynamic load allowance.

c. Dynamic amplification factor for TT530 fatigue loading

A specific additional dynamic amplification factor of 1.3 should be taken into account within 6m of expansion joints or other discontinuities (including the ends of integral bridges), as required by BS EN 1991-2[3] and previously required by BS5400 *Steel concrete and composite bridges* part 10 Code of practice for fatigue[6]. The Eurocode applies the factor to axle loads, reducing linearly from 1.3 to 1.0 at 6m from the joint. For simplicity the *Bridge manual* adopts the option to apply a constant factor to the derived actions.

d. Loading from multiple lanes

In most steel structures the fatigue effects at each component are dominated by fatigue loading from the lane causing the highest stress range at the component under consideration (Lane 1 as defined in 3.2.6(d)). However, a component located between marked lanes or supporting multiple lanes (box girder flanges for example) can have similar stress ranges from traffic in either lane, and the total damage from traffic in both lanes must be considered using Miner's summation or equivalent. The exponents applied to stress ranges (5 for steel structures) will substantially reduce the influence of adjacent lanes, causing lower fatigue damage at the component.

Infrequent occurrence of simultaneous loading from 2 lanes is allowed for by the factor $K_b Z$ which is based upon UK Highways Agency report *Derivation of the UK National Annex to clause 4.6: Fatigue load models: Eurocode 1: Actions on structures – part 2: Traffic loads on bridges*[7].

e. Heavy-vehicles-per-lane-per-day

Guidance on use of available information on heavy vehicle counts is provided in the appendix to C3.2.6 below.

A minimum first year count of 25 heavy-vehicles-per-day in each direction is specified for secondary collector and access roads. This provides a minimum standard for bridge structures on very low volume roads and urban streets.

The allocation of heavy-vehicles-per-day in one direction into heavy-vehicles-per-lane-per-day in that direction (table 3.1) is based on the AS 5100.2[1] requirements with the following additional considerations:

C3.2.6 continued

- observations from the Auckland Harbour Bridge WiM (weigh-in-motion) stations, during long periods with heavy vehicles restricted to 2 lanes, that up to 80% used 1 of the 2 available lanes (see research report 547(2))
- a requirement for 2 lanes damage summations that the total counts should match the direction total, except that for 3 lanes (45% in the accompanying lane) the combined total of 110% considers the greater potential for unconstrained future growth on the higher capacity roads.

f. Cycle counts for the TT530 fatigue loading

The cycle count formula for the TT530 fatigue vehicle loading is split into its component parts to clarify the function of each part.

The equivalent number of cycles of TT530 load effect per heavy vehicle (0.6 to 2.0) is an average value allowing for the full HPMV mass limits on roads with a high proportion of fully laden freight vehicles in the considered direction (route factor = 1.0), and the additional stress cycles caused by each axle group. This part may be compared with $0.125L^{-0.5}$ for M1600 and 0.25 for A160 fatigue loadings in AS5100.2(1) (for example, 0.04 at L=10m for M1600 compared with 1.0 at L=10m for TT530 fatigue loading).

The long term multiplier (100,000) was reduced from 160,000 in AS5100.2(1) and research report 547(2) to reflect a lower expectation of growth in vehicle masses above present HPMV limits over the design life, compared with the initial assumptions (which included 30% growth in axle set mass limits). The 100,000 multiplier equates to 274 times the first-year fatigue loading compared with 438 for the AS5100.2(1) formula.

Background to the choice of long-term multiplier for the *Bridge manual* fatigue load model follows:

> The commentary to AS 5100.2(1) notes that in developing the fatigue design criteria, a fatigue life of 75 years has been assumed to correspond to a bridge design life of 100 years on the basis that:
>
> i. bridges will be inspected regularly and that intervention will occur when fatigue damage is detected. This process should ensure that fatigue damage is controlled; and
> ii. the uncertainty associated with the prediction of the fatigue life is such that only a relatively low percentage of bridges for which the theoretical design fatigue life has been reached actually exhibit fatigue damage.
>
> If a 75-year period is assumed used for accumulation of equivalent cycle counts, the long-term multiplier applied to year-one fatigue loadings in AS 5100.2(1) amounts to approximately 4% per annum geometric growth. The AS 5100.2(1) commentary indicates that the growth allowance considers average vehicle mass increase over time, annual rates of increases of freight volumes from 5% on major interstate routes down to 1% lesser routes, with volumes capped at saturation levels of 4,000-5,000 heavy-vehicles per-lane-per-day.
>
> Growth levels considered for New Zealand loadings (research report 547(2)) identified that the AS 5100.2(1) growth level (438 times the first year fatigue loading) could be reached or exceeded through a range of scenarios, such as 3% per annum linear volume growth with 0.7% per annum vehicle mass growth (capped at 30% above expected HPMV levels).

C3.2.6 continued

The reduced growth multiplier adopted for the *Bridge manual* (274 times the first-year fatigue loading) considers the following:

- The base TT530 fatigue vehicle calibration of 0.6 equivalent cycles per heavy vehicle for span lengths over 16.7m (research report 547[2]) is based on conservative estimates for adoption of the full higher mass HPMV limits. Proportions of vehicles operating at the full HPMV limits so far been lower than allowed for due to adoption of lower mass configurations such as 50MAX.
- Waka Kotahi NZ Transport Agency considers the initial expectation of 30% further increase in axle group mass limits over time to be unrealistic for New Zealand roads in view of other constraints such as pavement damage considerations.
- Increases in design live loadings for bridges to the levels recommended in research report 539 *A new vehicle loading standard for road bridges in New Zealand*[8] have not yet occurred, but smaller increases above current *Bridge manual* loadings are anticipated.
- Capping the assumed mass growth at 15% above HPMV levels while retaining the 3% per annum linear volume increase rate over a 75 year period leads to the adopted multiplier of 100,000 (274 times the first year fatigue loading) which is equivalent to approximately 3% geometric increase for 75 years.
- Principal Inspections at 6-yearly frequency as specified in specification NZTA S6 *Bridges, geotechnical structures and other significant structures inspection policy*[9] fulfils a key assumption for the 75-year period adopted for AS 5100.2[1] fatigue loadings.
- The added requirement to use the safe life approach (*Bridge manual* clause 4.3.3(l)) and corresponding capacity reduction factors should provide additional reliability.

The growth multiplier could be increased in a future amendment if design live loadings for bridges are increased significantly to cater for larger vehicle mass increases.

Route factor selection

The range of route factors for *typical* New Zealand road types is 0.3–0.8, replacing 0.3–0.9 in the *Bridge manual* 3rd edition up to amendment 3, or 0.3–1.0 in AS 5100.2[1]. The specified route factors allow for general access by HPMV conforming vehicles on all route types. The maximum route factor = 1.0 is reserved for routes where there is a high proportion of freight vehicles and most of those vehicles travelling in one or both directions are fully loaded, whereas the 0.8 factor for typical long haul freight routes allows for typical proportions of partly loaded or empty vehicles in both directions. The 0.4 factor for high-volume urban motorways and arterial routes is applicable to major urban freight routes where around half of the heavy vehicle mix are 2-axle trucks and buses. The 0.6 factor is relevant to the motorway sections at the urban fringes where the heavy vehicle mix is less diluted by the lighter vehicles, and to other rural routes.

For information on selection of route factors suited to fatigue assessments of bridges restricted to Class 1 conforming vehicles or to estimates of accumulated fatigue damage prior to introduction of HPMV, refer to research report 547[2].

C3.2.6 continued

g. Service life adjustment

The service life factors in AS/NZS 5100.6 *Bridge design* part 6 Steel and composite construction[10] clause 13.9.2.2 assume that effective annual cycles continue at the average rate over the 75-year or 100-year period. However, for extended service lives it must be assumed that ongoing fatigue damage will accumulate at the increased rate including growth to end of that period. For an extension to service life past 100 years it is assumed that heavy traffic volumes per lane may be limited by capacity constraints, and that controls on vehicle loadings would be acceptable.

For the adopted long term cycle count multiplier of 100,000 (approximately 274 times the first year design fatigue loading) assuming caps on vehicle mass growth and no further increases in annual heavy vehicle counts per lane, the annual damage increment including growth would be approximately 6 times the first year fatigue loading, amounting to 2.2% increase in cycle counts per additional year of service life.

Appendix to C3.2.6 Guidance for estimation of heavy vehicle counts for use in fatigue loadings

The heavy vehicle counts used in fatigue loadings are required to be based on an appropriate value for the number of heavy-vehicles-per-lane-per-day expected in the first year the bridge will open. This requires the designers and/or road controlling authority to forecast the expected average heavy vehicle counts, typically based on forecast AADT (annual average daily traffic) and percentage of heavies. For bridges at new locations, bridges replacing structures with capacity restrictions, and bridges on upgraded highways the heavy traffic count estimates should consider the volumes likely to be attracted from nearby alternative routes.

The heavy vehicle counts used in fatigue loading estimates must allow for all vehicles with gross mass exceeding 3500kg. This includes short wheelbase 2-axle commercial vehicles and buses which cannot be clearly distinguished from light vehicles at most traffic counting stations.

This appendix includes guidance on interpretations of route classes and available heavy traffic count data but does not address volume forecasts.

Road classifications

The *One network road classification – functional classification*[11] lists minimum heavy commercial vehicle (HCV) daily flows, and maps reproduced as figures 2.1(a) to (c) in the *Bridge manual* show the categories for all state highways and selected main roads in urban centres. A web hosted ArcGIS map[12] provides classifications for all roads including urban streets. (It is noted that work to update the ONRC classifications to a One Network Framework (ONF) is underway.)

Research report 547[2] noted that state highway classifications did not appear to be a reliable guide as to appropriate route factors and heavy vehicle counts, so suggested that local knowledge and heavy traffic forecasts would be needed to guide the selection of an applicable route type and associated route factor. Analysis of classified heavy vehicle counts at a selection of Waka Kotahi NZ Transport Agency telemetry sites presented in research report 547[2] found that the average daily HCV counts for 2011 generally exceeded the minimums for the applicable ONRC functional categories. Also, the ONRC category for the sample sites did not correlate well with route factors based on the heavy vehicle type mixes indicated by the count data.

Guidance on interpretation of heavy traffic count data

Sources of traffic count data held by Waka Kotahi NZ Transport Agency include:

- AADT and estimated heavy vehicle percentages for all state highway traffic count stations published through an interactive map or annually in traffic data booklets on the Waka Kotahi NZ Transport Agency website[13]
- annual WiM reports[14] covering a small number of sites
- raw count data from WiM stations and telemetry sites held in the Waka Kotahi NZ Transport Agency TMS database
- data and summaries held by regional offices and consultants.

Comments on interpretation of count data are as follows:

- HCV counts as defined in the *Monetised benefits and costs manual*[15] normally exclude buses (passenger transport class) and refer to vehicles and combinations with at least 3 axles; whereas "heavy vehicle" counts must include 2-axle vehicles classed as medium commercial vehicles (MCV). Site specific traffic reports sometimes include 2-axle vehicles in "HCV" counts so clarifications of count basis may be necessary.

Appendix to C3.2.6 continued

- The minimum HCV counts for the ONRC functional categories should be assumed to refer to vehicles with at least 3 axles as per the *Monetised benefits and costs manual*[15]. Those counts appear to be bare minimum values, which should be increased to align with heavy traffic survey data.
- AADT reporting[13] by Waka Kotahi NZ Transport Agency gives annual daily traffic counts and heavy vehicle percentages at multiple locations on all state highways. However, the reported heavy vehicle percentages may be inaccurate for various reasons including:
  - sample data may be short term (a few weeks per year) and skewed by seasonal variations
  - counts may rely on lengths to distinguish between light and heavy vehicles, which can be heavily skewed by numbers of SUVs, utility vehicles and light vans, especially in urban areas
  - heavy vehicle percentages may just be assumptions based on other linked roads.
- The best quality data would come from a nearby WiM site on the route.
- The next best data would come from axle classified counts listing vehicle counts by Waka Kotahi NZ Transport Agency vehicle class, for representative time periods. Proportions of 2-axle vehicles could be compared to those for similar sample locations included in research report 547[2] (table 9.3 and appendix D). Proportions of truck and trailer combinations in each direction would assist in selection of route factor.
- If vehicle counts are classified by numbers of axles only, assume that all vehicles with 3 or more axles are HCVs, and scale-up the HCV counts to estimate heavy vehicle counts using ratios as follows:

Route description	Route factor	Ratio of HV counts to 3+ axle counts	Examples (from sample sites in research report 547[2])
Freight routes with a very high proportion of fully loaded long vehicles in one or both directions.	1.0	1.3	SH5 (Eskdale) SH35 (Hamanatua Bridge) SH45 (Ohawe Beach Rd)
Typical long-haul freight routes, national and regional routes including expressways	0.8	1.4	SH1N (Tokoroa), SH2 (Te Puke) SH27 (Kaihere), SH1S (Waipara)
Motorways, other rural freight routes	0.6	1.4	SH1N (Drury, Paekakariki)
High-volume urban motorways and urban arterial routes	0.4	2.0	SH1N (AHB)
Urban roads	0.3	2.0	

References for C3

(1) Standards Australia AS 5100.2:2017 Bridge design. Part 2 Design loads.

(2) Waka Kotahi NZ Transport Agency (2014) *Fatigue design criteria for road bridges in New Zealand*. Research report 547, Wellington.

(3) British Standards Institution BS EN 1991-2:2003 *Eurocode 1: Actions on structures.* Part 2 Traffic loads on bridges.

(4) Standards Australia AS 5100.2 Supp 1-2007 *Bridge design–Design loads–Commentary (Supplement to AS 5100.2-2004)*.

(5) American Association of State Highway and Transportation Officials (2020) *LRFD Bridge design specification, 9th edition.* Washington DC, USA.

(6) British Standards Institution BS 5400-10:1980 *Steel concrete and composite bridges*. Part 10 Code of practice for fatigue. Withdrawn.

(7) Flint & Neill Partnership (2004) *Derivation of the UK National Annex to clause 4.6: Fatigue load models: Eurocode 1: Actions on structures – part 2: Traffic loads on bridges*. Report 738/20-Rp01-v1 for UK Highways Agency.

(8) Waka Kotahi NZ Transport Agency (2013) *A new vehicle loading standard for road bridges in New Zealand*. Research report 539, Wellington

(9) Waka Kotahi NZ Transport Agency (2020) NZTA S6 *Bridges, geotechnical structures and other significant structures inspection policy*. Wellington.

(10) Standards Australia and Standards New Zealand jointly AS/NZS 5100.6:2017 *Bridge design*. Part 6 Steel and composite construction.

(11) Waka Kotahi NZ Transport Agency (2013) *One network road classification – functional classification*. Wellington.

(12) Waka Kotahi NZ Transport Agency *One network road classification*. Last accessed 17 March 2022. <nzta.maps.arcgis.com/apps/webappviewer/index.html?id=95fad5204ad243c39d84c37701f614b0>

(13) Waka Kotahi NZ Transport Agency (2019) *State highway traffic volumes 1975–2020*. Last accessed 17 March 2022. <www.nzta.govt.nz/resources/state-highway-traffic-volumes>

(14) Waka Kotahi NZ Transport Agency (2018) *Weigh-in-motion (WiM) report*. Last accessed 17 March 2022. <www.nzta.govt.nz/resources/weigh-in-motion>

(15) Waka Kotahi NZ Transport Agency (2020) *Monetised benefits and costs manual*. Wellington.

(This page is intentionally blank)

C4 Analysis and design criteria

In this section

C4.2 Reinforced concrete and prestressed concrete

C4.2.1 General

e. Shrinkage and creep effects in concrete

New Zealand average relative humidities

Relative humidity data is available from the NIWA CliFlo(1) database which can be analysed to determine appropriate average relative humidities for locations throughout New Zealand for use in assessing the shrinkage and creep of concrete.

The following outlines the process that needs to be adopted to access and analyse the NIWA data through the internet, as the process is not obvious from the NIWA website:

Bring up the CliFlo database: <http://cliflo.niwa.co.nz/>.

Establish an On-Line Subscription to CliFlo, and then Login. The subscription will be valid for 2 years and allow the subscriber to download up to 2,000,000 lines of data, but with a limit of 40,000 lines of data per individual search.

Ensure that your internet browser has its security settings set to allow pop-up menus on the NIWA website.

In the Database Query form, make the following selections:

In panel 1: - Click "Select Datatype" and select "Daily and Hourly Observations" from the pop-up menu, then select "Hly Air T" as the option.

In panel 2: - Click "Choose Stations" and then on the pop-up menu click against "region" and from the drop-down list select the region closest to the site of interest. Then click on "Get Station List" This will open as a new webpage. From the listing of stations select an appropriate station near the site of interest to download the data for, by clicking on its "Select" tick box. Confirm that the stations start and end dates encompass the period of time for which data is sought. Then at the bottom of the screen click on "Replace Selected Stations".

Return to the Database Query form by clicking on its webpage tab at the top of the screen.

In panel 3: - Input the start and end dates for the period of time for which data is required. It is suggested that a recent ~5 year period be specified. (40,000 lines of hourly data = 4.566 years)

In panel 4: - Against "Split data into date and time columns" click against "No (single data column)", and against "File download option" select "Excel file" from the drop-down list.

Then click "Send Query" and wait. The website will eventually return an Excel file named wgenf.genform1_proc. Open the file using Microsoft Excel (ignoring any messages about inappropriate file naming). Check that the file contains RH data for each line of data supplied, and that the data is hour by hour for 24 hours of each day, as for some stations some RH data is missing. That data is missing is usually evident from inspection of the first and last few pages of output.

C4.2.1 continued

For datasets that are complete, calculate the average RH by summing the RH data column (column E) and dividing the sum by the number of data rows (≤40,000).). It is suggested that, for each individual site, 2 data searches be undertaken for consecutive periods and averaged to provide an average RH across 9 years' worth of data.

Note that 40,000 lines of data equates to ~700 pages of A4 output, so printing the output file is not recommended.

C4.3 Structural steel and composite construction

C4.3.3 Application of AS/NZS 5100.6(2)

l. Fatigue loading (section 13)

The modifications to AS/NZS 5100.6 *Bridge design* part 6 Steel and composite construction(2) include damage equivalent factors (λ) for the T530 fatigue loading model and provide amendments for errors in the initially published code version (March 2017).

Requirement to use the safe life method

The changes in the 2017 code originated in the Eurocodes, and NA to BS EN 1993-1-9 *UK National Annex to Eurocode 3: Design of steel structures* part 1-9: Fatigue(3) recommended that fatigue design of new structures should usually be based on safe life principles (unless otherwise agreed with the relevant authority). NA to BS EN 1993-1-9(3) and related guideline document PD 6695-1-9 *Recommendations for the design of structures to BS EN 1993-1-9*(4) provide clarification on what in-service inspection and maintenance regimes for fatigue damage tolerant structures may entail (significantly more than necessary for normal principal inspections). In view of those recommendations, the damage tolerant approach is not appropriate for new bridges and the safe life method is considered necessary.

Selection of capacity reduction factor

NA to BS EN 1993-1-9(3) and PD 6695-1-9(4) also clarify the meanings of consequence classes CC1-CC3. It is apparent from PD 6695-1-9(4) that "high" consequence of failure (CC3) was intended to relate to loss of life or "very great" economic consequence, while "medium" consequence of failure (CC2) aligns with "considerable" economic consequences resulting from loss of service.
NA to BS EN 1990 *UK National Annex for Eurocode – Basis of structural design*(5) and NA to BS EN 1993-2 *UK National Annex to Eurocode 3: Design of steel structures* part 2 Steel bridges(6) confirm that fatigue in bridges should be treated as CC2 and recommend $\phi_{Mf} = {}^{1}/_{1.1}$ for all safe life fatigue assessments regardless of consequence class, thus supporting the use of $\phi_{Mf} = 0.85$ generally.

An exception is required for bridges with fracture critical components (also known as FCM – fracture critical members) where failure would lead to overall collapse of the structure. For the *Bridge manual* these are considered to have high consequence of failure in view of potential for loss of life and the corresponding safe life capacity reduction factor $\phi_{Mf} = 0.75$ is required.

C4.3.3 continued

Damage equivalent factors (λ) for the TT530 fatigue loading model

The derivation of the damage equivalent factors (λ) to be used with the TT530 fatigue loading model aimed to produce the same outcomes as evaluations based on damage accumulation using a Miners sum. The purpose of the λ-factors is to adjust the stress range for the fatigue design vehicle at the applicable number of design vehicle cycles to the damage equivalent stress range value at 2 million cycles.

The required derivations provided in *Transfer of Australasian bridge design to fatigue verification system of Eurocode 3*(7) were modified based on the following:

- The lifetime numbers of cycles of loading for the TT530 vehicle are generally more than 1×10^7 except for very low daily heavy vehicle counts, for which fatigue is unlikely to be a governing consideration.
- Therefore exponent m=5 was used for all derivations, with $1/m$ = 0.2 as used in the code, and it can be assumed that normal stress ranges for the fatigue design vehicle will be lower than the S-N curve knee point at $1\text{x}10^7$ cycles.
- For shear stress ranges the S-N curve knee point is at $1\text{x}10^8$ cycles, and the exponent changes from m =5 to m =9 in equation 13.10.1(6). Use of m =5 for derivation of damage equivalent factors for shear stress ranges is conservative for higher cycle counts.
- A fixed adjustment factor must be applied to normal stress ranges (no adjustment is required for shear stress ranges) to account for the different S-N curve slope m =3 between 2×10^6 and 1×10^7 cycles (similar to figure 4 in *Transfer of Australasian bridge design to fatigue verification system of Eurocode 3*(7)). Hence a stress type adjustment factor λ_S is included to address the discrepancy:

  $$\lambda_S = \left(\frac{2\times10^6}{1\times10^7}\right)^{\left(\frac{1}{5}-\frac{1}{3}\right)} = 1.239$$

- The λ_L factor for consideration of effective span length is calculated from the equivalent cycles of TT530 loading per heavy vehicle and varies from $2.0^{0.2} = 1.149$ for L≤5m to $0.6^{0.2} = 0.903$ for L≥16.7m rounded to 2 decimal places. Eg $\lambda_L = 1.00$ for L=10m.
- The λ_C factor for heavy-vehicles-per-lane-per-day provides the adjustment between lifetime heavy vehicle counts including long term growth multiplier and 2 million cycles, thus:

  $\lambda_C = \left(\frac{100{,}000}{2{,}000{,}000}\times \text{hvpd}\right)^{0.2}$ where hvpd = heavy-vehicles-per-lane-per-day

- The multiple lane adjustment factor λ_M was adapted from the λ_4 factor defined by BS EN 1993-2 *Eurocode 3 – Design of steel structures* part 2 Steel bridges(8) clause 9.5.2(6), in conjunction with the adjustments in NA to BS EN 1991-2 UK *National Annex to Eurocode 1: Actions on structures* part 2 Traffic loads on bridges(9) clause NA.2.26. The K_bZ factor from NA to BS EN 1991-2(9) is intended to allow for side-by-side running, or coincident vehicles from opposing directions, of a small proportion of heavy vehicles (giving a small increase in average stress range). The factor provided in the *Bridge manual* is considerably less onerous than table 13.9.2.2(E) of AS/NZS 5100.6(2).

C4.3.3 continued

- The service life adjustment factor λ_Y amends the factor in AS/NZS 5100.6[2] to consider the growth in effective cycles per year (as for clause 3.2.6(g)). As noted in C3.2.6(g) the adopted long-term cycle count multiplier (100,000) is approximately 274 times the first year fatigue load and effective cycles per year are assumed to grow to 6 times the first year fatigue load. For example, the factor for 120 years is calculated from:

$$\left(1 + {}^{20 \times 6}/_{274}\right)^{0.2} = (1 + 20 \times 0.022)^{0.2} = 1.08$$

Shear connectors

The damage equivalent factor λ_V within clause 13.9.6 required clarification to reference the slope m specified for the applicable detail category. Alternatively, the values derived for m =5 may conservatively be used.

Fatigue strength – general (corrections to clause 13.10.1)

Corrections to typographical errors in AS/NZS 5100.6[2] are provided in this amendment.

Clause 13.11.1 – verification formats

The reference to the alternative fatigue life verification formats in appendix I enables the use of a Miner's sum format similar to NZS 3404 *Steel structures standard*[10] and AS 5100:2004[11] for summation of damage for multiple lanes of loading, but including the $K_b Z$ factor applied to the total.

The outcomes should be close to those for the damage equivalent stress range approach, as demonstrated by the worked example in appendix C4A (a rework of the two-span multi-girder bridge fatigue assessment in appendix F of the Waka Kotahi NZ Transport Agency research report RR 525 *Steel-concrete composite bridge design guide*[12]).

Worked example – appendix C4A

A worked example of fatigue assessment calculations following the new *Bridge manual* fatigue design criteria is provided in appendix C4A. The two span multi-girder bridge example structure is based on appendix F of the *Steel-concrete composite bridge design guide* [12].

Fatigue assessment calculation results based on previous code methods (NZS 3404[10] or AS 5100.6[2]) for both M1600 and TT530 loading models are included for comparison with the results for TT530 loading using the damage equivalent factors provided in amendment 4 of the *Bridge manual*.

C4.3.5 Fatigue design

It is recommended that fatigue design parameters are recorded in project hand-over documentation to inform asset managers of the assumed lifetime fatigue loading and design assumptions to be considered in future modifications and maintenance programming.

References for C4

(1) National Institute of Water and Atmospheric Research CliFlo – The national climate database. Last accessed 22 March 2022. <http://cliflo.niwa.co.nz/>.

(2) Standards Australia and Standards New Zealand jointly AS/NZS 5100.6:2017 *Bridge design*. Part 6 Steel and composite construction.

(3) British Standards Institution (2008) NA to BS EN 1993-1-9:2005 *UK National Annex to Eurocode 3: Design of steel structures.* Part 1-9 Fatigue.

(4) British Standards Institution PD 6695-1-9:2008 *Recommendations for the design of structures to BS EN 1993-1-9*.

(5) British Standards Institution (2004) NA to BS EN 1990:2002+A1:2005 *UK National Annex for Eurocode – Basis of structural design.*

(6) British Standards Institution (2008) NA+A1:2012 to BS EN 1993-2:2006 *UK National Annex to Eurocode 3: Design of steel structures.* Part 2 Steel bridges.

(7) Hobbacher AF, Hicks SJ, Karpenko M, Thole F and Uy B (2016) *Transfer of Australasian bridge design to fatigue verification system of Eurocode 3*. Journal of Constructional Steel Research, vol 122, July, 532–542.

(8) British Standards Institution BS EN 1993-2:2006 *Eurocode 3 – Design of steel structures.* Part 2 Steel bridges. (Under review)

(9) British Standards Institution (2008) NA+A1:2020 to BS EN 1991-2:2003 UK *National Annex to Eurocode 1: Actions on structures.* Part 2 Traffic loads on bridges.

(10) Standards New Zealand NZS 3404 Parts 1 and 2:1997 *Steel structures standard*.

(11) Standards Australia AS 5100.6-2004 *Bridge design*. Part 6 Steel and composite construction. Superseded.

(12) Waka Kotahi NZ Transport Agency (2013) *Steel-concrete composite bridge design guide*. Research report 525, Wellington.

Appendix C4A Worked example – Two Span Multi-Girder Bridge, Fatigue Assessment Calculation

In this section

C4A.1 Introduction

Refer to Waka Kotahi NZ Transport Agency research report 525 *Steel-concrete composite bridge design guide*[1] appendix F (referred to as the design guide in the following) for the example bridge details and design calculations. Summary details and dimensions of the bridge superstructure are as follows:

- 28m continuous spans, 14.3m wide x 250mm thick deck slab, four 1100mm deep I-girders at 3.7m spacing
- 9.0m wide carriageway with 2 x 3.5m lanes, 1.0m shoulders, no median, footpaths outside the edge barriers on both sides
- span girders: 600x40 bottom flange, 500x25 top flange, 20 web plate, grade 300, 21.7m long
- pier girders: 700x60 bottom flange, 600x50 top flange, 20 web plate, grade 300, 2 x 6.3m long
- slab reinforcing DH16-150 T&B generally, or DH25-150 T&B longitudinal rebar over the pier section
- intermediate bracing diaphragms between pairs of girders at 3 points per span
- design loadings in accordance with the *Bridge manual* 3rd edition, amendment 0 excluding group 4 load combinations (with HO) for simplicity. Inspection of the design calculations indicated no spare capacity for the pier girder section, but somewhat conservative design of the mid-span sections
- outer girders are below the footpath so the interior girders are more critical for fatigue loading.

The following example fatigue assessment calculations use the TT530 fatigue load model set out in clause 3.2.6 of the *Bridge manual* 3rd edition amendment 4 with application rules for AS/NZS 5100.6:2017 *Bridge design* part 6 Steel and composite construction[2] set out in clause 4.3.3(I), plus the M1600 fatigue load model as implemented in amendment 0 of the *Bridge manual*. These calculation results are intended to be an addendum to those in section F14 of the design guide[1]. To facilitate comparisons with the design guide[1] and fatigue assessments in accordance with AS 5100.6-2004[3], the verification formats used in the example calculations for both load models are consistent with AS 5100.6-2004[3] and the damage accumulation format in AS/NZS 5100.6:2017[2] appendix I section I1.6.

The example calculations are repeated using the characteristic nominal stress range (λ-factor) method (AS/NZS 5100.6[2] clause 13.9 as amended by *Bridge manual* clause 4.3.3(I)) for the TT530 fatigue load model only.

While the design guide[1] example calculation was for an urban road (route factor=0.3), the following example uses parameters for a high volume freight route with 1,500 heavy vehicles per direction per day to illustrate the importance of fatigue design loading for high volume routes. For this illustrative example the lane positions are based on one lane in each direction and no median strip or barrier, whereas a real-world version would be expected to have two lanes in one direction or would have a median strip and/or barrier. Calculations for one lane loaded (representing a two-lane carriageway) are included.

The fatigue detail categories and fatigue strength curves used below are taken from AS/NZS 5100.6[2]. The safe life approach will be used, with $\phi_{Mf} = 0.85$. Only the bending stress checks for the span and pier sections and shear checks for the pier section are illustrated in the example below. Checks at other locations would also be required, as illustrated in the design guide[1] example.

C4A.2 Fatigue assessment (RR 525 design guide section F14)

C4A.2.1 Basic loadings for fatigue design (F14.1)

Two fatigue design loadings are considered below:

- M1600 vehicle loading as modified by the *Bridge manual* 3rd edition amendment 0 (vehicle restricted to the marked lanes) and as described in design guide[1] clause F14.1.
- TT530 vehicle loading as set out in clause 3.2.6 of the *Bridge manual* 3rd edition amendment 4.

The year one average daily heavy vehicle count for both loadings is 1,500 trucks per direction with route factor = 0.8 (based on a long haul freight route).

C4A.2.2 Analysis model

The bridge was modelled in CSiBridge using the automated I-girder bridge template with shell finite elements representing the deck slab and I-girder webs and beam elements for I-girder flanges, diaphragm bracing, and substructure. Demands for the composite slab and girder sections were compiled by the software. A similar approach was used for the SCI Eurocode version of this example bridge (*Composite highway bridge design: worked examples*[4]). Alternatively, plane grillage models are commonly used – as illustrated in the design guide[1].

Modelling assumptions and properties for the fatigue load analysis followed common practice for ultimate limit state live load cases, including:

- short term elastic material properties as for appendix F of the design guide[1]
- deck longitudinal membrane effective stiffness reduced to 16% within 0.15L of the pier (transformed stiffness neglecting concrete in tension as per AS/NZS 5100.6[2] clause 4.4.3)
- deck plate bending stiffnesses reduced to 50% to allow for cracked slab sections.

Due to eccentricity of the main girders below the deck slab, the effects of bending moments on the composite sections should be combined with axial force effects to correctly calculate stress ranges. That step would not be required with a plane grillage model (as used in the design guide[1] example).

Figure C4A.1: Analysis model geometry – wire frame outline

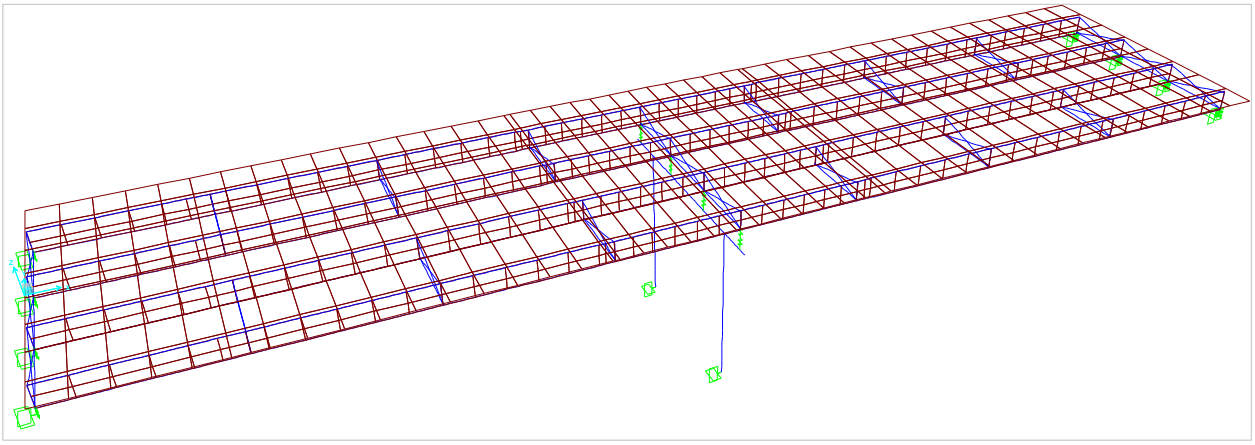

Figure C4A.2: Analysis model – rendered cross section at diaphragm

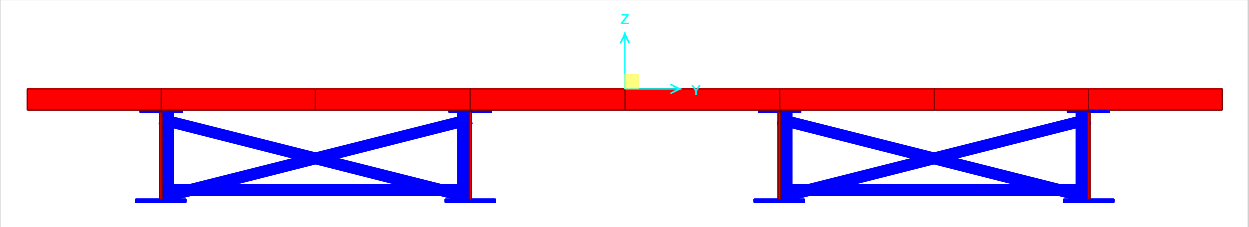

C4A.2.3 Range of effects due to passage of fatigue vehicles (F14.2)

The maximum bending moment, shear force, and bending stress ranges for the two design vehicles are tabulated in tables C4A.1 to C4A.3, and the TT530 vehicle live load bending moment envelope for the most critical girder composite section is shown in figure C4A.3.

Table C4A.1: Worst bending effects (table F.42)

		TT530 vehicle × 1.0		M1600 vehicle × 0.7(1+0.3)	
		Pier M_X (kNm)	Span M_X (kNm)	Pier M_X (kNm)	Span M_X (kNm)
Lane 1	Positive	0	781	0	1415
	Negative	-608	-175	-1579	-328
	Range	608	956	1579	1743
Lane 2	Positive	0	482	0	925
	Negative	-292	-130	-896	-251
	Range	292	612	896	1176

Table C4A.2: Worst shear effects (table F.43)

		TT530 vehicle × 1.0		M1600 vehicle × 0.7(1+0.3)	
		Pier F_X (kN)	Span end F_X (kNm)	Pier F_X (kN)	Span end F_X (kN)
Lane 1	Positive	233	174	452	334
	Negative	0	-12	0	-23
	Range	233	186	452	356
Lane 2	Positive	88	77	197	163
	Negative	-2	-10	-5	-19
	Range	90	87	202	182

In addition, the concurrent axial forces must also be considered for stress calculations in FE slab + eccentric beam models (figure C4A.4), but the resulting stress evaluations are performed by the software (figure C4A.5).

It may be noted that the factored M1600 vehicle moments and shear forces are significantly higher than the values presented in the design guide[1]. For verification of the CSiBridge model, the serviceability limit state HN72 loading results were compared with tables F.15 and F.18 in the design guide[1] and found to be within 5%, and therefore the results in this example are considered to be sufficiently accurate.

Figure C4A.3: Interior girder bending moment envelope for TT530 in lane 1 (kNm)

Figure C4A.4: Interior girder axial force envelope for TT530 in lane 1 (kN)

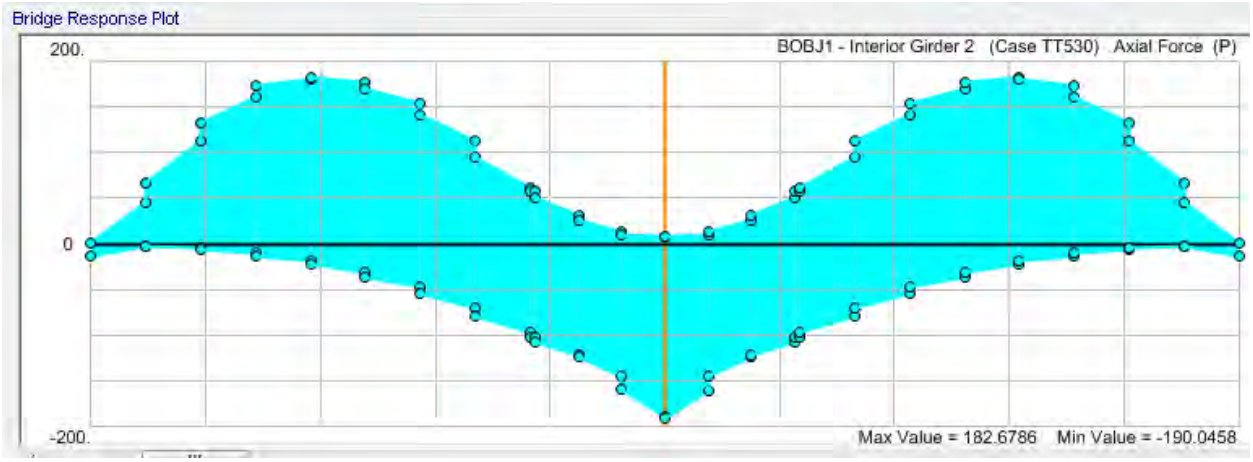

Figure C4A.5: Interior girder bottom flange stress envelope for TT530 in lane 1 (MPa)

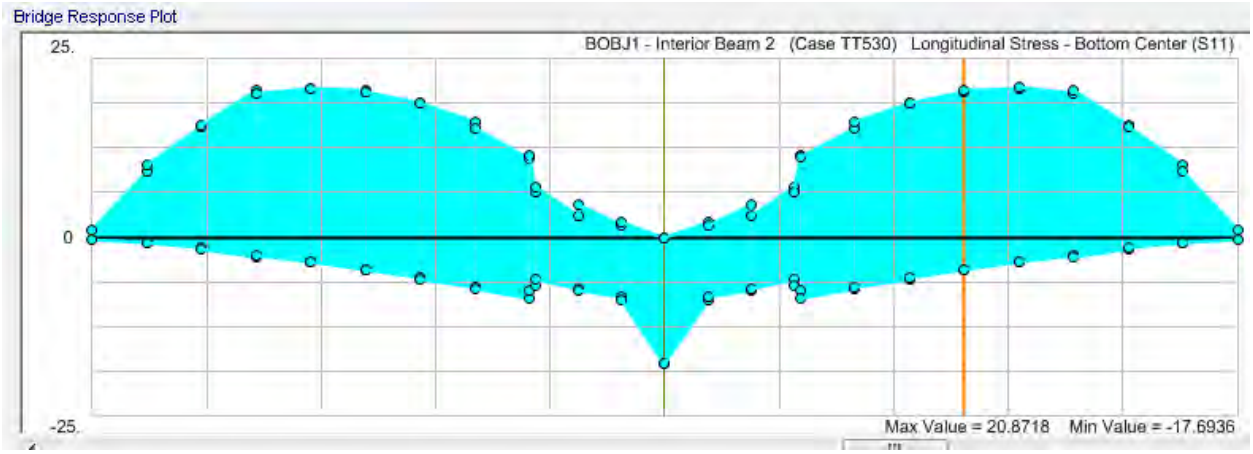

C4A.2.3 continued

The corresponding stress ranges at the bottom flange centre line are tabulated in table C4A.3, for the longitudinal positions with maximum range – which are not necessarily the same points as for maximum absolute values. Stress ranges for the pier section top (tension) and bottom flange centre line are also shown.

The stress ranges for vehicles in the adjacent lane are also given, for combinations of two lanes using a Miners sum or multiple lane adjustment λ-factor.

C4A.2.3 continued

Table C4A.3: Worst stress ranges at centre of girder top and bottom flanges

	TT530 vehicle × 1.0			M1600 vehicle × 0.7(1+0.3)		
	Pier, top $\Delta\sigma_{max}$ (MPa)	Pier, soffit $\Delta\sigma_{max}$ (MPa)	Span, soffit $\Delta\sigma_{max}$ (MPa)	Pier, top $\Delta\sigma_{max}$ (MPa)	Pier, soffit $\Delta\sigma_{max}$ (MPa)	Span, soffit $\Delta\sigma_{max}$ (MPa)
Lane 1 Range	9.1	17.7	24.9	21.2	34.7	45.5
Lane 2 Range	4.9	6.7	16.0	12.2	19.6	30.6
Ratio K_b	0.54	0.38	0.64	0.58	0.56	0.67

C4A.2.4 Equivalent cycle counts for design fatigue loading (F14.1)

For equal spans, the effective span length for both negative and positive bending moments is L = 28m.

For the M1600 loading, 1500 trucks/lane/day, route factor = 0.8, the total number of cycles is:

$$n = 1500 \times 2 \times 10^4 \times 28^{-0.5} \times 0.8 = 4.54 \times 10^6$$

For TT530 loading and L = 28m the equivalent cycles per truck is 0.6, and the total number of cycles is:

$$n = 1500 \times 0.6 \times 1 \times 10^5 \times 0.8 = 72 \times 10^6$$

Note that the number of cycles of TT530 loading is considerably higher than M1600, but the design stress ranges are much lower.

C4A.2.5 Assessment of structural steel details – pier girder section (F14.3)

The design guide[1] example showed that top flange stress ranges were less than for the bottom flange in this structure, so only the bottom flange is considered here.

The detail categories likely to be relevant are 71 or 80 for web stiffener welds to the flange, or 40 for a bearing attachment plate weld to the underside of the bottom flange; and $\phi = 0.85$ for safe life will apply. The knee point on the S-N curves is at 1×10^7 cycles, $0.585\Delta\sigma_C$ in AS/NZS 5100.6[2].

The assessments in table C4A.4 show that the bottom flange has adequate fatigue life at stiffener welds but standard fillet welds to the bearing plates would not be acceptable in this case. The outcomes for TT530 loading are the same as for M1600 loading. A minimum detail category of 56 would be required for compliance in this instance.

Table C4A.4: Assessment of structural steel details – pier girder section

Assessment	TT530 vehicle × 1.0	M1600 vehicle × 0.7(1+0.3)
Stress ranges: lane 1 lane 2	$\Delta\sigma_{max} = 17.7\text{MPa}$ $\Delta\sigma_{max} = 6.7\text{MPa}$	$\Delta\sigma_{max} = 34.7\text{MPa}$ $\Delta\sigma_{max} = 19.6\text{MPa}$
Cycle count	$n = 72 \times 10^6$ in both lanes (N>10^7)	$n = 4.54 \times 10^6$ in both lanes (N<10^7)
Design fatigue strength, detail category 71 at web stiffener weld (if 50–80mm attachment length), lane 1 only	$\Delta\sigma_c = 71\text{MPa}$ $\Delta\sigma_R = 0.585\Delta\sigma_C \left(\frac{1\times10^7}{n}\right)^{\frac{1}{m}} = 41.5\left(\frac{10}{72}\right)^{\frac{1}{5}} = 28$ $\phi_{Mf}\Delta\sigma_R = 0.85\times28 = 24\text{MPa} > \Delta\sigma_{max}$ - OK stress ratio = 0.74 (lane 1 only)	$\Delta\sigma_c = 71\text{Mpa}$ $\Delta\sigma_R = \Delta\sigma_C \left(\frac{2\times10^6}{n}\right)^{\frac{1}{m}} = 71\left(\frac{2}{4.54}\right)^{\frac{1}{3}} = 54$ $\phi_{Mf}\Delta\sigma_R = 0.85\times54 = 46\text{MPa} > \Delta\sigma_{max}$ - OK stress ratio = 0.76 (lane 1 only)
Two lane combination using Miner's sum (Refer to AS/NZS 5100.6(2) appendix I clauses I1.5, I1.6)	$\Delta\sigma_1 = 17.7\text{MPa}, \Delta\sigma_2 = 6.7\text{MPa}$ $n_1 = n_2 = 72\times10^6$ (>10^7) $\phi_{Mf}0.585\Delta\sigma_C = 0.85\times41.5 = 35.3\text{MPa}$ ($\Delta\sigma_1, \Delta\sigma_2$ below knee point at 10^7 cycles) $N_{Ri} = 1\times10^7\left(\frac{0.585\Delta\sigma_C}{\Delta\sigma_i}\right)^m$ from eq. 13.10.1(5) $N_{R1} = 1\times10^7\left(\frac{35.3}{17.7}\right)^5 = 315\times10^6$ By inspection, lane 2 can be neglected. Miners sum: $D_d = \sum\frac{n_i}{N_{Ri}} = \frac{72}{315} + 0 = 0.23 < 1.0$ (OK) Within AS/NZS 5100.6(2) equation I1.6(2) use of m=5 is recommended because TT530 fatigue load cycle counts exceed 1×10^7: $\sqrt[m]{D_d} = \sqrt[5]{0.23} = 0.74$ (approximates the stress ratio for lane 1)	$\Delta\sigma_1 = 34.7\text{MPa}, \Delta\sigma_2 = 19.6\text{MPa}$ $n_1 = n_2 = 4.54\times10^6$ (<10^7) $\phi_{Mf}0.585\Delta\sigma_C = 0.85\times41.5 = 35.3\text{MPa}$ ($\Delta\sigma_1, \Delta\sigma_2$ below knee point at 10^7 cycles) $N_{Ri} = 1\times10^7\left(\frac{0.585\Delta\sigma_C}{\Delta\sigma_i}\right)^m$ from eq. 13.10.1(5) $N_{R1} = 1\times10^7\left(\frac{35.3}{34.7}\right)^5 = 10.9\times10^6$ $N_{R2} = 1\times10^7\left(\frac{35.3}{19.6}\right)^5 = 189\times10^6$ Miners sum: $D_d = \sum\frac{n_i}{N_{Ri}} = \frac{4.54}{10.9} + \frac{4.54}{189} = 0.44 < 1.0$ (OK) Within AS/NZS 5100.6(2) equation I1.6(2) use m=3 with M1600 fatigue loadings: $\sqrt[m]{D_d} = \sqrt[3]{0.44} = 0.76$ (approximates the stress ratio for lane 1)
Two lane combination, with allowance for multiple presence (clause 3.2.6(d))	$Z = 1.5$ for L≥20m, $K_b = 0.38$ $ZK_b = 1.5\times0.38 = 0.57 < 1.0$ (no additional effect to be considered)	$Z = 1.5$ for L≥20m, $K_b = 0.54$ $ZK_b\ 1.5\times0.57 = 0.86 < 1.0$ (no additional effect to be considered)
Design fatigue strength, detail category 40 at bearing plate weld for (t>50, t_c<t), lane 1 only	$\Delta\sigma_c = 40\text{MPa}$ $\Delta\sigma_R = 0.585\Delta\sigma_C \left(\frac{1\times10^7}{n}\right)^{\frac{1}{m}} = 23.4\left(\frac{10}{72}\right)^{\frac{1}{5}} = 16$ $\phi_{Mf}\Delta\sigma_R = 0.85\times16 = 13\text{MPa} < \Delta\sigma_{max}$ - NG	$\Delta\sigma_c = 40\text{MPa}$ $\Delta\sigma_R = \Delta\sigma_C \left(\frac{2\times10^6}{n}\right)^{\frac{1}{m}} = 40\left(\frac{2}{4.54}\right)^{\frac{1}{3}} = 30$ $\phi_{Mf}\Delta\sigma_R = 0.85\times30 = 26\text{MPa} < \Delta\sigma_{max}$ - NG

C4A.2.6 Assessment of structural steel details – span girder section (F14.5)

The design guide[1] example showed that top flange stress ranges were negligible, so only the bottom flange is considered here.

The most onerous detail category would likely be 80 for web stiffener welds to the flange.

The assessments in table C4A.5 show that the bottom flange has adequate fatigue life at stiffener welds. The outcome for TT530 loading is similar to that for the M1600 loading. The contribution from the 2nd lane was more significant for the M1600 loading (15% of the total damage sum compared with 10% for the TT530 loading).

Table C4A.5: Assessment of structural steel details – span girder section

Assessment	TT530 vehicle × 1.0	M1600 vehicle × 0.7(1+0.3)
Stress ranges: lane 1 lane 2	$\Delta\sigma_{max} = 24.9\text{MPa}$ $\Delta\sigma_{max} = 16.0\text{MPa}$	$\Delta\sigma_{max} = 45.5\text{MPa}$ $\Delta\sigma_{max} = 30.6\text{MPa}$
Cycle count	$n = 72 \times 10^6$ in both lanes (N>10^7)	$n = 4.54 \times 10^6$ in both lanes (N<10^7)
Design fatigue strength, detail category 80 at web stiffener (no size effect), lane 1	$\Delta\sigma_c = 80\text{MPa}$ $\Delta\sigma_R = 0.585\Delta\sigma_C\left(\frac{1\times10^7}{n}\right)^{\frac{1}{m}} = 46.8\left(\frac{10}{72}\right)^{\frac{1}{5}} = 32$ $\phi_{Mf}\Delta\sigma_R = 0.85\times32 = 27\text{MPa} > \Delta\sigma_{max}$ - OK stress ratio = 0.93 (lane 1 only)	$\Delta\sigma_c = 80\text{Mpa}$ $\Delta\sigma_R = \Delta\sigma_C\left(\frac{2\times10^6}{n}\right)^{\frac{1}{m}} = 80\left(\frac{2}{4.54}\right)^{\frac{1}{3}} = 61$ $\phi_{Mf}\Delta\sigma_R = 0.85\times61 = 52\text{MPa} > \Delta\sigma_{max}$ - OK stress ratio = 0.88 (lane 1 only)
Two lane combination using Miner's sum (Refer to AS/NZS 5100.6[2] appendix I clauses I1.5, I1.6)	$\Delta\sigma_1 = 24.9\text{MPa}, \Delta\sigma_2 = 16.0\text{MPa}$ $n_1 = n_2 = 72\times10^6$ (>10^7) $\phi_{Mf}0.585\Delta\sigma_C = 0.85\times46.8 = 39.8\text{MPa}$ ($\Delta\sigma_1, \Delta\sigma_2$ < strength at 10^7 cycles) $N_{Ri} = 1\times10^7\left(\frac{0.585\Delta\sigma_C}{\Delta\sigma_i}\right)^m$ from eq. 13.10.1(5) $N_{R1} = 1\times10^7\left(\frac{39.8}{24.9}\right)^5 = 104\times10^6$ $N_{R2} = 1\times10^7\left(\frac{39.8}{16.0}\right)^5 = 952\times10^6$ Miners sum: $D_d = \sum\frac{n_i}{N_{Ri}} = \frac{72}{104} + \frac{72}{952} = 0.77 < 1.0$ (OK)	$\Delta\sigma_1 = 45.5\text{MPa}, \Delta\sigma_2 = 30.6\text{MPa}$ $n_1 = n_2 = 4.54\times10^6$ (<10^7) $\phi_{Mf}0.585\Delta\sigma_C = 0.85\times80 = 68\text{MPa}$ (strength at 2x10^6 cycles) $N_{Ri} = 2\times10^6\left(\frac{\sigma_C}{\Delta\sigma_i}\right)^m$ from eq. 13.10.1(1) $N_{R1} = 2\times10^6\left(\frac{68}{45.5}\right)^5 = 6.68\times10^6$ $N_{R2} = 2\times10^6\left(\frac{39.8}{30.6}\right)^5 = 37.2\times10^6$ Miners sum: $D_d = \sum\frac{n_i}{N_{Ri}} = \frac{4.54}{6.68} + \frac{4.54}{37.2} = 0.80 < 1.0$ (OK)
Two lane combination, with allowance for multiple presence (clause 3.2.6(d))	$Z = 1.5$ for L≥20m, $K_b = 0.64$ $ZK_b = 1.5\times0.64 = 0.96$ < 1.0 (no additional effect to be considered)	$Z = 1.5$ for L≥20m, $K_b = 0.67$ ZK_b $1.5\times0.67 = 1.005$ $D_d = 0.80\times1.005 = 0.804$ (increase is negligible)
Stress ratio estimate (see table C4A.4)	$\sqrt[m]{D_d} = \sqrt[5]{0.77} = 0.95$	$\sqrt[m]{D_d} = \sqrt[5]{0.804} = 0.93$

C4A.2.7 Assessment of shear connections (F14.6)

The maximum shear force ranges at the pier are 233kN for the TT530 vehicle and 452kN for the M1600 vehicle (table C4A.2). Shear stresses in the 6mm web/flange fillet welds (design guide[1] section F11.5) and shear connectors (design guide[1] section F11.6) should be considered. Relevant short-term section properties for calculation of shear flows are provided in the design guide[1] table F.35.

a. Shear connectors at pier (F14.6.1)

The relevant detail category from AS/NZS 5100.6[2] table 13.10.1(F) is 90 with m=8 for shear stress on the nominal cross section area of headed shear studs (AS/NZS 5100.6[2] clause13.10.2). For the pier section where the top flange is in tension, interaction between the shear stress on the stud area and normal stress range in the flange must also be checked (AS/NZS 5100.6[2] clause 13.11.2). By inspection, shear force ranges for vehicles in the adjacent lane 2 have an insignificant effect relative to lane 1 when the m=8 exponent (or m=5 for web shear stress) is applied to stress ratios and therefore ignored in this example.

The assessments in table C4A.6 indicate that the shear connector fatigue lives with TT530 loading or M1600 load are adequate, but the M1600 fatigue loading is more critical.

Table C4A.6: Assessment of shear connections – shear connectors at pier

Assessment	TT530 vehicle × 1.0	M1600 vehicle × 0.7(1+0.3)
Shear force range (lane 1)	233kN	452kN
Calculate shear force per stud from shear flow at slab-flange interface	$\frac{A_t y_c}{I_t} = 0.761\text{m}^{-1}$ 19mm studs, 3 rows, 0.15m spacing $233 \times 0.761 \times \frac{0.15}{3} = 8.9\text{kN/stud}$	$\frac{A_t y_c}{I_t} = 0.761\text{m}^{-1}$ 19mm studs, 3 rows, 0.15m spacing $452 \times 0.761 \times \frac{0.15}{3} = 17.2\text{kN/stud}$
Shear stress range	$\Delta_\tau = \frac{8.9\text{kN}}{283\text{mm}^2} = 31\text{MPa}$	$\Delta_\tau = \frac{17.2\text{kN}}{283\text{mm}^2} = 61\text{MPa}$
Cycle count	$n = 72 \times 10^6$	$n = 4.54 \times 10^6$
Design fatigue strength, detail category 90 with m=8 for shear studs	$\Delta\tau_c = 90\text{MPa}$ $\Delta\tau_R = \Delta\tau_C\left(\frac{2\times10^6}{n}\right)^{\frac{1}{m}} = 90\left(\frac{2}{72}\right)^{\frac{1}{8}} = 57$ $\phi_{Mf}\Delta\tau_R = 0.85\times57 = 49\text{MPa} > \Delta\tau$ - OK	$\Delta\tau_c = 90\text{MPa}$ $\Delta\tau_R = \Delta\tau_C\left(\frac{2\times10^6}{n}\right)^{\frac{1}{m}} = 90\left(\frac{2}{4.54}\right)^{\frac{1}{8}} = 81$ $\phi_{Mf}\Delta\tau_R = 0.85\times81 = 69\text{MPa} > \Delta\tau$ - OK
Top flange stress range (conservatively use max range rather than concurrent values)	$\Delta\sigma_{max} = 9\text{MPa}$	$\Delta\sigma_{max} = 21\text{MPa}$
Design fatigue strength, detail category 80	$\Delta\sigma_c = 80\text{MPa}$ $\Delta\sigma_R = 0.585\Delta\sigma_C\left(\frac{1\times10^7}{n}\right)^{\frac{1}{m}} = 46.8\left(\frac{10}{72}\right)^{\frac{1}{5}} = 32$ $\phi_{Mf}\Delta\sigma_R = 0.85\times32 = 27\text{MPa} > \Delta\sigma_{max}$	$\Delta\sigma_c = 80\text{MPa}$ $\Delta\sigma_R = \Delta\sigma_C\left(\frac{2\times10^6}{n}\right)^{\frac{1}{m}} = 80\left(\frac{2}{4.54}\right)^{\frac{1}{3}} = 61$ $\phi_{Mf}\Delta\sigma_R = 0.85\times61 = 52\text{MPa} > \Delta\sigma_{max}$
Check shear – tension stress interaction	$\frac{\Delta\sigma_{max}}{\phi_{Mf}\Delta\sigma_R} + \frac{\Delta\tau}{\phi_{Mf}\Delta\tau_R} = \frac{9}{27} + \frac{31}{49} = 0.97 < 1.3$ - OK	$\frac{\Delta\sigma_{max}}{\phi_{Mf}\Delta\sigma_R} + \frac{\Delta\tau}{\phi_{Mf}\Delta\tau_R} = \frac{21}{52} + \frac{61}{69} = 1.29 < 1.3$ - OK

C4A.2.7 continued

b. Web-flange weld shear assessment

The relevant detail category from AS/NZS 5100.6(2) table 13.10.1(F) is 80 with m=5 for fillet weld longitudinal shear stress. The effect of fatigue loads in lane 2 is ignored as noted in C4A.2.7(a).

The assessments in table C4A.7 show that the web-flange welds have adequate fatigue life. The outcome for TT530 loading is the same as for the M1600 loading.

Table C4A.7: Assessment of shear connections – web-flange weld shear assessment

Assessment	TT530 vehicle × 1.0	M1600 vehicle × 0.7(1+0.3)
Shear force range (lane 1)	233kN	452kN
Shear flow at flange-web connection	$\frac{A_t y_c}{I_t} = 0.873 m^{-1}$ $233 \times 0.873 = 204 kN/m$ 2 x 6mm fillet welds, t_t = 8.4mm	$\frac{A_t y_c}{I_t} = 0.873 m^{-1}$ $452 \times 0.873 = 395 kN/m$
Shear stress range	$\Delta_\tau = \frac{204}{8.4} = 24 MPa$	$\Delta_\tau = \frac{395}{8.4} = 47 MPa$
Cycle count	$n = 72 \times 10^6$ (N>10^7)	$n = 4.54 \times 10^6$ (N<10^7)
Design fatigue strength, detail category 80 with m=5	$\Delta\tau_c = 80 MPa$ $\Delta\tau_R = \Delta\tau_C \left(\frac{2\times10^6}{n}\right)^{\frac{1}{m}} = 80\left(\frac{2}{72}\right)^{\frac{1}{8}} = 39$ $\phi_{Mf}\Delta\tau_R = 0.85\times39 = 33 MPa > \Delta\tau$ - OK	$\Delta\tau_c = 80 MPa$ $\Delta\tau_R = \Delta\tau_C \left(\frac{2\times10^6}{n}\right)^{\frac{1}{m}} = 80\left(\frac{2}{4.54}\right)^{\frac{1}{8}} = 68$ $\phi_{Mf}\Delta\tau_R = 0.85\times68 = 57 MPa > \Delta\tau$ - OK

C4A.2.8 Fatigue assessments using AS/NZS 5100.6(2) section 13.9

The preceding assessments for the TT530 fatigue load model are repeated below, using the damage equivalent factors (λ) for the TT530 fatigue load model provided in *Bridge manual* clause 4.3.3(l):

$\lambda = \lambda_C \times \lambda_S \times \lambda_L \times \lambda_R \times \lambda_M \times \lambda_Y$

λ_C = factor for heavy-vehicles-per-lane-per-day for first year of service
= $(0.05 \times 1500)^{0.2} = 2.37$

λ_S = stress type adjustment factor (new – not included in AS/NZS 5100.6(2))
= 1.24 for normal stress ranges or 1.0 for shear stress ranges

λ_L = factor for consideration of effective span length
= $0.6^{0.2} = 0.90$ for L ≥ 16.67m

λ_R = route factor adjustment
= $0.8^{0.2} = 0.96$ for route factor = 0.8

λ_M = multiple lane adjustment factor
= $\left[\left(1 + \frac{N_2}{N_1} K_b^5\right) K_b Z\right]^{0.2}$

λ_Y = for service life adjustment factor
= 1.0 for 100 year service life and regular inspections

For assessments of shear stud connectors using AS/NZS 5100.6(2) clauses 13.9.6 and 13.10.2 (m=8) the damage equivalent factor λ_v is recalculated by replacing 5 with 8 and 0.2 with 0.125 in the above in the above equations for λ_C, λ_L, λ_R, λ_M.

C4A.2.8 continued

For sections not within 6m of expansion joints or other discontinuities, use dynamic load allowance $\alpha = 0$.

a. Pier girder section

Assessment	TT530 vehicle × 1.0
Stress range (lane 1)	$\Delta\sigma_{max} = 17.7\text{MPa}$
Multiple lane adjustment	Negligible: $K_b = 0.38$, $K_bZ = 1.0$, if $N_1 = N_2$ then $\lambda_M = 1.0016$
Damage equivalent factor	$\lambda = 2.37 \times 1.24 \times 0.90 \times 0.96 \times 1.0 \times 1.0016 = 2.54$
Nominal stress range	$\Delta\sigma_{E,2} = (1+\alpha)\lambda\Delta\sigma_{max} = 1.0 \times 2.54 \times 17.7 = 45.0\text{MPa}$
Design fatigue strength, detail category 71 at web stiffener weld	$\Delta\sigma_c = 71\text{MPa}$ (if 50-80mm attachment length) $\phi_{Mf}\Delta\sigma_c = 0.85 \times 71 = 60\text{MPa} > \Delta\sigma_{E,2}$ - OK

The assessment outcome is the same as in C4A.2.5, ie a minimum detail category of 56 would be required for compliance in this instance.

b. Span girder section

Assessment	TT530 vehicle × 1.0
Stress range (lane 1)	$\Delta\sigma_{max} = 24.9\text{MPa}$
Multiple lane adjustment	$K_b = 0.64$, $K_bZ = 1.0$, for $N_1 = N_2$ $\lambda_M(1 + 0.64^5) = 1.021$
Damage equivalent factor	$\lambda = 2.37 \times 1.24 \times 0.90 \times 0.96 \times 1.0 \times 1.021 = 2.59$
Nominal stress range	$\Delta\sigma_{E,2} = (1+\alpha)\lambda\Delta\sigma_{max} = 1.0 \times 2.59 \times 24.9 = 64.5\text{MPa}$
Design fatigue strength, detail category 80 at web stiffener	$\Delta\sigma_c = 80\text{MPa}$ $\phi_{Mf}\Delta\sigma_c = 0.85 \times 80 = 68\text{MPa} > \Delta\sigma_{E,2}$ - OK Demand/resistance $(D/R) = 64.5/68 = 0.95$
Compare with Miner's sum from C4A.2.6 (see AS/NZS 5100.6[2] appendix I clause I1.6 for basis)	Miners sum for 2 lane combination: $D_d = 0.77$ $\sqrt[5]{D_d} = \sqrt[5]{0.77} = 0.95$ This matches the D/R value above, showing that the outcomes are identical.

The assessment outcome is the same as in C4A.2.6. The 2nd lane contribution increases the equivalent nominal stress by 2%.

c. Web-flange weld shear assessment

Assessment	TT530 vehicle × 1.0
Shear stress range	$\Delta\tau_{max} = 24\text{MPa}$ (as in C4A.2.7(b))
Multiple lane adjustment	Negligible: $\lambda_M = 1.0$
Damage equivalent factor	$\lambda = 2.37 \times 1.0 \times 0.90 \times 0.96 \times 1.0 \times 1.0 = 2.05$
Nominal stress range	$\Delta\tau_{E,2} = (1+\alpha)\lambda\Delta\tau_{max} = 1.0 \times 2.05 \times 24 = 49\text{MPa}$
Design fatigue strength, detail category 80 with m=5	$\Delta\tau_c = 80\text{MPa}$ $\phi_{Mf}\Delta\tau_c = 0.85 \times 80 = 68\text{MPa} > \Delta\tau_{E,2}$ - OK

C4A.2.8 continued

d. Shear connectors at pier

Assessment	TT530 vehicle × 1.0
Shear stress range	$\Delta\tau_{max} = 31.3\text{MPa}$ (as in C4A.2.7(a))
Multiple lane adjustment	Negligible: $\lambda_M = 1.0$
Damage equivalent factor, recalculate with m=8	$\lambda_v = (0.05 \times 1500)^{0.125} \times 1.0 \times 0.6^{0.125} \times 0.8^{0.125} \times 1.0 \times 1.0 = 1.57$ Note that the λ-value for shear stress ranges with m=5 (see C4A.2.8(c)) is a conservative alternative to this recalculation.
Nominal stress range	$\Delta\tau_{E,2} = (1+\alpha)\lambda\Delta\tau_{max} = 1.0 \times 1.57 \times 31.3 = 49\text{MPa}$
Design fatigue strength, detail category 80 with m=5	$\Delta\tau_c = 90\text{MPa}$ $\phi_{Mf}\Delta\tau_c = 0.85 \times 90 = 78\text{MPa} > \Delta\tau_{E,2}$ - OK
Normal stress range	$\Delta\sigma_{max} = 9\text{MPa}$ (as in C4A.2.7(a))
Damage equivalent factor	$\lambda = 2.37 \times 1.24 \times 0.90 \times 0.96 \times 1.0 \times 1.0 = 2.54$
Nominal stress range	$\Delta\sigma_{E,2} = (1+\alpha)\lambda\Delta\sigma_{max} = 1.0 \times 2.54 \times 9.0 = 23\text{MPa}$
Design fatigue strength, detail category 80	$\Delta\sigma_c = 80\text{MPa}$ $\phi_{Mf}\Delta\tau_c = 0.85 \times 80 = 68\text{MPa}$
Check interaction, AS/NZS 5100.6(2) equation 13.11.2(2)	$\frac{23}{68} + \frac{49}{78} = 0.97 < 1.3$ OK (same result as in C4A.2.7(a))

C4A.3 References

(1) Waka Kotahi NZ Transport Agency (2013) *Steel-concrete composite bridge design guide*. Research report 525, Wellington.

(2) Standards Australia and Standards New Zealand jointly AS/NZS 5100.6:2017 *Bridge design*. Part 6 Steel and composite construction.

(3) Standards Australia AS 5100.6-2004 *Bridge design*. Part 6 Steel and composite construction. Superseded.

(4) Iles, DC (2010) *Composite highway bridge design: worked examples*. SCI Publication P357. The Steel Construction Institute, Silwood Park, UK.

C5 Earthquake resistant design of structures – Commentary to the provisions for displacement based design

In this section

C5.1 General

The topics of this commentary are presented in the order that a designer would be expected to address them in, whereas the order in section 5 of the *Bridge manual* differs to group requirements relevant to both displacement-based design and force-based design together and to group requirements relevant to one or other of the design methods separately. Cross-referencing is provided to the relevant clauses in the *Bridge manual*.

The approach in these provisions has been provided as an alternative to the force-based approach in the *Bridge manual* and utilizes displacement-based principles. As noted in *Displacement-based seismic design of structures*(1), force-based seismic design of bridges is based on a number of assumptions that are invalid, and which can result in inappropriate global strength, and/or poor distribution of strength between different structural elements participating in seismic resistance. Areas of particular concern with current force-based seismic design of bridges include the following:

- *Elastic stiffness of piers*. It is incorrectly assumed that elastic stiffness of piers (reinforced concrete or steel) is independent of strength. For reinforced concrete piers a value of $0.5I_{gross}$ is often assumed. However, it can easily be shown that, dependent on axial load and reinforcement content, the stiffness can be as low as $0.12I_{gross}$ and as high as $0.9I_{gross}$ (see figure C5.1). The consequence can be significant errors in calculation of structural periods, and hence required design strength.
- *Distribution of design strength to structural elements in proportion to elastic stiffness*. Elastic stiffness is irrelevant once piers respond inelastically. The correct value to use is the secant stiffness to maximum design displacement. The errors induced by force-based design are particularly serious when a combination of elastic (superstructure flexure) and inelastic load paths (pier flexure) contribute to seismic resistance.
- *The assumption that a given ductility factor is appropriate for all bridges of a given configuration (e.g. cantilever piers with bearing supported superstructures).* In fact, bearing flexibility and column aspect ratio (height/width) can result in large variation of ductility capacity.
- *The assumption that the equal displacement approximation is valid*. In fact, displacements predicted on the basis of elastic stiffness often underestimate the true inelastic displacements. This error is compounded by errors in estimated elastic stiffness, as noted above.
- *The inability of force-based design methodology to correctly account for foundation flexibility and foundation damping.*

Direct displacement-based seismic design (DDBD) does not suffer from any of the above defects, and is simple to apply. The procedure is of similar complexity to the equivalent-lateral force procedure in force-based seismic design.

Even if force-based design is adopted, the influence of the errors noted above can be greatly reduced by adopting appropriate parts of this commentary, such as distribution of design base shear between different piers, or determining whether a bridge in a low seismic region can be expected to respond elastically. Information in this commentary can also be used to justify reductions in transverse reinforcement of piers compared with requirements of NZS 3101.1&2 *Concrete structures standard*(2), where appropriate.

C5.1 continued

Figure C5.1: Stiffness of circular bridge columns as a function of axial load ratio and flexural reinforcement content (*Displacement-based seismic design of structures*[1])

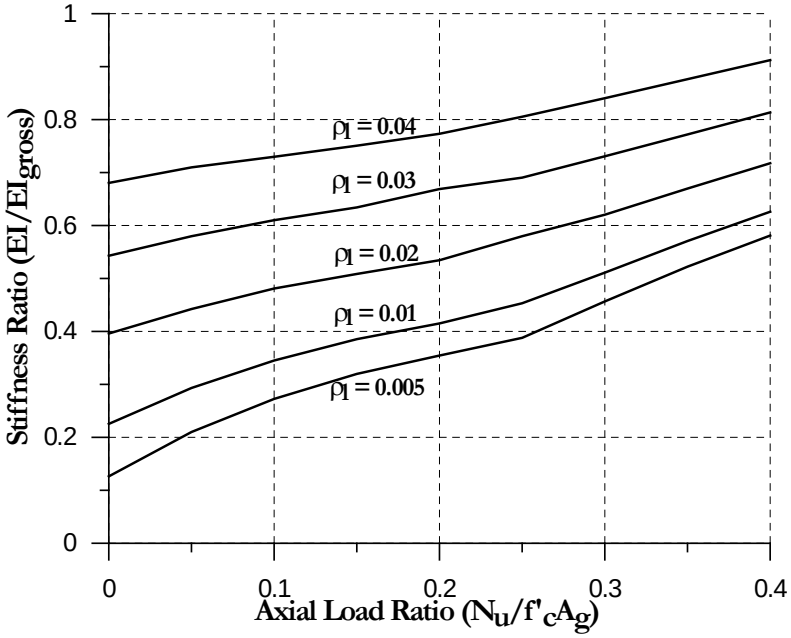

Limitations are placed on categories of bridges that can be designed, with confidence, by DDBD without additional verification. For structures that do not comply with these limitations, and for bridges of high importance, DDBD can still be used to determine the distribution of required strength, but the design should be verified by modal response-spectrum analysis using effective member stiffness and equivalent viscous damping or by non-linear time-history analysis regardless of requirements of 5.4.1. Bridges with subtended angles between abutments less than 90 degrees may be treated as straight bridges in design, as extensive non-linear time-history analyses indicate the error imposed by this approximation is minimal (see *Comparison of the seismic performance of equivalent straight and curved bridges due to transverse seismic excitation*[3]).

The format of the provisions has been prepared to be as compatible as possible with the recently prepared displacement-based bridge seismic design code for Australian conditions, while recognizing differences imposed by the higher seismicity in New Zealand, and current design practice. This should facilitate interaction between construction and design practice in the two countries.

There has been considerable discussion in recent years as to the validity of using structural performance factors, as specified in NZS 1170.5 *Structural design actions* part 5 Earthquake actions – New Zealand[4]. In buildings the combination of effects such as unquantified excess strength, and conservatism in material strengths for design, and strength reduction factors provide some justification for S_p values less than 1.0. However, in bridge design, excess strength is much less common than in buildings, and displacement-based design uses expected, rather than dependable material strengths, and flexural strength reduction factors for plastic hinges are taken as 1.0. As a consequence structural performance factors are taken as 1.0. This conforms with practice in overseas bridge seismic design codes including and AASHTO *Guide specifications for LRFD seismic bridge design*[5], Caltrans *Seismic design criteria*[6] and Eurocode 8[7], none of which use a structural performance factor.

C5.2 Design limit state (5.1)

NZS 1170.5[4] requires consideration of three limit states: two serviceability limit states (SLS1 and SLS2) and one "ultimate" limit state (ULS) when determining required strength. Because of the annual probability of exceedance for the three limit states, current force-based design will generally result in SLS2 governing the required strength for bridges designated as appropriate for the maximum specified ductility demand of μ=6, making this ductility limit irrelevant.

SLS2 requires full functionality to be maintained (table 5.1). Knock-off elements "should not be damaged or dislodged".

Although the performance objective for the SLS2 earthquake response is satisfactory, it is not clear that the structural strength should be determined from this limit state. It should be noted that potential for damage to structural elements (eg plastic hinge regions of columns) cannot be correlated well with the design ductility level. Damage potential is related to reinforcing steel tension strain and to concrete compression strain. These depend strongly on structural configuration. For example, plastic hinge damage will occur at lower ductility levels for slender piers than for squat piers, and multi-column bents with flexible cap beams will suffer damage at lower displacement ductility factors than will cantilever columns. It is thus inappropriate to use a specified ductility level at SLS2 to determine required strength.

It should also be noted that for bridges designed for some level of ductility at the ULS, structural damage at the SLS2 limit state will be minor or non-existent, and associated with spalling or permanently open crack width in the bridge piers. This type of damage would not affect the primary functionality of the bridge to carry full traffic loading, and repairs could be carried out with the bridge in service.

The requirement for avoiding damage to knock-off devices etc, is however important. This is related primarily to maximum displacement response rather than to designed strength. Assuming the "equal-displacement" approximation holds (it is a coarse, but adequate approximation at low ductility levels), strength would be irrelevant to displacement demand, except for very stiff structures, which are uncommon for bridges.

The discussion above is presented in a form appropriate for force-based design, but the conclusions are also relevant to DDBD. Currently strength is illogically dictated by SLS2 and this requirement should be dropped. Strength should be determined by the ULS limit state, but displacement-sensitive elements of the bridge (such as knock-off devices) should be checked at SLS2. Design limit state SLS1 should be completely dropped as irrelevant for bridges. This approach has been adopted for DDBD.

Finally, it should be noted that "ultimate" is an inappropriate description for the ULS, as it gives the impression that seismic intensity greater than the ULS would cause failure. In fact, the ULS has been formulated as a "damage control" limit state (DCLS), and the limit-state strains defined in the commentary should provide a capacity for displacement corresponding to at least 1.5ULS. The intent is that bridges responding at the DCLS (this terminology will be used in preference to ULS in these provisions) should be economically repairable.

C5.3 Bridge classification and importance level (2.1.3)

Different requirements, including different methods of analysis and consideration of vertical acceleration effects are defined for different importance levels. The principal difference between designs at different importance levels will, however, be in the return period defined for each importance level.

C5.4 Design seismicity (5.2.4)

The design seismicity is directly compatible with both NZS 1170.5[4] and the *Bridge manual*, but is expressed in terms of displacement spectra, rather than acceleration spectra. Figure 5.2 and table 5.5 present the spectral shapes in graphical and tabular forms. It will be noted that NZS 1170.5[4] implies a displacement plateau initiating at T=3 seconds. The implication is that elastic displacement demand for bridges with elastic fundamental periods greater than T=3 seconds will not exceed the displacement predicted for T=3 seconds.

C5.5 Design displacement spectrum for earthquake response

C5.5.1 Elastic design spectrum for horizontal earthquake response (5.2.4)

The design firm shall ensure that there is sufficient site information to form the basis of the structure options report or structure design statement. The bridge site information summary given in appendix E is a suitable checklist. However, it is the design firm's responsibility to ensure that the information is sufficiently comprehensive to enable sound judgement to be made on all aspects of the design. This applies particularly to subsurface and hydrological information and if these or other data are not adequate the design firm shall obtain the necessary information before the structure design statement is produced.

C5.5.2 Elastic design spectrum for vertical response (5.2.4)

Recent recordings of vertical response in near-field conditions (eg Christchurch, 2011) indicate that vertical peak ground accelerations (PGAs) and response accelerations can be very large. It is suggested that for these conditions, the vertical response spectrum should equal the horizontal spectrum in the low-period range of response. Where near-field conditions are not expected, the common assumption of vertical response ordinates equal to ⅔ of the horizontal ordinates should be conservative.

On the other hand, recorded accelerograms indicate that the vertical response spectrum tends to decrease rapidly as period increases. Because of this, it is suggested that the displacement spectrum for vertical response should reach a plateau at 1.5 seconds, rather than 3.0 seconds, as is the case for horizontal response. This is still considered to be a conservative approximation.

The vertical acceleration response spectra presented in NZS 1170.5[4] has been revised by amendment 1 promulgated in September 2016. In most cases vertical response spectra, where required, will be utilized to determine elastic forces in superstructures or pier cap beams. In these cases it will generally be more convenient to express the vertical spectrum in acceleration, rather than displacement format.

C5.5.3 Reduced design displacement spectrum for ductile response (5.4.2, 5.4.3)

In DDBD the effects of ductility are expressed by equivalent viscous damping which modifies the elastic 5% spectra. This approach is more accurate than the "equal displacement" approximation used for periods greater than about 1 second in force-based design, which does not recognize the influence of different hysteretic rules on ductile displacement demand. It also allows the effect of abutment damping and foundation rotation to be directly incorporated in the design process. Equation (5–17) is taken from a superseded version of Eurocode 8[7]; the relationships between ductility and equivalent viscous damping in 5.4.3 have been calibrated to be compatible with equation (5–17). Note that a revised expression for the influence of damping on the elastic spectra is provided in the current version of Eurocode 8[7]; this should not be used, as it would require recalibration of the damping/ductility relationships of 5.4.3.

The reduced efficiency of ductility and damping in reducing displacement response in near-field forward-directivity effects is expressed by a different value for the power parameter (α) applied in equation (5–17). Though this near-field expression is believed to be conservative, (see *Scaling of spectral displacement ordinates with damping ratios*[8]) it should be considered tentative until further data is available.

C5.6 Seismic mass distribution (5.3.8)

The section is self-explanatory. With very tall piers higher mode effects may become significant, and further discretization of mass up the pier height may be advisable. Note, however, that this will primarily be needed to determine the influence of higher modes on pier response, and will not influence the basic displacement-based design determination of total base shear force. Further information on mass distribution for analysis and design is available in *Displacement-based seismic design of structures*[1].

C5.7 Pier elastic flexibility

C5.7.1 Pier yield curvature (5.3.4)

The elastic stiffness is dependent on strength, as influenced by reinforcement content and axial load, in the case of reinforced concrete, and by plate thickness in the case of structural steel, and hence is not known at the start of the design process. The yield curvature (ϕ_y) depends only weakly on the section shape (circular or rectangular, or even architectural, within limits). It is also not strongly dependent on the material of the pier, reinforced concrete or structural steel. The value given in equation (5–8) is an average of all section shapes and materials, and is accurate to within 15% in all cases. This is accurate enough for most designs. More accurate values are provided in chapter 4 of *Displacement-based seismic design of structures*[1]. Note that the yield curvature is effectively independent of strength, and is thus known at the start of the design process, if section sizes have been determined. The yield curvature is used in DDBD to determine the structural ductility demand corresponding to the DCLS displacement profile, and is a fundamental parameter in DDBD.

Once the required structural strength of a section has been determined, the effective elastic stiffness can be found from equation (5–9).

C5.7.2 Yield displacement of piers (5.3.4)

With the section yield curvature known, the pier yield displacements can be determined at the start of the design process, before strength has been determined. As well as being needed for DDBD, the yield displacements can be used to determine whether the piers can be expected to respond elastically to the DCLS seismic intensity.

As indicated in equation (5–10), the yield displacement of the pier depends on the structural displacement of the pier plus any lateral displacement of the foundation. To obtain the lateral displacement of the superstructure at the pier position this will be further modified by the deflection of any bearings. The structural displacement, in turn, depends on the condition of fixity at the top and bottom of the pier. Some common examples for longitudinal response are illustrated in figure C5.2.

For complex section shapes 5.3.4 may be too coarse, and more detailed analyses may be required. In such cases, cracking and non-linearity of materials should be modelled. First yield displacement should be determined at steel yield strain or concrete compression strain of 0.002, whichever occurs first, with the equivalent bi-linear yield deformation calculated by linear extrapolation of the first-yield deformation to the nominal moment capacity at the critical section. Refer to *Displacement-based seismic design of structures*[1] for details.

Different values of the flexibility coefficient (C_1) will apply for each case. For example, in figure C5.2(a) the superstructure is bearing-supported, and the footing is considered rigid against rotation and translation. The effective height is measured to the centre of the bearing and includes an allowance for strain-penetration into the base. For this case the coefficient is C_1=⅓. For the case in figure C5.2(b), representing longitudinal response of a pier monolithically connected to a stiff superstructure the coefficient C_1=⅙. Note that the same pier in the transverse direction would have an effective height of $H + h_{ss}/2$ and the coefficient would be C_1=⅓. Further details, including appropriate values for C_1 for pile columns (figure C5.2(e)) are provided in *Displacement-based seismic design of structures*[1].

Bearing and soil flexibility will increase the yield displacement, and a preliminary, conservative check may be made ignoring these.

Figure C5.2: Some possible fixity conditions for pier longitudinal response (*Displacement-based seismic design of structures*[1])

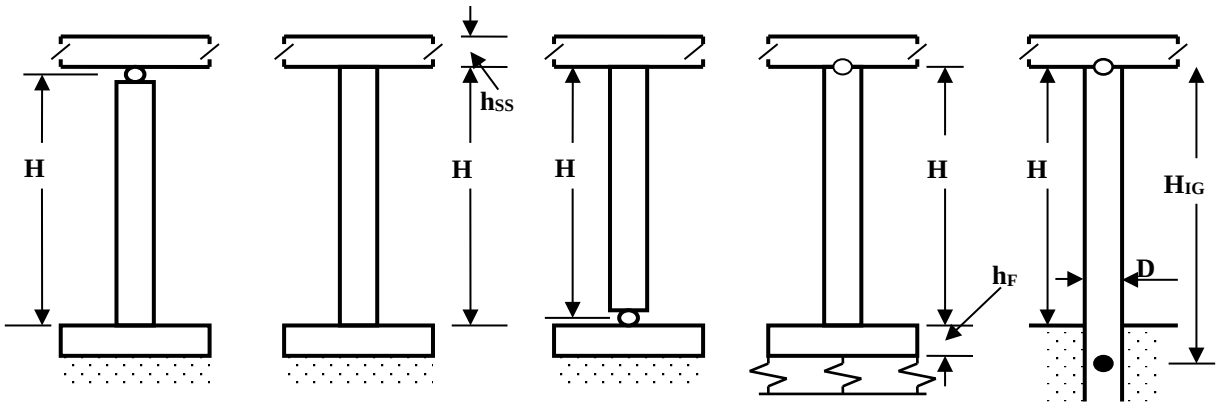

(a) Rigid base, pinned top (b) Rigid base, fixed top (c) Pinned base, fixed top (d) Flexible base (e) Pile/column

C5.7.2 continued

Equation (5–10) includes an allowance for strain penetration. This recognizes that for reinforced concrete piers, the reinforcement strain does not immediately drop to zero at the support (eg the foundation pad), but is gradually reduced due to bond. Adding a length L_{sp} based on experimental measurements, to the effective height of the pier is a simple method for allowing for this. Note that for the longitudinal response case of figure C5.2(b) a strain penetration length would need to be added to both top and bottom of the column.

Note that the structural component of yield displacement depends only on the pier geometry, the yield strain, and the end fixity conditions, and is independent of the strength. For example, increasing the flexural strength of a reinforced concrete section increases its stiffness proportionately, and the yield curvature remains unchanged. The same happens for a structural steel section where the strength is altered by, for example, increasing the flange thickness.

The structural component of yield displacement corresponding to cases (a) and (b) in figure C5.2 are plotted in figures C5.3(a) and C5.3(b) respectively for a yield stress of 500MPa, for a variety of pier diameters (circular columns) or depths (rectangular columns) and heights. Total yield displacement will often exceed the structural component of displacement, due to deformation of the soil, or of the bearings.

For example, consider the pier on a spread footing in figure C5.2(d). If the length of the spread footing in the direction of the seismic shear force is L and the width B, and the soil vertical subgrade coefficient is k_v, then the additional yield displacement at the bearing due to foundation rotation will be:

$$\Delta_f = \frac{(M_N + V_N h_f)(H + h_f)}{\left(k_v\left(\frac{L^3 B}{12}\right)\right)} \qquad \text{(C5-1)}$$

Where:

M_N = the design moment at the base of the column

V_N = the design shear at the base of the column

h_f = the foundation slab thickness defined in figure C5.2(d)

Figure C5.3(a): Yield displacements for prismatic piers of reinforced concrete or structural steel F_y=500MPa (bearing and foundation flexibility ignored) – cantilever pier (single bending)

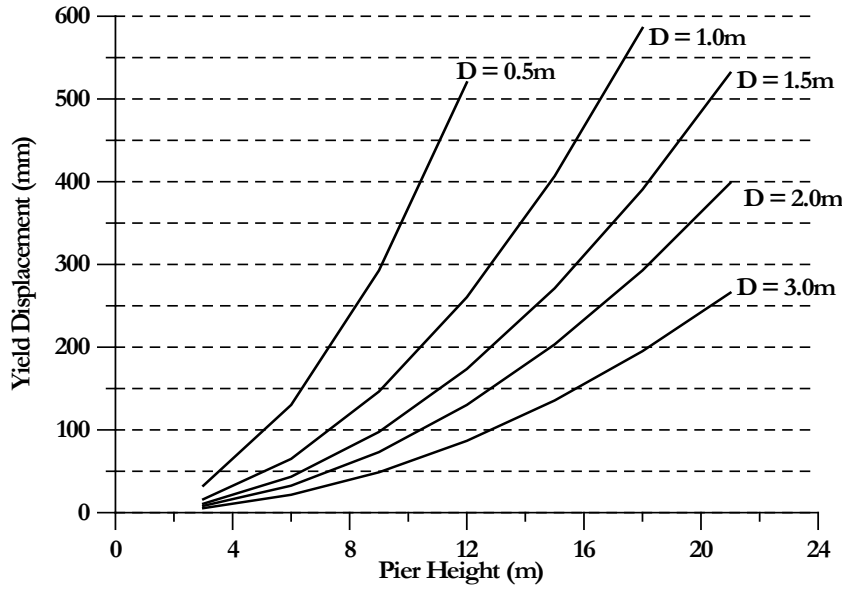

Figure C5.3(b): Yield displacements for prismatic piers of reinforced concrete or structural steel F_y=500MPa (bearing and foundation flexibility ignored) – pier in double bending

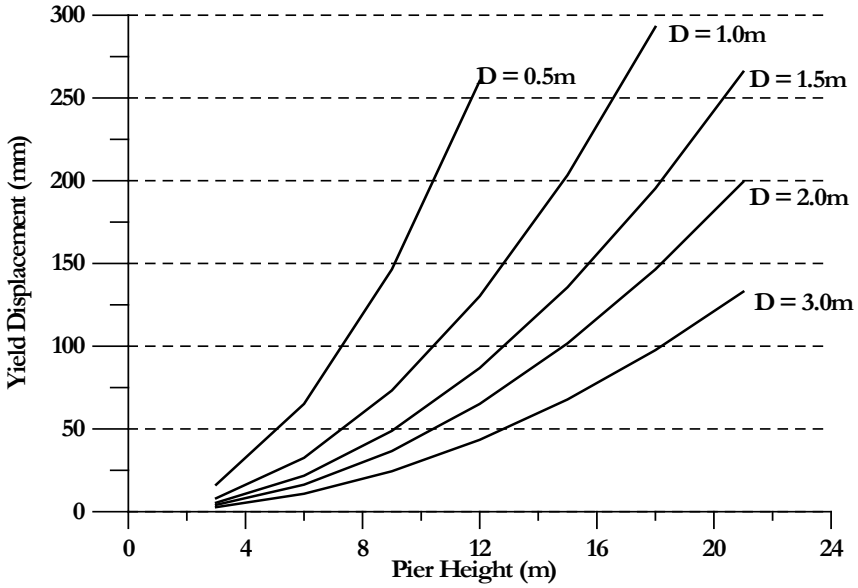

C5.8 Seismic analysis for design strength of plastic hinges

C5.8.1 General (5.4.1)

This section defines the basic DDBD design process. With long bridges it is very unlikely that the ground motion at different piers or abutments, separated by a distance that is significant by comparison with the seismic wave length, will be synchronous (perfectly in phase) and coherent (of same amplitude). Variations in soil properties along the bridge also affect this. Consequently there is little point in designing as though the seismic input at all points of a bridge is perfectly in phase and of equal amplitude. Further information on this phenomenon is available in *Seismic design and retrofit of bridges*[9]. As a consequence, it is suggested that long bridges be conceptually separated into segments (frames) delineated by movement joints.

The procedure for displacement-based seismic design of bridges has been outlined in some detail elsewhere (*Displacement-based seismic design of structures*[1]) and is only briefly described here. There are four stages in the process:

1. representation of the bridge as an equivalent single degree of freedom (SDOF) structure (figure C5.4(a))
2. representation of the seismic response by the effective stiffness at the design response displacement (figure C5.4(b))
3. determination of the relationship between displacement ductility demand and equivalent viscous damping (figure C5.4(c))
4. representation of seismicity by displacement spectra for different levels of equivalent viscous damping (figure C5.4(d)).

The design procedure is typically represented by the following sequence:

a. Determine the critical displacement capacities of the piers from code-specified strain or drift limits (5.4.5).

b. Estimate the inelastic mode shape (see C5.9.1 and figure C5.6) and hence determine the critical pier.

C5.8.1 continued

c. Scale the inelastic mode shape (equation (5–34)) so that the critical pier just reaches its limit state.

d. Determine the characteristic equivalent SDOF displacement (equation (5–20)) and mass (equation (5–21)) for the frame.

e. Determine the equivalent viscous damping (equation (5–23)) for the frame from the damping of the bridge components (5.4.3(f)).

f. Enter the displacement spectra set (eg figure C5.4(d)) with the characteristic displacement and equivalent viscous damping, and determine the effective period at peak displacement response.

g. From the calculated period, determine the equivalent effective stiffness (equation (5–21)).

h. From the effective stiffness and the characteristic displacement, determine the frame design lateral earthquake force (total base shear) (equation (5–19)).

i. Distribute the design force to the mass locations in proportion to mass and displacement (equation (5–39)).

j. Analyse the frame, using effective stiffness values for the piers, to determine moments in plastic hinges (5.4.7).

k. Use capacity design principles to determine required shear strength etc (5.6.1).

For a frame under longitudinal seismic response the critical pier will normally be the shortest one, if the different piers have different heights. The design displacements will be the same for all columns. The procedure to estimate design displacement of the critical pier is outlined in 5.4.5. Yield displacements for all piers will differ, if the heights are different, and will be given by equation (5–10) with the displacement of any bearings also added. Hence the ductility demand, and the damping will be different for the different piers. For piers with negligible foundation or bearing deformation the ductility demand of each pier (i), can thus be found as:

$$\mu_i = \frac{\Delta_d}{\Delta_{yi}} \qquad \text{(C5-2)}$$

Where foundation and/or bearing flexibility are significant, and the damping associated with the foundation or bearing deformation is conservatively assumed to be 5%, then equation (C5-2) will still apply, where the ductility is related to the total design and yield displacement of the pier plus bearing/foundation. However, if different values of damping are assigned to foundation or bearing flexibility, and deformation associated with these is significant (say more than 20% of total deformation), then the structural ductility (μ_{si}) should be separately determined from equation (C5-3):

$$\mu_{si} = \frac{\left(\Delta_d - \Delta_{yf} - \Delta_b\right)}{\left(C_1 \phi_{yi}\left(H + L_{sp}\right)^2\right)} \qquad \text{(C5-3)}$$

The effective damping for the pier will then include contributions from structural deformation of the pier, and from foundation and bearing compliance, where appropriate, in accordance with equation (5–23). Since the shear force transmitted through the bearings into the pier and subsequently to the foundation is essentially constant (ignoring small variations due to pier mass), equation (5–23) simplifies, for a given pier, to:

$$\xi_e = \frac{\left(\Delta_s \xi_s + \Delta_b \xi_b + \Delta_f \xi_f\right)}{\Delta_d} \qquad \text{(C5-4)}$$

where the suffixes s, b and f refer to structure, bearing and foundation respectively, and the displacement components are measured at the height of the pier centre of mass (see 5.3.8).

C5.8 continued

Note that under transverse response, the design displacement at each pier will generally be different, depending on the transverse mode shape (see C5.9). The approach may require some iteration when the seismic inertia forces are carried by two or more different load paths (eg superstructure flexure to abutments, and pier inelastic bending to foundations under transverse seismic response). An initial estimate of the proportion of the total seismic inertia forces carried by superstructure flexure is made, enabling the system damping to be found in accordance with equation (5–23). This is checked by structural analysis after the design base shear is determined, and the seismic forces are distributed to the different mass locations in accordance with equation (5–39). Guidance is given in *Displacement-based seismic design of structures*[1].

The sequence of code clauses in 5.4 does not follow the above sequence, but defines the basic equation for required strength, then explains how to determine the components of the basic equation.

Figure C5.4: Fundamentals of DDBD of bridges

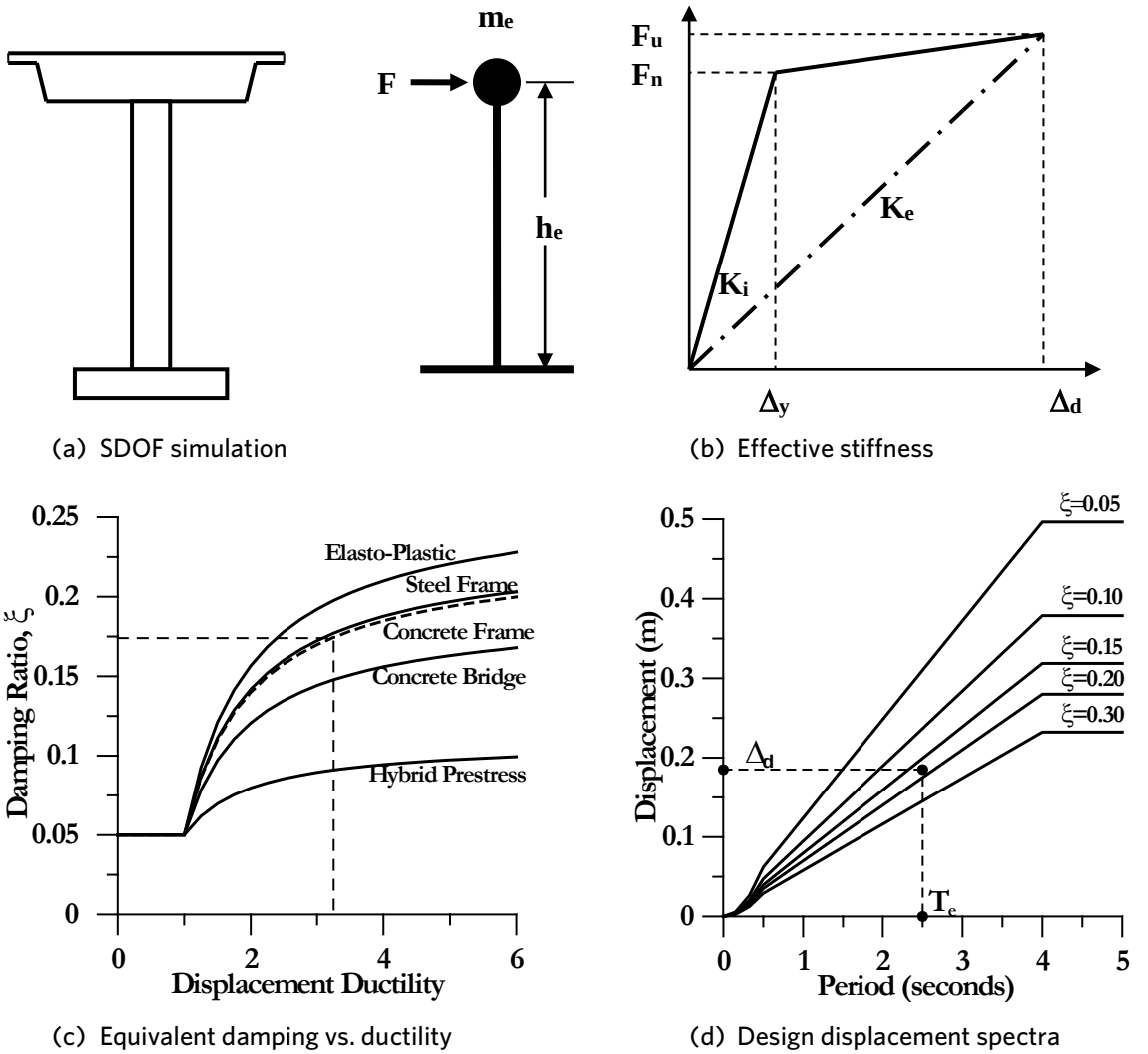

(a) SDOF simulation

(b) Effective stiffness

(c) Equivalent damping vs. ductility

(d) Design displacement spectra

C5.8.2 Design lateral earthquake force (5.4.3(a))

Equation (5–19) expresses the relationship shown in figure C5.4(b), that the design force is the product of the design displacement and the effective stiffness.

C5.8.3 Frame characteristic design displacement (5.4.3(b))

Equation (5–20) defines the characteristic (equivalent single degree of freedom (SDOF)) displacement of the multi degrees of freedom frame. This is based on the displacement mode shape and the critical displacement of a pier, as defined in 5.4.3 and 5.4.4. For longitudinal response, the mode shape is normally unity (ie all piers have the same displacement), and the displacement capacity of the critical (shortest) pier corresponding to the damage control limit state strains (see 5.3.5) defines the scaling of the displacement mode shape to obtain the design displacement.

C5.8.4 Frame effective stiffness (5.4.3(c))

The effective stiffness of the SDOF model of the frame, needed in equation (5–19) is found from the effective period, and is defined in equation (5–21). Note that this equation is a simple inversion of the standard equation for the period of a SDOF structure.

C5.8.5 Frame effective mass (5.4.3(d))

Equation (5–21) requires the equivalent mass participating in the fundamental inelastic mode. This mass is defined in equation (5–22). Under longitudinal response the frame effective mass will normally be the total seismic mass of the frame, as defined in 5.3.8. Under transverse response with significant flexibility the frame mass will still be close to the total mass – often as high as 95%.

Note that a common, uninformed, criticism of DDBD is that it only considers the fundamental mode whereas modal analysis considers sufficient modes to capture 90% of the total structural mass.

Dividing the bridge into frames separated by movement joints, for reasons discussed in C5.8.1, means that fewer modes are needed to capture sufficient mass, and modes with strong anti-symmetric deformation components participate only to an insignificant degree. It should be noted that the higher modes in a single frame do not contribute significantly to the displacements at the pier tops, and hence are not significant in determining pier design forces. Forces in components of bridges that are sensitive to higher mode effects, such as bridge transverse superstructure moments, and, particularly, abutment forces, are determined by capacity design considerations (see 5.6.1).

C5.8.6 Frame effective period (5.4.3(e))

The effective period, corresponding to design displacement response is found from the elastic design spectrum for horizontal earthquake response (5.2.4), with modifications for different damping values in accordance with equation (5–17), and as represented conceptually in figure C5.4(d) (displacement spectra set) entering with the design displacement, and using the displacement spectrum corresponding to the calculated equivalent viscous damping. Normally this is done analytically, rather than graphically.

Note that the inelastic fundamental period of almost all bridges supported by ductile piers will be greater than 1.0 sec. Examination of figure 5.2 indicates that it is conservative, and only slightly in error to assume that the displacement/period relationships for all four soil conditions are linear from T=0 to T=3.0 sec. If this approximation is made, the effective period (T_e) is given by:

$$T_e = 3.0\frac{\Delta_d}{M_\xi \Delta_h(3.0)} \qquad \text{(C5-5)}$$

where M_ξ is given by equation (5–17).

C5.8.7 Frame equivalent viscous damping (5.4.3(f))

The area of greatest complexity in displacement-based design of bridges is associated with determining the equivalent viscous damping. Consider the typical bridge shown in figure C5.5 under transverse seismic response. The ends of the bridge are restrained by shear keys, but there is some flexibility of the abutments, meaning that the abutment reactions will dissipate some energy by damping. The piers have different heights, different response displacements, and different yield displacements, so the damping of each pier will be different. Foundation flexibility and bearing displacement may influence the pier damping as discussed in C5.8.1. Finally, the superstructure carries some of the inertia forces back to the abutments, and some elastic damping of the superstructure needs to be considered.

Equation (5–23) defines the structure equivalent viscous damping as a composite of the damping values for each of the structural components (piers, abutments, and superstructure). It is necessary to know the shear force carried by each component, their displacement, and their equivalent viscous damping.

First consider a single pier with flexible foundations, flexible bearings and structural ductility. Deflections at the pier top at design displacement response are Δ_f, Δ_b and Δ_s from the three components respectively, and damping values for the three components are ξ_f, ξ_b and ξ_s respectively, found from the data provided in 5.4.3(g). The shear force corresponding to the three deformations are essentially the same, and hence the effective damping for the pier is given by equation (C5-6):

$$\xi_p = \frac{\left(\Delta_b\xi_b + \Delta_f\xi_f + \Delta_s\xi_s\right)}{\left(\Delta_b + \Delta_f + \Delta_s\right)} \qquad \text{(C5-6)}$$

To determine the global (system) damping, the displacement, damping ratio, and proportion of total design force carried by each pier must be estimated, and the proportion of total design force carried back to the abutments by superstructure flexure, and abutment deformation and damping must be determined.

The procedure is outlined in detail in *Displacement-based seismic design of structures*[1] with reference to design examples. Further details are presented in C5.8.8. Note that the structural damping of a pier may include components of displacement and damping associated with pier, bearing and foundation deformation, in accordance with equation (5–23).

Figure C5.5: Components contributing to damping under transverse response (*Displacement-based seismic design of structures*[1])

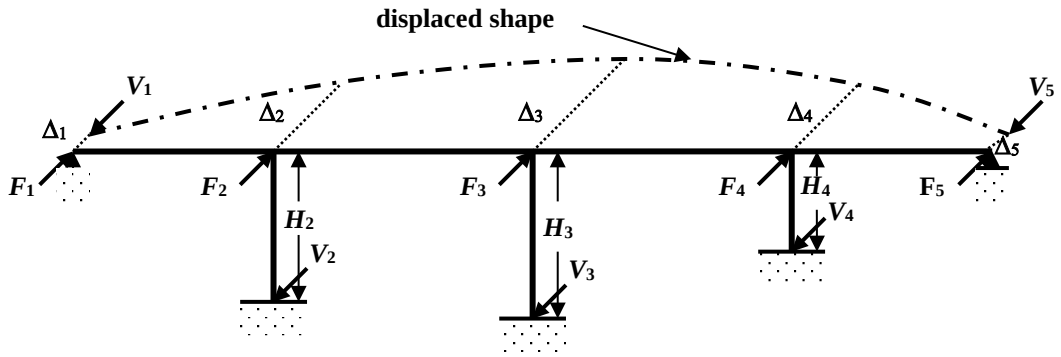

C5.8.8 Equivalent viscous damping of component actions (5.4.3(g))

Pier structural damping is defined in terms of displacement ductility demand at the design displacement. Note that the ductility demand will be known at the start of the design process, since the design displacement will be defined (5.4.4), and the yield displacement is also known and is independent of design strength (5.3.4).

C5.8.8 continued

Pile/column designs (figure C5.2(e)) are a special case, as the displacement and damping resulting from foundation and structural deformation are difficult to separate. The values in 5.4.3(g) are simplified from detailed analytical work given in *Direct displacement-based seismic design of drilled shaft bents with soil-structure interaction*[10].

This clause also defines the damping associated with foundation rotation, with superstructure flexure, and with abutment displacement. For the latter, a conservatively low estimate of 0.12 (12%) is assumed. The actual value will depend on the shear strain of soil in the abutment region, and can be difficult to compute without expert geotechnical advice.

Note that systems identification analyses related to actual seismic response of two bridges with integral superstructure/abutment designs (Melloland, and Painter Ave) in Californian earthquakes have resulted in damping values of at least 25% (see *Displacement based seismic assessment of existing bridges in regions of moderate seismicity*[11]).

The equations for damping associated with rotation of spread footings on soil (equations (5–26) and (5–27)) are simplified from work by Paolucci et al (*Interazione dinamica non-lineare terreno-struttura nell'ambito della progettazione sismica agli spostamenti*[12]). A more detailed analysis of the variation of foundation rotational stiffness and damping as a function of foundation rotational angle and bearing capacity, based on the work of Paolucci et al[12] is available in *A model code for the displacement-based seismic design of structures*[13]. The damping associated with bearing flexibility will depend on the type of bearing adopted and the bearing displacement. Manufacturers' data, or local test results should be used where available.

With designs where the piers are deliberately designed to rock on structural foundations (as distinct from the structural foundation rocking on the soil), the equivalent viscous damping should be taken as ξ_{eq}=0.05, unless special damping elements are provided between the pier and structural foundation. In the latter case, damping should be based on the type of special damping element provided.

C5.9 Design displacements

C5.9.1 Design displacement profile (5.4.4)

The design displacement profile requires knowledge of both the deflected shape and the magnitude of displacements. For longitudinal response, this is straightforward as displacements of all piers will be effectively identical, and thus the design displacement will be equal to the displacement capacity of the critical (normally the shortest) pier, given in 5.4.5, measured at the deck level.

For transverse response, since the displaced shape, and in particular the magnitude of the displacements will not be known with any accuracy at the start of the design process, it is suggested that a displacement modal shape, of arbitrary magnitude, be adopted. Note that the designer will generally have a good idea of the shape. For example, lateral displacement of a bridge constrained transversely by shear keys at abutments, with internal flexible piers can be approximated with adequate accuracy by a sine or parabolic shape. The displacement capacities of the various piers are then calculated, based on the strain limits, and the displacement shape is scaled until the first pier reaches its displacement capacity. This is expressed by equation (5–34).

The critical structural element will normally be a pier. However, it may be bearing or an energy dissipating device. The critical displacement will be calculated at a mass location, and will include all contributing elastic and inelastic displacement components.

C5.9.1 continued

Chapter 10 of *Displacement-based seismic design of structures*[1] gives advice on displacement shapes for bridges. Examples of possible transverse displacement shapes are presented in figure C5.6 for bridges with both stiff and flexible superstructures.

This is used as the basis of displacement-based design. An inelastic mode shape is assumed (see figure C5.6, for examples), and then scaled in accordance with equation (5–34) so that the critical pier or abutment just reaches its limit-state displacement, defined in 5.4.5. These limit-state displacements are calculated from the permissible strains for the damage control limit state, defined in 5.3.5.

Figure C5.6: Different possible transverse displacement profiles for bridges (*Displacement-based seismic design of structures*[1])

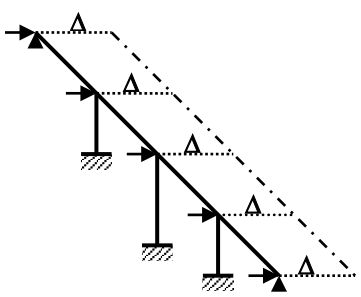

(a) Symmetrical, free at abutments, rigid superstructure translation

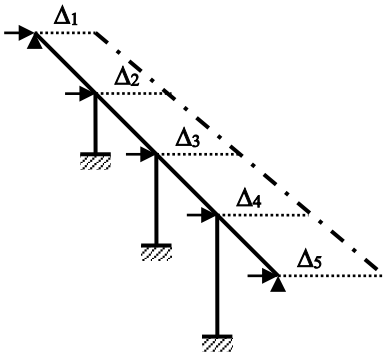

(b) Asymmetrical, free at abutments, rigid superstructure translation and rotation

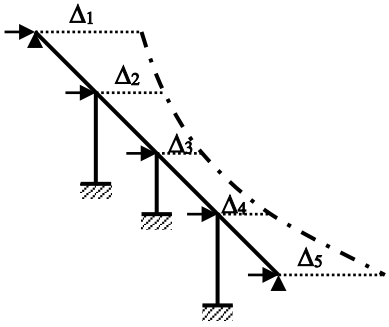

(c) Symmetrical, free at abutments, flexible superstructure

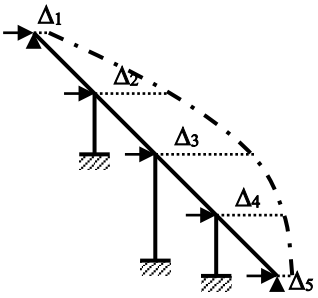

(d) Symmetrical, restrained at abutments, flexible superstructure

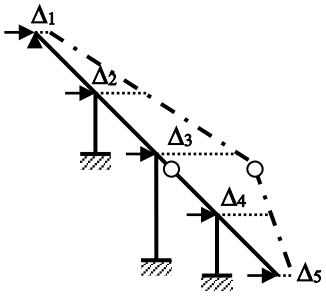

(e) Internal movement joint, rigid superstructure, restrained at abutments

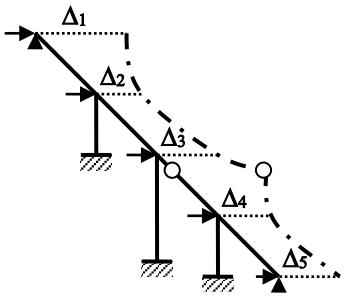

(f) Internal movement joint, free at abutments, flexible superstructure

C5.9.2 Strain limits for ultimate limit state (5.3.5)

The strain in reinforcing steel in potential plastic hinges is related to anti-buckling requirements, and low-cycle fatigue. In conjunction with transverse reinforcement spacing requirements of 5.6.4 equation (5–11) is expected to provide adequate resistance against buckling or fracture. The strain limits at maximum strength specified in equation (5–11) are conservative values based on code requirements for reinforcing steel. The conservatism is higher for 300E steel, since the ultimate strain is higher than for 500E, and the effective post-yield modulus will reduce, increasing the probability of buckling.

Minimum volumetric confinement steel ratios of 0.005 and 0.006 are defined in 5.6.4 for circular and rectangular sections respectively. These lower limits apply when columns are designed for elastic response. Using these equations, displacement-based design would allow some limited ductility corresponding to this minimum confinement ratio, since the permitted steel strain from equation (5–11) would be 0.015.

C5.9.2 continued

Equation (5–12) defines the permitted concrete compression strain as a function of transverse reinforcement ratio and confinement steel properties. This is a well-established and conservative expression (*Seismic design and retrofit of bridges*[9] and *Displacement-based seismic design of structures*[1]).

Note that in the design situation, a required ultimate compression strain, corresponding to a required displacement may be calculated, and the required confining steel ratio can be determined from inverting equation (5–12). Note further that the confinement steel ratio of 0.005 suggested for elastic response of circular columns (see previous paragraph) would typically result in a permissible concrete compression strain of about 0.01. This would imply considerable ductility, which could be taken advantage of in displacement-based design, or used as protection against seismic demand exceeding the design level.

For circular columns, the volumetric ratio of confinement is given by:

$$\rho_s = \frac{4A_b}{D's} \qquad \text{(C5-7)}$$

Where:

A_b = the area of the hoop or spiral confinement with pitch circle diameter of D' measured to the centre of the spiral, which has a spacing or pitch of s along the column axis

For rectangular column sections, the volumetric ratio of confinement is the sum of the area ratios of confinement in the two orthogonal section directions:

$$\rho_s = \rho_{ax} + \rho_{ay} = \frac{\sum A_{bx}}{d'_y s} + \frac{\sum A_{by}}{d'_x s} \qquad \text{(C5-8)}$$

Where:

$\sum A_{bx}$ and $\sum A_{by}$ = the total areas of transverse reinforcement in the x and y directions of the section within a spacing of s along the column axis

d'_x and d'_y = the confined core dimensions of the section in the x and y directions, measured to the centreline of the peripheral hoop

For hollow piers, a maximum compression strain of 0.005 is specified, since experimental research indicates that spalling of external cover can rapidly shift the neutral axis, increasing the compression strain on the inside surface, and causing spalling of the inside cover. This can result in a rapid compression failure (see *Displacement-based seismic design of structures*[1], chapter 10). The value of 0.005 should still provide adequate reserve of performance for the collapse limit state (see *Flexural strength and ductility of circular hollow reinforced concrete columns without confinement on inside face*[14]).

C5.9.3 Displacement capacity of piers (5.4.5)

The displacement capacity of a pier at the damage control limit state is the sum of the yield displacement (Δ_y) given by equation (5–10), and the plastic displacement (Δ_p) given by equation (5–36). Since for reinforced concrete piers the plastic displacement depends on the plastic curvature, which in turn depends on the ultimate (damage control) limit strains, variations in the limit strains by varying the volumetric ratio of lateral reinforcement can be used to increase or decrease the plastic displacement.

Note that for reinforced concrete sections the limit state reinforcement tension and concrete compressive strains will not occur simultaneously. Curvatures corresponding to each limit should be calculated, and the lower one adopted for design. Thus if c is the distance from the extreme compression fibre of the concrete to the neutral axis and d is the distance from the extreme compression fibre to the reinforcing bar furthest from the neutral axis, then the limit state curvatures corresponding to the concrete and reinforcement limit strains are, respectively,

C5.9.3 continued

concrete: $\phi_{cd} = \frac{\varepsilon_{cd}}{c}$ (C5-9)

reinforcement: $\phi_{sd} = \frac{\varepsilon_{sd}}{(d-c)}$ (C5-10)

The lower of ϕ_{cd} and ϕ_{sd} is chosen as the design limit state curvature (ϕ_{ls}) for the section.

In equation (5–37) the plastic hinge length for reinforced concrete piers is expressed as the sum of the strain penetration length, and a section of column length proportional to the distance to the column point of contraflexure. The constant of proportionality depends on the shape of the post-elastic stress-strain curve for the flexural reinforcement, expressed by the ratio of ultimate to yield strength of the reinforcement. If this ratio is large, plasticity spreads to a greater extent up the column than if it is small.

Note that the plastic hinge length is a mathematical convenience based on constant plastic curvature, and provides the correct plastic rotation as that expected from the pier, where plastic curvature will decrease with distance from the critical section, and will be distributed over a greater length than L_p. For this reason, the plastic end region, over which special transverse confinement is needed, given in 5.6.4(e) is greater than L_p. With knowledge of the plastic rotation capacity of critical section, the structural plastic displacement can be readily found, and added to the yield displacement. If foundation and bearing flexibility are an issue, the corresponding displacements would need to be added. For a simple cantilever column with height L_c to the point of contraflexure (or centre of bearing), the design displacement will thus be:

$$\Delta_d = \Delta_y + \theta_p L_C + \Delta_{yf} + \Delta_b \quad \text{(C5-11)}$$

Where:

Δ_{yf} = lateral displacement at superstructure resulting from foundation deformation

Δ_b = lateral displacement of pier-cap bearing

Δ_y = structural component of yield displacement

$= C_1 \phi_y (H + L_{sp})^2$ (see 5.3.4) (C5-12)

For structural steel piers, the strain penetration length should be taken as zero.

C5.10 Distribution of design lateral force (5.4.6)

The displacement-based design process directly yields the total base shear force (sum of shears at the base of all piers plus abutment base shears) for the frame under consideration. This base shear force is distributed to the mass locations chosen during the seismic mass distribution (5.3.8) in accordance with equation (5–39).

C5.11 Seismic design moments in potential plastic hinges (5.4.7)

This section requires that structural analysis under the design lateral forces should not be based on elastic stiffness, but on the effective secant stiffness to maximum design displacement. Thus ductile members will have their elastic stiffness reduced approximately by their displacement ductility factor. This enables the moment demands at the potential plastic hinges to be determined by a structural analysis that is compatible with the principles of displacement-based design summarized in figure C5.4.

C5.11 continued

Note that this procedure requires the effective stiffness of the piers to be known, which implies that both displacement, and flexural strength of the piers are known before the analysis proceeds. In practice the actual strengths will not be known at this stage, but if rational decisions are made about the relative pier strengths, the analysis is greatly simplified. The normal assumption will be to use uniform flexural strength in all piers, resulting from, eg constant section size and equal reinforcement ratios in all piers.

Note also that this analysis also provides a check on displacements. The displacement profile from the analysis should correspond to the initial design assumption. In the case of a bridge with two load paths (eg transverse seismic response with superstructure elastic flexure and inelastic column flexure, as illustrated in figure C5.5), the proportion of the total lateral inertia force carried by superstructure flexure and column bending will need to be assumed at the start of the design, in order to determine the equivalent viscous damping. If the displacements from the analysis differ from the assumed displacement profile, adjustments will need to be made, by a simple iterative process to this proportion. The procedure is outlined in detail in *Displacement-based seismic design of structures*(1).

Note further that analyses reported in *Displacement-based seismic design of structures*(1) show that if the structure represented by figure C5.5 has columns with identical stiffness in both longitudinal and transverse directions (eg circular cantilever columns with bearings-supported superstructure), then longitudinal design, which is much simpler, will always govern.

C5.12 Vertical seismic response (5.3.3)

Since no ductility is permitted for vertical response of superstructures, conventional analysis using modal superposition, or time-history analysis may be used to determine design seismic moments induced in superstructures or cap-beams. In simply supported spans, equivalent lateral force procedures will be adequate. Although ductility is not permitted, some moment redistribution (up to 30%) may be adopted to reduce peak superstructure moments resulting from the combination of seismic and gravity actions.

The reduced damping associated with vertical response of structural steel or prestressed superstructures implies increased seismic response. The vertical design spectrum defined in 5.2.4(c) should thus be increased by use of equation (5–17) where ξ is taken as 0.02 or 0.03 for structural steel or prestressed concrete respectively. The value for α in equation (5–17) should be taken as 0.5 in all cases.

C5.13 Required moment capacity

C5.13.1 At potential plastic hinge locations (5.6.2(a), 5.6.2(b)(i))

This is a significant deviation from current seismic design practice in New Zealand. For force-based design for (say) gravity loads, the use of flexural strength reduction factors is essential to provide protection for the unlikely case that material strengths are less than specified, for errors in dimensions and placement of reinforcing steel, and for errors in analytical procedures. Uncertainty in load values is accounted for mainly by load factors associated with, eg dead and live load values. The consequence of strength being less than applied load is certain failure.

C5.13.1 continued

In seismic response these arguments do not apply. The flexural strength of the bridge is expected to be reached under design excitation when design permits ductility. Hence load factors are currently not applied to seismic forces since the requirement that moment capacity must exceed moment demand is meaningless. The same argument applies to flexural strength reduction factors. There is no point in using a conservative estimate of moment capacity, since the actual capacity will be achieved in design-level response. All that will be achieved by use of flexural strength reduction factors is a (possible, though not certain) reduction in ductility demand below the adopted design level. Protection against failure is increased only marginally, if at all.

As a consequence Priestley et al (in *Seismic design and retrofit of bridges*[9] and *Displacement-based seismic design of structures*[1]) have argued that flexural strength reduction factors should not be used for estimating flexural strength of potential plastic hinge regions. This approach has also been adopted by the Applied Technology Council (see *Improved seismic design criteria for California bridges: Provisional recommendations: ATC32*[15]) and has been standard practice for the California Department of Transportation (Caltrans) for almost 20 years.

Using conservative estimates of expected material strengths, rather than lower 5% characteristic strengths, and eliminating flexural strength reduction factors for design, results in obvious design efficiencies. It has a secondary economic advantage when capacity design (5.6.1) is considered. Note that *Seismic design and retrofit of bridges*[9], *Displacement-based seismic design of structures*[1] and ATC32[15], also permit the consideration of strain-hardening of flexural reinforcement and enhanced compression strength of concrete from confinement by transverse reinforcement to be considered when estimating flexural strength in potential plastic hinges. This is particularly relevant for displacement based design, since the required strength relates to the design displacement, rather than the "yield" displacement as in force-based design.

Values for expected strengths will depend on local data for steel and concrete strengths. In the absence of local data, the values listed in table 5.7 may be used.

Generally, moments induced in potential plastic hinge regions by gravity, creep and shrinkage, and temperature are small compared with seismic moments. Since non-seismic moments are typically based on elastic analyses of the bridge frame, often without consideration of column cracking, it is inappropriate to directly add them to seismic moments, which are adjusted for pier ductility, either by use of a ductility factor (force-based design) or by analysis using reduced member stiffness (displacement based design). A more appropriate method for determining the level of gravity moment to be added to the seismic moment is to reduce the gravity moments by the pier ductility factor, or to carry out the non-seismic-load analysis using the same reduced pier stiffness used for seismic moment determination. These more rational approaches result in greatly reduced non-seismic moments in potential plastic hinges.

A detailed discussion of this issue is provided in *Displacement-based seismic design of structures*[1]. Since the level of gravity moment to be added to seismic moment becomes very small, with the approach outlined above, it is recommended that the design moment in potential plastic hinges be the greater of (a) the factored non-seismic-moments without consideration of seismic effects, and (b) the pure seismic moment, determined from the DDBD procedure, without consideration of non-seismic moments. This may imply some limited moment redistribution between potential plastic hinges, but this level will always be acceptable.

Note that if factored non-seismic moments govern, then conventional strength reduction factors should apply.

C5.13.2 At other locations (5.6.2(a), 5.6.2(b)(ii))

In regions where plastic hinges must not develop, the dependable moment capacity, determined using conventional estimates of material strengths, and strength reduction factors as used for gravity-load design, should exceed the moment demand corresponding to formation of over-strength capacity in plastic hinge locations. This is illustrated in more detail in C5.16. In these cases, gravity and seismic moments are directly added, though again the gravity moments should take into account the reduced stiffness of potential plastic hinges.

C5.14 P-delta effects (5.3.7)

The provisions here are taken from *Displacement-based seismic design of structures*[1] and result from extensive non-linear time-history analyses of reinforced concrete and steel structures.

C5.15 Design abutment forces (5.4.8)

The DDBD analysis procedure is a single mode approach, using design lateral forces that recognize the reductions of member forces resulting from pier ductility. Although this is suitable for determining the design moments in plastic hinges, it is non-conservative when abutment reactions are considered, since the analysis approach implies that these will also be reduced as a consequence of pier ductility. In fact, higher mode effects, which have only minor significance to plastic hinge moments, can significantly increase the abutment reactions above the value predicted from the lateral analysis using ductility-reduced lateral forces. This is the reason that failures of abutments and shear keys are the most common form of damage to bridges in earthquakes.

Elastic modal superposition analysis can significantly underestimate abutment forces when ductile response is expected and elastic forces are reduced by a ductility factor. It has been found (see *Displacement-based design of continuous concrete bridges under transverse seismic excitation*[16] and *Displacement-based seismic design of structures*[1]) that a modified form of modal superposition analysis, where the stiffness of ductile piers is reduced by the expected ductility factor, while members responding elastically (eg superstructure) retain their elastic stiffness provides results that are in close agreement with results from non-linear time history analyses. In this "effective stiffness" modal analysis, the damping used should be the global damping used in the structural displacement-based design.

This procedure can also be used for design verification of bridge seismic response.

The magnitude of the abutment reactions can be accurately estimated by either of the two methods (effective modal superposition, or non-linear time-history analysis) presented in C5.15. When elastic response to the design earthquake is assured, abutment reactions may be determined by conventional elastic modal analysis.

C5.16 Design displacements (5.6.1 – 5.6.3)

It is essential that inelastic deformations only occur in intended plastic hinges, and that non-ductile inelastic modes be avoided. To ensure this is the case, a hierarchy of failure is required where, eg the dependable shear strength of a bridge pier exceeds the shear associated with maximum feasible flexural strength, noting that with ductile design, it is the actual, not design level of flexural strength that will be developed. If the flexural strength is high because material strengths exceed the expected values (the normal situation) or as a result of reinforcement strain-hardening, then the corresponding elevated shear force, rather than the design level shear force will be developed.

Similar arguments apply to the required flexural strength of sections that must not form plastic hinges (eg cap beam sections). The best, and least conservative way to determine the actual moment capacity of potential plastic hinges is to carry out a moment-curvature analysis, using actual material strengths, with strain-hardening of reinforcement and confinement of concrete modelled, and checking the resultant moment at the design curvature for the pier. This will almost always result in a moment amplification factor significantly lower than the default option of 1.5 in the case of steel grade 500 reinforcement or 1.7 in the case of grade 300 reinforcement. Actual upper-bound material strengths should be based on local information. Commonly used values, included in table 5.7 are:

reinforcement: $f_y^\circ = 1.25 f_y$ (C5-13)

concrete: $f'^\circ_c = 1.7 f'_c$ (C5-14)

Where:

f_y = reinforcement yield strength

f'_c = characteristic concrete compression strength

Equilibrium considerations are illustrated in figure C5.7 which represents a simple two-column bent, subjected to lateral seismic force and applied vertical loads from superstructure beams. The demand seismic moments for the left column are shown by the dashed line, and will have been calculated without considering any moment contribution from gravity loads P, in accordance with 5.6.2. (Note, however, that the gravity loads P must be considered when determining the moment capacity of the piers). The maximum feasible moments in the column (overstrength moments) are shown by the solid line, and have a value of M_b° at the bottom and M_t° at the top. Note that the sketch shows column-top moments at the beam centre line, which requires extrapolation from the critical moment at the soffit of the cap beam.

The column overstrength moments are found from moment-curvature analyses using actual material strengths, or by multiplying the design moments by 1.5 or 1.7 depending on the grade of reinforcement, as above. The design shear force for the column is thus:

$$V_c = \frac{(M_b^\circ + M_t^\circ)}{H} \quad \text{(C5-15)}$$

At the joint between the column and the cap beam, the moments must be in equilibrium. For convenience of illustration, it is assumed that the moment at the top of the right column is also M_t° (this will not generally be the case, because of different seismic axial force levels between left and right columns). Hence the maximum design positive cap beam moment, which occurs under the left point load P, is:

$$M_{cb} = M_t^\circ \left(1 - \frac{2a}{L}\right) + Pa \quad \text{(C5-16)}$$

C5.16 continued

The maximum cap beam shear, which occurs between the right column and the right point load P is:

$$V_{cb} = \frac{2M_t^o}{L} + P \qquad \text{(C5-17)}$$

Note that in the above example that vertical seismic response has not been considered. When vertical acceleration is included this would cause an increase in the free cap beam moments (Pa) that would be added to equation (C5-16).

Figure C5.7: Equilibrium considerations for capacity design of a bridge bent (*Displacement-based seismic design of structures*[1])

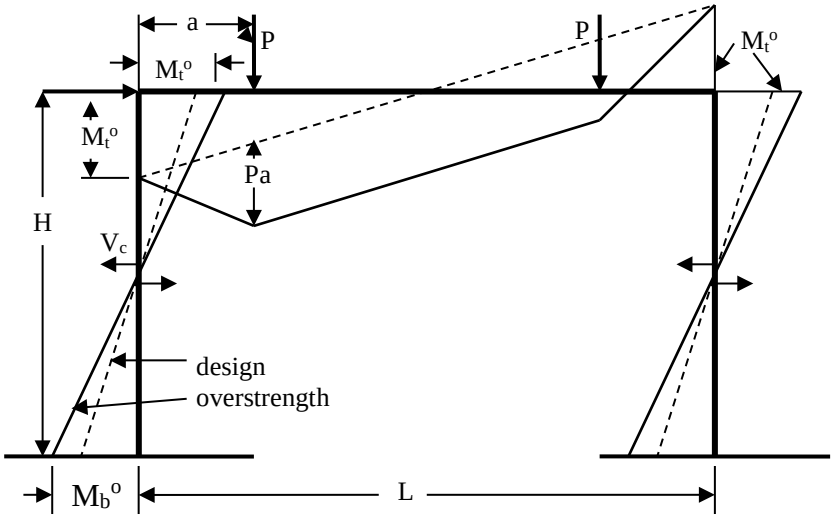

Shear strength of compression members: It is recommended that shear strength of concrete compression members be determined by the modified UCSD model. This has been shown in independent assessments to provide the best estimate deterministic models of shear strength. Full details are provided in *Displacement-based seismic design of structures*[1], and only a summary of the procedure is provided here. An alternative approach is to use modified compression field theory as detailed in the *LRFD bridge design specifications*[17].

In the modified UCSD model, the dependable shear strength of concrete sections is found from the additive equation:

$$V_{des} = \phi_s V_{cap} = \phi_s\left(V_c + V_s + V_p\right) \qquad \text{(C5-18)}$$

Where:

V_c = shear strength component provided by concrete mechanism

V_s = shear strength component provided by transverse reinforcement

V_p = shear strength component provided by axial force mechanisms

a. Concrete shear resisting mechanism

This reduces with increasing ductility as a result of a decrease in effectiveness in aggregate interlock as crack width increases. The shear strength provided by concrete mechanisms is given by equation (C5-19):

$$V_c = k\sqrt{f'_{ce}}\,A_e = \alpha\beta\gamma\sqrt{f'_{ce}}\,\left(0.8A_g\right) \qquad \text{(C5-19)}$$

C5.16 continued

Where:

$$1.0 \leq \alpha = 3 - \frac{M}{VD} \leq 1.5 \quad \text{(C5-20)}$$

$$\beta = 0.5 + 20\rho_l \leq 1.0 \quad \text{(C5-21)}$$

In equation (C5-20) M and V are the moment and shear force at the critical section of the member, of section depth D. In equation (C5-21) ρ_l is the longitudinal reinforcement ratio of the section and A_g is the gross section area. The coefficient γ in equation (C5-19) depends on the curvature ductility demand, and is given in figure C5.8.

b. Axial load component

The axial load in a compression member enhances the shear strength as a consequence of the inclination of the axial force relative to the member axis, as shown in figure C5.9 for a beam, and figure C5.10 for a column. To provide a conservative lower bound to the axial load component the lateral component of the inclined compression strut is reduced by 15%. Hence:

$$V_P = 0.85P \tan\zeta \quad \text{(C5-22)}$$

where ζ is defined in figure C5.9 and figure C5.10 for beams and columns respectively.

Figure C5.8: Ductility component of concrete shear-resisting mechanisms

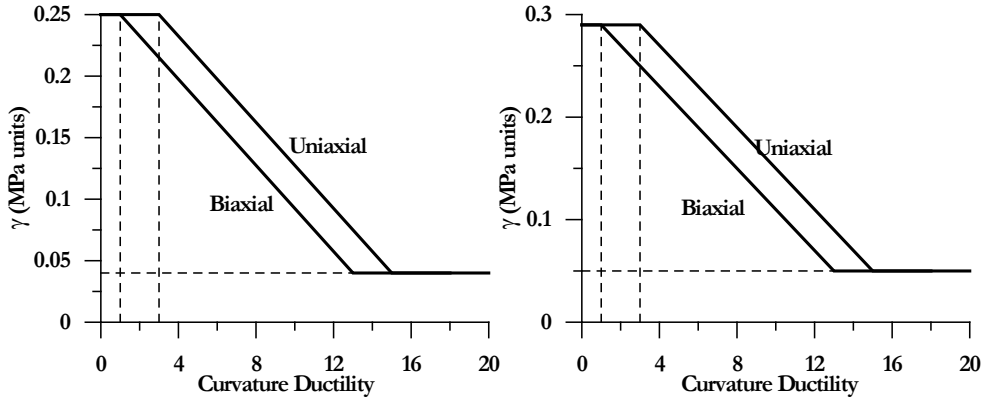

(a) Design of new members (b) Assessment of existing members

Figure C5.9: Contribution of axial force to shear strength of a cap beam

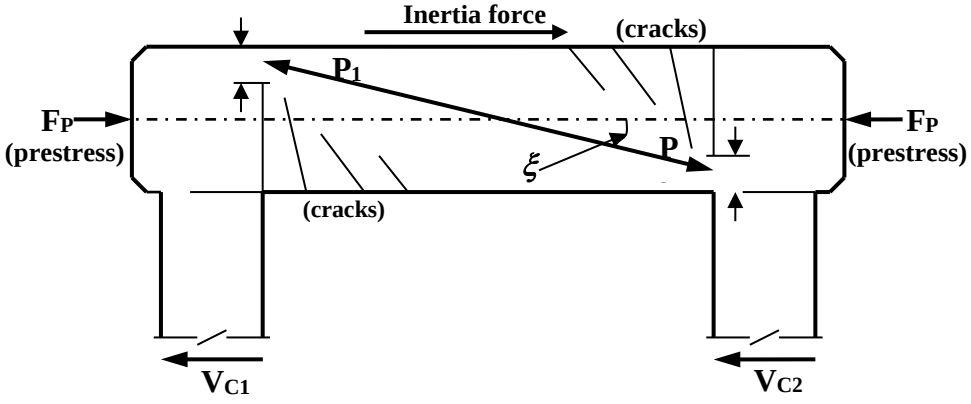

C5.16 continued

Figure C5.10: Contribution of axial force to column shear strength (*Displacement-based seismic design of structures*[1])

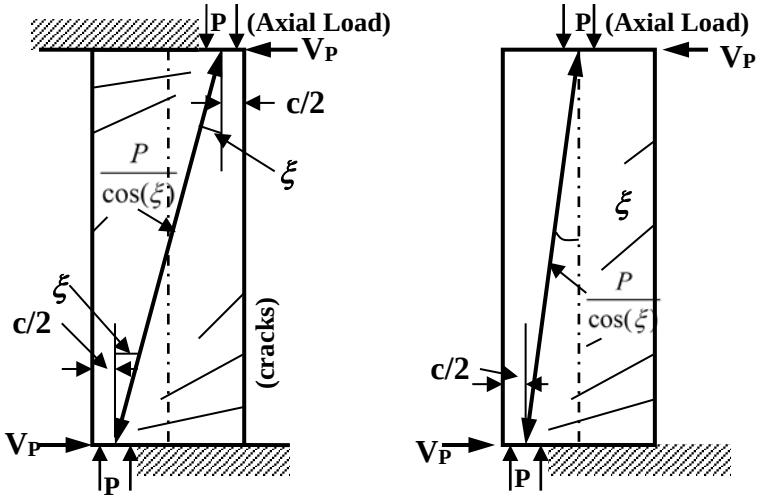

(a) Double bending (b) Single bending

c. Transverse reinforcement truss shear-resisting mechanism

The strength of transverse reinforcement truss mechanisms is illustrated in figure C5.11 for rectangular and circular columns. The rectangular column illustration is also relevant for beams.

Figure C5.11: Effectiveness of transverse reinforcement for shear resistance of columns (*Displacement-based seismic design of structures*[1])

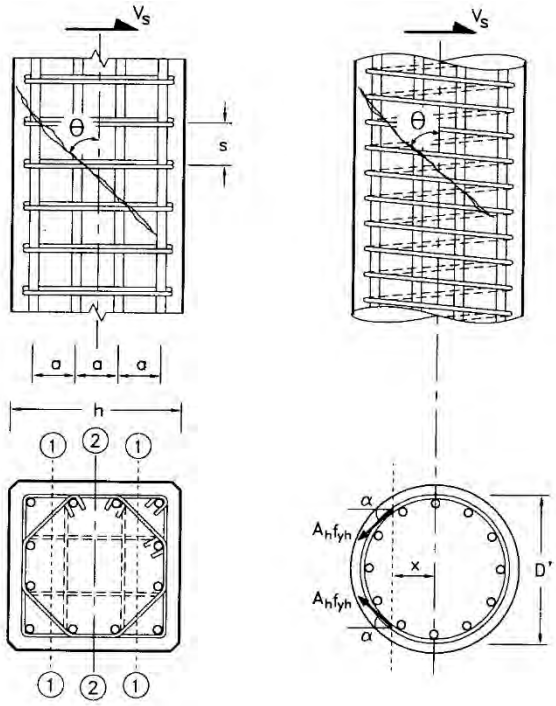

(a) Rectangular column (b) Circular column

For design, the angle of the critical crack to the column axis is taken as θ=35°. The yield capacity of all bars of transverse reinforcement crossing the critical crack is summed, providing the following equations for shear strength:

C5.16 continued

Rectangular column $$V_s = \frac{A_v f_{yh}(D - c - c_o)\cot(35°)}{s} \quad \text{(C5-23)}$$

Where:

A_v = the effective area of hoops in a single layer, as discussed above

For a circular column with circular hoops or spirals:

Circular column $$V_s = \frac{\pi}{2}\frac{A_h f_{yh}(D - c - c_o)\cot(35°)}{s} \quad \text{(C5-24)}$$

In equations (C5-23) and (C5-24), c is the depth of the flexural compression zone from the extreme compression fibre to the neutral axis, c_o is the cover measured to the centre of the peripheral hoop, spiral or tie, and s is the spacing of tie sets, spirals or hoops along the column axis.

For assessment of existing bridge columns, somewhat less conservative assumptions apply. These are defined in *Displacement-based seismic design of structures*(1).

C5.17 Span – support overlap at non-integral abutments (5.7.2(d))

The minimum support overlap at non-integral abutments at which linkages are not provided, expressed by equation (5–51) is made up of a number of components as follows:

- The first component represents the maximum feasible response displacement of the frame. A simple expression for this is the corner period elastic displacement ($\Delta(3.0)$) found from the displacement spectrum (see 5.2.4). Note that this will always be conservative, and will exceed the peak ground displacement.
- The second component, a function of length, reflects thermal and creep and shrinkage effects.
- The third component, related to average pier height is generally reflects the effect of rotation of the pier foundations due to travelling surface waves.
- The fourth component is related to bridge width. If the seating is wide, transverse displacement will inevitable involve rotation about the vertical axis, inducing a longitudinal component at the ends of the seating. The value of $0.005W$ is considered to be conservative, particularly since peak transverse and longitudinal response are not expected to occur simultaneously.
- There is also the question of skew, which is allowed for in the support overlap requirements of most seismic bridge codes. It does not seem that this should be a modifier to the bridge length or bridge height components, and in fact is only significant for skew angles above about 40°. It could be applied to the $\Delta(3.0)$ component. Skew response is thought to be limited to a value dictated by the gap between the bridge end diaphragms and the abutments. Unseating of skew bridges has generally occurred at the acute corners of bridges with very small seating lengths and short spans. The science behind such equations is questionable. It is considered better to have a conservative seating length that will cope with all reasonable skew angles and that equation (5–51) is sufficiently conservative in this respect.
- Finally, a minimum seating length of 400 mm, as previously applied in situations of no linkage, is retained.

A more complete discussion of the issues is provided in *Seismic design and retrofit of bridges*(9), pp418-421.

C5.18 References

(1) Priestley MJN, Calvi GM and Kowalsky MJ (2007) *Displacement-based seismic design of structures*. IUSS Press, Pavia, Italy.

(2) Standards New Zealand NZS 3101.1&2:2006 *Concrete structures standard*. (Incorporating Amendment No. 3: 2017)

(3) Khan E, Kowalsky MJ and Nau JM (2012) *Comparison of the seismic performance of equivalent straight and curved bridges due to transverse seismic excitation*. Proceedings, 15WCEE, Lisboa, Portugal.

(4) Standards New Zealand NZS 1170.5:2004 *Structural design actions*. Part 5 Earthquake actions – New Zealand. (Incorporating Amendment No. 1: 2016)

(5) American Association of State Highway and Transportation Officials (2011) *Guide specifications for LRFD seismic bridge design.* 2nd edition. Washington DC, USA.

(6) California Department of Transportation (Caltrans) (2013) *Seismic design criteria.* Version 1.7, Sacramento, CA, USA.

(7) British Standards Institution BS-EN 1998-2:2005 *Eurocode 8. Design of structures for earthquake resistance*. Part 2 Bridges.

(8) Bommer JJ and Mendis R (2005) *Scaling of spectral displacement ordinates with damping ratios*. Earthquake engineering and structural dynamics vol.34, no. 2, pp 145-165.

(9) Priestley MJN, Sieble F and Calvi GM (1996) *Seismic design and retrofit of bridges.* John Wiley and Sons, New York, NY, USA.

(10) Suarez V and Kowalsky MJ (2007) *Direct displacement-based seismic design of drilled shaft bents with soil-structure interaction*. Journal of earthquake engineering, vol.11, no. 6, pp 1010-1030

(11) Bimschas M (2010) *Displacement based seismic assessment of existing bridges in regions of moderate seismicity*. IBK report no. 326. vdf Hochschulverlag, ETH Zürich, Switzerland.

(12) Paolucci R, Prisco d.C, Figini R, Petrini L and Vecchiotti M (2009) *Interazione dinamica non-lineare terreno-struttura nell'ambito della progettazione sismica agli spostamenti*. Progettazione Sismica, vol. 1, no. 2, EUCENTRE, Pavia, Italy.

(13) Sullivan TJ, Priestley MJN and Calvi GM (2012) *A model code for the displacement-based seismic design of structures*, DBD12. IUSS Press, Pavia, Italy.

(14) Zahn F, Park R and Priestley MJN (1990) *Flexural strength and ductility of circular hollow reinforced concrete columns without confinement on inside face*. ACI Structural Journal vol.87, no.2, pp 1757-1772.

(15) Applied Technology Council (ATC) (1996) *Improved seismic design criteria for California bridges: Provisional recommendations: ATC32*. Redwood City, CA, USA.

(16) Alvarez JC (2004) *Displacement-based design of continuous concrete bridges under transverse seismic excitation*. MSc thesis, Rose School. IUSS Pavia, Italy.

(17) Washington DC, USA. American Association of State Highway and Transportation Officials (AASHTO) (2014) *LRFD Bridge design specifications, customary U.S. units, 7th edition*. Washington DC, USA.

Appendix C5A Displacement based design worked example 1 – Maitai River Bridge

In this section

C5A.1 Bridge description

The Maitai River Bridge was constructed in 1988 and is located at the mouth of the Maitai River, about 0.6km north of the central business area of Nelson City. The bridge has five precast prestressed concrete I beam spans with a cast in-situ reinforced concrete deck. The superstructure is supported on four piers with single 1.4m diameter reinforced concrete columns and hammerhead type column caps. Each pier has a 1.8m diameter cylinder foundation that consists of a reinforced concrete core cast in a 12mm thick steel liner. The cylinders were placed by excavation and top driving of the steel shell. Typical details of the structure are shown in figure C5A.1 to figure C5A.3.

Figure C5A.1: Maitai River Bridge (looking south)

The prestressed I beams are seated on lead rubber bearings on both the piers and abutments. The bearings provide energy dissipation and act as base isolators to limit the lateral loads on the substructure during earthquake loading. The bearings are shown on the drawings as having dimensions of 280x230x131mm on the piers and 380x300x175mm on the abutments. They are prevented from sliding by locating dowels in top and bottom plates with the top plate cast into the beams and the bottom plate anchored with four holding down bolts. Details of the bearings are shown on the drawings except for the rubber hardness (or rubber shear modulus). A hardness of 53 IRHD was assumed for the worked examples.

Shear keys on the hammerhead column caps are located each side of twin transverse beams formed by diaphragms at the end of the spans. For longitudinal earthquake response there is a clearance of 75mm between the diaphragm beams and the shear keys. In the transverse direction there is also a clear gap of 75mm between the keys and the bottom flange of the beams. There are deck joints on the centre-line of the piers and no linkage bolts between the diaphragms either side of the joints so the spans can displace independently and hammering contact between the diaphragm beams may occur during strong longitudinal response.

Figure C5A.2: Typical details of Maitai River Bridge

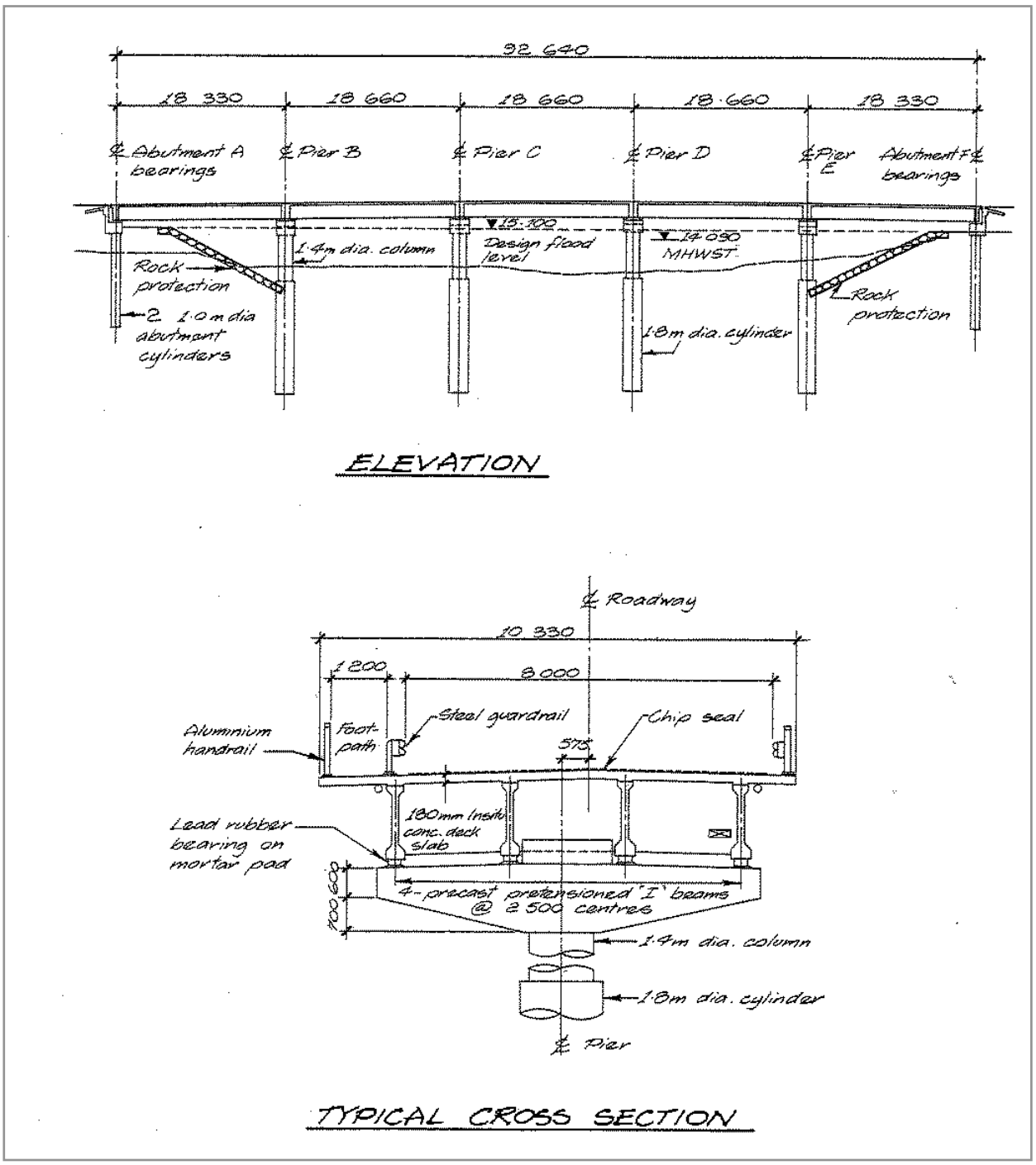

C5A.1 continued

The 1.4m diameter columns are reinforced with 34 D32 longitudinal bars with a specified minimum yield stress of 275MPa. Confinement over a 1.5m length at the base of the column is provided by D20 hoops at 125mm spacing. All four columns have a height of 7.62m measured from the top of the cylinders to the top of the hammer-head pier caps. Although the bridge is base isolated, the pier columns were designed to have a relatively high resistance to lateral load and details at the base of the columns provide for moderate amounts of ductility in the unlikely event of a plastic hinge developing.

The main longitudinal reinforcement in the 1.8 m diameter cylinder foundations consists of 36 D32 bars (275MPa specified minimum yield).

C5A.1 continued

Figure C5A.3: Typical details of bridge piers

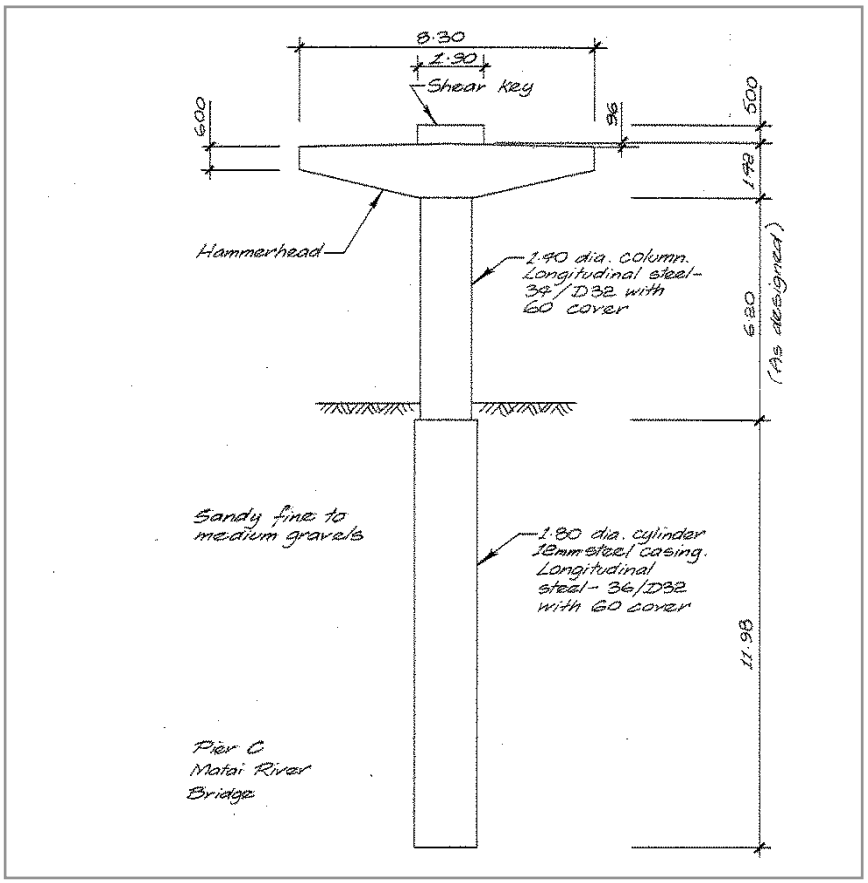

Figure C5A.4: SPT results for cylinder foundation

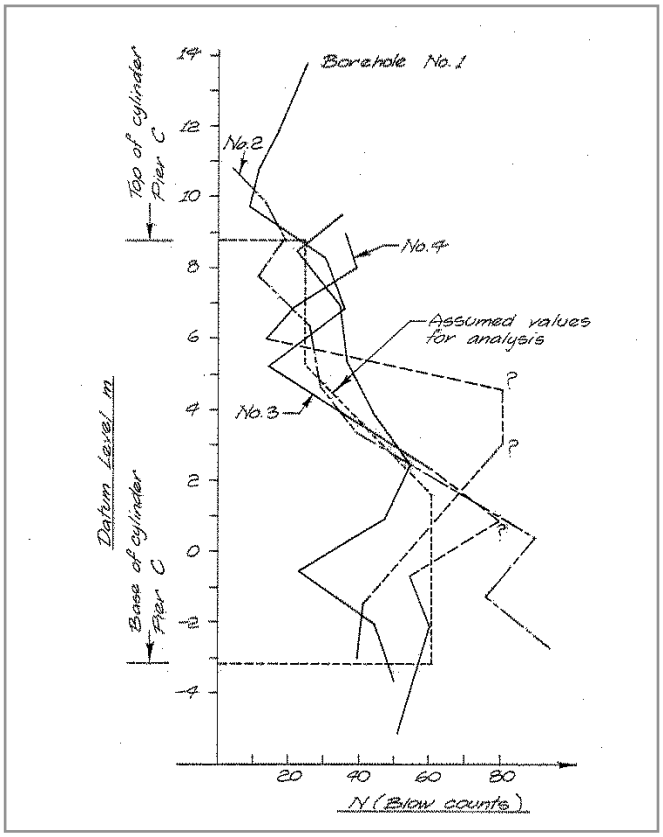

C5A.1 continued

Four investigational bore holes were drilled to provide foundation design data. The upper sections of the foundation cylinders are embedded in unweathered to moderately weathered fine gravels in a matrix of yellowish brown silty fine sand with a trace of clay. In the upper layers the soil is medium dense with the coarser gravel layers towards the bottom of the cylinders becoming dense to very dense. The investigational work showed that the foundation soil was relatively uniform over the extent of the bridge site. A summary of the standard penetration test (SPT) results is shown in figure C5A.4.

The bridge site is within the tidal influence of Nelson Harbour and the tops of the foundation cylinders are between 3.2 to 3.7m below mean sea level. The maximum tidal range is about 4.0m and thus the cylinder tops are below ground water level during the complete tidal range.

Static lateral load tests were carried out during construction of the bridge to determine the stiffness of three of the completed piers and their cylinder foundations. The maximum load applied at the tops of the piers was 325kN which is about 52% of the load estimated to develop the ultimate flexural strengths of the columns based on estimates of probable steel yield and concrete compressive strengths.

C5A.2 Example cases analysed

Three different configurations of the bridge were considered in the example calculations and for each case both transverse and longitudinal directions of loading were analysed. (Note that the example calculations were undertaken using an annual probability of exceedance of 1/2500 for this bridge having been written prior to the change of annual probabilities of exceedance introduced in amendment 3 to the *Bridge manual*.)

For case 1 the foundation was assumed to be rigid and the superstructure supported on rigid bearings on the piers and sliding bearings (no restraint) at the abutments. This is not a good representation of the as-built bridge. However, the rigid foundation assumption simplifies the analysis and provides a convenient introduction to the displacement based design (DBD) method. For case 2 the bridge foundation piles were assumed to be flexible and the superstructure supported on elastomeric bearings on the piers and abutments. Case 3 represented the as-constructed bridge with the superstructure mounted on lead-rubber bearings on the piers and abutments.

It is uncertain whether the bridge site should be subsoil category C or D, although it is probably a category C site. Both C and D categories were considered for the case 1 and 2 analyses. Only category C was assumed for case 3 as lead-rubber bearings should not be used on a soft or deep soil site.

For all cases the basic weights and geometry of the as-constructed bridge were used in the analyses. For cases 1 and 2 the column reinforcement details and the column diameter for soil category C were modified so that the flexural strength and ductility of the piers approximately matched the earthquake load demands. Steel reinforcement yield strengths were taken as either 300 or 500MPa instead of the specified value of 275MPa. The column reinforcement details, column diameter and lead-rubber bearings for case 3 were based on the as-constructed bridge but it was found that the usually accepted requirement that the substructure remain elastic when using a base isolation system to support the superstructure was not satisfied. The flexural strength of the piers was increased for this case by using a reinforcement yield strength of 500MPa.

C5A.2 continued

For case 2 (elastomeric bearings without lead cores) it was found that the plan dimensions of the pier bearings shown on the drawings for the lead rubber bearings were insufficient to limit the shear strain in the bearings to approximately 1.0. For the example analyses the dimensions were increased from 280x230mm to 350x280mm for soil category C and to 380x380mm for soil category D. For both soil categories the abutment bearing plan dimensions were taken as 380x300mm, which is the size of the lead rubber bearings shown on the drawings.

For each case the modified design was checked against the DBD provisions of section 5 of the *Bridge manual*. For case 1 and in the transverse loading direction of case 2, two types of analysis procedures were used. The first type was a design approach and the second a review type procedure. The design approach is more direct and does not involve any iteration when the shape of the first mode of vibration is known. The review approach is more appropriate for checking a given design but is rather more complicated with iteration steps required. Only the review analysis procedure was used for case 2 in the longitudinal load direction and in both loading directions for case 3. The analysis procedures are described below for each analysis case.

A summary of the analysis case, load direction, soil category and analysis procedure used in the 16 separate analyses (nine transverse and seven longitudinal load directions) undertaken for this example is given in table C5A.1.

Table C5A.1: Bridge configuration cases and analysis methods for example calculations

Analysis case	Case description	Load direction	Subsoil category	Method	Column diameter (m)
1	Rigid foundation and bearings. Unrestrained at abutments	Transverse	C	Review	1.2
				Design	
		Longitudinal	C	Review	1.2
				Design	
		Transverse	D	Review	1.4
				Design	
		Longitudinal	D	Review	1.4
				Design	
2	Flexible foundation and elastomeric bearings Abutments restrained by elastomeric bearings and piles	Transverse	C	Review	1.2
				Design	
			D	Review	1.4
				Design	
		Longitudinal	C	Review	1.2
			D		1.4
3	Flexible foundation and lead-rubber bearings. Abutments restrained by lead-rubber bearings and piles	Transverse	C	Review	1.4
		Longitudinal			

C5A.2 continued

A summary of the main results is given in table C5A.2.

For case 3 the ratio of the flexural capacities of the piers to the demands from the response moments were 1.6 and 1.8 for the transverse and longitudinal directions respectively.

Overstrength of the lead cores or rubber stiffness variations in the bearings is unlikely to result in the piers reaching their flexural capacities under a DCLS event. The piers have sufficient ductility to withstand displacement demands 1.5 times greater than expected in the DCLS earthquake.

Table C5A.2: Summary of Main Results

Analysis case	Load direction	Subsoil	Method	Column diameter (m)	No. D32 main bars in column	Steel yield stress (MPa)	Hoop diameter /spacing (mm)	Column moments (kNm)		Column ductility	
								Capacity	Demand	Capacity	Demand
1	Transverse	C	Review	1.2	20	300	16/100	3700	3700	4.2	3.3
			Design						3500		3.5
	Longitudinal	C	Review	1.2	20	300	16/100	3700	3700	4.3	3.7.
			Design						3800		3.5
	Transverse	D	Review	1.4	28	500	20/100	7750	7750	3.2	2.7
			Design						7200		3.0
	Longitudinal	D	Review	1.4	28	500	20/100	7750	7750	3.5	2.9
			Design						7600		3.0
2	Transverse	C	Review	1.2	20	300	16/120	3700	3800	3.7	2.8
			Design						3200		3.5
		D	Review	1.4	28	500	20/100	7750	7900	3.7	2.3
			Design						6200		3.0
	Longitudinal	C	Review	1.2	20	300	16/120	3700	3700	3.8	2.8
		D		1.4	28	500	20/100	7750	7800	4.0	2.3
3	Transverse	C	Review	1.4	34	500	20/125	8200	5200	-	-
	Longitudinal								4600	-	-

C5A.3 Two-degree of freedom dynamic model

The two-degree-of-freedom dynamic model shown in figure C5A.5 was used in the review analysis procedure for case 2 (elastomeric bearings on piers and abutments) and case 3 (lead-rubber bearings on piers and abutments). The model takes into account the pier cap mass in a more correct manner than simply lumping it with the superstructure mass or using an equivalent single mass model. This is important when a significant part of the total mass acting on the piers is in pier caps located beneath flexible superstructure bearings.

Figure C5A.5: Two-degree-of-freedom model for bridge on elastomeric or lead-rubber bearings

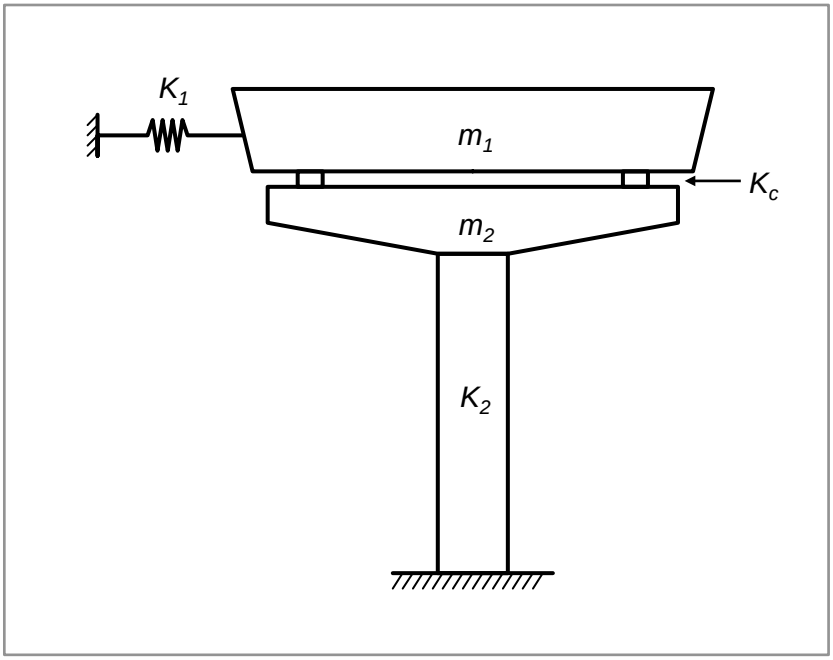

The spring K_1 shown in figure C5A.5 was used to represent the stiffness of the abutments in the longitudinal direction analyses but was not used in the transverse direction analyses.

The model in figure C5A.5 is analogous to the simple spring-mass linear model shown in figure C5A.6, which has been presented as an illustrative example for two-degree-of freedom systems in *Vibration theory and applications*[1] and elsewhere.

Figure C5A.6: Two-degree-of-freedom example used in texts on structural dynamics (from *Vibration theory and applications*[1])

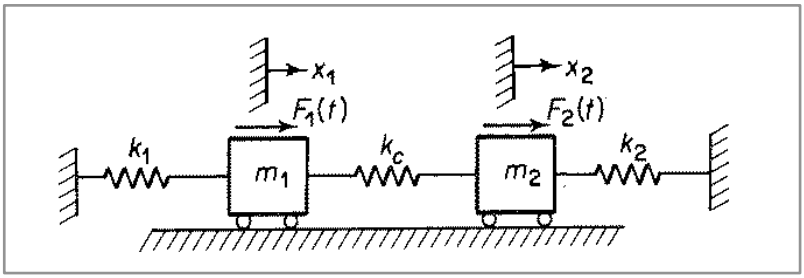

C5A.3 continued

One limitation of using the simple linear model shown in figure C5A.6 for dynamic analysis of the two-mass bridge model shown in figure C5A.5 is that rotation in the plastic hinge at the base of a pier may result in a significant additional displacement of the superstructure mass that is not represented by the sum of the horizontal translation components of displacement at the top of the pier and from shear in the bearings. The effect of pier base rotation on the dynamic response is significant when there is a significant height difference between the centre of gravities of the superstructure and pier masses.

To incorporate the effects of pier base rotation into the analysis for transverse response of the two-mass bridge model the modified model shown in figure C5A.7 was used.

Figure C5A.7: Two-degree-of-freedom model for significant rotation at pier base

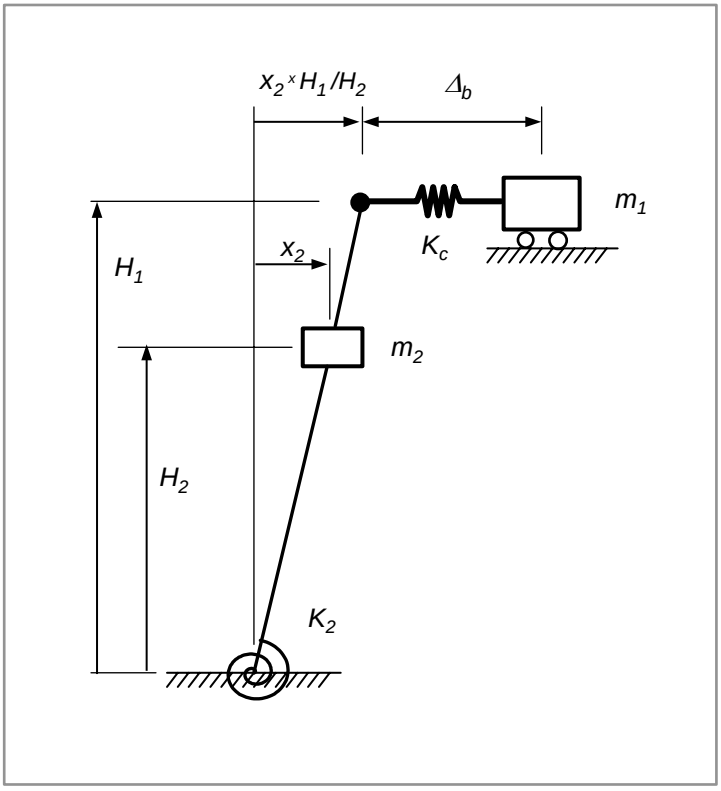

It is convenient to define parameters, x_1 and aa to allow the analysis of the simplified model (figure C5A.7) to follow the solution given by Thompson for the "horizontal" two-degree-of freedom model shown in figure C5A.6. These parameters are defined as:

$$x_1 = x_2 + \Delta_b$$

$$aa = \left(\frac{H_1}{H_2} - 1\right)$$

Where:

Δ_b = the displacement in the spring representing the bridge bearings of the model shown in figure C5A.5

H_1 = the height of the superstructure mass m_1

H_2 = the height of the pier mass m_2

C5A.3 continued

The equations of motion for free vibration of the two masses of the model are then given by:

$$m_1(\ddot{x}_1 + aa\ddot{x}_2) + K_c(x_1 - x_2) = 0$$
$$m_2\ddot{x}_2 + K_2x_2 + K_c(x_2 - x_1) = 0 \quad \text{(C5A-1)}$$

Where:

K_c = the effective horizontal stiffness of the bearings (see figure C5A.5)

K_2 = the effective horizontal stiffness of the pier

Following *Vibration theory and applications*[1], equations (C5A-1) are solved by setting:

$$x_1 = A_1 \sin \omega t$$

$$x_2 = A_2 \sin \omega t$$

Cramer's rule is then used to evaluate the determinate of the resulting equations to give the following frequency equation:

$$\omega^4 - \left[\frac{K_1 + K_c}{m_1} + \frac{K_2 + K_c(1 + aa)}{m_2}\right]\omega^2 + \frac{K_1K_2 + (K_1 + K_2)K_c}{m_1m_2} = 0 \quad \text{(C5A-2)}$$

Where:

ω = the angular natural frequency for the two modes of vibration

Equation (C5A-2) can be written as:

$$\omega^4 - B\omega^2 + C = 0 \quad \text{(C5A-3)}$$

Equation (C5A-3) is a quadratic equation in ω^2 which has the solution:

$$\omega^2 = \frac{-B \pm \sqrt{B^2 - 4C}}{2} \quad \text{(C5A-4)}$$

Using equation (C5A-4) the first mode period is derived as:

$$T = \frac{2\pi}{\omega} \quad \text{(C5A-5)}$$

The mode shapes are given by:

$$\frac{A_1}{A_2} = \frac{K_2 + K_c - m_2\omega^2}{K_c} \quad \text{(C5A-6)}$$

The springs and masses in the model represent the following bridge parameters:

K_1 = the sum of the abutment stiffnesses for longitudinal response. For transverse response of piers supporting simply supported spans $K_1 = 0$

K_c = sum of the stiffness of the bearings on the pier

K_2 = stiffness of the pier for transverse horizontal displacement at the centre of gravity of the pier mass or the sum of the pier stiffnesses for longitudinal response

m_1 = mass of the superstructure supported by the pier for transverse response or the total mass of the superstructure for longitudinal response

m_2 = mass of the pier cap plus ⅓ of the mass of the column for transverse response and the sum of these items for longitudinal response

The total displacement of the superstructure mass is given by:

$$x_s = \Delta_b + x_2(1 + aa) \quad \text{(C5A-7)}$$

C5A.3 continued

The mode shape *A* is given by:

$$A = \frac{x_1}{x_2} = \frac{x_2 + \Delta_b}{x_2} \quad \text{(C5A-8)}$$

From equations (C5A-7) and (C5A-8):

$$x_2 = \frac{x_s}{(A + aa)} \quad \text{(C5A-9)}$$

$$\Delta_b = x_s[1 - \frac{(1 + aa)}{(A + aa)}] \quad \text{(C5A-10)}$$

The base moment in the pier of the model is given by:

$$M_b = (m_1 x_s H_1 + m_2 x_2 H_2)\omega^2 \quad \text{(C5A-11)}$$

The displacement in the bearings is given by:

$$\Delta_b = \frac{m_1 x_1 \omega^2}{K_c} \quad \text{(C5A-12)}$$

and for lead-rubber bearings,

$$K_c = \frac{Q_d}{\Delta_b} + K_d \quad \text{(C5A-13)}$$

Where Q_d and K_d are the characteristic strength and post yield stiffness of the lead rubber bearings (Q_d=0 for elastomeric bearings).

The shear in the pier is given by:

$$V_b = (m_1 x_s + m_2 x_2)\omega^2 \quad \text{(C5A-14)}$$

For longitudinal bridge response, equations (C5A-11) and (C5A-14) need to be modified if restraint is provided by the abutments. For this case the shear forces in the piers are calculated by subtracting the shear forces developed by the abutment stiffness from the inertia forces acting on the superstructure.

C5A.4 Response to earthquake ground motion

From vibration theory for the response of multi-degree-of-freedom structures to a ground acceleration of $\ddot{y}(t)$ the normal coordinates for mode r are given in *Dynamics of structures*(2):

$$\xi_r(t) = P_r D \quad \text{(C5A-15)}$$

Where:

P_r = the modal participation factor for mode r

D = the displacement response of a single-degree-of –freedom system

The participation factor is given by:

$$P_r = \frac{\{\varphi_r\}^T\{M\}}{\{\varphi_r\}^T[M]\{\varphi\}} \quad \text{(C5A-16)}$$

C5A.4 continued

Where:

$\{\varphi_r\}$ = the mode shape in mode r

$[M]$ = the diagonal mass matrix

$\{M\}$ = the mass vector

For a two mass system with the mode shapes normalised so that the superstructure modal displacements are 1.0, the participation factor for the first mode is:

$$P_1 = \frac{\left(m_1 + \Delta_{1,2} m_2\right)}{\left(m_1 + \left(\Delta_{1,2}\right)^2 m_2\right)} \quad \text{(C5A-17)}$$

Where:

$\Delta_{1,2}$ = the first mode normalised displacement of m_2

The first mode earthquake response displacements for the superstructure and pier $Z_{1,1}$ and $Z_{1,2}$ are given by:

$$Z_{1,1} = P_1 D$$
$$Z_{1,2} = \Delta_{1,2} P_1 D \quad \text{(C5A-18)}$$

C5A.5 Abutment stiffness for longitudinal response

In the analyses the stiffness of the abutments was modified using an approximate procedure to allow for the inertia load acting on the abutment and Mononobe-Okabe active earth pressure acting on the abutment backwall. It was conservatively assumed that these forces are in phase with the inertia force acting on the superstructure.

The effective stiffness of the abutment being pulled away from the soil backfill is given by:

$$K_{ea} = \frac{F_s}{\Delta_b + \Delta_a} \quad \text{(C5A-19)}$$

Where:

F_s = the superstructure force acting on the abutment

Δ_b, Δ_a = the displacement in the bearing and the displacement of the abutment respectively relative to the ground remote from the abutment as shown in figure C5A.8

Equation (C5A-19) can be written as:

$$K_{ea} = \frac{F_s}{\frac{F_s}{K_b} + \frac{F_a + F_s}{K_a}} \quad \text{(C5A-20)}$$

Where:

K_b, K_a = the stiffness of the bearings and the abutment structure (essentially the piles) acting alone

F_a = the sum of the inertia force from the mass of the abutment and the active pressure force on the backwall

C5A.5 continued

Equation (C5A-20) can be simplified to:

$$K_{ea} = \frac{K_b K_a}{K_a + K_b\left(1 + \frac{F_a}{F_s}\right)} \qquad \text{(C5A-21)}$$

Figure C5A.8: Abutment model for pull loading from superstructure

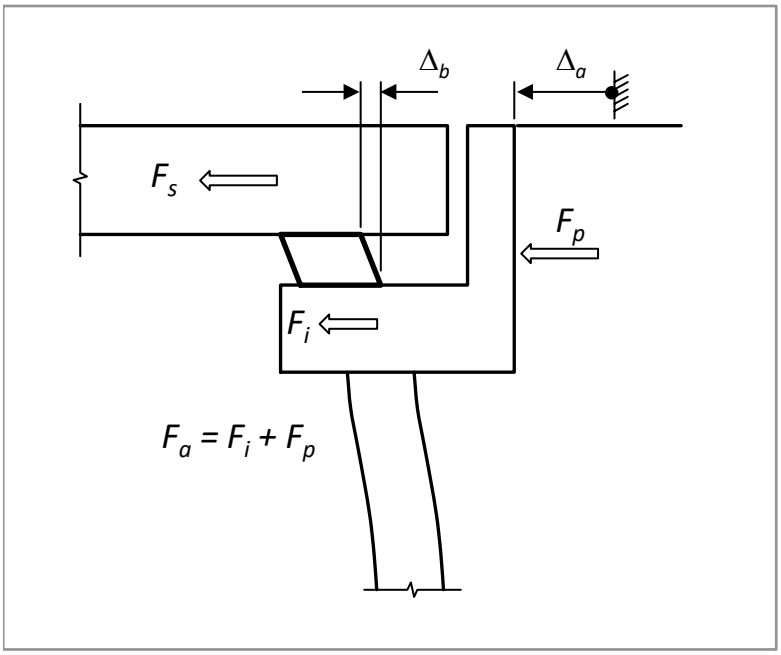

C5A.6 Analysis for case 1: rigid foundations and bearings

C5A.6.1 Review type analysis procedure

In a "review" type of analysis procedure the pier section reinforcement details and column diameter are assumed to be known. The inelastic displacement capacity of the pier is calculated from these properties and compared with the displacement demand from the code defined displacement response spectrum. In general the capacity and demand will not be equal and the process gives a ratio of capacity/demand for the pier section based on the earthquake design level inelastic displacement.

To determine the displacement demand from the design displacement spectrum it is necessary to have an effective period of vibration and the equivalent viscous damping for the inelastic pier (based on the ductility and foundation interaction). The damping is used to modify the 5% code spectrum by calculating a damping modified corner period. The linear relationship assumed for the response spectrum displacement between zero and the modified corner period can then be used together with the effective period of vibration at maximum displacement response to calculate the inelastic displacement demand. However, both the effective period and the equivalent viscous damping are dependent on the demand displacement so an iterative procedure is necessary to determine the demand displacement.

C5A.6.1 continued

A convenient starting point for the iteration is to use an approximate ductility demand calculated by using the elastic period and the elastic response spectrum to calculate an approximate maximum elastic displacement demand. The yield displacement is calculated from the height and diameter of the column (equation (5–10)) and the shear force at yield is calculated from the flexural capacity of the section (moment curvature or strength analysis) to give the elastic stiffness of the pier. An elastic period is calculated from the elastic stiffness and the effective mass of the superstructure carried by the pier. The maximum elastic demand displacement divided by the yield displacement gives an approximate ductility demand ("equal displacement" rule).

The approximate ductility demand can then be used to calculate an equivalent viscous damping, and the elastic period and the approximate ductility demand can be used to calculate the effective or secant period at maximum displacement. A displacement demand can then be calculated (or scaled) from the damping modified displacement response spectrum. The ductility demand is then iterated until the assumed ductility agrees with the ductility demand calculated (or scaled) from the damping modified displacement response spectrum.

The main steps in the review analysis procedure are summarised as follows:

a. Calculate the yield displacement from equation (5–10).

b. Use moment curvature or a section strength analysis to calculate the flexural capacity of the section.

c. Calculate the shear force at flexural capacity then calculate the elastic stiffness from the shear force and yield displacement.

d. From the longitudinal and confining reinforcement details calculate the limiting reinforcement and concrete strains.

e. From the neutral axis depth and the limiting strains calculate the damage limit state curvature.

f. Calculate the plastic hinge length and use this and the plastic curvature limit to calculate the plastic rotation and the plastic displacement limit at the top of the pier.

g. From the yield displacement and the plastic displacement limit calculate the ductility capacity for the pier.

h. Calculate the elastic period: $T = 2\pi\sqrt{\frac{m}{k}}$

   (Where k and m are the stiffness at yield and the effective mass respectively).

i. Calculate the elastic displacement demand from displacement response spectrum and elastic period.

j. Estimate the approximate ductility demand from the yield displacement and elastic response displacement.

k. Use the approximate ductility demand as starting point for iteration to determine the more correct ductility demand using DBD equivalent damping theory.

l. Calculate the equivalent viscous damping from the ductility demand assumption and equation (5–23).

m. Calculate the effective period (secant stiffness) from the elastic period and the approximate ductility demand.

n. Calculate the inelastic displacement demand from the effective period and the damping modifier (equation (5–17)).

C5A.6.1 continued

o. Calculate the ductility demand from the inelastic displacement demand and the yield displacement.

p. Iterate the estimated ductility demand until this agrees with the calculated demand in step (o).

q. Compare the ductility demand with the ductility capacity calculated from the material strain limits.

r. Calculate the P-Δ moment using the inelastic displacement demand from step (n). Using the provisions of clause 5.3.7 check that the moment capacity with any added P-Δ moment is satisfactory.

s. Check that the shear strength of the pier is satisfactory.

t. If the above procedure is part of the design process it may be necessary to modify the pier flexural capacity by modifying the section details to provide an economical (or safe) design with the capacity/demand ratio approximately equal to 1.0. If no change is made to the column diameter the yield displacement is unchanged as this is independent of the reinforcement details. However, the shear force in the pier is dependent on its flexural capacity which may change resulting in a change to the elastic stiffness and elastic period. These changes will affect the displacement demand and it therefore becomes necessary to repeat the complete analysis process if the reinforcement details are changed to modify the flexural and ductility capacities.

The above analysis procedure is used in the examples that are given in the Austroads *Design guideline for earthquakes*[3].

Figure C5A.9: Main steps in DBD analysis (from Priestley el al publications)

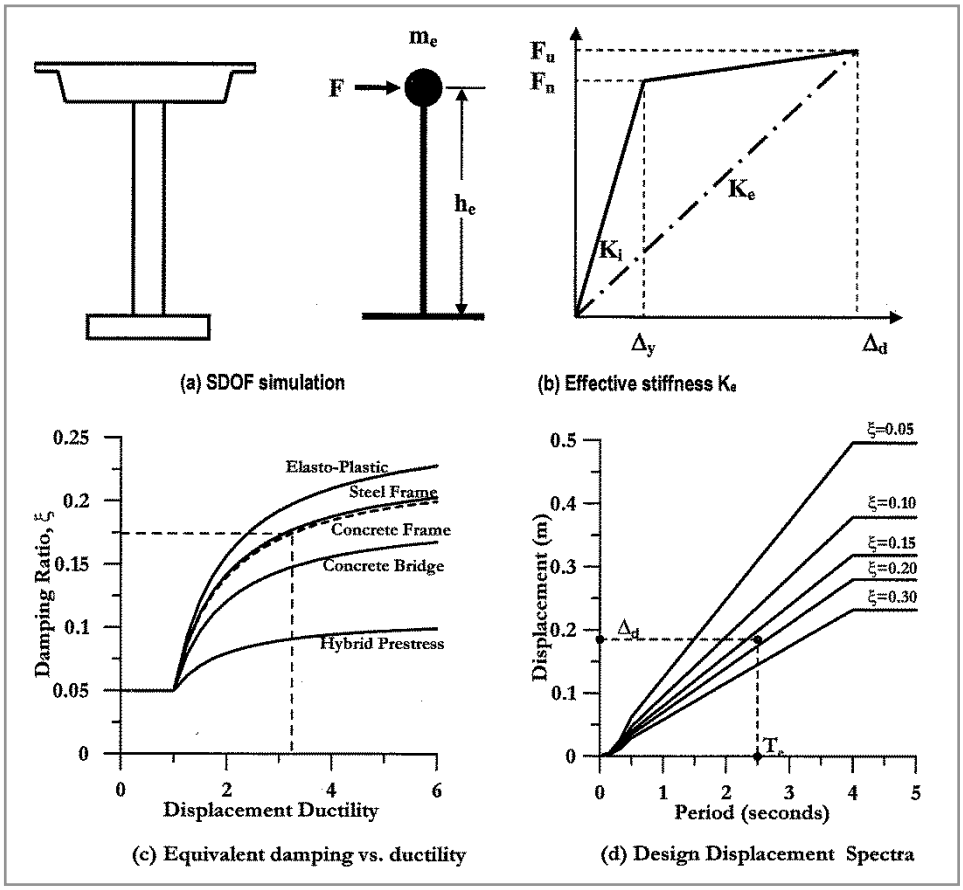

C5A.6.1 continued

Figure C5A.9, which appears in a number of Priestley et al publications (for example see *Performance based seismic design*[4]), is useful for interpreting some of the above steps. In figure C5A.9(b) all the "capacity" force, displacement and stiffness parameters are known when the critical section reinforcement details are selected. However, the demand Δ_d (and K_e) is unknown. This is calculated by selecting a trial value, calculating K_e and T_e, entering figure C5A.9(c) to determine the equavalent damping, and then using figure C5A.9(d) to predict the demand displacement. Iteratons are required on the selected trial Δ_d until it agrees with the value from figure C5A.9(d).

C5A.6.2 Design type analysis procedure

An alternative to the above procedure is to use a "design" type of analysis. In this procedure the design demand ductility level (or a demand drift ratio) and the column diameter are assumed to be known at the start of the design process. These parameters enable the shear force and the corresponding base moment capacity required to satisfy the demand ductility ratio to be calculated. The reinforcement details are then selected to provide the demand moment strength and the confinement to meet the selected ductility demand. Iterations will be required in this step but when it is completed the demand and capacity will be approximately equal. For a design analysis when the pier section details are not determined from an existing bridge or by previous experience this procedure may be more direct than the "review" procedure in C5A.6.1.

The main steps in the design analysis procedure are summarised as follows:

a. Calculate the yield displacement from equation (5–10).

b. Calculate the design level inelastic displacement using the yield displacement and the selected ductility demand (or capacity).

c. From the selected ductility demand calculate the equivalent viscous damping (see figure C5A.9(c)).

d. Calculate the damping modifier for the design displacement response spectrum and adjust the 5% damping spectrum.

e. From the design inelastic displacement calculated in step (b), calculate the effective secant response period by scaling from the modified spectrum corner period (see figure C5A.9(d)).

f. Using the effective period calculate the secant stiffness for the design level inelastic response.

g. From the secant stiffness and the design level inelastic displacement calculate the required design base shear (see figure C5A.9(b)).

h. From the base shear and the effective height calculate the required moment capacity at the base of the pier.

i. Using moment curvature or section strength analyses determine the reinforcement details to give the required flexural capacity.

j. Select the longitudinal and confinement reinforcement details and calculate the limiting reinforcement and concrete strains.

k. From the neutral axis depth and the limiting strains calculate the design (or damage) limit state curvature.

l. Calculate the plastic hinge length and use this and the plastic curvature limit to calculate the plastic rotation and the plastic displacement limit at the top of the pier.

C5A.6.2 continued

m. From the yield displacement and the plastic displacement limit calculate the ductility capacity for the pier. Iterate the reinforcement details as necessary to give agreement between the calculated capacity and the selected demand capacity.

n. Calculate the P-Δ moment using the inelastic displacement demand from step (l). Using the provisions of clause 5.3.7 check that the moment capacity with any added P-Δ moment is satisfactory.

o. Check that the shear strength of the pier is satisfactory.

The above analysis procedure is used in DBD examples given in chapter 6 (by Priestley, Kowalsky and Calvi) of *Bridge engineering handbook: Seismic design*[5].

C5A.7 Analysis for case 2: flexible foundation and elastomeric bearings

C5A.7.1 Review type analysis procedure

a. Carry out steps (a) to (j) as described for case 1 in C5A.6.1. The elastic period of vibration calculation follows the method outlined above for the two-mass model.

b. Calculate the displacements of the superstructure and the pier and the shears and moments in the pier at the yield displacement level. A minor adjustment can made to the pier stiffness to ensure that the base moment from the model agrees with the flexural capacity of the pier. The yield level actions are not used directly in the analysis but are useful checks on similar actions calculated for the inelastic response.

c. Modify the pier stiffness using the approximate ductility demand estimated from the yield and elastic response displacements.

d. Calculate the effective period and elastic design displacement using the two-mass model.

e. From the elastic design displacement and an estimate of the damping, estimate the inelastic displacement demand.

f. From the mode shape and the estimated inelastic displacement demand, calculate the bearing and pier displacements and the force actions in the bearings and piers.

g. Calculate the equivalent viscous damping from the displacements and shears in the piers and bearings using equation (5–22).

h. Calculate the damping modifier and the inelastic displacement demand from the damping modified spectrum.

i. Compare the calculated inelastic displacement demand with the trial displacement demand determined in step (e). Iterate the estimated displacement demand until close agreement is obtained.

j. Using the converged displacement demand, check the pier base moment. Adjust the assumed ductility in the pier and iterate steps (c) to (i) until the calculated base moment is in reasonable agreement with the flexural capacity of the pier.

k. Carry out the iterations in steps (i) and (j) until convergence for both the base moment and the inelastic displacement response is achieved. The iteration function in Excel (set under the "Excel Options" and "Formulas" tabs) is a convenient method of undertaking this double iteration.

l. Calculate the ductility demand from the pier top displacement and the yield displacement and compare with the ductility capacity calculated from material strain limits.

C5A.7.1 continued

m. Calculate the P-Δ moment using the inelastic displacement demand from step (k). Using the provisions of clause 5.3.7, check that the moment capacity with any added P-Δ moment is satisfactory.

n. Check that the shear strength of the pier is satisfactory.

Both the transverse and longitudinal responses are calculated using the above procedure. The longitudinal response is more complicated because of the interaction at the abutments. The abutments are assumed to respond elastically and the shears carried by them can be calculated using the superstructure demand displacement. For calculating the moments in the piers the total longitudinal inertia load is reduced by these shears. Alternatively the moments can be calculated from the shears in the bearings and the inertia load from the piers (see equations (C5A-11) and (C5A-13)).

An adjustment should be made to the stiffness of the pulled abutment to allow for the abutment displacement resulting from the inertia load on the abutment and the active earthquake pressure on the back wall. The forces on the abutment can be estimated using the peak ground acceleration. Because the forces from the superstructure will not necessarily be in phase with the abutment forces it is difficult to accurately adjust the abutment stiffness. It is conservative to assume that the superstructure and abutment inertia forces are in phase and to modify the stiffness using equation (C5A-21).

C5A.7.2 Design type analysis procedure

The design type analysis procedure for case 2 generally follows the steps given in C5A.6.2 for the case 1 analysis. However, several modifications are required. Firstly the design inelastic displacement for an equivalent single mass system is calculated using equation (5–19). This displacement is then used to calculate the effective secant period and stiffness. The inertia forces acting at the two mass levels are calculated using equation (5–20).

The other important modification is that with a two-mass model (or multi-mass model) to calculate the combined effective damping an estimate needs to be made of the first mode shape. In the present example this shape gives the relative displacement between the two masses. It can be checked once the effective period of vibration is calculated and the inertia forces acting on the masses are known. Iteration may be required to obtain a good estimate of the mode shape or alternatively the two-mass dynamic model used in the review analysis procedure can be used.

C5A.8 Analysis for case 3: lead-rubber bearings (review type analysis)

C5A.8.1 Transverse response

a. Calculate the stiffness from the yield displacement and the flexural moment capacity of the pier. Assume the pier remains elastic at the maximum displacement response of the superstructure for the DCLS displacement spectrum.

b. Assume a displacement in the bearings based on the acceptable limits for the configuration of the bearing selected.

c. Calculate the stiffness of the bearings (see equation (C5A-13)). The bearing stiffness depends on the displacement in the bearing.

d. Calculate the period of vibration and mode shape using the two-mass model. From the period, calculate the elastic design displacement.

e. From the mode shape, calculate the displacement of the superstructure and the pier top and the shear forces in the bearings and pier.

C5A.8.1 continued

f. Calculate the equivalent viscous damping using equation 1.16 of *Introduction to seismic isolation*[6] for the bearings, equation (5–31) for the piers and equation (5–22) to calculate the overall damping.

g. From the damping reduction modifier (equation (5–17)) and the elastic design displacement, calculate the demand displacement for the superstructure.

h. Calculate the displacement in the bearings using the mode shape and compare with the assumed displacement selected in step (b). Iterate until there is reasonable agreement between these displacements.

i. Calculate the pier base moment to check that there is a reasonable margin against yield. If not, strengthen the pier and repeat the analysis.

j. Design the pier transverse reinforcement to give moderate ductility and the required shear strength.

C5A.8.2 Longitudinal response

The analysis for the longitudinal response generally follows the procedure above for the transverse response except that stiffness of the abutments and the lead-rubber bearings supporting the superstructure on the abutments needs to be considered. The stiffness of the abutments is dominated by the bearings and this stiffness is required to calculate the period of vibration.

Because the stiffness of the bearings on both the abutments and piers is dependent on the displacement in them there is no straightforward analysis procedure. One method of analysis is to assume both a displacement of the superstructure and a displacement in the pier bearings. The bearing displacement can then be iterated to get convergence as outlined above for the transverse analysis. This is followed by iterations on the superstructure response so that the assumed response agrees with the demand response as calculated in step (g). Successive iterations are required to obtain convergence for both the demand displacement of the superstructure and the displacement in the pier bearings. The iteration function in Excel provides a convenient method of speeding up the analysis.

After convergence is obtained for the displacements, the base moment in the piers should be checked and compared with their yield strength as undertaken in step (i) for the transverse analysis.

As for case 2 longitudinal response analysis (see C5A.7.1), the stiffness of the pulled abutment should be adjusted to allow for the displacement from its inertia force and the active soil pressure force acting on it.

C5A.9 Spreadsheet analysis

C5A.9.1 Analysis case 1: rigid foundations and bearings: subsoil category C: transverse and longitudinal directions (see page C5–57)

a. Structural inputs

The weights and height dimensions were based on the bridge drawings. The calculation of the weights is summarised on the separate spreadsheet titled *Geometric and weight input parameters* (page C5–55).

A single span was considered (tributary mass assumption) with the total dynamic mass taken as the sum of the mass of a superstructure span plus the mass of a pier cap and one-third of the pier column. The mass of the column was assumed to act at the bottom of the pile cap as proposed in C5.

C5A.9.1 continued

In the longitudinal direction the piers are pinned at their tops so the effective height for the analysis is the height of the pier. Because the pier bearings can transfer axial loads under transverse loading they provide overturning fixity rather than a pinned joint between the superstructure and piers. For this loading direction the effective height for the transverse analysis was taken as the height of the centre-of-gravity of the dynamic mass.

For the purpose of the example the column diameter and reinforcement details were modified from the as-built structure (see C5A.2).

b. Earthquake inputs

The earthquake inputs were from the *Bridge manual* (same as NZS 1170.5 *Structural design actions* part 5 Earthquake actions – New Zealand [7]) for a 2,500 year return period event. The bridge would have been designed to the earthquake load requirements of the *Highway bridge design brief*[8], which was based on NZS 4203 *General structural design and design loads for buildings*[9]. Neither the *Highway bridge design brief*[8] nor NZS 4203[9] used return period factors. They used a force based design approach with coefficients based on assumed ductility factor reductions. It is therefore difficult to make a direct comparison between the design loads and the current force based provisions of the *Bridge manual* but the current 2,500 year loads would be approximately 50% greater than the design loads.

c. Calculated structural parameters

The steel areas and volumetric ratio are required for the column strength and ductility calculations. *Gen-Col*[10] was used to calculate the moment capacity of the columns and the depth of the neutral axis. (Moment curvature analysis software can be used for these calculations.)

d. Yield displacements

The yield curvature was calculated using equation (5–8) and the yield strain based on the probable yield strength of the reinforcement as given in table 5.7.

The yield displacement was calculated from the curvature using equation (5–10) and C_1=0.333 (as given in C5.7.2).

e. Elastic period

The shear force at the flexural capacity of the column was calculated from the flexural capacity and the effective height of the superstructure dynamic mass. This was used to calculate an effective elastic stiffness based on the pier yield displacement. The period was calculated by substituting the effective stiffness and dynamic mass into the conventional period equation for a single-degree-of- freedom structure.

f. Elastic displacement

An elastic displacement response (assuming no yield) was calculated from the elastic period and the displacement spectrum 3 second corner period displacement. Based on the equal displacement assumption for elastic and inelastic response this displacement divided by the yield displacement gives an approximate ductility demand.

C5A.9.1 continued

g. Strain limits for plastic rotation

Strain limits were calculated using equations (5–11) and (5–12). The confined compressive strength of the concrete was calculated using empirical equations given in *Seismic design and retrofit of bridges*[11]. (Alternatively this parameter can be selected from charts in *Seismic design and retrofit of bridges*[11].)

The neutral axis depth from the strength analysis was used to calculate the steel and concrete strains and these were compared with the strain limits to determine whether the steel or concrete strain governed. For this example, the steel strain limit governed and was used to calculate the limit state curvature by dividing it by the distance of the extreme bar from the neutral axis.

h. Plastic hinge lengths

Plastic hinge lengths were calculated using equations (5–36) and (5–37). Based on typical steel test results for grade 300 reinforcement the f_u/f_y ratio was taken as 1.4.

Because of the different fixity conditions at the top of the pier for the two response directions the heights to the point of contraflexure differ resulting in a small difference between the plastic hinge lengths for each direction.

i. Ductility factor capacities

Both the limit state displacement capacities and ductility factors for the piers were calculated using conventional expressions.

j. Damping

To calculate the damping a ductility demand is estimated and then iterated until it agrees with the ductility calculated from the ductile displacement demand which is calaculated from the damping reduced spectrum. The ductile displacement demand depends on the secant period and the equivalent viscous damping which are unknown at this point of the analysis.

Damping from inelastic action in the piers was calculated using equation (5–31) and the assumed ductility demand. The damping modifier was calculated from the damping and equation (5–17).

k. Effective period

The effective period was calculated from the elastic period and the assumed ductility demand. Recalling that $\mathrm{T_e} = 2\pi\sqrt{\frac{\mathrm{m_e}}{\mathrm{k_e}}}$ the ratio between the secant and elastic period is proportional to the square root of the assumed ductility since ductility is inversely proportional to the effective stiffness.

l. Ductile displacement demand

The elastic spectrum displacement was calculated from the elastic spectrum corner period displacement using the ratio of the 3 second corner period and the secant period. The ductile displacement demand was then calculated by reducing the elastic spectrum demand by the damping modifier.

The ductility demand was then calculated from the ductile displacement demand by dividing by the yield displacement. A comparison was then made between the assumed ductility and the calculated ductility. Iteration was continued until close agreement was obtained.

C5A.9.1 continued

m. Check P-Δ moment

The P-Δ moment at the base of the piers was calculated using conventional procedures. There are two components to the moment; a component from the superstructure displacement and dynamic weight force, and a component from the displacement of the lower two-thirds of the columns and the gravity force from this lower section. The component from the lower column section is small and can be neglected.

The ratio of the P-Δ moment to the pier moment capacity was checked. If this ratio is less than 0.1 no increase is required to the design moment capacity. In this example, the ratio was between 0.1 and 0.25. In this range the design capacity should be increased by 50% of the P-Δ moment. (P-Δ moment ratios greater than 0.25 are unacceptable. Refer to clause 5.3.7.)

n. Required moment capacity

The analysis showed that the required moment demand on the columns, including the P-Δ increase, was approximately equal to the capacity calculated for the assumed reinforcement details.

C5A.9.2 Analysis case 2: flexible foundations and bearings: subsoil category C and D: transverse direction (see page C5–71)

a. Structural inputs

The weights and height dimensions were based on the bridge drawings. The calculation of the weights is summarised on the separate spreadsheet titled *Geometric and weight input parameters* (page C5–55).

It was necessary to calculate the centre of gravities (CoG's) of both the superstructure and the piers as these points define the location for the application of the inertia forces.

A single span was considered (tributary mass assumption) with the total dynamic mass taken as the sum of the mass of a superstructure span plus the mass of the pier cap and one-third of the pier column. The mass of the column was assumed to act at the bottom of the pile cap as proposed in C5.

For the purpose of the example the column diameter for soil category C was taken as 1.2m instead of the 1.4m as-built diameter. The reinforcement details were modified from the as-built structure for both soil categories (see C5A.2).

b. Foundation stiffness inputs

These were calculated on a separate spreadsheet titled: *Analysis case 2 (flexible foundation & elastomeric bearings): pier pile stiffness: transverse analysis* (page C5–69). The stiffness parameters for the tops of the cylinder (translation and rotation) were calculated using the elastic continuum method given in *Aseismic pile foundation design analysis*[12]. A linear increase of soil stiffness with depth was assumed and the cylinders were assumed to be long although some are marginally shorter than the minimum length required for this assumption. The increase in the soil modulus with depth (parameter m) was based on the results from the cylinder testing carried out during construction (see C5A.1).

c. Inputs for elastomeric bearings on piers

The overall dimensions of the bearings are shown on the drawings (see C5A.1). For the purpose of the example these were adjusted to give a more satisfactory strain level in the bearings. The rubber thickness, side covers and shear modulus were based on typical values used in bridge bearings.

C5A.9.2 continued

d. Earthquake inputs

Earthquake inputs were from the *Bridge manual* (same as NZS 1170.5[7]) for a 2,500 year return period event. The bridge would have been designed to the earthquake load requirements of the *Highway bridge design brief*[8] which was based on NZS 4203[9]. Neither the *Highway bridge design brief*[8] nor NZS 4203[9] used return period factors. They used a force based design approach with coefficients based on assumed ductility factor reductions. It is therefore difficult to make a direct comparison between the design loads and the current force based provisions of the *Bridge manual* but the current 2,500 year loads would be approximately 50% greater than the design loads.

e. Calculated structural parameters

The steel areas and volumetric ratio are required for the column strength and ductility calculations.

The cracked stiffness of the pier was calculated to provide a comparison and check on the pier yield stiffness used to calculate the elastic period of vibration (see below). The reduction in stiffness from cracking was based on the pier stiffness ratio given in figure 4.12 of *Displacement-based seismic design of structures*[13].

f. Yield displacements

The yield curvature was calculated using equation (5–8) and the yield strain based on the probable yield strength of the reinforcement as given in table 5.7.

To estimate the displacement component from the foundations at the yield capacity of the pier it is necessary to know the moment and shear acting on the foundation. These were estimated from the flexural capacity calculated using *Gen-Col*[10].

The yield displacement was calculated using equation (5–10) and C_1=0.333 (as given in C5.7.2). The pier yield displacement was based on the centre of gravity of the pier. This is a convenient reference point as the inertia force from the pier is applied at this location.

g. Elastic period of vibration

The elastic period of vibration was calculated using the two-mass model and equations (C5A-1) to (C5A-6).

It is not essential to calculate the elastic period of vibration but it provides a useful check on the ductility demand calculations and the performance of the elastomeric bearings.

For the elastic period calculations the stiffness of the pier was estimated using the yield displacement and an approximation to the yield shear force obtained by dividing the flexural capacity by the height to the centre of gravity of the total mass. Using an iterative process the pier stiffness was adjusted until the moment at the base of the pier from the first mode response of the model was equal to the flexural capacity of the column.

h. Displacement in bearings at pier yield capacity

The displacement of the superstructure when the pier reaches its flexural capacity was calculated from the yield displacement and the first mode shape of the two-mass model. A correction was made to the superstructure for the column base rotation (see equation (C5A-9)).

C5A.9.2 continued

The displacement in the bearings can be calculated using equation (C5A-8) or (C5A-12). Both are used on the spreadsheet to check the analysis.

The first mode shear in the pier was calculated by summing the shear in the bearings and the inertia force acting at the pier centre of gravity. The shear in the bearings was calculated from the bearing displacement and stiffness.

A check was made on the shear strain in the bearing by dividing the displacement by the thickness of rubber in the bearing. For this example the bearing dimensions were adjusted to give a shear strain of less than 1.0 which is considered an acceptable limit for earthquake loading.

i. Elastic displacement

The displacement based on assumed elastic response was calculated from the displacement spectrum 3 second corner period displacement. To get the correct superstructure displacement this single-degree-of-freedom response needs to be adjusted using the participation factor (equation (C5A-17)).

The pier centre of gravity displacement was calculated from the superstructure displacement using the mode shape corrected for base rotation (equation (C5A-9)). After subtracting the foundation displacement component the pier centre of gravity displacement was divided by the pier yield displacement to give an approximate ductility demand based on the equal displacement assumption for elastic and inelastic response.

j. Strain limits for plastic rotation and curvatures

Strain limits were calculated using equations (5–11) and (5–12). The confined compressive strength of the concrete was calculated using empirical equations given in *Seismic design and retrofit of bridges*[11]. (Alternatively this parameter can be selected from charts given in *Seismic design and retrofit of bridges*[11].)

The neutral axis depth from the strength analysis was used to calculate the steel and concrete strains and these were compared with the limits to determine whether the steel of concrete strain governed. The steel strain governed for the soil category C example and the concrete strain for soil category D. The limit state curvatures were calculated by dividing the steel strain by the distance of the extreme bar from the neutral axis for the soil category C example and the concrete strain by the neutral axis distance for the soil category D case.

k. Plastic hinge lengths and ductility factor capacity

The plastic hinge lengths were calculated using equations (5–36) and (5–37). Based on typical steel test results the f_u/f_y ratio was taken as 1.4 for grade 300 reinforcement and 1.2 for grade 500.

For calculating the plastic hinge length the distance to the point of contraflexure was assumed to be the height of the CoG of the total mass. Both the limit state displacement capacities and ductility factors for the piers were calculated using conventional expressions.

l. Ductility iteration for superstructure response

The stiffness of the piers was estimated from trial values for the ductility demand and the shear force in the pier. Initial trials can be estimated from the previous calculations for elastic displacement response.

C5A.9.2 continued

Using the trial pier stiffness, the two-mass model was used to calculate an effective period of vibration and an estimate of the design elastic spectrum displacement (unreduced by damping) for the superstructure mass. The iteration of the ductility is carried out until the moment at the base of the pier is equal to the flexural capacity minus any P-Δ correction. The moment is calculated using equation (C5A-11). The moment is dependent on the damping reduced displacement demands on the two masses which in turn are dependent on the overall system damping. These parameters are not accurately known at this point. The method used on the spreadsheet was to estimate a displacement demand for the superstructure mass and to iterate both the ductility demand and the displacement demand simultaneously until the base moment and the displacement demand converged (moment equal to capacity with P-Δ modification and demand displacement equal to the trial demand displacement). The iteration function in Excel was found to be helpful for this process.

m. Damping and ductility demand

The shear force in the bearings and piers (required for the damping calculation) was estimated from the trial displacement demand on the superstructure mass. Equations (C5A-10) and (C5A-12) were used to estimate the displacement in the bearings. The shear force in the bearings was then estimated from the displacement and bearing stiffness. The shear in the pier was calculated by adding the inertia force acting on the pier mass and the shear force in the bearings.

Damping from the piers was estimated using equation (5–31) for pile/columns assuming that the cylinder/column structure has similar damping to a pile/column. Damping in the pier bearings was taken as the 0.05 default value given in clause 5.4.4.

The system damping was calculated using equation (5–22). Damping in the superstructure was neglected as it is small in comparison to the damping from the other components.

The ductility demand was then calculated from the ductile displacement demand on the pier (total displacement of the pier mass minus the foundation component) dividing by the yield displacement. A comparison was then made between the assumed ductility and the calculated ductility. Iteration was continued until close agreement was obtained between the assumed and calculated values for both the pier ductility and the displacement demand on the superstructure mass.

n. Check P-Δ moment

The P-Δ moment at the base of the piers was calculated using conventional procedures. There are two components to the moment; a component from the superstructure displacement and weight, and a component from the pier displacement and weight (assumed to act at the centres of gravity of the pier). The gravity force from the lower two-thirds of the column was neglected as it was not included in the pier weight. The cylinder top displacement of approximately 7 mm was also neglected and could be subtracted from the total displacements to make a small reduction in the P-Δ moment.

The ratio of the P-Δ moment to the pier moment capacity was checked. If this ratio is less than 0.1 no increase is required to the design moment capacity. When the ratio is between 0.1 and 0.25 the design capacity should be increased by 50% of the P-Δ moment. (P-Δ moment ratios greater than 0.25 are unacceptable. Refer to clause 5.3.7.)

C5A.9.2 continued

For both the soil category C and D examples the ratio of the P-Δ moment to the design capacity moment exceeded 0.1 and an increase in capacity was therefore required.

o. Required moment capacity

The analysis showed that the required moment demand on the columns, including the P-Δ increase, was marginally lower than capacities calculated for the assumed reinforcement details.

C5A.10 References

(1) Thomson WT (1965) *Vibration theory and applications*. Prentice-Hall Inc, Upper Saddle River, NJ, USA.

(2) Clough RW and Penzien J (1993) *Dynamics of structures*. McGraw-Hill Education, New York, NY, USA.

(3) Austroads (2012) *Bridge design guidelines for earthquakes*, AP-T200-12. Sydney, NSW, Australia.

(4) Priestley MJN (2000) *Performance based seismic design*. Proceedings of the Twelfth World Conference on Earthquake Engineering, Auckland.

(5) Chen WF and Duan L (2014) *Bridge engineering handbook: Seismic design*, 2nd edition. CRC Press, Boca Raton, FL, USA.

(6) Buckle IG (2013) *Introduction to seismic isolation*. Appendix E of *Base isolation 101*, seminar TR54, New Zealand Concrete Society.

(7) Standards New Zealand NZS 1170.5:2004 *Structural design actions*. Part 5 Earthquake actions – New Zealand. (Incorporating Amendment No. 1: 2016)

(8) Ministry of Works and Development (1978) *Highway bridge design brief*, CDP 701/D. Superseded.

(9) Standards New Zealand NZS 4203: 1984 *General structural design and design loads for buildings*. Superseded.

(10) Society of Structural Engineers *Gen-Col*. Last accessed 28 September 2018. <www.sesoc.org.nz/software/>. (Available to members only.)

(11) Priestley MJN, Sieble F and Calvi GM (1996) *Seismic design and retrofit of bridges*. John Wiley and Sons, New York, NY, USA.

(12) Pender MJ (1993) *Aseismic pile foundation design analysis*. Bulletin of the New Zealand Society for Earthquake Engineering, vol. 26 no. 1, pp 49-161.

(13) Priestley MJN, Calvi GM and Kowalsky MJ (2007) *Displacement-based seismic design of structures*. IUSS Press, Pavia, Italy.

C5A.11 Spreadsheets

Table C5A.3: Spreadsheet index

Maitai River Bridge

Geometric and Weight Input Parameters

Prepared: J Wood

Edit Date: 21-Aug-17 Print Date: 21-Aug-17

Item	Sym	Value	Units	Comment / Formula
Weight of Superstructure				
Unit weight of concrete	w_{con}	25	kN/m^3	Including reinforcement
Beam length	L_s	18.40	m	
Length of bridge deck	L_d	93.9	m	
Length of centre spans	L_{cs}	18.66	m	
Cross-section area of beams	A_b	0.326	m^2	From drawings
Weight of I beams per span	W_b	600	kN	Total of 4 beams per span
Weight of deck per span	W_{de}	895	kN	Including paps - neglecting taper at Abut F
Weight of surfacing per span	W_{su}	154	kN	40 mm thick seal with unit wt = 20 kN/m^3
Wt handrails/guardrail per span	W_h	23	kN	Assume = 1.2 kN/m
Weight of services per span	W_{se}	20	kN	Assumed value
Weight of diaphragms per span	W_{di}	210	kN	
Total weight of span	W_s	1,902	kN	
Height CoG Superstructure				
Height CoG deck	H_d	1.63	m	Above bottom of beams
Area of central section of beams	A_{bc}	0.292	m^2	From drawing dimensions
Overall CoG of superstructure	H_{su}	1.18	m	Above bottom of beams (ignores cross-fall)
Superstructure O/A height	H_{st}	1.72	m	Bottom of beams to top of deck
Ratio CoG ht over superstructure ht	R_h	0.69		
Height of pier bearings	H_{bea}	0.181	m	
Height CoG super above pier cap	H_{cog}	1.361	m	$H_{cog} = H_{bea} + H_{su}$
Height of pier	H_{cap}	7.621	m	Top of cylinder to top of pier cap
Height CoG super above cylinder	H_s	8.982	m	$H_s = H_{cap} + H_{cog}$
Weight of Pier Cap				
Maximum depth of pier cap	H_{ca}	1.421	m	From drawings
Weight of pier cap	W_c	399	kN	
Weight of Pier Columns				
Pier column height	H_{col}	6.200	m	From drawings
Diameter of columns	D_c	1.40	m	Reduced to 1.2 m for some cases
Weight of each column - 1.4 dia	W_{co}	239	kN	
Weight of each column - 1.2 dia	W_{cor}	175	kN	
Total Weights				
Axial force at base of column - 1.4 dia	N_{ct}	2,539	kN	$N_{ct} = W_s + W_c + W_{co}$
Axial force at base of column - 1.2 dia	N_{ctr}	2,476	kN	$N_{ctr} = W_s + W_c + W_{cor}$
Dynamic wt of span - 1.4 dia column	W_d	2,380	kN	Superstructure + pier cap + 1/3 column
Dynamic wt of span - 1.2 dia column	W_{dr}	2,359	kN	Superstructure + pier cap + 1/3 column

Item	Symbol	Value	Units	Comment / Formula
Height of CoG of Pier Cap, Total and Dynamic Mass				
Height CoG of pier cap	H_c	6.967	m	Above pile cylinder top
Height CoG total mass - 1.4 dia col	H	8.113	m	$H = (H_{col}/2*W_{co}+H_c*W_c+W_s*H_s)/N_{ct}$
Height CoG total mass - 1.2 dia col	H_r	8.241	m	$H = (H_{col}/2*W_{cor}+H_c*W_c+W_s*H_s)/N_{ctr}$
Ht CoG dynamic mass -1.4 dia col	H_e	8.552	m	$H_e = (H_{col}*W_{co}/3+H_c*W_c+W_s*H_s)/W_d$
				1/3 column mass at underside of pier cap
Ht CoG dynamic mass -1.2 dia col	H_{er}	8.573	m	$H_{er} = (H_{col}*W_{cor}/3+H_c*W_c+W_s*H_s)/W_{dr}$
Weight of Abutments				
Weight of each abutment	W_a	930	kN	Calculated from drawings
				does not include approach slab

Maitai River Bridge

Analysis Case 1: Rigid Foundations and Bearings: Soil Subsoil Category C: Review Method

Transverse and Longitudinal Directions

Prepared: J Wood

Edit Date: 21-Aug-17 Print Date: 21-Aug-17

Item	Symbol	Value		Units	Comment / Formula
		Trans	Long		
Structural Inputs					
Dynamic wt of superstructure on pier	W_s	2,359		kN	Includes pier cap + 1/3 column. See p. C5-55
Effective height superstructure	H_e	8.573	7.621	m	Trans: centre dynamic mass above pile top Long: top of pier above pile top
Column diameter	D_c	1.2		m	
Diameter longitudinal bars	d_b	32		mm	
Diameter transverse hoops	d_t	16		mm	
Number of longitudinal bars	N_b	20			
Spacing transverse hoop bars	s_t	100		mm	
Cover to hoops	c_v	40		mm	
Specified concrete 28 day strength	f_c	35		MPa	
Specified steel yield stress	f_y	300		MPa	Longitudinal and transverse steel
Earthquake Inputs					
Site Subsoil Category		C			
Zone Factor	Z	0.27			Nelson
Return Period Factor	R_u	1.8			2,500 year return period
Corner period spectral shape factor	$\Delta_h(3)$	985		mm	From BM Table 5.5
Corner period displacement	$\Delta(3)$	479		mm	$\Delta(3) = R_u*Z*\Delta_h(3)$
Calculated Structural Parameters					
Cover to longitudinal bars	c_o	56		mm	From cover to hoops
Gross column section area	A_g	1.13		m^2	$A_g = \pi*D_c^2/4$
Area of longitudinal steel	A_s	16,085		mm^2	$A_s = N_b\ \pi*d_b^2/4$
Check longitudinal steel area ratio	ρ_l	0.0142			$\rho_l = A_s/(10^6 *A_g)$
Check minimum required steel area	A_{sm}	15,080		mm^2	$A_{sm} = 4*10^6\ A_g/f_y$: BM Clause 5.6.4(f)
Check maximum permitted steel area	A_{sma}	67,858		mm^2	$A_{sma} = 18*10^6\ A_g/f_y$: BM Clause 5.6.4(f)
Area of transverse reinforcement	A_t	201		mm^2	$A_t = \pi*d_t^2/4$
Volumetric ratio transverse steel	ρ_s	0.00728			$\rho_s = 4*A_t / (1000*(D_c - (2*c_v + dt)/1000)*s_t)$ Depth of core taken on centre-line of hoops Adopt Priestley et al 1996 rather than NZS 3101
Yield Displacement					
Probable yield strength reinforcement	f_{ye}	330		MPa	$f_{ye} = 1.1*f_y$: BM Table 5.7
Young's modulus reinforcement	E_s	200,000		MPa	
Yield strain	ε_y	0.00165			$\varepsilon_y = f_{ye} / E_s$
Yield curvature	ϕ_{yy}	2.96E-03		1/m	$\phi_{yy} = 2.15*\varepsilon_y / D_c$: Eq (5-8)
Strain penetration length	L_{sp}	0.232		m	$L_{sp} = 0.022*f_{ye}*d_b /1000$: See def of terms for Eq (5-10)

Item	Symbol	Trans	Long	Units	Comment / Formula
Coefficient for column fixity	C_1	0.333			See Bridge Manual Commentary C5
Yield displacement	Δ_y	76	61	mm	$\Delta_y = C_1*\phi_{yy}*(H_e + L_{sp})^2 *1000$: Eq (5-10)
Elastic Period					
Flexural strength	M_n	3,400		kN m	Flexural strength analysis: f_y = 330 MPa Reduced from 3,672 kNm to allow for P-Δ. See below
Shear force at flexural capacity	V	397	446	kN	$V = M_n / H_e$
Elastic stiffness	k	5,191	7,341	kN/m	$k = V/(\Delta_y/1000)$
Elastic period	T_{el}	1.35	1.14	s	$T_{el} = 2*\pi*(W_s/(9.81*k))^{1/2}$
Elastic Displacement					
Elastic spectrum displacement	$\Delta(T_{el})$	216	181	mm	$\Delta(T_{el}) = \Delta(3)*T_{el}/3$
Approximate ductility demand	μ	2.82	2.99		$\mu = \Delta(T_{el})/(\Delta_y)$: Equal disp. assumption
Strain Limits for Plastic Rotation					
Yield strength transverse reinf.	f_{sy}	300		MPa	
Strain at max stress lateral reinf.	ε_{sut}	0.12			BM Clause 5.3.5(b)
Strain at max stress longitudinal reinf.	ε_{sul}	0.12			BM Clause 5.3.5(a)
Design comp strength plastic hinge	f_{ce}	45.5		MPa	$f_{ce} = 1.3*f_c$: BM Table 5.7
Average confining stress	f_{ld}	1.04			$f_{ld} = 0.95*f_{sy}*\rho_s/2$: From Priestley et al, 1996
Confined comp strength concrete	f_{cc}	52.3		MPa	$f_{cc}= f_{ce}*(2.254*(1+7.94*f_{ld}/f_{ce})^{1/2}- 2*f_{ld}/f_{ce}-1.254)$ Priestley et al 1996, Eq (5.6)
Reinforcement limiting strain	ε_{sd}	0.029			$\varepsilon_{sd} = 0.015+6*(\rho_s - 0.005) \le 0.5\ \varepsilon_{sul}$: Eq (5-11)
Concrete limiting strain	ε_{cd}	0.011			$\varepsilon_{cd} = 0.004+(1.4*\rho_s*f_{sy}*\varepsilon_{sut}) / f_{cc}$: Eq (5-12)
Neutral axis depth	c	282		mm	From moment strength analysis
Check using empirical formula	c_c	276		mm	$c_c = D_c*(0.2+0.65*W_s/(1000*f_{ce}*A_g))*1000$ Priestley et al 2007. Eq (10.8)
Distance extreme bar to neutral axis	b_{na}	846		mm	$b_{na} = D_c*1000 - c - c_o - d_b/2$
Concrete strain from steel strain	ε	0.0096			$\varepsilon = \varepsilon_{sd}*c / b_{na}$ Steel limiting strain governs
Limit state curvature	ϕ_{ls}	0.0339		1/m	ϕ_{ls} = IF($\varepsilon > \varepsilon_{cd}$, ε_{cd} / (c/1000), ε_{sd} / (b_{na} /1000))
Plastic curvature	ϕ_p	0.0310		1/m	$\phi_p = \phi_{ls} - \phi_{yy}$
Plastic Hinge Length					
Ratio steel ultimate over yield stress	f_u/f_y	1.4			From Pacific Steel test results
Hinge length parameter	k_{lp}	0.080			$k_{lp} = 0.2*(f_u / f_y - 1) \le 0.8$: Eq (5-38)
Distance to point of contraflexure	L_c	8.57	7.62	m	$L_c = H_e$
Plastic hinge length	L_p	0.92	0.84	m	$L_p = k_{lp}*L_c + L_{sp} \ge 2*L_{sp}$: Eq (5-37)
Ductility Factor Capacity					
Plastic rotation	θ_p	0.0284	0.0261	rad	$\theta_p = \phi_p*L_p$
Plastic displacement	Δ_p	244	199	mm	$\Delta_p = \theta_p*L_c*1000$: Eq (5-36)
Limit state displacement capacity	Δ_{ls}	320	260	mm	$\Delta_{ls} = \Delta_y + \Delta_p$
Ductility capacity	μ_{ls}	4.19	4.27		$\mu_{ls} = \Delta_{ls}/\Delta_y$ Capacity > Approximate demand Design probably OK

Item	Symbol	Trans	Long	Units	Comment / Formula
Damping at Displacement Demand					
Assumed ductility demand	$\mu_{ld a}$	3.31	3.62		Iterate until μ_{ld} (see below) = $\mu_{ld a}$ Iteration necessary since demand depends on T_e and ξ_e which are unknown at this point. Approx demand from elast displ (see above) can be used as initial estimate of ductility.
Equivalent viscous damping	ξ_e	0.149	0.152		$\xi_e = 0.05+0.444*(\mu_{ld a} - 1)/(\mu_{ld a}*\pi)$: Eq (5-24)
Damping modifier	M_ξ	0.644	0.637		$M_\xi = (0.07/(0.02+\xi_e))^{0.5}$: Eq (5-17)
Effective Period					
Effective period	T_e	2.46	2.16	s	$T_e = T_{el}*(\mu_{ld a})^{1/2}$: for elasto-plastic response Stiffness at displacement capacity = $k/\mu_{ld a}$
Ductile Displacement Demand					
Elastic spectrum displacement	$\Delta(T_e)$	393	345	mm	$\Delta(T_e) = \Delta(3)*T_e /3$
Ductile displacement demand	$\Delta_d(T_e)$	253	220	mm	$\Delta_d(T_e) = M_\xi*\Delta(T_e)$
Ductility demand	μ_{ld}	3.31	3.62		$\mu_{ld} = \Delta_d(T_e)/\Delta_y$
Ratio: ductility capacity/demand	R_{cd}	1.27	1.18		$R_{cd} = \mu_{ls}/\mu_{ld}$
Check P-Δ Moment					
Dynamic weight x disp demand	$M_{p\text{-}\Delta s}$	597	519	kN m	$M_{p\text{-}\Delta s} = W_s*\Delta_d(T_e)/1000$
Additional P-Δ from lower 2/3 column	$M_{p\text{-}\Delta c}$	11	11	kN m	Minor contribution - could be neglected
Total P-Δ	$M_{p\text{-}\Delta}$	607	530	kN m	
Ratio: $M_{p\text{-}\Delta}$ / M_n	M_{rat}	0.179	0.156		> 0.1. Increase in moment capacity required BM Clause 5.3.7
Moment Capacity					
Required moment capacity	M_{bp}	3,704	3,665	kN m	$M_{bp} = M_{p\text{-}\Delta}/2 + M_n$
Capacity of section with 20/D32 bars	M_{bc}	3,672	3,672	kN m	OK : M_{bc} approximately equal to M_{bp}

Reference:

Priestley M J N, Seible F and Calvi G M, 1996. *Seismic Design and Retrofit of Bridges* . John Wiley & Sons Inc

Priestley M J N, Calvi G M and Kowalsky, 2007. *Displacement-Based Seismic Design of Structures* . IUSS Press.

Maitai River Bridge

Analysis Case 1: Rigid Foundations and Bearings: Soil Subsoil Category D: Review Method

Transverse and Longitudinal Directions

Prepared: J Wood

Edit Date: 21-Aug-17 Print Date: 21-Aug-17

Item	Symbol	Value		Units	Comment / Formula
		Trans	Long		
Structural Inputs					
Dynamic wt of superstructure on pier	W_s	2,380		kN	Includes pier cap + 1/3 column. See p. C5-55
Effective height superstructure	H_e	8.552	7.621	m	Trans: centre dynamic mass above pile top Long: top of pier above pile top
Column diameter	D_c	1.4		m	
Diameter longitudinal bars	d_b	32		mm	
Diameter transverse hoops	d_t	20		mm	
Number of longitudinal bars	N_b	28			
Spacing transverse hoop bars	s_t	100		mm	
Cover to hoops	c_v	40		mm	
Specified concrete 28 day strength	f_c	35		MPa	
Specified steel yield stress	f_y	500		MPa	Longitudinal and transverse steel
Earthquake Inputs					
Site Subsoil Category		D			
Zone Factor	Z	0.27			Nelson
Return Period Factor	R_u	1.8			2500 year return period
Corner period spectral shape factor	$\Delta_h(3)$	1,585		mm	From BM Table 5.5
Corner period displacement	$\Delta(3)$	770		mm	$\Delta(3) = R_u*Z*\Delta_h(3)$
Calculated Structural Parameters					
Cover to longitudinal bars	c_o	60		mm	From cover to hoops
Gross column section area	A_g	1.54		m^2	$A_g = \pi*D_c^2/4$
Area of longitudinal steel	A_s	22,519		mm^2	$A_s = \pi*d_b^2/4*N_b$
Check longitudinal steel area ratio	ρ_l	0.0146			$\rho_l = A_s/(10^6*A_g)$
Check minimum required steel area	A_{sm}	12,315		mm^2	$A_{sm} = 4*10^6\ A_g\ /f_y$: BM 5.6.4(f)
Check maximum permitted steel area	A_{sma}	55,418		mm^2	$A_{sma} = 18*10^6\ \ A_g\ /f_y$: BM 5.6.4(f)
Area of transverse reinforcement	A_t	314		mm^2	$A_t = \pi*d_t^2/4$
Volumetric ratio transverse steel	ρ_s	0.00967			$\rho_s = 4*A_t / (1000*(D_c - (2*c_v+dt)/1000)*s_t)$ Depth of core taken on centre-line of hoops Adopt Priestley et al 1996 rather than NZS 3101
Yield Displacement					
Probable yield strength reinforcement	f_{ye}	550		MPa	$f_{ye} = 1.1*f_y$: BM Table 5.7
Young's modulus reinforcement	E_s	200,000		MPa	
Yield strain	ε_y	0.00275			$\varepsilon_y = f_{ye} / E_s$
Yield curvature	ϕ_{yy}	4.22E-03		1/m	$\phi_{yy} = 2.15*\varepsilon_y / D_c$: Eq (5-8)
Strain penetration length	L_{sp}	0.387		m	$L_{sp} = 0.022*f_{ye}*d_b /1000$: See def of terms for Eq (5-10)

Item	Symbol	Trans	Long	Units	Comment / Formula
Coefficient for column fixity	C_1	0.333			See Bridge Manual Commentary C5
Yield displacement	Δ_y	112	90	mm	$\Delta_y = C_1*\phi_{yy}*(H_e + L_{sp})^2*1000$: Eq (5-10)
Elastic Period					
Flexural strength	M_n	7,751		kN m	Flexural strength analysis: f_y = 550 MPa (P- Δ effects not significant - see below)
Shear force at flexural capacity	V	906	1,017	kN	$V = M_n / H_e$
Elastic stiffness	k	8,057	11,266	kN/m	$k = V/(\Delta_y /1000)$
Elastic period	T_{el}	1.09	0.92	s	$T_{el} = 2*\pi*(W_s/(9.81*k))^{1/2}$
Elastic Displacement					
Elastic displacement	$\Delta(T_{el})$	280	237	mm	$\Delta(T_{el}) = \Delta(3)*T_{el}$ /3
Approximate ductility demand	μ	2.49	2.62		$\mu = \Delta(T_{el})/(\Delta_y)$: equal displ assumption
Strain Limits for Plastic Rotation					
Yield strength transverse reinf.	f_{sy}	500		MPa	
Strain at max stress lateral reinf.	ε_{sut}	0.10			BM Clause 5.3.5(b)
Strain at max stress longitudinal reinf.	ε_{sul}	0.10			BM Clause 5.3.5(a)
Design comp strength plastic hinge	f_{ce}	45.5		MPa	$f_{ce} = 1.3*f_c$: BM Table 5.7
Average confining stress	f_{ld}	2.30			$f_{ld} = 0.95*f_{sy}*\rho_s/2$: From Priestley et al, 1996
Confined comp strength concrete	f_{cc}	59.7		MPa	$f_{cc}= f_{ce}*(2.254*(1+7.94*f_{ld}/f_{ce})^{1/2}- 2*f_{ld}/f_{ce}-1.254)$ Priestley et al 1996, Eq 5.6
Reinforcement limiting strain	ε_{sd}	0.0430			$\varepsilon_{sd} = 0.015+6*(\rho_s - 0.005) \le 0.5\ \varepsilon_{sul}$: Eq (5-11)
Concrete limiting strain	ε_{cd}	0.0153			$\varepsilon_{cd} = 0.004+(1.4*\rho_s*f_{sy}*\varepsilon_{sut}) / f_{cc}$: Eq (5-12)
Neutral axis depth	c	364		mm	From moment strength analysis
Check using empirical formula	c_c	311		mm	$c_c = D_c*(0.2+0.65*W_s/(1000*f_{ce}*A_g))*1000$ Priestley et al 2007. Eq (10.8)
Distance extreme bar to neutral axis	b_{na}	960		mm	$b_{na} = D_c*1000 - c - c_o - d_b/2$
Concrete strain from steel strain	ε	0.0163			$\varepsilon = \varepsilon_{sd}*c / b_{na}$ Concrete limiting strain governs
Limit state curvature	ϕ_{ls}	0.0421		1/m	ϕ_{ls} = IF($\varepsilon > \varepsilon_{cd}$, ε_{cd} / (c/1000), ε_{sd} / (b_{na} /1000))
Plastic curvature	ϕ_p	0.0379		1/m	$\phi_p = \phi_{ls} - \phi_{yy}$
Plastic Hinge Length					
Ratio steel ultimate over yield stress	f_u / f_y	1.2			From Pacific Steel test results
Hinge length parameter	k_{lp}	0.040			$k_{lp} = 0.2*(f_u / f_y - 1) \le 0.8$: Eq (5-38)
Distance to point of contraflexure	L_c	8.55	7.62	m	$L_c = H_e$
Plastic hinge length	L_p	0.77	0.77	m	$L_p = k_{lp}*L_c + L_{sp} \ge 2*L_{sp}$: Eq (5-37)
Ductility Factor Capacity					
Plastic rotation	θ_p	0.0293	0.0293	rad	$\theta_p = \phi_p*L_p$
Plastic displacement	Δ_p	251	224	mm	$\Delta_p = \theta_p*L_c*1000$: Eq (5-36)
Limit state displacement capacity	Δ_{ls}	363	314	mm	$\Delta_{ls} = \Delta_y + \Delta_p$
Ductility capacity	μ_{ls}	3.23	3.48		$\mu_{ls} = \Delta_{ls}/\Delta_y$ Capacity > Approximate demand Design probably OK

Item	Symbol	Trans	Long	Units	Comment / Formula
Damping at Displacement Demand					
Assumed ductility demand	μ_{Ida}	2.72	2.95		Iterate until μ_{Id} (see below) = μ_{Ida} Iteration necessary since demand depends on T_e and ξ_e which are unknown at this point. Approx demand from elast displ (see above) can be used as initial estimate of ductility.
Equivalent viscous damping	ξ_e	0.139	0.143		$\xi_e = 0.05+0.444*(\mu_{Ida} - 1)/(\mu_{Ida}*\pi)$: Eq (5-24)
Damping modifier	M_ξ	0.663	0.654		$M_\xi = (0.07/(0.02+\xi_e))^{0.5}$: Eq (5-17)
Effective Period					
Effective period	T_e	1.80	1.58	s	$T_e = T_{el}*(\mu_{Ida})^{1/2}$: for elasto-plastic response Stiffness at displacement capacity = k/μ_{Ida}
Ductile Displacement Demand					
Elastic spectrum displacement	$\Delta(T_e)$	462	407	mm	$\Delta(T_e) = \Delta(3)*T_e /3$
Ductile displacement demand	$\Delta_d(T_e)$	306	266	mm	$\Delta_d(T_e) = M_\xi*\Delta(T_e)$
Ductility demand	μ_{Id}	2.72	2.95		$\mu_{Id} = \Delta_d(T_e)/\Delta_y$
Ratio: ductility capacity/demand	R_{cd}	1.19	1.18		$R_{cd} = \mu_{Is}/\mu_{Id}$
Check P-Δ Moment					
Dynamic weight x disp demand	$M_{p\text{-}\Delta s}$	728	633	kN m	$M_{p\text{-}\Delta s} = W_s*\Delta_d(T_e)/1000$
Additional P-Δ from lower 2/3 column	$M_{p\text{-}\Delta c}$	13	13	kN m	Minor contribution - could be neglected
Total P-Δ	$M_{p\text{-}\Delta}$	741	646	kN m	
Ratio: $M_{p\text{-}\Delta}$ / M_n	M_{rat}	0.096	0.083		< 0.1. No increase in moment capacity reqd See BM Clause 5.3.7
Moment Capacity					
Required moment capacity	M_{bp}	7,751	7,751	kN m	$M_{bp} = M_n$
Capacity of section with 28/D32 bars	M_{bc}	7,751	7,751	kN m	OK : $M_{bc} = M_{bp}$

Reference:

Priestley M J N, Seible F and Calvi G M, 1996. *Seismic Design and Retrofit of Bridges*. John Wiley & Sons Inc

Priestley M J N, Calvi G M and Kowalsky, 2007. *Displacement-Based Seismic Design of Structures*. IUSS Press.

Maitai River Bridge

Analysis Case 1: Rigid Foundations and Bearings: Soil Subsoil Category C: Design Analysis Procedure

Transverse and Longitudinal Directions

Prepared: J Wood

Edit Date: 21-Aug-17 Print Date: 21-Aug-17

Item	Symbol	Value		Units	Comment / Formula
		Trans	Long		
Structural Inputs					
Dynamic wt of superstructure on pier	W_s	2,359		kN	Includes pier cap + 1/3 column
Effective height superstructure	H_e	8.573	7.621	m	Trans: centre dynamic mass above pile top Long: top of pier above pile top
Column diameter	D_c	1.2		m	
Design ductility limit	μ_d	3.5			Reasonable limit for concrete piers A higher limit results in a significant P-Δ mom
Diameter longitudinal bars	d_b	32		mm	
Diameter transverse hoops	d_t	16		mm	
Number of longitudinal bars	N_b	20			Adjusted to give required moment capacity
Spacing transverse hoop bars	s_t	100		mm	Adjusted to give required ductility - see below
Check maximum permitted spacing	s_c	173		mm	$s_c = (3+6*(f_u/f_y - 1))*d_b$: Eq (5-48) Where f_u/f_y taken as 1.4 (see below)
Cover to hoops	c_v	40		mm	
Specified concrete 28 day strength	f_c	35		MPa	
Specified steel yield stress	f_y	300		MPa	Longitudinal and transverse steel
Earthquake Inputs					
Site Subsoil Category		C			
Zone Factor	Z	0.27			Nelson
Return Period Factor	R_u	1.8			2500 year return period
Spectrum corner period	T_c	3.0		s	From BM Fig 5.2
Corner period spectral shape factor	$\Delta_h(3)$	985		mm	From BM Table 5.5
Corner period displacement	$\Delta(3)$	479		mm	$\Delta(3) = R_u*Z*\Delta_h(3)$
Yield Displacement					
Probable yield strength reinforcement	f_{ye}	330		MPa	$f_{ye} = 1.1*f_y$: BM Table 5.7
Young's modulus reinforcement	E_s	200,000		MPa	
Yield strain	ε_y	0.00165			$\varepsilon_y = f_{ye} / E_s$
Yield curvature	ϕ_{yy}	2.96E-03		1/m	$\phi_{yy} = 2.15*\varepsilon_y / D_c$: Eq (5-8)
Strain penetration length	L_{sp}	0.232		m	$L_{sp} = 0.022*f_{ye}*d_b /1000$: See def of terms for Eq (5-10)
Coefficient for column fixity	C_1	0.333			See Bridge Manual Commentary C5
Yield displacement	Δ_y	76	61	mm	$\Delta_y = C_1*\phi_{yy}*(H_e + L_{sp})^2*1000$: Eq (5-10)
Design Base Shear					
Design maximum inelastic disp.	Δ_d	267	213	mm	$\Delta_d = \mu_d*\Delta_y$
Equivalent viscous damping ratio	ξ_e	0.151			$\xi_e = 0.05+0.444*(\mu_d - 1)/(\mu_d*\pi)$: Eq (5-24)
Damping modifier	M_ξ	0.64			$M_\xi = (0.07/(0.02+\xi_e))^{0.5}$: Eq (5-17)
Corner disp. of mod spectrum	Δ_{cm}	306		mm	$\Delta_{cm} = \Delta(3)*M_\xi$: Eq (5-18)

Item	Symbol	Trans	Long	Units	Comment / Formula
Effective structure period	T_e	2.62	2.08	s	$T_e = T_c*\Delta_d / \Delta_{cm}$
Effective secant stiffness	K_e	1,384	2,188	kN/m	$K_e = 4*\pi^2*W_s/(9.81*T_e^2)$
Design base shear	V_b	370	465	kN	$V_b = K_e*\Delta_d$ /1000
Required design base mom capacity	M_n	3,173	3,546	kN m	$M_n = V_b*H_e$: does not include P - Δ effects
Calculated Structural Parameters					
Cover to longitudinal bars	c_o	56		mm	From cover to hoops
Gross column section area	A_g	1.13		m^2	$A_g = \pi*D_c^2/4$
Area of longitudinal steel	A_s	16,085		mm^2	$A_s = N_b*\pi*d_b^2/4$
Check longitudinal steel area ratio	ρ_l	0.0142			$\rho_l = A_s/(10^6*A_g)$
Check minimum required steel area	A_{sm}	15,080		mm^2	$A_{sm} = 4*10^6\ A_g/f_y$: BM Clause 5.6.4(f)
Check maximum permitted steel area	A_{sma}	67,858		mm^2	$A_{sma} = 18*10^6\ A_g/f_y$: BM Clause 5.6.4(f)
Area of transverse reinforcement	A_t	201		mm^2	$A_t = \pi*d_t^2/4$
Volumetric ratio transverse steel	ρ_s	0.00728			$\rho_s = 4*A_t / (1000*(D_c - (2*c_v+dt)/1000)*s_t)$ Depth of core taken on centre-line of hoops Adopt Priestley et al, 1996 rather than NZS 3101 OK: min required = 0.005 : BM Clause 5.6.4(h)(i)
Strain Limits for Plastic Rotation					
Yield strength transverse reinf.	f_{sy}	300		MPa	
Strain at max stress lateral reinf.	ε_{sut}	0.12			BM Clause 5.3.5(b)
Strain at max stress longitudinal reinf.	ε_{sul}	0.12			BM Clause 5.3.5(a)
Design comp strength plastic hinge	f_{ce}	45.5		MPa	$f_{ce} = 1.3*f_c$: BM Table 5.7
Average confining stress	f_{ld}	1.04			$f_{ld} = 0.95*f_{sy}*\rho_s/2$: From Priestley et al, 1996
Confined comp strength concrete	f_{cc}	52.3		MPa	$f_{cc} = f_{ce}*(2.254*(1+7.94*f_{ld}/f_{ce})^{1/2} - 2*f_{ld}/f_{ce} - 1.254)$ Priestley et al 1996, Eq (5.6)
Reinforcement limiting strain	ε_{sd}	0.029			$\varepsilon_{sd} = 0.015+6*(\rho_s - 0.005) \le 0.5\ \varepsilon_{sul}$: Eq (5-11)
Concrete limiting strain	ε_{cd}	0.0110			$\varepsilon_{cd} = 0.004+(1.4*\rho_s*f_{sy}*\varepsilon_{sut}) / f_{cc}$: Eq (5-12)
Neutral axis depth	c	282		mm	From moment strength analysis
Check using empirical formula	c_c	276		mm	$c_c = D_c*(0.2+0.65*W_s/(1000*f_{ce}*A_g))*1000$ Priestley et al 2007. Eq (10.8)
Distance extreme bar to neutral axis	b_{na}	846		mm	$b_{na} = D_c*1000 - c - c_o - d_b/2$
Concrete strain from steel strain	ε	0.0096			$\varepsilon = \varepsilon_{sd}*c / b_{na}$ Steel limiting strain governs
Limit state curvature	ϕ_{ls}	0.0339		1/m	$\phi_{ls} = IF(\varepsilon > \varepsilon_{cd}, \varepsilon_{cd}/(c/1000), \varepsilon_{sd}/(b_{na}/1000))$
Plastic curvature	ϕ_p	0.0310		1/m	$\phi_p = \phi_{ls} - \phi_{yy}$
Plastic Hinge Length					
Ratio steel ultimate over yield stress	f_u/f_y	1.4			From Pacific Steel test results
Hinge length parameter	k_{lp}	0.080			$k_{lp} = 0.2*(f_u/f_y - 1) \le 0.8$: Eq (5-38)
Distance to point of contraflexure	L_c	8.57	7.62	m	$L_c = H_e$
Plastic hinge length	L_p	0.92	0.84	m	$L_p = k_{lp}*L_c + L_{sp} \ge 2*L_{sp}$: Eq (5-37)

Item	Symbol	Trans	Long	Units	Comment / Formula
Ductility Factor Capacity					
Plastic rotation	θ_p	0.0284	0.0261	rad	$\theta_p = \phi_p * L_p$
Plastic displacement capacity	Δ_p	244	199	mm	$\Delta_p = \theta_p * L_c * 1000$: Eq (5-36)
Limit state displacement capacity	Δ_{ls}	320	260	mm	$\Delta_{ls} = \Delta_y + \Delta_p$
Ductility capacity	μ_{ls}	4.19	4.27		$\mu_{ls} = \Delta_{ls}/\Delta_y$: OK > 3.5
Check P-Δ Moment					
Dynamic weight x disp. demand	$M_{p\text{-}\Delta}$	631	502	kN m	$M_{p\text{-}\Delta} = W_s * \Delta_d$ /1000 Ignores minor contribution from lower col.
Ratio: $M_{p\text{-}\Delta}$ / M_n	M_{rat}	0.20	0.14		> 0.1. Increase in moment capacity required < 0.25 so less than maximum limit See BM Clause 5.3.7
Moment Capacity					
Required moment capacity	M_{bp}	3,489	3,797	kN m	$M_{bp} = M_n + M_{p\text{-}\Delta}/2$
Capacity of section with 20/D32 bars	M_{bc}	3,672		kN m	OK: M_{bc} approximately equal to M_{bp}

References:

Priestley M J N, Seible F and Calvi G M, 1996. *Seismic Design and Retrofit of Bridges*. John Wiley & Sons Inc

Priestley M J N, Calvi G M and Kowalsky, 2007. *Displacement-Based Seismic Design of Structures*. IUSS Press.

Maitai River Bridge

Analysis Case 1: Rigid Foundations and Bearings: Soil Subsoil Category D: Design Analysis Procedure

Transverse and Longitudinal Directions

Prepared: J Wood

Edit Date: 21-Aug-17 Print Date: 21-Aug-17

Item	Symbol	Value		Units	Comment / Formula
		Trans	Long		
Structural Inputs					
Dynamic wt of superstructure on pier	W_s	2,380		kN	Includes pier cap + 1/3 column
Effective height superstructure	H_e	8.552	7.621	m	Trans: centre dynamic mass above pile top Long: top of pier above pile top
Column diameter	D_c	1.4		m	
Design ductility limit	μ_d	3.0			Reasonable limit for concrete piers A higher limit results in a significant P-Δ mom
Diameter longitudinal bars	d_b	32		mm	
Diameter transverse hoops	d_t	20		mm	
Number of longitudinal bars	N_b	20			Adjusted to give required moment capacity
Spacing transverse hoop bars	s_t	100		mm	Adjusted to give required ductility - see below
Check maximum permitted spacing	s_c	134		mm	$s_c = (3+6*(f_u/f_y - 1))*d_b$: Eq (5-48) Where f_u/f_y taken as 1.4 (see below)
Cover to hoops	c_v	40		mm	
Specified concrete 28 day strength	f_c	35		MPa	
Specified steel yield stress	f_y	500		MPa	Longitudinal and transverse steel
Earthquake Inputs					
Site Subsoil Category		D			
Zone Factor	Z	0.27			Nelson
Return Period Factor	R_u	1.8			2500 year return period
Spectrum corner period	T_c	3.0		s	From BM Fig 5.3
Corner period spectral shape factor	$\Delta_h(3)$	1,585		mm	From BM Table 5.5
Corner period displacement	$\Delta(3)$	770		mm	$\Delta(3) = R_u*Z*\Delta_h(3)$
Yield Displacement					
Probable yield strength reinforcement	f_{ye}	550		MPa	$f_{ye} = 1.1*f_y$: BM Table 5.7
Young's modulus reinforcement	E_s	200,000		MPa	
Yield strain	ε_y	0.00275			$\varepsilon_y = f_{ye} / E_s$
Yield curvature	ϕ_{yy}	4.22E-03		1/m	$\phi_{yy} = 2.15*\varepsilon_y / D_c$: Eq (5-8)
Strain penetration length	L_{sp}	0.387		m	$L_{sp} = 0.022*f_{ye}*d_b /1000$: See def of terms for Eq (5-10)
Coefficient for column fixity	C_1	0.333			See Bridge Manual Commentary C5
Yield displacement	Δ_y	112	90	mm	$\Delta_y = C_1*\phi_{yy}*(H_e + L_{sp})^2*1000$: Eq (5-10)
Design Base Shear					
Design maximum inelastic disp.	Δ_d	337	271	mm	$\Delta_d = \mu_d*\Delta_y$
Equivalent viscous damping ratio	ξ_e	0.144			$\xi_e = 0.05+0.444*(\mu_d - 1)/(\mu_d*\pi)$: Eq (5-24)
Damping modifier	M_ξ	0.65			$M_\xi = (0.07/(0.02+\xi_e))^{0.5}$: Eq (5-17)
Corner disp. of mod spectrum	Δ_{cm}	503		mm	$\Delta_{cm} = \Delta(3)*M_\xi$: Eq (5-18)

Item	Symbol	Trans	Long	Units	Comment / Formula
Effective structure period	T_e	2.01	1.62	s	$T_e = T_c*\Delta_d / \Delta_{cm}$
Effective secant stiffness	K_e	2,363	3,669	kN/m	$K_e = 4*\pi^2*W_s/(9.81*T_e^2)$
Design base shear	V_b	798	994	kN	$V_b = K_e*\Delta_d$ /1000
Required design base mom capacity	M_n	6,821	7,574	kN m	$M_n = V_b*H_e$: does not include P - Δ effects
Calculated Structural Parameters					
Cover to longitudinal bars	c_o	60		mm	From cover to hoops
Gross column section area	A_g	1.54		m^2	$A_g = \pi*D_c^2/4$
Area of longitudinal steel	A_s	16,085		mm^2	$A_s = N_b*\pi*d_b^2/4$
Check longitudinal steel area ratio	ρ_l	0.0104			$\rho_l = A_s/(10^6*A_g)$
Check minimum required steel area	A_{sm}	12,315		mm^2	$A_{sm} = 4*10^6\ A_g/f_y$: BM Clause 5.6.4(f)
Check maximum permitted steel area	A_{sma}	55,418		mm^2	$A_{sma} = 18*10^6\ A_g/f_y$: BM Clause 5.6.4(f)
Area of transverse reinforcement	A_t	314		mm^2	$A_t = \pi*d_t^2/4$
Volumetric ratio transverse steel	ρ_s	0.00967			$\rho_s = 4*A_t / (1000*(D_c - 2*c_v+dt)/1000)*s_t)$ Depth of core taken on centre-line of hoops Adopt Priestley et al, 1996 rather than NZS 3101 OK: min required = 0.005 : BM Clause 5.6.4(h)(i)
Strain Limits for Plastic Rotation					
Yield strength transverse reinf.	f_{sy}	500		MPa	
Strain at max stress lateral reinf.	ε_{sut}	0.10			BM Clause 5.3.5(b)
Strain at max stress longitudinal reinf.	ε_{sul}	0.10			BM Clause 5.3.5(a)
Design comp strength plastic hinge	f_{ce}	45.5		MPa	$f_{ce} = 1.3*f_c$: Table 5.7
Average confining stress	f_{ld}	2.30			$f_{ld} = 0.95*f_{sy}*\rho_s/2$: From Priestley et al, 1996
Confined comp strength concrete	f_{cc}	59.7		MPa	$f_{cc} = f_{ce}*(2.254*(1+7.94*f_{ld}/f_{ce})^{1/2} - 2*f_{ld}/f_{ce} - 1.254)$ Priestley et al 1996, Eq 5.6
Reinforcement limiting strain	ε_{sd}	0.043			$\varepsilon_{sd} = 0.015+6*(\rho_s - 0.005) \le 0.5\ \varepsilon_{sul}$: Eq (5-11)
Concrete limiting strain	ε_{cd}	0.0153			$\varepsilon_{cd} = 0.004+(1.4*\rho_s*f_{sy}*\varepsilon_{sut}) / f_{cc}$: Eq (5-12)
Neutral axis depth	c	364		mm	From moment strength analysis
Check using empirical formula	c_c	311		mm	$c_c = D_c*(0.2+0.65*W_s/(1000*f_{ce}*A_g))*1000$ Priestley et al, 2007 Eq (10.8)
Distance extreme bar to neutral axis	b_{na}	960		mm	$b_{na} = D_c*1000 - c - c_o - d_b/2$
Concrete strain from steel strain	ε	0.0163			$\varepsilon = \varepsilon_{sd}*c / b_{na}$ Concrete limiting strain governs
Limit state curvature	ϕ_{ls}	0.0421		1/m	$\phi_{ls} = IF(\varepsilon > \varepsilon_{cd}, \varepsilon_{cd}/(c/1000), \varepsilon_{sd}/(b_{na}/1000))$
Plastic curvature	ϕ_p	0.0379		1/m	$\phi_p = \phi_{ls} - \phi_{yy}$
Plastic Hinge Length					
Ratio steel ultimate over yield stress	f_u/f_y	1.2			From Pacific Steel test results
Hinge length parameter	k_{lp}	0.040			$k_{lp} = 0.2*(f_u/f_y - 1) \le 0.8$: Eq (5-38)
Distance to point of contraflexure	L_c	8.55	7.62	m	$L_c = H_e$
Plastic hinge length	L_p	0.774	0.774	m	$L_p = k_{lp}*L_c + L_{sp} \ge 2*L_{sp}$: Eq (5-37)

Item	Symbol	Trans	Long	Units	Comment / Formula
Ductility Factor Capacity					
Plastic rotation	θ_p	0.0293	0.0293	rad	$\theta_p = \phi_p * L_p$
Plastic displacement capacity	Δ_p	251	224	mm	$\Delta_p = \theta_p * L_c * 1000$
Limit state displacement capacity	Δ_{ls}	363	314	mm	$\Delta_{ls} = \Delta_y + \Delta_p$
Ductility capacity	μ_{ls}	3.23	3.48		$\mu_{ls} = \Delta_{ls}/\Delta_y$: OK > 3.0
Check P-Δ Moment					
Axial load x displacement demand	$M_{p\text{-}\Delta}$	803	645	kN m	$M_{p\text{-}\Delta} = W_s * D_d$ /1000 Ignores minor contribution from lower col.
Ratio: $M_{p\text{-}\Delta}$ / M_n	M_{rat}	0.12	0.09		> 0.1 in transverse direction Increase in mom cap reqd in trans direction < 0.25 so less than maximum limit See BM clause 5.3.7
Moment Capacity					
Required moment capacity	M_{bp}	7,223	7,574	kN m	$M_{bp} = M_n + M_{p\text{-}\Delta}/2$ (Transverse direction)
Capacity of section with 20/D32 bars	M_{bc}	7,751		kN m	OK : $M_{bc} > M_{bp}$

References:

Priestley M J N, Seible F and Calvi G M, 1996. *Seismic Design and Retrofit of Bridges*. John Wiley & Sons Inc

Priestley M J N, Calvi G M and Kowalsky, 2007. *Displacement-Based Seismic Design of Structures*. IUSS Press.

Maitai River Bridge

Analysis Case 2 (Flexible Foundation & Elastomeric Bearings): Pier Pile Stiffness

Transverse Analysis

Analyses for longitudinal and other analysis cases are similar with M_a, H_e, and H_c adjusted to appropriate values

Prepared: J Wood

Edit Date 21-Aug-17 Print Date: 21-Aug-17

Item	Symbol	Value	Units	Formula / Comments
Input Parameters				
Cylinder pile diameter inside shell	D_i	1.800	m	
Thickness of steel shell	t_s	10	mm	Design value. 12 mm used in construction
Cylinder pile length	L	11.980	m	Length at Pier C
Specified concrete strength	f_c	35	MPa	
Moment applied to pile top	M_a	7,750	kN m	Flexural capacity of 1.4 m dia pier column
Effective height of superstructure	H_e	8.552	m	Height of CoG of dynamic mass
Shear applied to pile top	V	906	kN	$V = M_a / H_e$: approximate, see Page C5-73
				For Soil D more exact shear is 868 kN
Height CoG of Column/3 + Pier Cap	H_c	6.967	m	See Page C5-56
Assumed inc of soil E with depth	m	10	MPa/m	Based on pile test results. Linear variation
Calculated Parameters				
Cylinder pile outside diameter	D	1.820	m	$D = D_i + 2*t_s/1000$
I for concrete core	I_c	0.515	m^4	$I_c = \pi*D_i^4/64$
I for shell	I_s	0.023	m^4	$I_s = \pi*(D^4 - D_i^4)/64$
Young's modulus for concrete	E_c	36,147	MPa	$E_c = 4700*Sqrt(f_c)*1.3$
				Priestley et al, 1996 Eq (5.2)
				Factor of 1.3 allows for E_c being typically
				20% - 50% greater than given by specified f_c
Combined shell + concrete core EI	EI	23,284	MN m^2	$EI = I_c*E_c + I_s*200{,}000$
Modified E_p to allow for shell	E_p	43,232	MPa	$E_p = EI/(\pi*D^4/64)$: Pender Eq 3.17
E value of soil at depth D	E_s	18.2	MPa	$E_s = m*D$: Pender Eq 3.23
Modulus ratio	K	2,375		$K = E_p / E_s$: Pender Eq 3.23
Pile Length / Diameter	L_{Dr}	6.58		$L_{Dr} = L / D$
Short pile length limit	L_r	6.21	m	$L_r = 0.07*D*(E_p / E_s)^{0.5}$: $L > L_r$: Pender Eq 3.35
Long pile length limit	L_a	13.29	m	$L_a = 1.3*D*(E_p / E_s)^{0.222}$: $L < L_a$: Pender Eq 3.27
				Pile is intermediate: assume long pile action
Depth of maximum moment	L_{Mmax}	5.45	m	$L_{Mmax} = 0.41\ L_a$: Pender Eq 3.29
Moment / Shear Ratio	e	8.552	m	$e = M_a / V$
	f	4.699		$f = M_a / (D*V)$: Pender Eq 3.18
Parameter a	a	2.819		$a = 0.6*e/D$: Pender Eq 3.30
Parameter b	b	0.107		$b = 0.17*f^{-0.3}$: Pender Eq 3.30
Parameter for maximum moment	I_{mh}	6.47		$I_{mh} = a*K^b$: Pender Eq 3.30
Maximum moment in pile	M_{max}	10,671	kN m	$M_{max} = I_{mh}*D*V$: Pender Eq 3.30

Item	Symbol	Value	Units	Formula / Comments
Flexibility and Stiffness: Long Pile: Linear Increase in E_s With Depth				
Flexibility coefficients:	f_{uHL}	0.00726	m/MN	$f_{uHL} = 3.2*K^{-0.333}/ (E_s*D)$
(Pender Eq 3.28)	f_{uML}	0.00110	MN^{-1}	$f_{uML} = 5.0*K^{-0.556} / (E_s*D^2)$
	$f_{\theta ML}$	0.00029	$(m\ MN)^{-1}$	$f_{\theta ML} = 13.6*K^{-0.778} / (E_s*D^3)$
Stiffness coefficients:	K_{HHL}	320	MN/m	$K_{HHL} = f_{\theta ML} / (f_{uHL}*f_{\theta ML} - f_{uML}^2)$
(Pender Eq 3.40)	K_{HML}	-1,204	MN	$K_{HML} = -f_{uML} / (f_{uHL}*f_{\theta ML} - f_{uML}^2)$
	K_{MML}	7,936	MN m	$K_{MML} = f_{uHL} / (f_{uHL}*f_{\theta ML} - f_{uML}^2)$
Pile head horizontal stiffness	K_{HtL}	60.0	MN/m	$K_{HtL} = (K_{HHL}*K_{MML} - K_{HML}^2) / (K_{MML} - e*K_{HML})$ Pender Eq 3.41
Pile head rotational stiffness	$K_{\theta tL}$	2,371	MN m/rad	$K_{\theta tL} = (K_{HHL}*K_{MML} - K_{HML}^2) / (K_{HHL} - K_{HML} / e)$ Pender Eq 3.42
Pile and Pier CoG Deflections from Foundation Flexibility				
Deflection at ground level	Δ_g	15	mm	$\Delta_g = V/(K_{HtL})$
Rotation at ground level	θ_g	3.3	mili rad	$\theta_g = M_a/K_{\theta tL}$
Deflection at pier CoG	Δ_t	38	mm	$\Delta_t = V/(K_{htL}) + M_a*H_c /K_{\theta tL}$

References:

Priestley M J N, Seible F and Calvi G M, 1996. *Seismic Design and Retrofit of Bridges* . John Wiley & Sons Inc

Pender M J, 1993. *Aseismic Pile Foundation Design Analysis,* NZSEE, Vol 26 No 1 pp 49 - 161

Maitai River Bridge

Analysis Case 2: Flexible Foundations and Bearings: Soil C and D: Review Method

Transverse Direction

Prepared: J Wood

Edit Date: 21/Aug/17 Print Date: 21-Aug-17

Item	Symbol	Value		Units	Comment / Formula
		Soil C	Soil D		
Structural Inputs					
Weight of superstructure on pier	W_s	1,902		kN	Excludes pier cap and column
Height of superstructure mass	H_s	8.982		m	Above pile cylinder top: see anal on p. C5-55
Height of CoG total mass	H	8.113		m	Above pile cylinder top: see anal on p. C5-56
Height of column	H_{col}	6.200		m	From drawings
Weight of pier cap	W_c	399		kN	See previous analysis on p. C5-55
Maximum depth of pier cap	H_{ca}	1.421		m	From drawings
Height of top of pier cap	H_{cap}	7.621		m	Above pile cylinder top
Height CoG of pier cap	H_c	6.967		m	Above pile cylinder top: see anal on p. C5-56
Column diameter	D_c	1.2	1.4	m	
Weight of pier column	W_{co}	175	239	kN	
Weight of pier cap + column/3	W_{cc}	457	478	kN	$W_{cc} = W_c + W_{co}/3$
Height CoG of pier	H_{cogc}	6.869	6.839	m	$H_{cogc} = (W_c*H_c+W_{co}*H_{col}/3)/W_{cc}$
					1/3 column mass at underside cap. See BM C5
Total dynamic weight of span	W_d	2,359	2,380	kN	$W_d = W_s+W_c+W_{co}/3$: not including abutments
Diameter longitudinal bars	d_b	32	32	mm	
Number of longitudinal bars	N_b	20	28		
Diameter of transverse hoop bars	d_t	16	20	mm	
Spacing transverse hoop bars	s_t	120	100	mm	
Cover to hoops	c_v	40		mm	
Specified concrete strength	f_c	35		MPa	
Specified steel yield stress	f_y	300	500	MPa	Longitudinal and transverse
Foundation Stiffness Inputs					
Horizontal stiffness at ground level	K_h	60		MN/m	See previous analysis on Page C5-70
Rotational stiffness at ground level	K_θ	2,370		MN m/ra	See previous analysis on Page C5-70
Inputs for Elastomeric Bearings on Piers					
Shear modulus	G_b	0.73		MPa	53 IRHD - Skellerup brochure
Width of bearing	B_b	350	380	mm	Size greater than on drawings Trans direction
Length of bearing	L_b	280	380	mm	Size greater than on drawings Long direction
Total thickness of bearing	t_t	131		mm	= (90 rubber + 24 plates + top and btm cover)
Thickness of rubber	t_r	90		mm	9 inner layers at 10 mm
					Bearings are dowelled. Ignore cover rubber.
Side cover	s_c	7		mm	Skellerup brochure
Number bearings on each pier	N_{be}	8			
Bonded area of rubber	A_{bl}	0.0894	0.1340	m^2	$A_{bl} = (B_b - 2*s_c)*(L_b - 2*s_c)/10^6$
					Cover rubber ignored. Some guidelines include it.
Shear stiffness	K_d	0.72	1.09	MN/m	$K_d = G_b*A_{bl}/(t_r/1000)$
Total stiffness of bearings on pier	K_{dt}	5,800	8,692	kN/m	$K_{dt} = 1000*K_d*N_{be}$

Item	Symbol	Soil C	Soil D	Units	Comment / Formula
Earthquake Inputs					
Site Subsoil Category		C	D		
Zone Factor	Z	0.27			Nelson
Return Period Factor	R_u	1.8			2,500 year return period
Corner period spectral shape factor	$\Delta_h(3)$	985	1,585	mm	From BM Table 5.5
Corner period displacement	$\Delta(3)$	479	770	mm	$\Delta(3) = R_u*Z*\Delta_h(3)$
Calculated Structural Parameters					
Cover to longitudinal bars	c_o	56	60	mm	From cover to hoops
Young's modulus concrete	E_c	29,580		MPa	$E_c = 5000*Sqrt(f_c)$: Priestley et al, 2007, Eq (4.43)
					Equation used to drive stiffness ratio curves.
Area of longitudinal steel	A_s	16,085	22,519	mm^2	$A_s = N_b*\pi*d_b^2/4$
Area of transverse reinforcement	A_t	201	314	mm^2	$A_t = \pi*d_t^2/4$
Volumetric ratio transverse steel	ρ_s	0.00607	0.00967		$\rho_s = 4*A_t / (1000*(D_c - (2*c_v + d_t)/1000)*s_t)$
					Depth of core taken on centre-line of hoops
					Adopt Priestley et al 1996 rather than NZS 3101
Area of pier column	A_g	1.131	1.539	m^2	$A_g = \pi*D_c^2/4$
Longitudinal reinforcement ratio	ρ_l	0.0142	0.0146		$\rho_l = A_s/(A_g*10^6)$
Axial force ratio in column	R_{af}	0.063	0.047		$R_{af} = (W_s+W_c+W_{co})/(A_g*f_c*1000)$
Pier stiffness ratio	R_{st}	0.38	0.37		From Priestley et al, 2007. Fig 4.12
Cracked stiffness of pier column	K_p	7,106	10,910	kN/m	$K_p = \Delta_y/\Delta_{yc}*(3*\pi*D_c^4*R_{st}*E_c*1000)/$
(displacements at CoG of pier)					$(64*(H_{cogc} + L_{sp})^3)$
					For comparison with yield stiffness based on pier
					yield disp & shear. Δ_y, Δ_{yc} and K_y calculated below
Yield Displacement at Top of Pier and Flexural Strength					
Probable yield stress for reinf.	f_{ye}	330	550	MPa	$f_{ye} = 1.1*f_y$: BM Table 5.7
Steel elastic modulus	Es	200,000		MPa	
Yield strain	ε_y	0.00165	0.00275		$\varepsilon_y = f_{ye} / E_s$
Yield curvature	ϕ_{yy}	0.00296	0.00422	1/m	$\phi_{yy} = 2.15*\varepsilon_y / D_c$: Eq (5-8)
Strain penetration length	L_{sp}	0.232	0.387	m	$L_{sp} = 0.022*f_{ye}*d_b/1000$: See def of terms
					for Eq (5-10)
Flexural strength of column -	M_n	3,500	7,500	kNm	Flexural strength anal: f_y = 330 & 550 MPa
used to calculate shear in column			Reduced from 3,672 kNm & 7,751 kNm to allow for P-Δ mom		
Shear in pier at flexural capacity	V_y	431	924	kN	$V_y = M_n/H$
					Approximate. See 1st mode shear below.
Coefficient for column fixity	C_1	0.33	0.33		See Bridge Manual Commentary C5
Pier CoG disp. due to foundn Δ & θ	Δ_f	17	37	mm	$\Delta_f = V_y/K_h + M_n*H_{cogc}/K_\theta$
Pier CoG disp. due to col. at yield	Δ_y	50	74	mm	$\Delta_y = C_1*\phi_{yy}*(H_{cogc} + L_{sp})^2*1000$: Eq (5-10)
Total displacement at CoG pier	Δ_{yc}	67	111	mm	$\Delta_{yc} = \Delta_y + \Delta_f$
Elastic Period of Vibration: See Equations (C5A-1) to (C5A-6)					
Calculate period of vibration assuming elastic response of pier					
Use two-degree of freedom vibration theory from Thompson, 1965 to calculate period and mode shape					
Pier stiffness modifier	S_{ma}	0.93	0.93		Used to adjust pier stiffness: iterate until $M_b = M_n$
					M_b calculated below
Pier stiffness at yield	K_y	5,986	7,776	kN/m	$K_y = S_{ma}*V_y/(\Delta_{yc}/1000)$
Height modifier for mass disps	aa	0.31	0.31		$aa = (H_s/H_{cogc} - 1)$
					Rotation of pier increases disp of W_s by (1+aa)

Item	Symbol	Soil C	Soil D	Units	Comment / Formula
Quadratic equation coefficient B	B_e	-321	-438	$(rad/s)^2$	$B_e = -9.81*(K_{dt}/W_s+(K_y+K_{dt}*(1+aa))/W_{cc})$
Quadratic equation coefficient C	C_e	3,844	7,151	$(rad/s)^4$	$C_e = 9.81^2*(K_y*K_{dt})/(W_s*W_{cc})$
Angular frequency first mode	ω_e	3.5	4.1	rad/s	$\omega_e = Sqrt((-B_e - Sqrt(B_e^2 - 4*C_e))/2)$
First mode period - elastic response	T_y	1.78	1.53	s	$T_y = 2*\pi/\omega_e$
Mode shape	A_{rae}	1.93	1.80		$A_{rae} = (K_y + K_{dt} - W_{cc}*\omega_e^2/9.81)/K_{dt}$
Displacement in Bearings at Pier Yield Capacity					
Disp of superstructure at pier yield	Δ_{sa}	150	234	mm	$\Delta_{sa} = \Delta_{yc}*(A_{rae} + aa)$: Eq (C5A-9)
Displacement in bearings	Δ_{bb}	62.5	88	mm	$\Delta_{bb} = \Delta_{yc}*(A_{rae} - 1)$: Eq (C5A-8)
Check disp in bearings	Δ_{bbc}	62.5	88	mm	$\Delta_{bbc} = W_s*\Delta_{sa}*\omega_e^2/(9.81*K_{dt})$: Eq (C5A-12)
Check base moment	M_b	3,522	7,526	kN m	$M_b = (W_s*\Delta_{sa}*H_s + W_{cc}*\Delta_{yc}*H_{cogc})*\omega_e^2/(1000*9.81)$ Eq (C5A-11)
Shear force in bearings	V_b	362	768	kN	$V_b = \Delta_{bb}*K_{dt}/1000$
Shear from inertia force on pier	V_{cs}	39	91	kN	$V_{cs} = (W_{cc}*\Delta_{yc}*\omega_e^2)/(9.81*1000))$
Base shear in 1st mode response	V_{ba}	401	860	kN	$V_{ba} = V_b + V_{cs}$
Shear strain in bearing rubber	ε_{by}	0.69	0.98		$\varepsilon_{by} = \Delta_{bb} / t_r$: acceptable if $\varepsilon_{by} < 1.0$.
Elastic Displacement					
Modal participitation factor	P_e	1.06	1.06		$P_e = (W_s+W_{cc}/A_{rae})/(W_s+W_{cc}/(A_{rae})^2)$ From Eq (C5A-17)
Elastic displacement superstruct	$\Delta(T_{el})$	300	414	mm	$\Delta(T_{el}) = P_e*\Delta(3)*T_y/3$
Elastic displacement at CoG pier	Δ_{coe}	176	238		$\Delta_{coe} = \Delta(T_{el})/(A_{ra}+aa)$: Eq (C5A-9)
Approx ductility demand on column	μ	3.20	2.74		$\mu = (\Delta_{coe} - \Delta_f)/(\Delta_y)$: equal disp. assumption
Strain Limits for Plastic Rotation & Curvatures					
Yield strength transverse reinf.	f_{sy}	300	500	MPa	
Strain at max stress lateral reinf.	ε_{sut}	0.12	0.10		BM Clause 5.3.5(b)
Strain at max stress longitud. reinf.	ε_{sul}	0.12	0.10		BM Clause 5.3.5(a)
Design comp strength plastic hinge	f_{ce}	45.5	45.5	MPa	$f_{ce} = 1.3*f_c$: Table 5.7
Average confining stress	f_{ld}	0.87	2.30		$f_{ld} = 0.95*f_{sy}*\rho_s/2$: From Priestley et al, 1996
Confined comp strength concrete	f_{cc}	51.2	59.7	MPa	$f_{cc} = f_{ce}*(2.254*(1+7.94*f_{ld}/f_{ce})^{1/2} - 2*f_{ld}/f_{ce} - 1.254)$ Priestley et al, 1996. Eq (5.6)
Reinforcement limiting strain	ε_{sd}	0.021	0.043		$\varepsilon_{sd} = 0.015+6*(\rho_s - 0.005) \le 0.5\ \varepsilon_{sul}$: Eq (5-11)
Concrete limiting strain	ε_{cd}	0.0100	0.0153		$\varepsilon_{cd} = 0.004+(1.4*\rho_s*f_{sy}*\varepsilon_{sut})/f_{cc}$: Eq (5-12)
Neutral axis depth	c	282	364	mm	From moment strength analysis
Check using empirical formula	c_{ce}	278	313	mm	$c_{ce} = D_c*10^3*(0.2+0.65*(W_{co}+W_c+W_s)/(10^3*f_{ce}*A_g))$ Priestley et al 2007. Eq (10.8) OK: reasonable agreement
Distance extreme bar to neutral axis	b_{na}	846	960	mm	$b_{na} = D_c*1000 - c - c_o - d_b/2$
Concrete strain from steel strain	ε	0.0071	0.0163		$\varepsilon = \varepsilon_{sd}*c / b_{na}$ Soil C: Steel limiting strain governs Soil D: Concrete limiting strain governs
Limit state curvature	ϕ_{ls}	0.0253	0.0421	1/m	$\phi_{ls} = IF(\varepsilon > \varepsilon_{cd}, \varepsilon_{cd}/(c/1000), \varepsilon_{sd}/(b_{na}/1000))$
Plastic curvature	ϕ_p	0.0224	0.0379	1/m	$\phi_p = \phi_{ls} - \phi_{yy}$

Item	Symbol	Soil C	Soil D	Units	Comment / Formula
Plastic Hinge Length and Ductility Factor Capacity					
Ratio steel ultimate over yield stress	f_u/f_y	1.4	1.2		From Pacific Steel test results
Hinge length parameter	k_{lp}	0.08	0.04		$k_{lp} = 0.2*(f_u / f_y - 1) \le 0.08$: Eq (5-38)
Distance to point of contraflexure	L_c	8.11	8.11	m	$L_c = H$
Plastic hinge length	L_p	0.88	0.77	m	$L_p = k_{lp}*L_c + L_{sp} \ge 2*L_{sp}$: Eq (5-37)
Plastic rotation	θ_p	0.0197	0.0293	rad	$\theta_p = \phi_p*L_p$
Plastic displacement	Δ_p	135	201	mm	$\Delta_p = \theta_p*H_{cogc}*1000$: Eq (5-36)
Limit state displacement capacity	Δ_{ls}	185	274	mm	$\Delta_{ls} = \Delta_y + \Delta_p$
Ductility capacity	μ_{ls}	3.73	3.73		$\mu_{ls} = \Delta_{ls}/\Delta_y$
			For Soil C & D:		Capacity > Approximate demand Design probably OK
Ductility Iteration for Superstructure Response					
Iterate assumed ductility in pier to give calculated base moment = yield base moment - (P-Δ moment/2)					
Assumed ductility demand on pier	μ_{ap}	2.76	2.28		Used to modify pier stiffness
Pier stiffness - modified for ductility	K	2,613	4,240	kN/m	$K = V_p/((\mu_{ap}*\Delta_y + \Delta_f)/1000)$: V_p calculated below
					For initial trial can use V_{ba} from above (pier yield)
Calculated base moment	M_{bc}	3,520	7,559	kN m	$M_{bc} = (W_s*\Delta_{de}*H_s + W_{cc}*\Delta_{cog}*H_{cogc})*\omega^2/(9.81*1000)$
					From Eq (C5A-11)
					Δ_{de}, Δ_{cog} and ω are calculated below
					OK: $M_{bc} = M_n$
Calculate period of vibration assuming equivalent elastic response of pier. See Equations (C5A-1) to (C5A-6) *Use two-degree of freedom vibration theory from Thompson, 1965 to calculate period and mode shape*					
Quadratic equation coefficient B	B_c	-249	-366	$(rad/s)^2$	$B_c = -9.81*(K_{dt}/W_s + (K + K_{dt}*(1+aa))/W_{cc})$
Quadratic equation coefficient C	C_c	1,678	3,899	$(rad/s)^4$	$C_c = 9.81^2*(K*K_{dt})/(W_s*W_{cc})$
Angular frequency	ω	2.6	3.3	rad/s	$\omega = Sqrt((-B_c - Sqrt(B_c^2 - 4*C_c))/2)$
First mode effective period	T	2.39	1.90	s	$T = 2*\pi/\omega$: T > Ty
Mode shape	A_{ra}	1.39	1.43		$A_{ra} = (K + K_{dt} - W_{cc}*\omega^2/9.81)/K_{dt}$
Participipation factor	P	1.04	1.05		$P = (W_s + W_{cc}/A_{ra})/(W_s + W_{cc}/A_{ra}^2)$
					From Eq (C5A-17)
Design disp. elastic spectrum	$\Delta(T)$	397	510	mm	$\Delta(T) = P*\Delta(3)*T/3$
Iterate displacement demand until $\Delta_d(T) = \Delta_{de}$					
Estimated displacement demand	Δ_{de}	263	356	mm	Displacement of superstructure mass
Calculated displacement demand	$\Delta_d(T)$	263	356	mm	$\Delta_d(T) = \Delta(T)*M_\xi$: M_ξ calculated below
Damping and Ductility Demand					
Displacement in bearings	Δ_i	61	87	mm	$\Delta_i = W_s*\Delta_{de}*\omega^2/(9.81*K_{dt})$: Eq (C5A-12)
Check displacement in bearings	Δ_{ic}	61	87	mm	$\Delta_{ic} = \Delta_{de}*(1 - (1+aa)/(A_{ra}+aa))$: Eq (C5A-10)
Shear strain in bearing rubber	ε_b	0.68	0.97		$\varepsilon_b = \Delta_i / t_r$: $\varepsilon_b < 1.0$: bearings OK
Disp at CoG of pier	Δ_{cog}	154	205	mm	$\Delta_{cog} = \Delta_{de}/(A_{ra}+aa)$: Eq (C5A-9)
Shear force in bearings	V_{pb}	354	758	kN	$V_{pb} = W_s*\Delta_{de}*\omega^2/9.81$
Inertia force from pier cap + column	F_{ci}	50	110	kN	$F_{ci} = \Delta_{cog}*\omega^2*W_{cc}/(1000*9.81)$
Shear force in pier	V_p	404	868	kN	$V_p = V_{pb} + F_{ci}$

Item	Symbol	Soil C	Soil D	Units	Comment / Formula
Viscous damping ratio for bearings	ξ	0.05	0.05		From BM Clause 5.4.3(g)(vi)
Damping from pier	ξ_e	0.17	0.15		$\xi_e = 0.10+0.04*(\mu_{ap} -1) \le 0.18$: Eq (5-32)
					Assume cylinder/column equivalent to pile/column
Combined damping bearings + pier	ξ_c	0.14	0.12		$\xi_c = (V_p*\Delta_{cog}*\xi_e + V_{pb}*\Delta_i*\xi)/(V_p*\Delta_{cog} + V_{pb}*\Delta_i)$:
					Eq (5-23)
Damping reduction factor	M_ξ	0.66	0.70		$M_\xi = (0.07/(0.02+\xi_c))^{0.5}$: Eq (5-17)
Ductility demand on pier column	μ_{Id}	2.76	2.28		$\mu_{Id} = (\Delta_{cog} - \Delta_f)/\Delta_y$
Ratio: ductility capacity/demand	R_{cd}	1.35	1.64		$R_{cd} = \mu_{Is}/\mu_{Id}$: $R_{cd} > 1.0$: Design OK
					Could increase hoop spacing for Soil D
Check P-Δ Moment					
Dynamic weight x disp demand	$M_{p-\Delta}$	571	775	kN m	$M_{p-\Delta} = (W_s*\Delta_{de} + W_{cc}*\Delta_{cog})/1000$
					Small contribution from lower col. ignored
Ratio: $M_{p-\Delta}$ / M_{bc}	M_{rat}	0.16	0.10		> 0.1. Increase in moment capacity required
					< 0.25 maximum limit. See BM clause 5.3.7
Moment Capacity					
Required moment capacity	M_{bp}	3,805	7,947	kN m	$M_{bp} = M_n + M_{p-\Delta}/2$
Capacities with 20 & 28 /D32 bars	M_{bca}	3,672	7,751	kN m	OK: capacities slightly less than demands

References:

Priestley M J N, Seible F and Calvi G M, 1996. *Seismic Design and Retrofit of Bridges*. John Wiley & Sons Inc

Priestley M J N, Calvi G M and Kowalsky, 2007. *Displacement-Based Seismic Design of Structures*. IUSS Press.

Thompson W T, 1965. *Vibration Theory and Applications*. Prentice-Hall Inc

Maitai River Bridge

Analysis Case 2 (Flexible Foundation & Elastomeric Bearings): Abutment Pile Stiffness

Longitudinal Analysis

Prepared: J Wood

Edit Date: 21-Aug-17 Print Date: 21-Aug-17

Item	Symbol	Value	Units	Formula / Comments
Input Parameters				
Cylinder pile diameter inside shell	D_i	1.00	m	
Thickness of steel shell	t_s	6	mm	Design value. 12 mm used in construction
Cylinder pile length	L	12.0	m	
Specified concrete strength	f_c	35	MPa	
Shear applied to pile top	V	1,000	kN	Nominal value for stiffness calculation
Height of brg seating above pile top	H_c	1.50	m	
Moment applied to pile top	M_a	1,500	kN m	$M_a = H_c*V$ (nominal value)
Assumed inc of soil E with depth	m	10	MPa/m	Based on pile test results. Linear variation
Calculated Parameters				
Cylinder pile outside diameter	D	1.012	m	$D = D_i + 2*t_s/1000$
I for concrete core	I_c	0.049	m^4	$I_c = \pi*D_i^4/64$
I for shell	I_s	0.002	m^4	$I_s = \pi*(D^4 - D_i^4)/64$
Young's modulus for concrete	E_c	36,147	MPa	E_c =4700*Sqrt(f_c)*1.3: Priestley et al, 1996 Eq (5.2) Factor of 1.3 allows for E_c being typically 20% - 50% greater than given by 28 day f_c
Combined shell + concrete core EI	EI	2,254	MN m^2	$EI = I_c*E_c + I_s*200{,}000$
Modified E_p to allow for shell	E_p	43,782	MPa	$E_p = EI/(\pi*D^4/64)$: Pender Eq 3.17
E value of soil at depth D	E_s	10.1	MPa	$E_s = m*D$
Modulus ratio	K	4,326		$K = E_p / E_s$
Pile Length / Diameter	L_{Dr}	11.86		$L_{Dr} = L / D$
Short pile length limit	L_r	4.66	m	$L_r = 0.07*D*(E_p / E_s)^{0.5}$: $L > L_r$
Long pile length limit	L_a	8.44	m	$L_a = 1.3*D*(E_p / E_s)^{0.222}$: $L < L_a$
				$L > L_a$: pile is long
Depth of maximum moment	L_{Mmax}	3.46	m	$L_{Mmax} = 0.41\ L_a$: Pender Eq 3.29
Moment / Shear Ratio	e	1.500	m	$e = M_a / V$
	f	1.482		$f = M_a / (D*V)$: Pender Eq 3.18
Parameter a	a	0.889		a = 0.6*e/D: Pender Eq 3.30
Parameter b	b	0.151		$b = 0.17*f^{-0.3}$: Pender Eq 3.30
Parameter for maximum moment	I_{mh}	3.15		$I_{mh} = a*K^b$: Pender Eq 3.30
Maximum moment in pile	M_{max}	3,188	kN m	$M_{max} = I_{mh}*D*V$: Pender Eq 3.30

Item	Symbol	Value	Units	Formula / Comments
Flexibility and Stiffness: Long Pile: Linear Increase in E_s With Depth				
Flexibility coefficients:	f_{uHL}	0.01923	m/MN	$f_{uHL} = 3.2*K^{-0.333}/ (E_s*D)$
(Pender Eq 3.28)	f_{uML}	0.00459	MN^{-1}	$f_{uML} = 5.0*K^{-0.556} / (E_s*D^2)$
	$f_{\theta ML}$	0.00192	$(m\ MN)^{-1}$	$f_{\theta ML} = 13.6*K^{-0.778} / (E_s*D^3)$
Stiffness coefficients:	K_{HHL}	121	MN/m	$K_{HHL} = f_{\theta ML} / (f_{uHL}*f_{\theta ML} - f_{uML}^2)$
(Pender Eq 3.40)	K_{HML}	-288	MN	$K_{HML} = -f_{uML} / (f_{uHL}*f_{\theta ML} - f_{uML}^2)$
	K_{MML}	1209	MN m	$K_{MML} = f_{uHL} / (f_{uHL}*f_{\theta ML} - f_{uML}^2)$
Pile head horizontal stiffness	K_{HtL}	38.3	MN/m	$K_{HtL} = (K_{HHL}*K_{MML} - K_{HML}^2) / (K_{MML} - e*K_{HML})$
Pile head rotational stiffness	$K_{\theta tL}$	201	MN m/rad	$K_{\theta tL} = (K_{HHL}*K_{MML} - K_{HML}^2) / (K_{HHL} - K_{HML} / e)$
Pile and Pier Seating Deflections and Seating Stiffness				
Deflection at ground level	Δ_g	26.1	mm	$\Delta_g = V/(K_{HtL})$
Rotation at ground level	θ_g	7.5	milli rad	$\theta_g = M_a /K_{\theta tL}$
Deflection at abutment seating level	Δ_p	37	mm	$\Delta_p = V/(K_{HtL}) + M_a*H_c /K_{\theta tL}$
Stiffness at seating level	K_a	27	MN/m	$K_a = V/\Delta_p$

References:

Priestley M J N, Seible F and Calvi G M, 1996. *Seismic Design and Retrofit of Bridges*. John Wiley & Sons Inc

Pender M J, 1993. *Aseismic Pile Foundation Design Analysis,* NZSEE, Vol 26 No 1 pp 49 - 161

Maitai River Bridge

Analysis Case 2: Abutment Passive Resistance and Stiffness

Longitudinal Analysis

Method:

Kahalili-Tehrani P, Taciroglu E, and Shamsadadi A, 2010.

Backbone curves for passive response of walls with homogenous backfills

Soil-Foundation-Structure Interaction,Taylor & Francis Group, London.

Prepared: J Wood

Edit Date: 21-Aug-17 Print Date: 21-Aug-17

Item	Symbol	Value	Units	Comment
Input Parameters				
Assumed friction angle	ϕ	35	deg	Dense gravel backfill
Assumed cohesion	c	0.0	kPa	
Assumed soil unit weight	γ_s	19.0	kN/m^2	
Strain at 50% ultimate stress	ε_s	0.0035		Estimated
Abutment wall height	H_w	3.455	m	From drawings: total height of pile cap and backwall
Abutment wall width	B_w	10.330	m	From drawings
Calculated Parameters				
Soil friction angle	ϕ_r	0.61	rad	ϕ_r = Radians(ϕ)
Beta parameter	β	4.42		$\beta = (1703-683.4*(\tan(\phi_r))^{1.23})*\varepsilon_s$
Alpha parameter	α	62		α = IF(f = 0,0.5*γ_s+2.63*c, $(5.62*(\tan(\phi_r))^2+0.53)*\gamma_s+(10.58*(\tan(\phi_r))^{1.79}+2.86)*c)$
n parameter	n	2.00		$n = IF(c = 0, 2, (0.9*(\tan(\phi_r))^{1.2} + 1.49)/(Sqrt(c))+0.9)$
η parameter	η	8.1		η = IF(c = 0, 14.36 - 7.49*Sqrt(tan(ϕ_r)), IF(ϕ < 5,15.47,18.1 - 9.38*Sqrt(tan(ϕ_r))))
a_r value	a_r	100		$a_r = (\eta - 1)*\alpha / \beta$
b_r value	b_r	1.38		$b_r = (\eta - 2) / \beta$

Abutment Force vs Disp Curve

Disp mm Δ	Force kN F	Dim Force F_d	Force/ Disp kN/mm
0	0	0.0	0
2	663	0.6	331
4	1,234	1.1	308
6	1,731	1.5	289
8	2,169	1.9	271
10	2,556	2.2	256
14	3,212	2.7	229
18	3,747	3.2	208
24	4,384	3.7	183
30	4,883	4.2	163

$F = (a_r*\Delta /10*H_w^n/(H_w + b_r*\Delta /10))*B_w$

$F_d = F /(0.5*\gamma_s*H_w^2*B_w)$

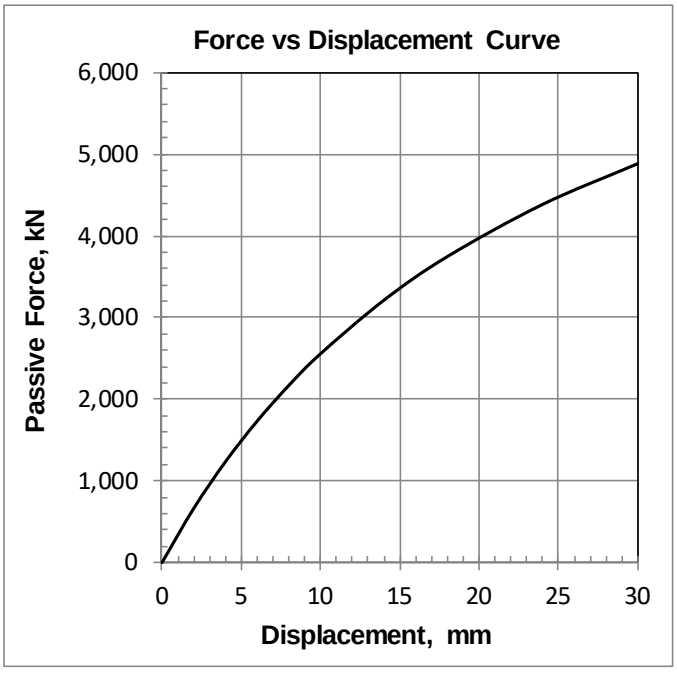

Maitai River Bridge

Analysis Case 2: Flexible Foundations and Bearings: Soil C & D: Review Method

Longitudinal Direction

Prepared: J Wood

Edit Date: 21-Aug-17 Print Date: 21-Aug-17

Item	Symbol	Value		Units	Comment / Formula
		Soil C	Soil D		
Structural Inputs					
Weight of superstructure on piers	W_s	9,500		kN	Five spans at 1,900 kN/span
Height of superstructure mass	H_s	8.982		m	Above pile cylinder top: see analysis on p. C5-55
Height of CoG total mass	H	8.113		m	Above pile cylinder top: see analysis on p. C5-56
Height of column	H_{col}	6.200		m	From drawings
Total weight of pier caps	W_c	1,596		kN	Four caps at 399 kN/cap: see analysis on p. C5-55
Maximum depth of pier cap	H_{ca}	1.421		m	From drawings
Height of top of pier cap	H_{cap}	7.621		m	Above pile cylinder top
Height CoG of pier cap	H_c	6.967		m	Above pile cylinder top: see analysis on p. C5-56
Weight of pier columns	W_{co}	673	916	kN	
Weight of pier caps + columns/3	W_{cc}	1,820	1,901	kN	$W_{cc} = W_c + W_{co}/3$
Height CoG piers	H_{cogc}	6.872	6.844	m	$H_{cogc} = (W_c*H_c+W_{co}*H_{col}/3)/W_{cc}$
					Column mass at underside cap. BM Comm C5
Total dynamic weight	W_d	11,320	11,401	kN	$W_d = W_s + W_c + W_{co}/3$: not including abuts
Weight of each abutment	W_a	930	930	kN	Does not include approach slab. Approach slab and soil above slab included in M-O active wedge.
Column diameter	D_c	1.2	1.4	m	
Diameter longitudinal bars	d_b	32	32	mm	
Number of longitudinal bars	N_b	20	28		
Diameter of transverse hoop bars	d_t	16	20	mm	
Spacing transverse hoop bars	s_t	120	100	mm	
Cover to hoops	c_v	40		mm	
Specified concrete strength	f_c	35		MPa	
Specified steel yield stress	f_y	300	500	MPa	Longitudinal and transverse
Foundation Stiffness Inputs					
Horizontal stiffness at ground level	K_h	60		MN/m	See previous analysis on Page C5-70
Rotational stiffness at ground level	K_θ	2,380		MN m/rad	See previous analysis on Page C5-70
Abutment Backfill and Backwall Dimensions					
Backfill friction angle	ϕ_b	35		deg	
Backfill friction angle - radians	ϕ_{br}	0.611		rad	
Soil unit weight	γ_s	19		kN/m^3	
Backwall height	H_w	3.46		m	
Backwall width	B_w	10.33		m	

Item	Symbol	Soil C	Soil D	Units	Comment / Formula
Inputs for Elastomeric Bearings on Piers					
Shear modulus	G_b	0.73		MPa	53 IRHD - Skellerup brochure
Width of bearing	B_b	350	380	mm	Size greater than on drawings Trans direction
Length of bearing	L_b	280	380	mm	Size greater than on drawings Long direction
Total thickness of bearing	t_t	131		mm	= (90 rubber + 24 plates + top and bot cover)
Thickness of rubber	t_r	90		mm	9 inner layers at 10 mm
					Bearings are dowelled. Ignore cover rubber.
Side cover	s_c	7		mm	Skellerup brochure
Total number bearings on piers	N_{be}	32			8 on each of 4 piers
Bonded area of rubber	A_{bl}	0.0894	0.1340	m^2	$A_{bl} = (B_b - 2*s_c)*(L_b - 2*s_c)/10^6$ Cover rubber ignored. Some guidelines include.
Shear stiffness	K_d	0.72	1.09	MN/m	$K_d = A_{bl} * G_b / (t_r/1000)$
Total stiffness of brgs on 4 piers	K_{dt}	23,198	34,769	kN/m	$K_{dt} = K_d * N_{be} * 1000$
Inputs for Elastomeric Bearings on Abutments					
Width of bearing	B_{ba}	380		mm	From drawings. Bridge transverse direction
Length of bearing	L_{ba}	300		mm	From drawings. Bridge longitudinal direction
Thickness of rubber	t_{ra}	100		mm	10 inner layers at 10 mm
Side cover	s_{ca}	10		mm	Skellerup brochure
Bonded area of rubber	A_{bra}	0.1008		m^2	7 mm side covers
Shear stiffness	K_{ra}	0.74		MN/m	$K_{ra} = A_{bra} * G_b / (t_{ra}/1000)$
Number bearings on each abut	N_{ba}	4			
Total stiffness bearings each abut	K_{rat}	2,943		kN m	$K_{rat} = K_{ra} * N_{ba} * 1000$
Earthquake Inputs					
Site Subsoil Category		C	D		
Zone Factor	Z	0.27			Nelson
Return Period Factor	R_u	1.8			2500 year return period
Peak ground acceleration	a_p	0.646	0.544	g	Soil C: $a_p = 1.33*Z*R_u$ Soil D: $a_p = 1.12*Z*R_u$
Corner period spectral shape factor	$\Delta_h(3)$	985	1,585	mm	From Table 5.5 in BM
Corner period displacement	$\Delta(3)$	479	770	mm	$\Delta(3) = R_u*Z*\Delta_h(3)$
Calculated Structural Parameters					
Cover to longitudinal bars	c_o	56	60	mm	From cover to hoops
Young's modulus concrete	E_c	29,580		MPa	$E_c = 5000*\mathrm{Sqrt}(f_c)$ Priestley et al, 2007 Eq (4.43)
					Equation used to derive stiffness ratio curves
Area longitudinal column steel	A_s	16,085	22,519	mm^2	$A_s = N_b * \pi * d_b^2/4$
Area transverse column reinf.	A_t	201	314	mm^2	$A_t = \pi * d_t^2/4$
Volumetric ratio transverse steel	ρ_s	0.00607	0.00967		$\rho_s = 4*A_t / (1000*(D - (2*c_v + d_t)/1000)*s_t)$
					Depth of core taken on centre-line of hoops
					Adopt Priestley et al 1996 rather than NZS 3101
Area of pier column	A_{co}	1.131	1.539	m^2	$A_{co} = \pi * D_c^2/4$
Longitudinal reinforcement ratio	ρ_l	0.0142	0.0146		$\rho_l = A_s/(A_{co}*10^6)$
Axial force ratio in column	R_{af}	0.062	0.047		$R_{af} = (W_s/5 + W_c/4 + W_{co}/4)/(A_{co}*f_c*1000)$
Pier stiffness ratio	R_{st}	0.38	0.37		From Priestley et al, 2007, Fig 4.12
Cracked stiffness of pier column	K_p	7,053	10,682	kN/m	$K_p = \Delta_y/\Delta_{yt} * (3*\pi*D^4*R_{st}*E_c*1000)/(64*(H_{cogc}+L_{sp})^3)$
(Displacements at CoG of pier)					Used for comparison with yield stiffness

Item	Symbol	Soil C	Soil D	Units	Comment / Formula
Yield Displacement at Top of Pier and Flexural Strength					
Probable yield stress for reinf.	f_{ye}	330	550	MPa	$f_{ye} = 1.1*f_y$: Table 5.7 in BM
Young's modulus steel	E_s	200,000		MPa	
Yield strain	ε_y	0.00165	0.00275		$\varepsilon_y = f_{ye} / E_s$
Yield curvature	ϕ_{yy}	0.00296	0.00422	1/m	$\phi_{yy} = 2.15*\varepsilon_y / D_c$: Eq (5-8)
Strain penetration length	L_{sp}	0.232	0.387	m	$L_{sp} = 0.022*f_{ye}*d_b$ /1000: Eq (5-10)
Coefficient for column fixity	C_1	0.333	0.333		See Appendix G in BM
Flexural strength of each column - used to calculate shear in column	M_n	3,500	7,751	kNm	Flexural strength analysis: Soil C, f_y = 330 MPa M_n reduced from 3,672 kNm to allow for P-Δ mom Soil D, f_y = 550 MPa: no P-Δ reduction required
Shear in pier at flexural capacity	V_y	459	1,017	kN	$V_y = M_n / H_{cap}$ Approximate. See 1st mode shear below.
Displacement from foundation	Δ_f	18	39	mm	$\Delta_f = V_y / K_h + M_n*H_{cogc} / K_\theta$
Disp from pier column at CoG pier	Δ_y	50	74	mm	$\Delta_y = C_1*\phi_{yy}*(H_{cogc} + L_{sp})^2*1000$: Eq (5-10)
Total yield disp at pier CoG	Δ_{yt}	68	113	mm	$\Delta_{yt} = \Delta_f + \Delta_y$
Overall Elastic Stiffness of Abutments					
Stiffness of two abutment piles	K_{api}	54,000		kN/m	See separate analysis on Page C5-77
Stiffness of abutment backwall	K_{aw}	300,000		kN/m	See separate analysis on Page C5-78 Stiffness at 5 mm displacement
Stiffness of push abutment	K_a	354,000		kN/m	$K_a = K_{api} + K_{aw}$
Stiffness push abut include brgs	K_{aa}	2,919		kN/m	$K_{aa} = 1/(1/K_a + 1/K_{rat})$
Abutment inertia force from PGA	F_i	601	506	kN	$F_i = W_a*a_p$
Inertia angle	α	0.574	0.50	rad	$\alpha = \text{Atan}(a_p)$
M-O active pressure coefficient	K_{AE}	1.054	0.793		$K_{AE} = (\text{Cos}(\phi_{br} - \alpha))^2 /$ $((\text{Cos}(\alpha))^2*(1+\text{Sqrt}(\text{Sin}(\phi_{br})*\text{Sin}(\phi_{br}-\alpha)/\text{Cos}(\alpha)))^2)$ Assuming zero friction on wall backface.
Active pressure force on abutment	F_{AE}	1,235	929	kN	$F_{AE} = 0.5*K_{AE}*H_w^2*B_w*\gamma_s$
Abutment inertia + active MO force	F_{ip}	1,836	1,435	kN	Reduces effective stiffness.
Assumed shear carried by pull abut	V_{ap}	522	786	kN	Iteration is required to determine V_{ap} See calculated value for V_{bu} below for ductile resp. Only approximate for yield response
Stiffness pull abut including brgs	K_{app}	2,362	2,551	kN/m	$K_{app} = K_{rat}*K_{api}/(K_{api}+K_{rat}*(1+F_{ip} / V_{ap}))$ From Eq (C5A-21)
Combined stiffness both abuts	K_{ab}	5,281	5,470	kN/m	$K_{ab} = K_{aa} + K_{app}$
Elastic Period of Vibration: See Equations (C5A-1) to (C5A-6)					
Calculate period of vibration assuming elastic response of pier *Use two-degree of freedom vibration theory from Thompson, 1965 to calculate period and mode shape*					
Pier stiffness modifier	S_{ma}	1.01	1.01		Used to adjust pier stiffness Iterate S_{ma} until $M_{be} = M_n$: M_{be} calculated below
Pier stiffness - elastic	K_y	27,486	36,411	kN/m	$K_y = S_{ma}*4*V_y / (\Delta_{yt}/1000)$: for all 4 piers
Quadratic equation coefficient B	B_e	-303	-409	$(\text{rad/s})^2$	$B_e = -9.81*((K_{dt} + K_{ab})/W_s + (K_y+K_{dt})/W_{cc})$
Quadratic equation coefficient C	C_e	5,038	8,819	$(\text{rad/s})^4$	$C_e = 9.81^2*((K_{ab}*K_y)+(K_{ab}+K_y)*K_{dt})/(W_s*W_{cc})$
Angular frequency	ω_e	4.21	4.78	rad/s	$\omega_e = \text{Sqrt}((-B_e - \text{Sqrt}(B_e^2 - 4*C_e))/2)$
First mode period - elast response	T_y	1.49	1.31	s	$T_y = 2*\pi/\omega$
Mode shape	A_{rae}	2.04	1.92		$A_{rae} = (K_y + K_{dt} - W_{cc}*\omega_e^2/9.81)/K_{dt}$

Item	Symbol	Soil C	Soil D	Units	Comment / Formula
Displacement in Bearings at Pier Yield Capacity					
Disp superstructure at pier yield	Δ_{sa}	138	217	mm	$\Delta_{sa} = A_{rae}*\Delta_{yt}$: From Eq (C5A-9)
Displacement in bearings	Δ_{bb}	70	104	mm	$\Delta_{bb} = \Delta_{sa} - \Delta_{sa}/A_{rae}$: From Eq (C5A-10)
Shear strain in bearing rubber	ε_{by}	0.78	1.15		$\varepsilon_{by} = \Delta_{bb} / t_r$:ε_{by} < 1.0 Soil C: > 0.1 Soil D For Soil D exceeding the limit may be acceptable
Disp at CoG pier cap + column	Δ_{cog}	68	113	mm	$\Delta_{cog} = \Delta_{sa} - \Delta_{bb}$: OK, $\Delta_{cog} = \Delta_{yt}$
Shear carried on push abutment	V_{ah}	403	632	kN	$V_{ah} = K_{aa}*\Delta_{sa}/1000$
Shear carried on pull abutment	V_{al}	326	553	kN	$V_{al} = K_{app}*\Delta_{sa}/1000$
Total shear force in pier bearings	V_b	1,634	3,609	kN	$V_b = \Delta_{bb}*K_{dt}/1000$
Shear in piers from cap/col inertia	V_{cs}	222	500	kN	$V_{cs} = (W_{cc}*\Delta_{cog}*\omega_e^2)/(9.81*1000)$: total from 4 piers
Total shear in piers - 1st mode resp	V_{ba}	1,855	4,109	kN	$V_{ba} = V_b + V_{cs}$
Total base shear on piers + abuts	V_{tt}	2,584	5,294	kN	$V_{tt} = V_{ba} + V_{ah} + V_{al}$
Check total inertia force	F_{in}	2,584	5,294	kN	$F_{in} = (W_s*\Delta_{sa}+ W_{cc}*\Delta_{cog})*\omega_e^2/(1000*9.81)$ From Eq (C5A-14)
Base shear in each pier	V_{ep}	464	1,027	kN	$V_{ep} = V_{ba}/4$
Check base moment (sum 4 piers)	M_b	13,974	30,962	kN m	$M_b = ((W_s*\Delta_{sa})*\omega_e^2/(1000*9.81) - V_{ah} - V_{al})*H_{cap}$ $+W_{cc}*\Delta_{cog}*H_{cogc}*\omega_e^2/(1000*9.81)$ From Eq (C5A-11)
Base moment on each pier	M_{be}	3,494	7,731	kN m	$M_{be} = M_b/4$: OK approximately = M_n
Modal participitation factor	P_e	1.05	1.05		$P_e = (W_s+W_{cc}/A_{rae})/(W_s+W_{cc}/(A_{rae})^2)$ From Eq (C5A-17)
Elastic displacement	$\Delta(T_{el})$	249	353	mm	$\Delta(T_{el}) = P_e*\Delta(3)*T_y/3$: at CoG of superst. mass
Elastic displacement at CoG pier	Δ_{coe}	120	184		$\Delta_{coe} = \Delta(T_{el})/A_{rae}$: Equation (C5A-9)
Approx ductility demand on cols	μ	2.06	1.97		$\mu = (\Delta_{coe} - \Delta_f)/\Delta_y$ Based on equal displacement approximation
Strain Limits for Plastic Rotation					
Yield strength transverse reinf.	f_{sy}	300	500	MPa	
Strain at max stress lateral reinf.	ε_{sut}	0.12	0.10		BM Clause 5.3.5(b)
Strain at max stress longitudinal reinf.	ε_{sul}	0.12	0.10		BM Clause 5.3.5(a)
Design comp strength plastic hinge	f_{ce}	45.5	45.5	MPa	$f_{ce} = 1.3*f_c$: BM Table 5.7
Average confining stress	f_{ld}	0.865	2.296	MPa	$f_{ld} = 0.95*f_{sy}*\rho_s/2$: From Priestley et al, 1996
Confined comp strength of concrete	f_{cc}	51.2	59.7	MPa	$f_{cc}= f_{ce}*(2.254*(1+7.94*f_{ld}/f_{ce})^{1/2}- 2*f_{ld}/f_{ce} -1.254)$ Priestley et al 1996, Eq (5.6)
Reinforcement limiting strain	ε_{sd}	0.021	0.043		$\varepsilon_{sd} = 0.015+6*(\rho_s-0.005) \le 0.5\ \varepsilon_{sul}$: Eq (5-11)
Concrete limiting strain	ε_{cd}	0.0100	0.0153		$\varepsilon_{cd} = 0.004+(1.4*\rho_s*f_{syf}*\varepsilon_{sut}) / f_{cc}$: Eq (5-12)
Neutral axis depth	c	282	364	mm	From moment strength analysis
Check using empirical formula	c_{ce}	277	313	mm	$c_c = D_c*10^3*(0.2+0.65*(W_{co}/4+W_c/4+W_s/5)/(10^3*f_{ce}*A_{co}))$ Priestley et al, 2007. Eq (10.8) OK: reasonable agreement
Distance extreme bar to neutral axis	b_{na}	846	960	mm	$b_{na} = D*1000 - c - c_o - d_b/2$
Concrete strain from steel strain	ε	0.0071	0.0163		$\varepsilon = \varepsilon_{sd}*c / b_{na}$ Soil C: Steel limiting strain governs Soil D: Concrete limiting strain governs
Limit state curvature	ϕ_{ls}	0.0253	0.0421	1/m	ϕ_{ls} = IF($\varepsilon > \varepsilon_{cd}$, ε_{cd} / (c/1000), ε_{sd} / (b_{na}/1000))
Plastic curvature	ϕ_p	0.0224	0.0379	1/m	$\phi_p = \phi_{ls} - \phi_{yy}$

Item	Symbol	Soil C	Soil D	Units	Comment / Formula
Plastic Hinge Length					
Ratio steel ultimate over yield stress	f_u/f_y	1.4	1.2		From Pacific Steel test results
Hinge length parameter	k_{lp}	0.08	0.04		$k_{lp} = 0.2*(f_u / f_y - 1) \le 0.08$: Eq (5-38)
Distance to point of contraflexure	L_c	7.62		m	$L_c = H_{cap}$
Plastic hinge length	L_p	0.84	0.77	m	$L_p = k_{lp}*L_c + L_{sp} \ge 2*L_{sp}$: Eq (5-37)
Ductility Factor Capacity					
Plastic rotation	θ_p	0.0188	0.0293	rad	$\theta_p = \phi_p*L_p$
Plastic displacement	Δ_p	144	224	mm	$\Delta_p = \theta_p*L_c*1000$: Eq (5-36)
Limit state displacement capacity	Δ_{ls}	193	297	mm	$\Delta_{ls} = \Delta_y + \Delta_p$
Ductility capacity	μ_{ls}	3.89	4.04		$\mu_{ls} = \Delta_{ls}/\Delta_y$
					Capacity > Approximate demand Design probably OK
Ductility Iteration for Superstructure Response					
Iterate assumed ductility in pier to give the calculated base moment in piers = flexural capacity					
Assumed ductility demand on pier	μ_{ap}	2.77	2.30		
Pier stiffness - modified	K	12,090	19,925	kN/m	$K_y = 4*V_{ebu}/((\mu_{ap}*\Delta_y + \Delta_f)/1000)$: V_{ebu} calc below
					For initial trial can use V_{ep} from above (at pier yield)
Calc base moment - total 4 piers	M_{bu}	14,061	31,125	kN m	$M_b = ((W_s*\Delta_{se})*\omega^2/(1000*9.81) - V_{au} - V_{bu})*H_{cap}$ $+W_{cc}*\Delta_{cou}*H_{cogc}*\omega^2/(1000*9.81)$
Calc base moment single pier	M_{bue}	3,515	7,781	kN m	$M_{bue} = M_{bu}$ /4
Calculate period of vibration assuming equivalent elastic response of pier					
Use two-degree of freedom vibration theory from Thompson, 1965 to calculate period and mode shape					
See Equations (C5A-1) to (C5A-7)					
Quadratic equation coefficient B	B_c	-220	-324	$(rad/s)^2$	$B_c = -9.81*((K_{dt} + K_{ab})/W_s+(K+K_{dt})/W_{cc})$
Quadratic equation coefficient C	C_c	2,598	5,285	$(rad/s)^4$	$C_c = 9.81^2*((K_{ab}*K)+(K_{ab}+K)*K_{dt})/(W_s*W_{cc})$
Angular frequency	ω	3.54	4.15	rad/s	$\omega_e = Sqrt((-B_c-Sqrt(B_c^2-4*C_c))/2)$
First mode period	T	1.77	1.51	s	$T_y = 2*\pi/\omega$
Mode shape	A_{ra}	1.42	1.48		$A_{ra} = (K+K_{dt} - W_{cc}*\omega^2/9.81)/K_{dt}$
Modal participitation factor	P	1.04	1.04		$P_e = (W_s+W_{cc}/A_{ra})/(W_s+W_{cc}/(A_{ra})^2)$
					From Eq (C5A-17)
Elastic design displacement	$\Delta(T)$	293	404	mm	$\Delta(T) = P*\Delta(3)*T/3$
Iterate displacement demand until $\Delta_d(T) = \Delta_{se}$					
Estimated superstructure demand	Δ_{se}	221	308	mm	
Calculated displacement demand	$\Delta_d(T)$	220	307	mm	$\Delta_d(T) = \Delta(T)*M_{su}$: M_{su} calculated below
Ductility Demand and Damping					
Disp at CoG of pier cap	Δ_{cou}	156	209	mm	$\Delta_{cou} = \Delta_{se}/A_{ra}$: From Eq (C5A-9)
Displacement in bearings	Δ_{bu}	65	99	mm	$\Delta_{bu} = \Delta_{se} - \Delta_{se}/A_{ra}$: From Eq (C5A-10)
Shear strain in bearing rubber	ε_{bu}	0.73	1.11		$\varepsilon_{by} = \Delta_{bu}/t_r$: $\varepsilon_{by} < 1.0$ Soil C: > 0.1 Soil D
					Overstrain of 11% acceptable
Shear carried on push abutment	V_{au}	645	899	kN	$V_{au} = K_{aa}*\Delta_{se}/1000$
Shear carried on pull abutment	V_{bu}	522	786	kN	$V_{bu} = K_{app}*\Delta_{se}/1000$
Total shear force in pier bearings	V_{bpu}	1,518	3,458	kN	$V_{bpu} = \Delta_{bu}*K_{dt}/1000$
Shear in piers from cap/col inertia	V_{cu}	362	697	kN	$V_{cu} = (W_{cc}*\Delta_{cou}*\omega^2)/(9.81*1000))$
Total shear in piers - 1st mode resp	V_{pu}	1,881	4,155	kN	$V_{pu} = V_{bpu} + V_{cu}$
Total shear on base of piers + abuts	V_{tu}	3,048	5,840	kN	$V_{tu} = V_{pu} + V_{au} + V_{bu}$
Check total inertia force	F_{inu}	3,048	5,840	kN	$F_{inu} = (W_s*\Delta_{se} + W_{cc}*\Delta_{cou})*\omega^2/(1000*9.81)$

Item	Symbol	Soil C	Soil D	Units	Comment / Formula
Base shear in each pier	V_{ebu}	470	1,039	kN	$V_{epu} = V_{pu}/4$
Ductility demand on piers	μ_{Id}	2.77	2.30		$\mu_{Id} = (\Delta_{cou} - \Delta_f)/\Delta_y$
Viscous damping ratio - bearings	ξ	0.05			From BM clause 5.4.3(g)(vi)
Damping from piers	ξ_{eu}	0.17	0.15		$\xi_{eu} = 0.10+0.04*(\mu_{Id} -1) \le 0.18$: Eq (5-32)
					Assume cylinder/column equivalent to pile/column
Combined damping brgs + piers	ξ_{cu}	0.104	0.101		$\xi_{cu} = (V_{pu}*\Delta_{cou}*\xi_{eu} + V_{bpu}*\Delta_{bu}*\xi+(V_{au}+V_{bu})*\Delta_{se}*\xi)/(V_{pu}*\Delta_{cou} + V_{pbu}*\Delta_{bu}+(V_{au}+V_{bu})*\Delta_{se})$: Eq (5-23)
Damping reduction factor	$M_{\xi u}$	0.75	0.76		$M_{\xi u} = (0.07/(0.02+\xi_{cu}))^{0.5}$: Eq (5-17)
Ratio: ductility capacity/demand	R_{cd}	1.40	1.76		$R_{cd} = \mu_{Is}/\mu_{Id}$: $R_{cd} > 1.0$: Designs OK
Check P-Δ Moment					
Axial load x displacement demand	$M_{p\text{-}\Delta}$	491	684	kN m	$M_{p\text{-}\Delta} = (W_s*\Delta_{se}/5 + W_{cc}*\Delta_{cou}/4)/1000$
					Ignores contribution from lower column sections
Ratio: $M_{p\text{-}\Delta}$ / M_{bu}	M_{rat}	0.14	0.09		> 0.1 Soil C. Increase in mom cap required
					< 0.25 maximum limit. See BM clause 5.3.7
Moment Capacity					
Reqd mom capacity each column	M_{bp}	3,761	7,781	kN m	IF(M_{rat} > 0.1, $M_{bp} = (M_{p\text{-}\Delta}/2 + M_{bue})$, M_{bue})
Capacity section with 20/D32 bars	M_{bca}	3,672		kN m	Soil C design: OK
Capacity section with 28/D32 bars	M_{bca}	7,751		kN m	Soil D design: OK

References:

Priestley M J N, Seible F and Calvi G M, 1996. *Seismic Design and Retrofit of Bridges*. John Wiley & Sons Inc

Priestley M J N, Calvi G M and Kowalsky, 2007. Displacement-Based Seismic Design of Structures. IUSS Press.

Thompson W T, 1965. *Vibration Theory and Applications*. Prentice-Hall Inc

Maitai River Bridge

Analysis Case 2: Flexible Foundations and Bearings: Soil C & D: Design Analysis Procedure

Transverse Direction

Prepared: J Wood

Edit Date: 21-Aug-17 Print Date: 21-Aug-17

Item	Sym	Value		Units	Comment / Formula
		Soil C	Soil D		
Structural Inputs					
Weight of superstructure on pier	W_s	1,900		kN	Excludes pier cap and column
Height of superstructure mass	H_s	8.982		m	Above pile cylinder top: see previous analysis
Height of CoG total mass	H	8.113		m	Check value. Not used in analysis
Height of column	H_{col}	6.200		m	From drawings
Weight of pier cap	W_c	399		kN	See calculations on Page C5-55
Maximum depth of pier cap	H_{ca}	1.421		m	From drawings
Height of top of pier cap	H_{cap}	7.621		m	Above pile cylinder top
Height CoG of pier cap	H_c	6.967		m	Calculated value. Ht above pile cylinder top
Column diameter	D_c	1.2	1.4	m	As designed = 1.4
Weight of pier column	W_{co}	175	239	kN	$W_{co} = 25*H_{col}*\pi*D_c^2/4$
Weight of pier cap + column/3	W_{cc}	457	478	kN	$W_{cc} = W_c + W_{co}/3$
Height CoG column/3 + pier cap	H_{cogc}	6.869	6.839	m	$H_{cogc} = (W_c*H_c+W_{co}*H_{col}/3)/W_{cc}$ Column mass at underside cap. See BM C5
Ductility limit adopted for analysis	μ_c	3.5	3.0		Adopting these values gives design disp < damping reduced spectrum corner disp Iteration requd if design disp > corner disp
Diameter longitudinal bars	d_b	32	32	mm	
Diameter transverse hoops	d_t	16	20	mm	
Number of longitudinal bars	N_b	20	28		As designed = 34 bars
Spacing transverse hoop bars	s_t	120	100	mm	As designed = 125 mm
Check maximum permitted spacing	s_{cc}	173	134	mm	$s_{cc} = (3+6*(f_u/f_y - 1))*d_b$: Eq (5-48)
Cover to hoops	c_v	40		mm	
Specified concrete 28 day strength	f_c	35		MPa	
Specified steel yield stress	f_y	300	500	MPa	Longitudinal and transverse steel
Foundation Stiffness Inputs					
Horizontal stiffness at ground level	K_h	60		MN/m	From analysis on Page C5-70
Rotational stiffness at ground level	K_θ	2,370		MN m/rad	From analysis on Page C5-70
Inputs for Elastomeric Bearings on Piers					
Shear modulus	G_b	0.73		MPa	53 IRHD - Skellerup brochure
Width of bearing	B_b	350	380	mm	Size greater than on drawings Trans direction
Length of bearing	L_b	280	380	mm	Size greater than on drawings Long direction
Total thickness of bearing	t_t	131		mm	=(90 rubber + 24 plates + top & bottom cover)
Thickness of rubber	t_r	90		mm	9 inner layers at 10 mm
Side cover	s_c	7		mm	Bearings are dowelled. Ignore cover rubber Skellerup brochure
Number bearings on each pier	N_{be}	8			
Bonded area of rubber	A_{bl}	0.0894	0.1340	m^2	$A_{bl} = (B_b - 2*s_c)*(L_b - 2*s_c)/10^6$
Shear stiffness	K_d	0.72	1.09	MN/m	$K_d = A_{bl}*G_b/(t_r/1000)$
Total stiffness of bearings on pier	K_{dt}	5,800	8,692	kN/m	$K_{dt} = 1000*K_d*N_{be}$: 8 bearings

Item	Sym	Soil C	Soil D	Units	Comment / Formula
Earthquake Inputs					
Site Subsoil Category		C	D		
Zone Factor	Z	0.27			Nelson
Return Period Factor	R_u	1.8			2500 year return period
Spectrum corner period	T_c	3.0		s	See BM Fig 5.2
Corner period spectral shape factor	$\Delta_h(3)$	985	1,585	mm	From Table 5.5 in BM
Corner period displacement	$\Delta(3)$	479	770	mm	$\Delta(3) = R_u*Z*\Delta_h(3)$
Yield Displacement					
Probable yield stress of reinf.	f_{ye}	330	550	MPa	$f_{ye} = 1.1*f_y$: BM Table 5.7
Youngs modulus for steel	E_s	200,000		MPa	
Yield strain	ε_y	0.00165	0.00275		$\varepsilon_y = f_{ye} / E_s$
Yield curvature	ϕ_{yy}	3.0E-03	4.2E-03	1/m	$\phi_{yy} = 2.15*\varepsilon_y / D_c$: Eq (5-8)
Strain penetration length	L_{sp}	0.232	0.387	m	$L_{sp} = 0.022*f_{ye}*d_b /1000$: Eq (5-10)
Coefficient for column fixity	C_1	0.333			See BM Commentary C5
Disp from pier column at CoG pier	Δ_y	50	74	mm	$\Delta_y = C_1*\phi_{yy}*(H_{cogc} + L_{sp})^2*1000$: Eq (5-10)
Design Base Shear					
Assumed mode shape	A_{ra}	1.27	1.26		Defined as ratio: (disp CoG pier + disp in bearing)/(disp CoG pier) The adopted value can be checked - see below and iteration used.
Disp at CoG pier from foundation	Δ_f	14	28	mm	$\Delta_f = M_b*H_{cogc} /K_\theta + V_b /K_h$ Iteration is required to calculate Δ_f since it depends on the base moment and shear
Design max inelastic disp at CoG pier	Δ_{dp}	188	248	mm	$\Delta_{dp} = \mu_c*\Delta_y + \Delta_f$
Mass height correction factor	aa	0.31	0.31		$aa = (H_s /H_{cogc} - 1)$
Design max inelastic disp superstruct	Δ_{ds}	296	390	mm	$\Delta_{ds} = \Delta_{dp}*(A_{ra} + aa)$: Equation (C5A-7)
Displacement in bearings	Δ_i	51	64	mm	$\Delta_i = \Delta_{ds} - \Delta_{dp}*(1+aa)$: Equation (C5A-10)
Design disp equiv single mass system	Δ_d	282	371	mm	$\Delta_d = (W_s*\Delta_{ds}^2 + W_{cc}*\Delta_{dp}^2)/(W_s*\Delta_{ds} + W_{cc}*\Delta_{dp})$ Eq (5-20)
Shear force in bearings	V_{pb}	294	561	kN	$V_{pb} = \Delta_i*K_{dt} /1000$
Viscous damping ratio for bearings	ξ	0.05			From BM clause 5.4.3(g)(vi)
Damping from pier	ξ_e	0.18	0.18		$\xi_e = 0.10+0.04*(\mu_c - 1) \le 0.18$: Eq (5-32)
Combined damping brgs + pier	ξ_c	0.16	0.16		$\xi_c = (V_b*\Delta_{dp}*\xi_e + V_{pb}*\Delta_i*\xi)/(V_b*\Delta_{dp} + V_{pb}*\Delta_i)$ Eq (5-23) Iteration is required since depends on V_b Alternatively an assumed value can be estimated from V_{pb}
Damping reduction factor	M_ξ	0.63	0.63		$M_\xi = (0.07/(0.02+\xi_c))^{0.5}$: Eq (5-17)
Corner period disp modified spectrum	Δ_{cm}	303	485	mm	$\Delta_c = \Delta(3)*M_\xi$
Frame effective weight	W_e	2,301	2,321	kN	$W_e = (W_s*\Delta_{ds} + W_{cc}*\Delta_{dp})/\Delta_d$: Eq (5-21)
Effective structural period	T_e	2.80	2.29	s	$T_e = T_c*\Delta_d /\Delta_{cm}$
Angular frequency	ω_{eq}	2.25	2.74	rad/s	$\omega_{eq} = 2\pi /T_e$
Effective secant stiffness	K_e	1,185	1,778	kN/m	$K_e = 4*\pi^2*W_e /(9.81*T_e^2)$: Eq (5-21)
Design base shear	V_b	334	659	kN	$V_b = K_e*\Delta_d /1000$: Eq (5-19)

Item	Sym	Soil C	Soil D	Units	Comment / Formula
Inertia force at superstructure level	F_s	290	568	kN	$F_s = V_b*(W_s*\Delta_{ds})/(W_s*\Delta_{ds}+W_{cc}*\Delta_{dp})$: Eq (5-39)
Inertia force at pier CoG level	F_{pi}	44	91	kN	$F_p = V_b*(W_{cc}*\Delta_{dp})/(W_s*\Delta_{ds}+W_{cc}*\Delta_{dp})$
Design base moment	M_b	2,909	5,724	kN m	$M_b = F_s*H_s+ F_{pi}*H_{cogc}$: excluding P - Δ increase
Effective stiffness of pier	K_p	1,779	2,657	kN/m	$K_p = V_b /\Delta_{dp}*1000$
Check mode shape	A_c	1.27	1.26		$A_c = (K_p + K_{dt} - W_{cc}*\omega_{eq}^2/9.81)/K_{dt}$
					From Eq (C5A-6)
Calculated Structural Parameters					
Cover to longitudinal bars	c_o	56	60	mm	From cover to hoops
Gross column section area	A_g	1.13	1.54	m^2	$A_g = \pi*D_c^2/4$
Area of longitudinal steel	A_s	16,085	22,519	mm^2	$A_s = N_b *\pi*d_b^2/4$
Check longitudinal steel area ratio	ρ_l	0.0142	0.0146		$\rho_l = A_s/(10^6*A_g)$
Check min required steel area	A_{sm}	15,080	12,315	mm^2	$A_{sm} = 4*10^6 *A_g /f_y$: BM clause 5.6.4(f)
Check max permitted steel area	A_{sma}	67,858	55,418	mm^2	$A_{sma} = 18*10^6 *A_g /f_y$: BM clause 5.6.4(f)
Area of transverse reinforcement	A_t	201	314	mm^2	$A_t = \pi*d_t^2/4$
Volumetric ratio transverse steel	ρ_s	0.00607	0.00967		$\rho_s = 4*A_t / (1000*(D_c - (2*c_v + dt)/1000)*s_t)$
					Depth of core taken on centre-line of hoops
					Adopt Priestley et al 1996 rather than NZS 3101
					OK: min required = 0.005: BM Clause 5.6.4(h)(i)
Strain Limits for Plastic Rotation					
Yield strength trans reinforcement	f_{sy}	300	500	MPa	
Strain at max stress lateral reinf.	ε_{sut}	0.12	0.10		BM Clause 5.3.5(b)
Strain at max stress long reinf.	ε_{sul}	0.12	0.10		BM Clause 5.3.5(a)
Design comp strength plastic hinge	f_{ce}	45.5	45.5	MPa	$f_{ce} = 1.3*f_c$: Table 5.7
Average confining stress	f_{ld}	0.865	2.296		$f_{ld} = 0.95*f_{sy}*\rho_s/2$: From Priestley et al, 1996
Confined comp strength concrete	f_{cc}	51.2	59.7	MPa	$f_{cc}= f_{ce}*(2.254*(1+7.94*f_{ld}/f_{ce})^{1/2}- 2*f_{ld}/f_{ce}-1.254)$
					Priestley et al, 1996, Eq (5.6)
Reinforcement limiting strain	ε_{sd}	0.021	0.043		$\varepsilon_{sd} = 0.015 + 6*(\rho_s - 0.005) \le 0.5\ \varepsilon_{sul}$: Eq (5-11)
Concrete limiting strain	ε_{cd}	0.0100	0.0153		$\varepsilon_{cd} = 0.004+(1.4*\rho_s*f_{sy}*\varepsilon_{sut}) / f_{cc}$: Eq (5-12)
Neutral axis depth	c	282	364	mm	From moment strength analysis
Check using empirical formula	c_c	277	313	mm	$c_c = D_c*1000*(0.2+0.65*(W_{co}+W_c+W_s)/(1000*f_{ce}*A_g))$
					Priestley et al, 2007, Eq (10.8)
					OK: reasonable agreement
Distance extreme bar to neutral axis	b_{na}	846	960	mm	$b_{na} = D_c*1000 - c - c_o - d_b /2$
Concrete strain from steel strain	ε	0.0071	0.0163		$\varepsilon = \varepsilon_{sd}*c / b_{na}$
				Soil C	Steel limiting strain governs
				Soil D	Concrete limiting strain governs
Limit state curvature	ϕ_{ls}	0.0253	0.0421	1/m	ϕ_{ls} = IF($\varepsilon > \varepsilon_{cd}$, ε_{cd} / (c/1000), ε_{sd} / (b_{na} /1000))
Plastic curvature	ϕ_p	0.0224	0.0379	1/m	$\phi_p = \phi_{ls} - \phi_{yy}$
Plastic Hinge Length					
Ratio steel ultimate / yield stress	f_u/f_y	1.4	1.2		From Pacific Steel's test results
Hinge length parameter	k_{lp}	0.08	0.04		$k_{lp} = 0.2*(f_u / f_y - 1) \le 0.8$: Eq (5-38)
Distance to point of contraflexure	L_c	8.11		m	$L_c = H$
Plastic hinge length	L_p	0.88	0.77	m	$L_p = k_{lp}*L_c + L_{sp} \ge 2*L_{sp}$: Eq (5-37)

Item	Sym	Soil C	Soil D	Units	Comment / Formula
Ductility Factor Capacity					
Plastic rotation	θ_p	0.0197	0.0293	rad	$\theta_p = \phi_p * L_p$
Plastic disp. capacity of pier	Δ_p	135	201	mm	$\Delta_p = \theta_p * H_{cogc} * 1000$: Eq (5-36)
Limit state disp. capacity pier	Δ_{ls}	185	274	mm	$\Delta_{ls} = \Delta_y + \Delta_p$: excludes foundation disp.
Ductility capacity	μ_{ls}	3.7	3.7		$\mu_{ls} = \Delta_{ls}/\Delta_y$: OK > 3.5 & 3.0 Soil C & D respect.
Max inelastic disp capacity at CoG pier	Δ_{dpc}	199	302	mm	$\Delta_{dpc} = \mu_{ls} * \Delta_y + \Delta_f$
Design disp capacity for superstruct	Δ_{cs}	253	380	mm	$\Delta_{cs} = \Delta_{dpc} * A_{ra}$: at CoG superstructure mass
Design disp capacity at equiv mass	Δ_{ce}	241	361	mm	$\Delta_{ce} = \Delta_{cs} * \Delta_d / \Delta_{ds}$
Check P-Δ Moment					
Axial load x displacement demand	$M_{p\text{-}\Delta}$	649	860	kN m	$M_{p\text{-}\Delta} = (W_s * \Delta_{ds} + W_{cc} * \Delta_{dp})/1000$ Ignores small component from lower 2/3 section of column
Capacities 20/D32 and 28/D32 bars	M_{bc}	3,672	7,751	kN m	
Ratio: $M_{p\text{-}\Delta} / M_{bc}$	M_{rat}	0.18	0.11		> 0.1. Increase in moment capacity required < 0.25 so less than maximum limit See BM Clause 5.3.7
Moment Capacity					
Required moment capacity	M_{bp}	3,234	6,154	kN m	$M_{bp} = M_b + M_{p\text{-}\Delta}/2$ OK: $M_{bc} > M_{bp}$

References:

Priestley M J N, Seible F and Calvi G M, 1996. *Seismic Design and Retrofit of Bridges*. John Wiley & Sons Inc

Priestley M J N, Calvi G M and Kowalsky, 2007. *Displacement-Based Seismic Design of Structures*. IUSS Press.

Maitai River Bridge

Analysis Case 3: Lead Rubber Bearings: Transverse Analysis

Prepared: J Wood

Edit Date: 21-Aug-17 Print Date: 21-Aug-17

Item	Symbol	Value	Units	Comment / Formula
Structural Inputs				
Weight of superstructure on pier	W_s	1,900	kN	Excludes pier. See analysis on Page C5-55
Height of superstructure mass	H_s	8.982	m	Above pile cylinder top. See analysis on Page C5-55
Height of CoG Total mass	H	8.113	m	See analysis on Page C5-56
Height of column	H_{col}	6.200	m	From drawings
Weight of pier cap	W_c	399	kN	See analysis on Page C5-55
Maximum depth of pier cap	H_{ca}	1.421	m	From drawings
Height of top of pier cap	H_{cap}	7.621	m	Above pile cylinder top
Height CoG of pier cap	H_c	6.967	m	Above pile cylinder top
Weight of pier column	W_{co}	239	kN	See analysis on Page C5-55
Weight of pier cap + column/3	W_{cc}	478	kN	$W_{cc} = W_c + W_{co}/3$
Height CoG column/3 + pier cap	H_{cogc}	6.839	m	$H_{cogc} = (W_c*H_c+W_{co}*H_{col}/3)/W_{cc}$ Column mass at underside cap. BM Comm C5
Total dynamic weight	W_d	2,378	kN	$W_d = W_s+W_c+W_{co}/3$: not including abutments
Column diameter	D	1.4	m	
Diameter longitudinal bars	d_b	32	mm	
Number of longitudinal bars	N_b	34		
Adopted concrete strength	f_c	40	MPa	Design value was 35 MPa
Adopted steel yield stress	f_y	500	MPa	Design value was 275 MPa
Inputs for Lead Rubber Bearings on Piers				
Shear modulus	G_b	0.73	MPa	53 IRHD - Skellerup brochure
Width of bearing	B_b	280	mm	From drawings. Transverse direction
Length of bearing	L_b	230	mm	From drawings. Longitudinal direction
Total thickness of bearing	t_t	131	mm	= (70 rubber + 51 plates + 10 top & bot cover)
Thickness of rubber	t_r	70	mm	From drawings: 10 inner layers at 7 mm Bearings are dowelled. Ignore cover rubber
Side cover	s_c	7	mm	From drawings
Number bearings on each pier	N_{be}	8		
Diameter of lead core	D_{cl}	75	mm	From drawings
Area of lead core	A_c	0.0044	m^2	$A_c = \pi*(D_{cl}/1000)^2/4$
Bonded area of rubber	A_{bl}	0.0530	m^2	$A_{bl} = (B_b - 2*s_c)*(L_b - 2*s_c)/10^6 - A_c$ Cover rubber ignored. Some guidelines include it.
Post yield shear stiffness	K_d	553	kN/m	$K_d = A_{bl}*G_b*1000/(t_r/1000)$
Total stiffness of bearings	K_{dt}	4,425	kN/m	$K_{dt} = K_d*N_{be}$
Yield strength of lead core	Q_d	35	kN	$Q_d = 6.23*D_{cl}^2/1000$: From Buckle, 2013.
Total yield strength of cores	Q_{dt}	280	kN	$Q_{dt} = N_{be}*Q_d$

Item	Symbol	Value	Units	Comment / Formula
Foundation Stiffness Inputs				
Horizontal stiffness at ground level	K_h	60	MN/m	See analysis on Page C5-70
Rotational stiffness at ground level	K_θ	2,380	MN m/rad	See analysis on Page C5-70
Earthquake Inputs				
Site Subsoil Category		C		Assumed for Case 3 analysis
Zone Factor	Z	0.27		Nelson
Return Period Factor	R_u	1.8		2,500 year return period
Corner period spectral shape factor	$\Delta_h(3)$	985	mm	From BM Table 5.5
Corner period displacement	$\Delta(3)$	479	mm	$\Delta(3) = R_u*Z*\Delta_h(3)$
Calculated Structural Parameters				
Young's modulus concrete	E_c	31,623	MPa	$E_c = 5000*Sqrt(f_c)$: Priestley et al, 2007, Eq (4.43)
				Eqn was used to derive stiffness ratio curves
Area of longitudinal steel	A_s	27,344	mm^2	$A_s = N_b*\pi*d_b^2/4$
Area of pier column	A_{co}	1.539	m^2	$A_{co} = \pi*D^2/4$
Longitudinal reinforcement ratio	ρ_l	0.0178		$\rho_l = A_s/(A_{co}*10^6)$
Axial force ratio in column	R_{af}	0.041		$R_{af} = (W_s+W_c+W_{co})/(A_{co}*f_c*1000)$
Pier stiffness ratio	R_{st}	0.37		From Priestley et al, 2007, Fig 4.12
Cracked stiffness of pier column	K_p	12,888	kN/m	$K_p = (3*R_{st}*E_c*1000*\pi*D^4)/(64*(H_{cap}+L_{sp})^3)$
				Based on top of pier ht. Used for period calc
				L_{sp} calculated below.
Yield Displacement at Top of Pier and Flexural Strength				
Probable yield stress for reinf.	f_{ye}	550	MPa	$f_{ye} = 1.1*f_y$: BM Table 5.7
Young's modulus steel	E_s	200,000	MPa	
Yield strain	ε_y	0.00275		$\varepsilon_y = f_{ye} / E_s$
Yield curvature	ϕ_{yy}	0.00422	1/m	$\phi_{yy} = 2.15*\varepsilon_y / D$: Eq (5-8)
Strain penetration length	L_{sp}	0.387	m	$L_{sp} = 0.022*f_{ye}*d_b /1000$: Eq (5-10)
Coefficient for column fixity	C_1	0.333		See Bridge Manual Commentary C5
Pier CoG disp. due to foundn Δ & θ	Δ_f	25	mm	$\Delta_f = V_p / K_h + M_{bc}*H_{cogc} / K_\theta$
				Iteration reqd: V_p and M_{bc} unknown at this point
Pier CoG disp. due to col. at yield	Δ_y	74	mm	$\Delta_y = C_1*\phi_{yy}*(H_{cogc} + L_{sp})^2*1000$: Eq (5-10)
Total displacement at CoG pier	Δ_{yt}	98	mm	$\Delta_{yt} = \Delta_f + \Delta_y$
Flexural strength of pier	M_n	8,200	kNm	Flexural strength analysis: f_y = 550 MPa
Displacement Iteration for Superstructure Response				
Iteration to find displacement in bearing and superstructure response at demand displacement				
Pier rotation modifier for super disps	aa	0.31		aa = (H_s /H_{cogc} - 1)
				Rotation of pier increases disp. of W_s
Assumed displacement in bearing	Δ_{ia}	57.2	mm	Iterate until $\Delta_{ia} = \Delta_i$
Calculated bearing displacement	Δ_i	57.2	mm	$\Delta_i = \Delta_d(T)*(1 - (1+aa)/(A_{ra}+aa))$
				See demand disp. and mode shape below Eq (C5A-10)
Shear strain in bearing rubber	ε_b	0.82		$\varepsilon_b = \Delta_i / t_r$: t_r < 1.0 bearings OK
Stiffness of columns	K	12,888	kN/m	K = K_p : columns do not reach yield but are likely to be cracked.
Bearing effective stiffness at Δ_{ia}	K_i	9,327	kN/m	$K_i = 1000*Q_{dt} /\Delta_i + K_{dt}$: Buckle, 2013, Eq (2.25)

Item	Symbol	Value	Units	Comment / Formula
Calculate period of vibration assuming elastic response of pier. See Equations (C5A-1) to (C5A-6) *Use two-degree of freedom vibration theory from Thompson, 1965 to calculate period and mode shape*				
Quadratic equation coefficient B	B_c	-564	$(rad/s)^2$	$B_c = -9.81*(K_i /W_s+(K+K_i*(1+aa))/W_{cc})$
Quadratic equation coefficient C	C_c	12,730	$(rad/s)^4$	$C_c = 9.81^2*(K*K_i)/(W_s*W_{cc})$
Angular frequency	ω	4.9	rad/s	$\omega = Sqrt((-B_c - Sqrt(B_c^2 - 4*C_c))/2)$
First mode period	T	1.29	s	$T = 2*\pi/\omega$
Mode shape	A_{ra}	2.26		$A_{ra} = (K+K_i - W_{cc}*\omega^2/9.81)/K_i$
Superstructure displacement	Δ_a	117	mm	$\Delta_a = \Delta_{ia} /(1 - (1+aa)/(A_{ra}+aa))$
Displacement at CoG of pier mass	Δ_p	45	mm	$\Delta_p = \Delta_a / (A_{ra}+ aa) < \Delta_{yt}$: pier remains elastic
Shear force in bearings	V_{pb}	533	kN	$V_{pb} = \Delta_i*K_i /1000$
Inertia force from pier cap	F_{ci}	52	kN	$F_{ci} = \Delta_p*\omega^2 *W_{cc} /(1000*9.81)$
Shear force on pier	V_p	586	kN	$V_p = V_{pb} + F_{ci}$
Viscous damping ratio for bearings	ξ	0.33		$\xi =2*Q_{dt} /(\pi* V_{pb})$: Buckle Eq (1.16)
Ductility demand on pier	μ_{ap}	1.00		Required for damping estimate
Damping from pier	ξ_e	0.10		$\xi_e = 0.10+0.04*(\mu_{ap} -1) \leq 0.18$: Eq (5-32)
Combined damping bearings+pier	ξ_c	0.23		$\xi_c = (V_p*\Delta_p*\xi_e + V_{pb}*\Delta_i*\xi)/(V_p*\Delta_p + V_{pb}*\Delta_i)$ Eq (5-23)
Damping reduction factor	M_ξ	0.53		$M_\xi = (0.07/(0.02+\xi_c))^{0.5}$: Eq (5-17)
Participitation factor	P	1.06		$P = (W_s+W_{cc} /A_{ra})/(W_s+W_{cc}/A_{ra}^2)$: Eq (C5A-17)
Elastic spectrum design disp.	$\Delta(T)$	219	mm	$\Delta(T) = P*\Delta(3)*T/3$
Displacement demand	$\Delta_d(T)$	117	mm	$\Delta_d(T) = \Delta(T)*M_\xi$
Force Actions on Pier				
Base moment	M_{bc}	5,149	kN m	$M_{bc} = (W_s*\Delta_a*H_s + W_{cc}*\Delta_p*H_{cogc})*\omega^2/(9.81*1000)$
Ratio pier moment capacity / demand	R_{cd}	1.59		Adequate overstrength to prevent yield at DCLS
Check pier shear / weight	R_{pw}	31	%	$R_{pw} = 100*V_p / W_s$

References:

Buckle I G, 2013. *Introduction to Seismic Isolation*. Notes in Base Isolation 101, Seminar TR54. NZ Concrete Soc.

Priestley M J N, Calvi G M and Kowalsky, 2007. *Displacement-Based Seismic Design of Structures.* IUSS Press.

Thompson W T, 1965. *Vibration Theory and Applications.* Prentice-Hall Inc

Maitai River Bridge

Analysis Case 3: Lead Rubber Bearings: Longitudinal Analysis

Prepared: J Wood

Edit Date: 16-Oct-17 Print Date: 15-Nov-17

Item	Symbol	Value	Units	Comment / Formula
Structural Inputs				
Number of spans	N_s	5		
Weight of superstructure span	W_s	1,900	kN	Excl pier cap and column. See analysis p. C5-55
Total weight of superstructure	W_{st}	9,500	kN	Five spans
Height of column	H_{col}	6.200	m	From drawings
Weight of pier cap	W_c	399	kN	From analysis on Page C5-55
Total weight of pier caps	W_{ct}	1,594	kN	Four caps
Maximum depth of pier cap	H_{ca}	1.421	m	From drawings
Height of top of pier cap	H_{cap}	7.621	m	$H_{cap} = H_{ca} + H_{col}$
Height CoG of pier cap	H_c	6.967	m	Above pile cylinder top. From analysis on p. C5-56
Weight of pier column	W_{co}	239	kN	From analysis on Page C5-55
Total weight of pier columns	W_{cot}	956	kN	Four columns
Wt of pier cap + column/3	W_{cc}	478	kN	$W_{cc} = W_c + W_{co}/3$
Total wt of pier cap + column/3	W_{cct}	1,913	kN	$W_{cct} = W_{ct} + W_{cot}/3$
Height CoG column/3 + pier cap	H_{cogc}	6.839	m	$H_{cogc} = (W_{ct}*H_c + W_{cot}*H_{col}/3)/W_{cct}$ Column mass assumed at underside cap. See Bridge Manual commentary C5
Total dynamic weight	W_d	11,413	kN	$W_d = W_{st} + W_{ct} + W_{cot}/3$: (excluding abutments)
Weight of each abutment	W_a	930	kN	Does not include approach slab. Approach slab and soil above included in M-O active wedge.
Column diameter	D	1.4	m	As designed
Diameter longitudinal bars	d_b	32	mm	As designed
Number of longitudinal bars	N_b	34		As designed
Adopted concrete strength	f_c	40	MPa	Design value was 35 MPa
Adopted steel yield stress	f_y	500	MPa	Design value was 275 MPa
Foundation Stiffness Inputs				
Hor stiffness each pile at ground level	K_h	60	MN/m	See analysis on Page C5-70
Rot stiffness each piler at ground level	K_θ	2,380	MN m/rad	See analysis on Page C5-70
Effective stiffness of two abutment piles	K_{api}	54,000	kN/m	At bearing level. See analysis on Page C5-77
Abutment Stiffness Inputs				
Backfill friction angle	ϕ_b	35	deg	Dense granular backfill
Backfill friction angle - radians	ϕ_{br}	0.611	rad	
Soil unit weight	γ_s	19	kN/m^3	
Backwall height	H_w	3.46	m	From drawings. Total of pile cap and backwall
Backwall width	B_w	10.33	m	From drawings
Passive soil stiffness of abut backwall	K_{aw}	300,000	kN/m	At 5 mm displacement. See analysis on Page C5-78
Stiffness of push abutment	K_a	354,000	kN/m	$K_a = K_{api} + K_{aw}$
Abutment inertia force from PGA	F_i	601	kN	$F_i = a_p*W_a$: see PGA (a_p) below

Item	Symbol	Value	Units	Comment / Formula
Inertia angle	α	0.574		α = Atan(a_p): see PGA below
Mononobe active pressure coefficient	K_{AE}	1.054		K_{AE} =(Cos(ϕ_{br} - α))^2/ ((Cos(α))^2*(1+Sqrt(Sin(ϕ_{br})*Sin(ϕ_{br}-α)/Cos(α)))^2) Assuming zero friction on wall backface.
Active pressure force on abutment	F_{AE}	1235	kN	F_{AE} = 0.5*K_{AE}*H_w^2*B_w*γ_s
Abutment inertia + active M-O force	F_{ip}	1,836	kN	F_{ip} = F_i + F_{AE}: reduces effective stiffness
Effective stiffness of pull abutment	K_{ap}	7,275	kN/m	K_{ap} = K_{api} / (1 + F_{ip} / V_{ap}): Not including reduction in stiffness from bearings From Introduction Eq (H-21) with k_b = ∞ Shear V_{ap} on pull abutment is calculated below
Inputs for Lead Rubber Bearings on Piers				
Shear modulus (piers and abutments)	G_b	0.73	MPa	53 IRHD - Skellerup brochure
Width of bearing	B_b	280	mm	From drawings. Transverse direction
Length of bearing	L_b	230	mm	From drawings. Longitudinal direction
Total thickness of bearing	t_t	131	mm	= (70 rubber + 51 plates + 10 top and bot cover)
Thickness of rubber	t_r	70	mm	10 inner layers at 7 mm
Side cover	s_c	7	mm	From drawings
Number bearings on all piers	N_{be}	32		
Diameter of lead core	D_{cl}	75	mm	From drawings
Area of lead core	A_c	0.0044	m^2	A_c = π*(D_{cl} /1000)^2/4
Bonded area of rubber	A_{bl}	0.0530	m^2	A_{bl} = (B_b - 2*s_c)*(L_b - 2*s_c)/10^6 - A_c
Post yield shear stiffness	K_d	553	kN/m	K_d = A_{bl} *G_b*1000/(t_r /1000)
Total stiffness bearings on all piers	K_{dt}	17,700	kN/m	K_{dt} = K_d*N_{be}
Yield strength of lead core	Q_d	35	kN	Q_d = 6.23*D_{cl}^2/1000 : from Buckle, 2013 notes.
Total yield strength all bearings	Q_{dt}	1,121	kN	Q_{dt} = N_{be}*Q_d
Inputs for Lead Rubber Bearings on Each Abutment				
Width of bearing	B_{ba}	380	mm	From drawings. Transverse direction
Length of bearing	L_{ba}	300	mm	From drawings. Longitudinal direction
Total thickness of bearing	t_{ta}	175	mm	= (117 rubber + 48 plates + 10 top and bot cover)
Thickness of rubber	t_{ra}	117	mm	From drawings: 9 inner layers at 13 mm
Side cover	s_{ca}	10	mm	From drawings
Number bearings on each abutment	N_{bea}	4		
Diameter of lead core	D_{cla}	75	mm	From drawings
Area of lead core	A_{ca}	0.0044	m^2	A_{ca} = π*(D_{cla} /1000)^2/4
Bonded area of rubber	A_{bla}	0.0964	m^2	A_{bla} = (B_{ba} - 2*s_{ca})*(L_{ba} - 2*s_{ca})/10^6 - A_{ca}
Post yield shear stiffness	K_{da}	601	kN/m	K_{da} = A_{bla} *G_b/(t_{ra} /1000)*1000
Total stiffness bearings on abutment	K_{dat}	2,405	kN/m	K_{dat} = K_{da}*N_{bea}
Yield strength of lead core	Q_{da}	35	kN	Q_{da} = 6.23*D_{cla}^2/1000 : from Buckle, 2013 notes
Total yield strength all bearings	Q_{dat}	140	kN	Q_{dat} = N_{bea}*Q_{da}

Item	Symbol	Value	Units	Comment / Formula
Earthquake Inputs				
Site Subsoil Category		C		Adopted for Case 3 analysis
Zone Factor	Z	0.27		Nelson
Return Period Factor	R_u	1.8		2,500 year return period
Peak ground acceleration	a_p	0.646	g	a_p =1.33*Z*R_u: required for M-O active pressure on abutments.
Corner period spectral shape factor	$\Delta_h(3)$	985	mm	From Table 5.5 in BM
Corner period displacement	$\Delta(3)$	479	mm	$\Delta(3) = R_u*Z*\Delta_h(3)$
Calculated Structural Parameters				
Youngs modulus concrete	E_c	31,623	MPa	E_c = 5000*Sqrt(f_c): Priestley et al, 2007, Eq (4.43) Equation was used to derive stiffness ratio curves.
Area of longitudinal steel	A_s	27,344	mm^2	$A_s = N_b*\pi*d_b^2/4$
Area of pier column	A_{co}	1.539	m^2	$A_{co} = \pi*D^2/4$
Longitudinal reinforcement ratio	ρ_l	0.0178		$\rho_l = A_s/(A_{co}*10^6)$
Axial force ratio in column	R_{af}	0.041		$R_{af} = (W_s+W_c+W_{co})/(A_{co}*f_c*1000)$
Pier stiffness reduction factor	R_{st}	0.37		From Priestley et al, 2007, Fig 4.12
Cracked stiffness of pier column	K_p	17,542	kN/m	$K_p = (3*R_{st}*E_c*1000*\pi*D^4)/(64*(H_{cogc}+L_{sp})^3)$ Based on pier CoG ht. Used for period calculation. L_{sp} calculated below.
Yield Displacement at Top of Pier and Flexural Strength				
Probable yield stress for reinf.	f_{ye}	550	MPa	f_{ye} = 1.1*f_y: BM Table 5.7
Young's modulus steel	E_s	200,000	MPa	
Yield strain	ε_y	0.00275		$\varepsilon_y = f_{ye} / E_s$
Yield curvature	ϕ_{yy}	0.00422	1/m	ϕ_{yy} = 2.15*ε_y / D: Eq (5-8)
Strain penetration length	L_{sp}	0.387	m	L_{sp} = 0.022*f_{ye}*d_b /1000: Eq (5-10)
Coefficient for column fixity	C_1	0.333		See Bridge Manual Commentary C5
Displacement pier CoG from foundation	Δ_f	24	mm	$\Delta_f = V_p/(4*K_h) + M_{bc}*H_c/K_\theta$ Iteration required: V_p and M_{bc} unknown at this point
Disp at pier CoG from pier column	Δ_{yc}	76	mm	$\Delta_{yc} = C_1*\phi_{yy}*(H_c + L_{sp})^2*1000$: Eq (5-10) At CoG of pier mass
Total yield displacement at CoG of pier	Δ_y	100	mm	$\Delta_y = \Delta_{yc} + \Delta_f$
Flexural strength	M_n	8,200	kNm	Flexural strength analysis: f_y = 500 MPa
Superstructure Response				
It is necessary to make assumptions for both the superstructure and pier bearing displacements then iterate until calculated values = assumed values. The iteration function in Excel can be used				
Assume disp of superstructure	Δ_{sa}	99.8	mm	Iterate until $\Delta_{sc} = \Delta_{sa}$
Calculated disp superstructure	Δ_{sc}	99.8	mm	$\Delta_{sc} = \Delta_d(T)$
Assume disp in pier bearings	Δ_{ba}	64.5	mm	Iterate until $\Delta_{ba} = \Delta_{bc}$
Calculated disp in pier bearings	Δ_{bc}	64.6	mm	$\Delta_{bc} = \Delta_{sa}*(1 - 1/A_{ra})$: using mode shape from below From Eq (C5A-10)
Cracked stiffness of 4 columns	K	70,166	kN/m	K = 4*K_p :(based on pier CoG height) Colmnns do not reach yield but likely to be cracked
Stiffness ratio for push abutment	γ_a	0.0108		$\gamma_a = (K_{dat}*\Delta_{sa}/1000 + Q_{dat})/(K_a*\Delta_{sa}/1000 - Q_{dat})$ Buckle, 2013, Eq 2.32

Item	Symbol	Value	Units	Comment / Formula
Stiffness ratio for pull abutment	γ_{ap}	0.649		$\gamma_{ap} = (K_{dat}*\Delta_{sa}/1000+Q_{dat})/(K_{ap}*\Delta_{sa}/1000 - Q_{dat})$
Effectiveness stiffness push abut	K_{ea}	3,784	kN/m	$K_{ea} = \gamma_a*K_a/(1 + \gamma_a)$: Buckle, Eq 2.31
Effective stiffness pull abutment	K_{eap}	2,863	kN/m	$K_{eap} = \gamma_{ap}*K_{ap}/(1 + \gamma_{ap})$
Effective stiffness of pier bearings	K_{eb}	35,086	kN/m	$K_{eb} = Q_{dt}/(\Delta_{ba}/1000) + K_{dt}$: Buckle, 2013, Eq 2.25
Calculate period of vibration and displacement of pier top assuming elastic response.				
Use two-degree of freedom vibration theory from Thompson, 1965 to calculate period and mode shape				
See Equations (C5A-1) to (C5A-6)				
Quadratic equation coefficient B	B_c	-583	$(rad/s)^2$	$B_c = -9.81*((K_{ea}+K_{eap}+K_{eb})/W_{st}+(K+K_{eb})/W_{cct})$
Quadratic equation coefficient C	C_c	16,740	$(rad/s)^4$	$C_c = 9.81^2*((K_{ea}+K_{eap})*K+(K_{ea}+K_{eap}+K)*K_{eb})/(W_{st}*W_{cct})$
Angular frequency	ω	5.5	rad/s	$\omega = Sqrt((-B_c - Sqrt(B_c^2 - 4*C_c))/2)$
Period two mass model	T	1.14	s	$T = 2*\pi/w$
Mode shape	A_{ra}	2.83		$A_{ra} = (K+K_{eb} - W_{cct}*\omega^2/9.81)/(K_{eb})$
Displacement at pier mass CoG	Δ_p	35.3	mm	$\Delta_p = \Delta_{sa}/A_{ra}$
Displacement in push abut bearings	Δ_{bau}	98.8	mm	$\Delta_{bau} = \Delta_{sa}/(1+ \gamma_a)$: Buckle, Eq 2.35
Shear strain in push abut bearings	ε	0.84		$\varepsilon = \Delta_{bau}/t_{ra}$: $\varepsilon < 1.0$: bearings OK
Displacement in pull abut bearings	Δ_{bap}	60.6	mm	$\Delta_{bap} = \Delta_{sa}/(1+ \gamma_{ap})$
Displacement of push abutment	Δ_a	1.1	mm	$\Delta_a = \Delta_{sa} - \Delta_{bau}$
Displacement of pull abutment	Δ_{ap}	39.3	mm	$\Delta_{ap} = \Delta_{sa} - \Delta_{bap}$
Effective stiffness push abut bearings	K_{eba}	3,825	kN/m	$K_{eba} = Q_{dat}/(\Delta_{bau}/1000) + K_{dat}$
Effective stiffness pull abut bearings	K_{ebb}	4,720	kN/m	$K_{ebb} = Q_{dat}/(\Delta_{bap}/1000) + K_{dat}$
Total of pier shears from pier CoG disp	V_p	2,474	kN	$V_p = \Delta_p*K/1000$
Shear force in pier bearings	V_{be}	2,263	kN	$V_{be} = \Delta_{ba}*K_{eb}/1000$
Check: bearing shear + cap inertia	V_{pc}	2,471	kN	$V_{pc} = V_{be} + W_{cct}*\Delta_p*\omega^2/(9.81*1000)$
Shear force on push abutment	V_a	378	kN	$V_a = \Delta_a*K_a/1000$
Check shear on push abutment	V_{ac}	378	kN	$V_{ac} = \Delta_{bau}*K_{eba}/1000$
Shear force on pull abutment	V_{ap}	286	kN	$V_{ap} = \Delta_{ap}*K_{ap}/1000$
Check shear on pull abutment	V_{apc}	286	kN	$V_{ac} = \Delta_{bap}*K_{ebb}/1000$
Total shear force on foundations	V_t	3,138	kN	$V_t = V_p + V_a + V_{ap}$
Check Bridge Inertia Forces				
Shear force from inertia of superstruct	V_{is}	2,929	kN	$V_{is} = W_{st}*\Delta_{sa}*\omega^2/(9.81*1000)$
Shear force from inertia of piers	V_{ip}	208	kN	$V_{ip} = W_{cct}*\Delta_p*\omega^2/(9.81*1000)$
Sum of inertia forces	V_{it}	3,138	kN	$V_{it} = V_{is} + V_{ip}$: OK $V_{it} = V_t$
Damping and Computed Response				
Damping from pier bearings	ξ	0.315		$\xi = 2*Q_{dt}/(\pi*V_{be})$: Buckle, 2013 Eq 1.16
Damping from push abut bearings	ξ_a	0.236		$\xi_a = 2*Q_{dat}/(\pi*V_a)$
Damping from pull abut bearings	ξ_{ap}	0.312		$\xi_{ap} = 2*Q_{dat}/(\pi*V_{ap})$
Ductility demand on piers	μ_a	1.00		See base moment below - elastic response
Damping from pier foundations	ξ_e	0.10		$\xi_e = 0.10+0.04*(\mu_a - 1) \le 0.18$: Eq (5-32)
Combined damping	ξ_c	0.240		$\xi_c = (V_p*\Delta_p*\xi_e+V_{be}*\Delta_{ba}*\xi+V_a*\Delta_{bau}*\xi_a+V_{ap}*\Delta_{bap}*\xi_{ap})$
(Ignores soil damping at abutments)				$/(V_p*\Delta_p+V_{be}*\Delta_{ba}+V_a*\Delta_{bau}+V_{ap}*\Delta_{bap})$: Eq (5-23)
Damping reduction factor	M_ξ	0.52		$M_\xi = (0.07/(0.02+\xi_c))^{0.5}$: Eq (5-17)
Participitation factor	P	1.06		$P = (W_s+W_{cc}/A_{ra})/(W_s+W_{cc}/A_{ra}^2)$: Eq (C5A-17)

Item	Symbol	Value	Units	Comment / Formula
Elastic spectrum design displacement	$\Delta(T)$	192	mm	$\Delta(T) = P*\Delta(3)*T/3$
Displacement demand	$\Delta_d(T)$	100	mm	$\Delta_d(T) = \Delta(T)*M_\xi$
Check base moment in each pier	M_{bc}	4,714	kN m	$M_{bc} = V_p*H_{cap}/4$: $M_{bc} < M_n$
Ratio pier moment capacity/demand	R_{cd}	1.74		$R_{cd} = M_n / M_{bc}$
				Overstrength more than adequate to prevent pier yield at DCLS
Check pier shear / weight on pier	R_{pw}	22	%	$R_{pw} = 100*V_p / W_d$

References:

Buckle I G, 2013. *Introduction to Seismic Isolation* . Base Isolation 101, Seminar Notes TR54. NZ Concrete Soc.

Priestley M J N, Calvi G M and Kowalsky, 2007. *Displacement-Based Seismic Design of Structures* . IUSS Press.

Thompson W T, 1965. *Vibration Theory and Applications.* Prentice-Hall Inc

Appendix C5B Displacement based design worked example 2 – Mangatewai-iti River Bridge

In this section

C5B.1 Bridge description

Constructed in 1983 the Mangatewai-iti River Bridge is located on State Highway 2 approximately 13km north of Dannevirke. The bridge has four simply supported precast prestressed concrete I beam spans with a cast insitu reinforced concrete deck continuous over the piers. The piers have single 1.52m diameter reinforced concrete columns with hammerhead type caps. Each pier has a 2.03m diameter cylinder foundation that consists of a reinforced concrete core cast in a 10mm thick steel liner. The central pier has a height of 13.2m measured from the top of the cylinder to the top of the hammerhead and the two outer piers have nearly equal heights of approximately 9.2m. Typical details of the structure are shown in figure C5B.1 to figure C5B.3.

On the piers the beams are seated on 380x300x119mm thick elastomeric bearings. At the abutments the beams sit on PTFE bearings which allow both unrestrained longitudinal and transverse displacements. The abutments are supported on twin 1.37m diameter cylinders.

The bottom section of the pier columns (all piers) are reinforced with 40 D32 longitudinal bars. Confinement over a 1.8m length at the base of the columns is provided by D16 hoops at 80mm spacing. The top of pier cylinders are reinforced with 54 D32 longitudinal bars. All the reinforcement had a specified minimum yield stress of 275MPa.

Bore logs included with the drawings show that the foundation cylinders are embedded in dense sand and gravels overlying siltstone at a depth varying between 15 to 20m.

In 1985 the bridge was subjected to snap-back lateral displacement testing as part of a research project undertaken by the University of Nevada-Reno, the University of Auckland and Computech Engineering Services Inc. System identification techniques were used to determine some of the important structural and soil stiffness parameters (*Large amplitude field response studies of two highway bridges subjected to simulated earthquake loads*[1]).

Figure C5B.1: Mangatewai-iti River Bridge looking to north

Figure C5B.2: Typical details of Mangatewai-iti River Bridge

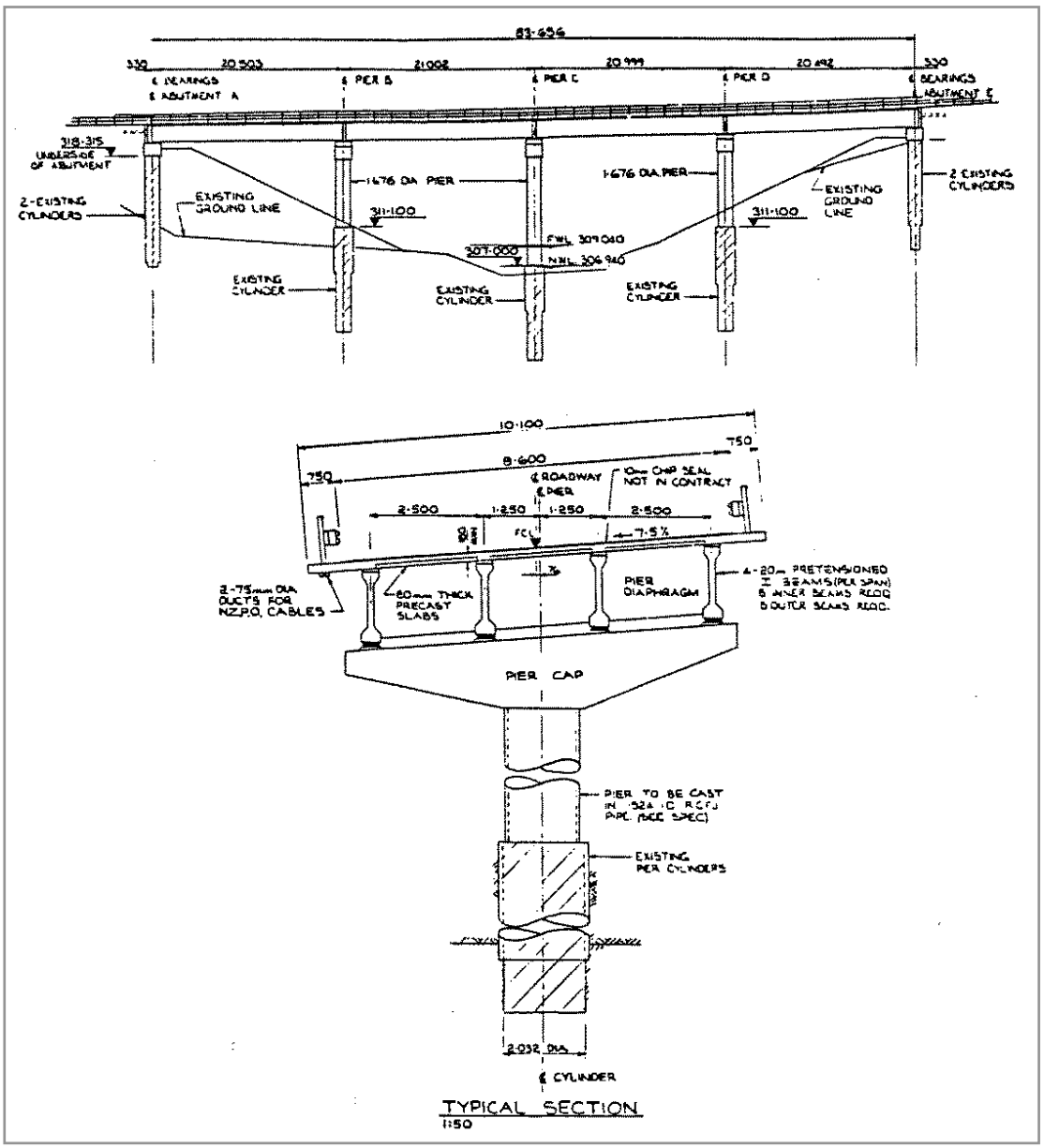

Figure C5B.3: Abutment seating showing sliding bearings (note lack of transverse restraint)

C5B.2 Example cases analysed

Only a single configuration of the bridge was considered for this example. Two minor changes were made to the as-designed bridge. The characteristic yield stress of the reinforcement in the piers was taken as 300MPa instead of the specified minimum of 275MPa. The columns at piers B and D were assumed to have equal heights of 7.7m instead of the actual heights of 7.2 and 7.9m respectively. Using equal heights for piers B and D makes the bridge symmetrical about the centre simplifying the analysis. The column of pier C was assumed to have its actual height of 11.7 m. Having a height difference between the central and outer piers adds analysis complexity and makes the analysis procedure different in a number of respects to that used in example 1 (see appendix C5A) where the piers were assumed to have uniform height.

(Note that the example calculations were undertaken using an annual probability of exceedance of 1/2500 for this bridge having been written prior to the change of annual probabilities of exceedance introduced in amendment 3 to the *Bridge manual*.)

Flexibility introduced by the cylinder pile foundations and the elastomeric bearings was considered in the analysis. The pier caps have significant mass and the appropriate inertia forces at both the centre of gravity of the superstructure and piers were applied. A worked example of a continuous bridge with differing height monolithic piers, a rigid foundation and inertia forces applied only at the centre of gravity of the superstructure is given in chapter 6 (by Priestley, Kowalsky and Calvi) of *Bridge engineering handbook: Seismic design*[(2)]. Reference to this simpler example is a useful starting point for the present more complex example.

For the longitudinal loading direction a single case was considered with the bridge assumed to slide on the abutment bearings with no influence of the abutments on the response except for the damping introduced by the abutment bearings. In the transverse direction two cases were considered. Firstly, the bridge was assumed to slide on the abutment bearings with a very rigid continuous superstructure spanning between the abutments to give uniform transverse displacement of the superstructure. (The analysis for this case is very similar to the longitudinal case.) In the second case the bridge was assumed to be restrained transversely by shear keys at the abutments. The flexibility introduced by the abutment cylinder foundations was included in the analysis but essentially the abutments are very rigid resulting in a very different response to that of the first case as the diaphragm action of the continuous and restrained deck reduces the displacements of the piers. This second case is more typical of New Zealand highway bridges and comparison of the results from the two cases illustrates the advantages of restraint at the abutments. (Restraint increases abutment costs but for this bridge the cost increase would have been minor because the abutments were supported on twin large diameter cylinders.)

The analysis procedure generally follows the method given in chapter 6 of *Bridge engineering handbook: Seismic design*[(2)]. Where appropriate the DBD provisions of section 5 of the *Bridge manual* (amendment 3) were applied. Essentially the *Bridge manual* provisions follow the basic analysis equations used in chapter 6 of *Bridge engineering handbook: Seismic design*[(2)]. For several of the cases considered in example 1, two types of analyses were undertaken with a design method used to determine the pier reinforcement details directly and a review method based on assuming the reinforcement details were known (or trial details chosen prior to the analysis). For example 2, it is necessary to know or select trial reinforcement details for the piers at the outset and there is no simple direct method of calculating the required capacity, confining reinforcement or ductility requirements.

C5B.3 Longitudinal analysis

The main steps in the spreadsheet analysis procedure are summarised as follows:

a. Structural inputs

   The weights and height dimensions were based on the bridge drawings. The calculation of the weights is summarised on the separate spreadsheet titled *Geometric and weight input parameters* (page C5–114). It is necessary to calculate the centres of gravity of both the superstructure and the piers as these points define the location for the application of the inertia forces.

   The transverse moment of inertia of the deck is required in the transverse analysis of the bridge for the case when the superstructure is restrained at the abutments. It is based on the moment of inertia of the deck section which is continuous across the piers. It would be increased by the beams that are simply supported but the increase from the beams is reasonably small and has been neglected for the example.

b. Elastomeric bearing Inputs

   The overall dimensions of the bearings are shown on the drawings. The rubber thickness, side covers and shear modulus were based on typical values used in bridge bearings.

c. Pier cylinder stiffness inputs

   These were calculated on a separate spreadsheet titled *Longitudinal analysis: Pier pile stiffness* (page C5–116). The stiffness of the tops of the cylinder (translation and rotation) has been calculated using the elastic continuum method of *Aseismic pile foundation design analysis*[3]. A linear increase of soil stiffness with depth was assumed and the cylinders were assumed to be long although some are marginally shorter than the minimum length required for this assumption. Insufficient information was available to derive a more exact soil model. (If SPT values are available for the foundation soils and show very variable layered properties a Winkler spring model could be used instead of the elastic continuum method.)

d. Earthquake inputs

   The earthquake inputs were from the *Bridge manual* (same as NZS 1170.5 *Structural design actions* part 5 Earthquake actions – New Zealand [4]) for a 2,500 year return period event. The bridge would have been designed to the earthquake load requirements of the *Highway bridge design brief*[5], which was based on NZS 4203 *General structural design and design loads for buildings*[6]. Neither the *Highway bridge design brief*[5] nor NZS 4203[6] used return period factors. They used a force based design approach with coefficients based on assumed ductility factor reductions. It is therefore difficult to make a direct comparison between the design loads and the current force based provisions of the *Bridge manual* but the current 2,500 year loads would be approximately 50% greater than the design loads.

e. Calculated structural parameters

   The steel areas and volumetric ratio are required for the column strength and ductility calculations. *Gen-Col*[7] was used to calculate the moment capacity of the columns and the depth of the neutral axis. (Moment curvature analysis software can be used for these calculations.)

C5B.3 continued

f. Strain limits for plastic rotation

Strain limits were calculated using equations (5–11) and (5–12). The confined compressive strength of the concrete was calculated using empirical equations given in *Seismic design and retrofit of bridges*[8]. (Alternatively this parameter can be selected from charts in *Seismic design and retrofit of bridges*[8].)

g. Plastic hinge lengths

Plastic hinge lengths were calculated using equations (5–36) and (5–37). Based on typical steel test results for grade 300 reinforcement the f_u/f_y ratio was taken as 1.4. As the piers are pinned at their tops for longitudinal displacements the distance to the point of contraflexure was taken as the distance from the top of the cylinders to the top of the piers.

h. Yield displacements

The yield displacements were calculated using equation (5–10) and C_1=0.333 (as given in C5.7.2). Displacements were calculated for both the top and the centre of gravity of the piers. The pier top values were used for ductility calculations and the centre of gravity values for calculating the pier inertia forces.

i. Ductility factor capacities

Both the limit state displacement capacities and ductility factors for the piers were calculated using conventional expressions. The pier tops were used as the reference point for these calculations. From the displacement capacities it is clear that the two shorter piers B and D control the design displacement although all three piers have similar ductility factor capacities.

j. Pier shears at limit state displacement

For piers that do not have significant mass and where the moment capacities are the same for each pier, the shears in the piers are inversely proportional to their heights (top of the pier where the pier is pinned at the top or height to the centre of gravity of superstructure for monolithic piers). For the present example, all the piers have the same moment capacity but because the pier inertia forces are not applied at the tops of the piers the shear ratio is only approximately equal to the inverse of the pier heights. A correction can be made to allow for this discrepancy but as indicated on the spreadsheet the correction is small. For this example it would be sufficiently accurate to base the ratio of the shear forces on the ratio of the pier heights.

At this stage of the analysis it is necessary to estimate the shears in the piers and the pier inertia forces and to adjust them by trial and error after calculating the total base shear at a later stage in the analysis. The pier shears and inertia forces are required to estimate the displacement from the foundation and bearing flexibility. In the simpler example given in chapter 6 of *Bridge engineering handbook: Seismic design*[2] there are no bearings and the foundation is assumed to be rigid. In this case the system damping can be calculated using the pier shear ratio with the actual pier shears calculated directly from the total base shear without the need for trial and error.

To initiate the trial and error the shear in pier B (and D) can be approximated by dividing the trial moment capacity by the height of the pier. The inertia forces acting on the piers can initially be assumed to be zero as these forces are relatively small in comparison to the shear forces at the base of the piers.

C5B.3 continued

It is convenient to use the iteration function in Excel to calculate the shears and inertia forces. After the first trial, the formulae iteration can be turned on (Tabs: File, Options, Formulas) followed by setting $V_{Bn} = V_B$ (trial value = calculated value) on the spreadsheet.

k. Displacements from foundations and bearings

The displacement components at the tops and centres of gravity of the piers from the foundation deformation were calculated using the shears and moments at the base of the piers and the translational and rotational stiffness of the cylinders.

The displacements in the bearings were calculated from the shears in the bearings (base shear minus inertia force on pier) and the total stiffness of the bearings on each pier.

The plastic displacement in pier C is required so that the ductility demand on pier C can be calculated for the damping calculation. The plastic displacement in pier C is obtained from the design limit state displacement of the superstructure less the contributions from the yield displacement and the displacement from the bearings and foundation. The design limit state displacement of the superstructure is computed by adding the bearing and foundation contributions to the limit state capacities (yield plus plastic displacement) of piers B and D.

l. Displacements at mass locations

The displacements at the centres of gravity of the piers were calculated from the pier yield and plastic displacements and the foundation displacement contribution. The characteristic design displacement was calculated by substituting the displacements at the mass locations into equation (5–3). Because the displacement of the superstructure is uniform along the length of the bridge the superstructure mass can be treated as a single point.

m. Effective mass

The effective mass is calculated using the characteristic design displacement in equation (5–21). Because the pier masses are relatively small compared to the total superstructure mass the effective mass is approximately equal to the total mass. (The effective mass should always be less than the total mass.)

n. Damping

Damping from the piers is calculated using equation (5–31). The damping ratio from the abutment sliding bearings has been taken as 0.25. This is consistent with the 0.25 value given in clause 5.4.4 for friction slabs. (The equivalent viscous damping ratio for a friction sliding device is theoretically $2/\pi$ so the value of 0.25 is conservative. The snap-back testing work on the bridge indicated that sliding at the bearings produced higher damping than indicated by a ratio of 0.25.)

Damping in the pier bearings was taken as the 0.05 default value given in clause 5.4.4. This is probably a conservative value.

The system damping was calculated using equation (5–22). Damping in the superstructure is neglected as it is small in comparison to the damping from the other components.

o. Effective period

The effective period was calculated from the limit state design displacement and the damping reduced displacement spectrum. It is assumed that the displacement spectrum is linear between zero period and the corner period of 3 seconds.

C5B.3 continued

The secant stiffness K_e was calculated from the effective period and effective mass using the standard single degree of freedom expression $T_e = 2\pi\sqrt{\frac{m_e}{k_e}}$ (from equation (5–21)).

The design base shear was obtained from the secant stiffness and the effective design displacement using equation (5–18).

p. Inertia forces

Inertia forces acting on the superstructure were calculated from the base shear and respective weights of the super structure and piers using equation (5–38).

q. Base Shears

The pier base shears were calculated by subtracting the abutment friction forces from the total base shear and using the pier shear ratio factor (approximately inversely proportional to the pier heights). A coefficient of friction of 0.05 was assumed for the PTFE sliding bearings. The shear force acting on the abutment bearings is a reasonably small proportion of the total base shear so the shears acting on the piers are not very sensitive to this assumption. (The *Bridge manual* specifies a coefficient of friction range of 0.02 to 0.15, so a lower value than assumed could be used and would increase the shears in the piers a small amount.)

The moments at the base of the piers were calculated from the shear in the bearings (base shear minus the pier inertia force) and the inertia forces using the appropriate pier heights.

r. Check P-Δ moment

The P-Δ moment at the base of the piers was calculated using conventional procedures. There are two components to the moment: a component from the superstructure displacement and gravity force, and a component from the pier displacement and gravity force (assumed to act at the centres of gravity of the piers). The gravity force from the lower two-thirds of the columns was neglected as it was not included in the pier weight. A correction for the cylinder top displacement has been applied although this is small and could be neglected. (The displacement of the superstructure included the cylinder top displacement.)

The ratio of the P-Δ moment to the pier moment capacity was checked. If this ratio is less than 0.1 no increase is required to the design moment capacity. If the ratio is between 0.1 and 0.25 the design capacity should be increased by 50% of the P-Δ moment. (P-Δ moment ratios greater than 0.25 are unacceptable. Refer to clause 5.3.7.)

s. Required moment capacity

The analysis shows that the required moment capacity of the piers is about 12% greater than the as-constructed capacity. In a design application the capacity should be increased by adding additional longitudinal bars or increasing the yield stress of the steel. Increasing the ductility capacity of the piers would also be option. By using 20mm diameter hoops at 100mm centres the ductility factors for piers B and D would be increased to approximately 5.3 and this would reduce the moment demand to about the as-built capacity. (With this level of ductility there would be a significant P-Δ moment which needs to be considered.) The as-designed ductility factors of approximately 4.0 are reasonable values to adopt for concrete bridge piers and it would probably be best to increase the pier flexural capacities.

C5B.4 Transverse analysis: Sliding bearings at abutments

The analysis procedure in the transverse analysis for the case when the superstructure is free to slide on PTFE bearings at the abutments is almost identical to the longitudinal analysis procedure, if the superstructure is assumed to form a rigid diaphragm so that the displacement of the superstructure at the tops of the piers is uniform. The deformation of the superstructure diaphragm in the present example was checked using structural analysis and assuming the transverse moment of inertia was the uncracked value for the deck (ignoring the simply supported beams). This showed that the relative displacement between the centre and side piers was approximately 3mm which is small in relation to the total superstructure limit state design displacement of about 430mm. Therefore a rigid deck diaphragm assumption is acceptable for the present example. (A check on the in-plane flexural capacity of the deck indicated that it had sufficient strength to cantilever over the length of the end spans.)

There are minor differences between both the analysis procedures and the results for the longitudinal and transverse sliding abutment bearing cases and these are summarised below.

a. Structural inputs

   The effective heights of the piers were taken as the height between the centre of gravity of the superstructure and the tops of the cylinder foundations rather than the height between the tops of the piers and the cylinders.

   Because the pier bearings can transfer axial loads they provide overturning fixity rather than a pinned joint between the superstructure and piers. The analysis was based on determining the displacements at these effective pier heights rather than the displacements at the tops of the piers, which in the longitudinal direction define the displacement of the superstructure.

b. Plastic hinge lengths

   The distances to the points of contraflexure were taken as the effective pier heights rather than the heights to the tops of the piers. This increases the plastic hinge lengths a small amount.

c. Yield displacements

   Yield displacements were calculated at the centres of gravity of the superstructure rather than at the tops of the piers. (Displacements were also calculated for the pier centres of gravity in a similar manner to the longitudinal displacement case.)

d. Ductility factor capacities

   The ductility capacities of the piers were based on the displacements at the centres of gravity of the piers rather than the tops of the piers. Alternatively they could be based on the displacements at the centre of gravity of the superstructure but it is perhaps more correct to use the centres of gravity of the piers. (The ductility factor capacities are only used in the damping calculations so the reference point is not very critical.)

   Using the pier centres of gravity (rather than the pier tops) increases the ductility factors from those calculated for the longitudinal direction by approximately 15%.

C5B.4 continued

e. Displacements at mass locations

The design limit state displacement of the superstructure and the characteristic design displacement for the longitudinal case increase from 365 and 354mm to 431 and 415mm respectively. This is mainly a consequence of the higher effective heights of the piers for the transverse analysis.

f. Effective mass

As expected the effective mass is similar for both displacement directions.

g. Damping

The damping in the transverse direction is a little higher for the transverse case which is mainly a consequence of the higher ductility demand on pier C (2.3 in the transverse direction compared to 2.1 in the longitudinal).

h. Effective period

The period is longer in the transverse direction by approximately 15% because of the greater characteristic design displacement (and the small increase in damping).

i. Base shears and moments

The longer period reduces the base shears and moments, with the moments reducing by about 9%.

j. Check P-Δ moment and required moment capacity

In the transverse direction the ratio of the P-Δ moment to the design capacity moment exceeds 0.1 and an increase in capacity is therefore required in this direction. However, even with this increase the required capacity is 5% less than for the longitudinal direction.

C5B.5 Transverse analysis: Restraint at abutments

The analysis procedure in the transverse analysis for the case when the superstructure is restrained at the abutments with rigid shear keys between the superstructure and abutment structure (but with flexible cylinder foundations) is similar to the transverse analysis procedure for sliding bearings at the abutments but there is one major difference. For the restrained abutments the displaced shape along the length of the superstructure becomes an important variable.

Following chapter 6 of *Bridge engineering handbook: Seismic design*[(2)], the analysis procedure is to assume a proportion of the total base shear, defined by a ratio = x, is transferred to the abutments and to assume a parabolic shape of the deflection profile along the length of the bridge with a small displacement at the abutments. The design limit state displacement for the critical pier fixes the magnitude of the displaced shape at a point along the length. Using these trial values the inertia forces acting at the mass points and the effective stiffness of the piers (shear force/trial displacements) were calculated. These parameters were then used as inputs to a structural model consisting of a horizontal continuous beam spanning between abutments with horizontal springs having the trial effective pier stiffnesses modelling the piers. The beam has the transverse moment of inertia of the superstructure (cracked if appropriate) to model the diaphragm action. The calculated displacements and x ratio from the structural model were then used for the next iteration with the process repeated until reasonable convergence is obtained. Revised inertia forces and effective stiffnesses were used in the structural model at each iteration.

C5B.5 continued

In the present example, the iteration process is rather complicated because in effect there are four variables that need to be iterated (shear and inertia forces acting on the piers, x ratio and displaced superstructure shape). The process can be simplified by using the Excel formula iteration function to calculate the pier shears and inertia forces as described for the longitudinal direction and the transverse response with sliding abutment bearings. For bridges with three or four spans and symmetrical about their centre point it is practical to carry out the structural analysis on the spreadsheet. To do this it is necessary to prepare a stiffness matrix (displacements and rotations as the unknown variables – a column matrix) for the end and centre beam spans and then to combine these in a total stiffness matrix for the symmetrical structure. The matrix inversion function in Excel can then be used to invert the stiffness matrix to allow the displacements to be calculated for the inertia force inputs. The displacement results can then be used as the next inputs to the iteration process. It appears best to set and adjust the x ratio manually in this iteration process.

Because the piers in the present example have significant mass, it is best to include these masses separately in the structural model. This can be done by calculating effective springs for the calculated displacement components above and below the centres of gravity of the pier masses and applying the pier inertia forces at nodes located at the junction of the two effective springs for each pier. The structural model for the present example is illustrated in figure C5B.4. By using symmetry, the number of degrees of freedom can be reduced to seven. These are the superstructure rotations at abutment A and pier B (ϕ_1, ϕ_2, rotation at pier C is zero), superstructure displacements at abutment A (Δ_3), and piers B (Δ_4) and C (Δ_5), and pier centre of gravity displacements at piers B (Δ_6) and C (Δ_7). (Inverting a 7x7 matrix is readily accomplished in Excel.)

Figure C5B.4: Bridge structural model (symmetrical about pier C)

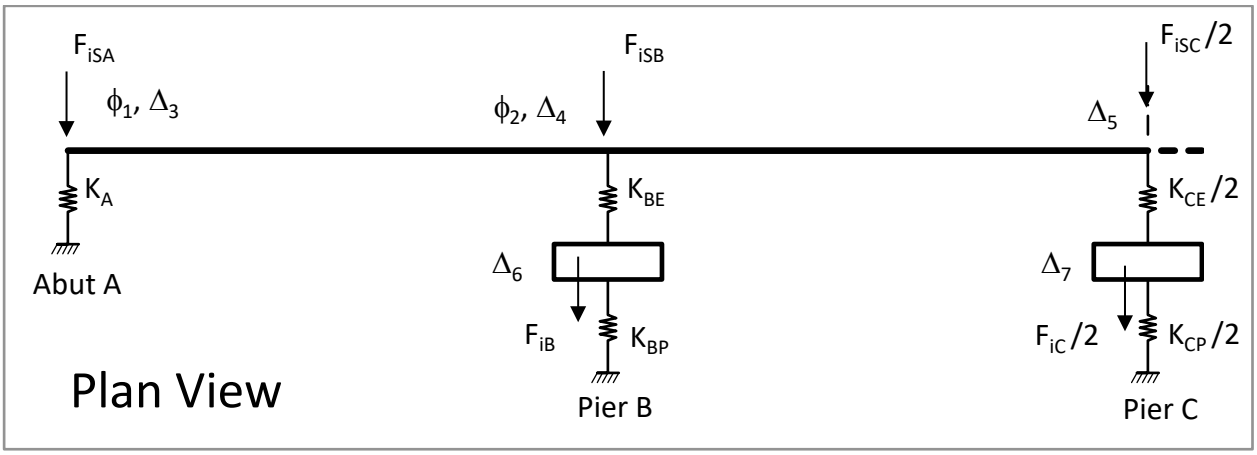

C5B.5 continued

In the present example trial and error results for the deflected shape of the superstructure showed that it was not possible for the limit state displacement at the ductility capacity of piers B and D to develop. The superstructure is sufficiently stiff to transfer a large proportion of the base shear to the abutments so that a viable solution can be obtained for displacements significantly less than the maximum based on the pier ductility capacities. In the example in chapter 6 of *Bridge engineering handbook: Seismic design*[(2)], the limit state displacement (at the central pier) was set as the iteration objective, but in the present example the moment capacity at the base of the piers needs to be used as the target objective. A successful iteration approach was to start with the superstructure displacements at the pier yield displacement limits and then proceed iteratively until the pier base moments were equal to the as-designed capacities (or adjusted capacities). The base moments are quite sensitive to the x ratio so it was best to iterate the x value manually and the displaced shape automatically using Excel formula iteration with the structural analysis based on the stiffness matrix approach.

The differences between the analysis procedures and the results for the two transverse cases are summarised below.

a. Structural inputs

   The inputs are the same as for the transverse sliding case except that the span lengths are included for calculating the superstructure inertia forces at the tops of each pier. (In this example the spans are approximately equal so that a reasonable approximation would be to base the inertia forces on the average span length.)

b. Superstructure displacement profile: Determine by trial and error to agree with structural analysis output

   The trial displacements were set to values calculated by the structural analysis model using Excel formula iteration and the structural analysis displacements calculated on the spreadsheet using the stiffness matrix inversion. Alternatively a separate structural analysis model can be set up using structural analysis software.

   The x ratio parameter was adjusted manually until the calculated bending moments at the base of the piers agreed with a target capacity value. In the present example the target capacity was taken at the required moment capacity indicated by the longitudinal displacement analysis.

   The displacements at the pier centres of gravity calculated by the structural analysis should agree with the displacements calculated from the displacement components (pier yield and plastic components, and the foundation and bearing components) as shown under the *Characteristic design displacement calculation* heading on the spreadsheet.

c. Ductility demands

   The ductility demands on the piers were calculated from the superstructure displacements (both the trial and iteration converged values). The plastic component is obtained by subtracting the yield, foundation and bearing components from the total displacement at the pier centre of gravity locations. The calculated ductility demands of 1.2 and 1.0 are significantly less than the ductility capacity limits of 4.2 and 4.6 for piers C and B respectively.

d. Superstructure inertia weights

   These were calculated from the span lengths and the unit weight of the superstructure (101kN/m). They are required to calculate the characteristic design displacement and the effective mass.

C5B.5 continued

e. Effective mass

The effective mass is approximately 25% less than the total mass. This difference occurs because the displacements of the superstructure near the abutments are significantly less than near the centre of the bridge.

f. Damping

The damping for this restrained abutment case is approximately 50% less than for the sliding bearing case. The overall damping is reduced by the lower ductility demands on the piers and the low damping assumed for the abutments. The damping ratio for the abutment structure was taken as 0.05 based on the small displacements calculated for the tops of the abutment piles.

g. Effective period

Because of the much stiffer structure resulting from the deck diaphragm action the period for the restrained abutment case is only 1.0 seconds compared to 2.7 seconds for the sliding bearing case.

h. Check P-Δ moment and required moment capacity

The smaller superstructure displacements result in the ratio of the P-Δ moment to the design capacity moment at the base of the piers being less than 0.1. No increase in moment capacity is therefore required for P-Δ action.

i. Structural analysis

The transverse moment of inertia of the superstructure was assumed to be 0.3 times the gross value for the deck on the basis that cracking was likely in the continuous deck over the piers. In design applications, a detailed analysis should be carried out to determine a more exact value. The correct value is probably higher than assumed but increasing the superstructure moment of inertia to 0.4 times the gross value would result in piers B and D remaining elastic. The value adopted best illustrated a typical analysis procedure for a long bridge (with long spans) when plastic displacement is expected in the piers.

Effective spring stiffness values for the structural model were calculated for the section of the piers below their centres of gravity. An effective spring value based on the displacement of the superstructure relative to the pier centres of gravity is also required for the structural model.

The structural model degrees of freedom are shown in figure C5B.4. Based on these degrees of freedom the stiffness matrices for the two beam sections (symmetrical structure about the pier C location) are listed below.

C5B.5 continued

The total stiffness matrix for the structural model is obtained by adding the values that have the same row and column designations in each of the individual matrices.

Stiffness matrix beam A-B: (Degree of freedom numbers in first row and column)

	1	2	3	4	6
1	$4E_{IA}$	$2E_{IA}$	$\frac{6E_{IA}}{L_{AB}}$	$-\frac{6E_{IA}}{L_{AB}}$	0
2	$2E_{IA}$	$4E_{IA}$	$\frac{6E_{IA}}{L_{AB}}$	$-\frac{6E_{IA}}{L_{AB}}$	0
3	$\frac{6E_{IA}}{L_{AB}}$	$\frac{6E_{IA}}{L_{AB}}$	$\frac{12E_{IA}}{{L_{AB}}^2}+K_A$	$-\frac{12E_{IA}}{{L_{AB}}^2}$	0
4	$-\frac{6E_{IA}}{L_{AB}}$	$-\frac{6E_{IA}}{L_{AB}}$	$-\frac{12E_{IA}}{{L_{AB}}^2}$	$\frac{12E_{IA}}{{L_{AB}}^2}+\frac{K_{BE}}{2}$	$-\frac{K_{BE}}{2}$
6	0	0	0	$-\frac{K_{BE}}{2}$	$\frac{(K_{BP}+K_{BE})}{2}$

Stiffness matrix beam B-C: (Degree of freedom numbers in first row and column)

	2	4	5	6	7
2	$4E_{IB}$	$\frac{6E_{IB}}{L_{Bc}}$	$-\frac{6E_{IB}}{L_{Bc}}$	0	0
4	$\frac{6E_{IB}}{L_{Bc}}$	$\frac{12E_{IB}}{{L_{BC}}^2}+\frac{K_{BE}}{2}$	$-\frac{12E_{IB}}{{L_{BC}}^2}$	$-\frac{K_{BE}}{2}$	0
5	$-\frac{6E_{IB}}{L_{Bc}}$	$-\frac{12E_{IB}}{{L_{BC}}^2}$	$\frac{12E_{IB}}{{L_{BC}}^2}+\frac{K_{CE}}{2}$	0	$-\frac{K_{CE}}{2}$
6	0	$-\frac{K_{BE}}{2}$	0	$\frac{(K_{BP}+K_{BE})}{2}$	0
7	0	0	$-\frac{K_{CE}}{2}$	0	$\frac{(K_{CP}+K_{CE})}{2}$

The calculated displacements at the seven degrees of freedom were obtained by post-multiplying the inverted stiffness matrix by the input force vector (inertia forces at the seven nodes).

A check on the displacement results can be made by post-multiplying the total stiffness matrix by the calculated displacement vector. This should return the input force vector. Beam forces can be obtained by post-multiplying the individual beam stiffness matrices by the appropriate displacement vector values. This gives the moment in the superstructure at pier B which can then be used to calculate the shear force transferred to the abutment.

C5B.6 Shear ratio in piers

The derivation of the shear force ratio for unequal piers with significant mass is summarised below for the longitudinal direction. The derivation for the transverse direction is essentially the same except that effective pier heights to the centre of gravity of the superstructure are used instead of the heights to the tops of the piers. (In the longitudinal direction the top of the pier is effectively pinned so the shear force is applied at the top of the pier. In the transverse direction the bearings act in tension and compression and apply an overturning moment as well as a shear to the pier top. Adjustment for this effect is made by applying the superstructure inertia force at the centre of gravity of the superstructure.)

The definition diagram for the following derivation is shown in figure C5B.5.

The moments and shears at the bases of the two different height piers are given by:

$$M_B = V_{Bb}H_B + F_B(H_B - h_B)$$
$$M_C = V_{Cb}H_C + F_C(H_C - h_C) \quad \text{(C5B–1)}$$

$$V_B = F_B + V_{Bb}$$
$$V_C = F_C + V_{Cb} \quad \text{(C5B–2)}$$

Setting $M_B = M_C$ and simplifying gives the pier shear ratio as:

$$\frac{V_C}{V_B} = \frac{H_B}{H_C} + \frac{(F_C h_C - F_B h_B)}{V_B H_C} \quad \text{(C5B–3)}$$

Figure C5B.5: Definition diagram for derivation of pier shear force ratio.

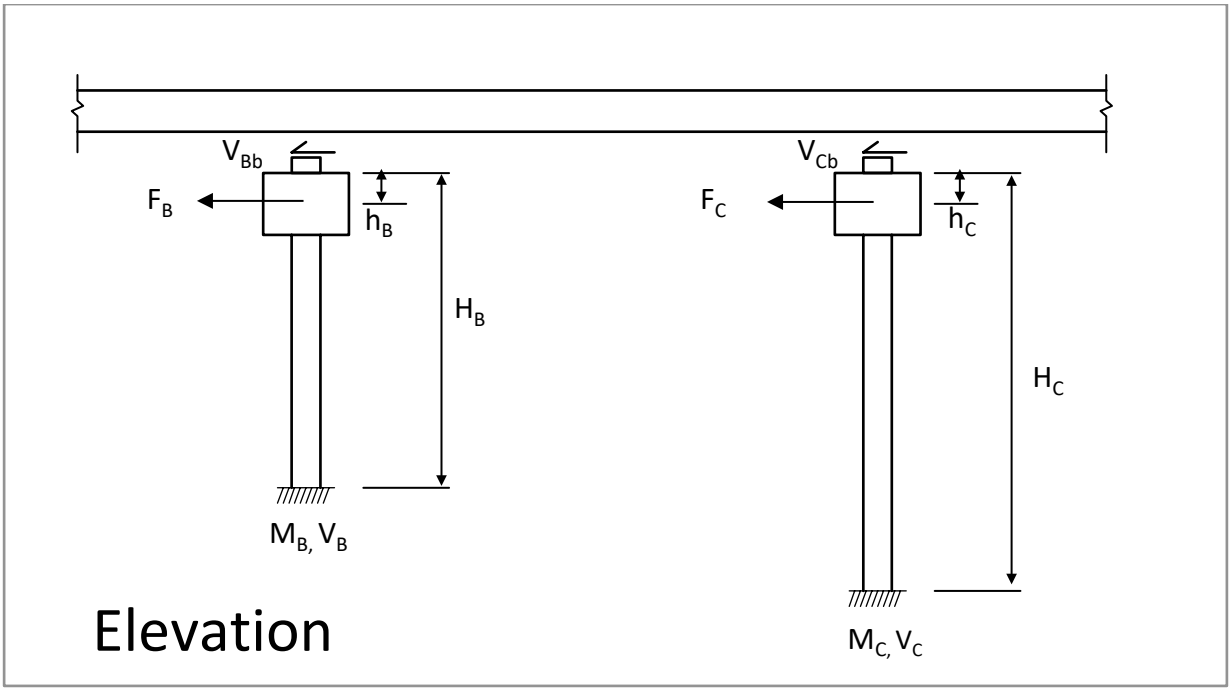

C5B.7 References

(1) Douglas BM and Buckle IG (1985) *Large amplitude field response studies of two highway bridges subjected to simulated earthquake loads*. Proceedings 2nd Joint US-NZ Workshop on the Seismic Resistance of Highway Bridges. Report ATC-12-1.

(2) Chen WF and Duan L (2014) *Bridge engineering handbook: Seismic design*, 2nd edition. CRC Press, Boca Raton, FL, USA.

(3) Pender MJ (1993) *Aseismic pile foundation design analysis*. Bulletin of the New Zealand Society for Earthquake Engineering, vol. 26 no. 1, pp 49-161.

(4) Standards New Zealand NZS 1170.5:2004 *Structural design actions*. Part 5 Earthquake actions – New Zealand. (Incorporating Amendment No. 1: 2016)

(5) Ministry of Works and Development (1978) *Highway bridge design brief*, CDP 701/D.

(6) Standards New Zealand NZS 4203: 1984 *General structural design and design loads for buildings*. Superseded.

(7) Society of Structural Engineers *Gen-Col*. Last accessed 28 September 2018. <www.sesoc.org.nz/software/>. (Available to members only.)

(8) Priestley MJN, Sieble F and Calvi GM (1996) *Seismic design and retrofit of bridges*. John Wiley and Sons, New York, NY, USA.

C5B.8 Spreadsheets

Table C5B.1: Spreadsheet index

Mangatewai-iti River Bridge

Geometric and Weight Input Parameters

Prepared: J Wood

Edit Date: 18-Aug-17 Print Date: 18-Aug-17

Item	Symbol	Value	Units	Comment/Formula
Weight of Superstructure				
Unit weight of concrete	w_c	25	kN/m^3	Including reinforcement
Beam length	L_s	20.0	m	
Length of bridge deck	L_d	83.7	m	
Length of centre spans	L_{cs}	21.0	m	
Length of end spans	L_{es}	20.5	m	
Weight of standard 20 m span I beam	W	17.0	t	From standard bridge drawings
Weight of I beams per span	W_b	667	kN	Total of 4 beams per span
Weight of deck per span	W_d	1,004	kN	Including paps
Weight of surfacing per span	W_s	170	kN	40 mm thick seal with unit wt = 20 kN/m^3
Wt handrails/guardrail per span	W_h	25	kN	1.2 kN/m
Weight of services per span	W_{se}	10	kN	Assumed value
Weight of diaphragms per span	W_{di}	221	kN	
Total weight of span	W_{st}	2,097	kN	
Weight of Pier Cap				
Maximum depth of pier cap	H_{ca}	1.5	m	From drawings
Weight of pier cap	W_{pc}	421	kN	
Weight of Pier Columns				
Pier C column height	H_C	11.70	m	
Pier B & D column heights	H_D	7.70	m	Average of heights of both columns
Diameter of columns (structural)	D_c	1.524	m	Neglecting pipe liner (Liner not included in strength calculations.)
Weight of Pier C columns	W_{cC}	534	kN	Neglecting pipe liner
Weight of Pier B & D columns	W_{cD}	351	kN	Neglecting pipe liner
Total Weights				
Axial force at base of Pier C column	N_{cC}	3,051	kN	
Axial force at base of Pier B & D cols	N_{cD}	2,869	kN	
Dynamic weight of bridge	W_{dy}	10,061	kN	Superstructure + caps + 1/3 columns
Height CoG Superstructure				
Height CoG deck	H_{de}	1.66	m	Above bottom of beams
Area of central section of beams	A_{bc}	0.292	m^2	From standard beam drawing dimensions
Height of CoG beams	H_{be}	0.66	m	Above bottom of beams
Overall CoG of superstructure	H_s	1.25	m	Above bottom of beams (ignores cross-fall)
Superstructure O/A height	H_{st}	1.75	m	Bottom of beams to top of deck
Ratio CoG over superstructure height	R_h	0.72		Check dimension - OK
Height of pier bearings	H_{bea}	0.119	m	From drawings
Ht CoG superstructure above pier cap	H_{cog}	1.37	m	
Height of Pier C	H_{pC}	13.20	m	Top of cylinder to top of pier cap
Ht CoG superstr above Pier C cylinder	H_{ct}	14.57	m	

Item	Symbol	Value	Units	Comment/Formula
Height of CoG of Total & Dynamic Mass				
Height CoG of Pier C pier cap	H_{coc}	12.63	m	Above top of cylinder
Height CoG total mass	H_{cot}	13.48	m	Above top of Pier C cylinder
Height of CoG dynamic mass	H_{cod}	14.11	m	1/3 column mass at underside of cap
Height of CoG of Pier Masses				
Height of CoG of Pier C mass	H_{cogC}	12.36	m	1/3 column at U/S cap: above Pier C cylinder
Height of CoG of Pier B & D mass	H_{cogD}	8.43	m	1/3 column at U/S cap: above Pier D cylinder
Deck Moment of Inertia				
MoI of deck section about vert axis	I_d	15.45	m^2	Deck slab only
MoI of beams about vert axis	I_b	9.13	m^2	Four beams about bridge CL
Specified concrete strength	f_{cd}	25	MPa	
Youngs modulus	E_c	28,200	MPa	
Flexural rigidity of deck	EI_d	436	GPa m^2	
Column Flexural Capacity				
Diameter of main bars	d_b	32	mm	
Number of bars	N_b	40		
Area of column	A_c	1.824	m^2	
Area of reinforcement	A_s	32,170	mm^2	
Reinforcement ratio	ρ	0.0176		
Axial force ratio Pier C	R_c	0.0515		$R_c = N_{cC}/(f_{ca}*A_c*1000)$
Adopted steel yield stress	f_y	300	MPa	275 MPa was the specified value
Steel yield stress for flexural capacity	f_{yc}	330	MPa	$f_{yc} = 1.1*f_y$
Specified concrete strength	f_c	25	MPa	
Conc strength for flexural capacity	f_{ca}	32.5	MPa	$f_{ca} = 1.3*f_c$
Cover to hoop steel	c	40	mm	From inside of pipe liner
Moment capacity from Gen-Col	M_u	7,887	kN m	Unreduced: based on 0.003 concrete strain
NA depth empirical formula	c_n	356	mm	$c_n = (0.2+0.65*R_c)*D_c*1000$
				Priestley et al, 2007. Eq (10.8)
NA depth from Gen-Col	d_{na}	376	mm	

Reference:

Priestley M J N, Calvi G M and Kowalsky, 2007. *Displacement-Based Seismic Design of Structures*. IUSS Press.

Mangatewai-iti River Bridge

Longitudinal Analysis: Pier Pile Stiffness

Prepared: J Wood

Edit Date: 18-Aug-17 Print Date: 18-Aug-17

Item	Symbol	Value	Units	Formulae / Comments
Input Structural Parameters				
Cylinder pile diameter inside shell	D_i	2.032	m	Inside of steel shell
Thickness of steel shell	t_s	10	mm	Design value.
Cylinder pile length	L	10.0	m	Pier C. Cylinders at other piers are longer
Specified concrete strength	f_c	25	MPa	
Height of Pier B	H_B	9.2	m	Top of pier above pile top
Shear applied to pile top at Pier B	V_B	906	kN	From structure longitudinal analysis (p. C5-120)
Moment applied to pile top	M_B	8,335	kN m	$M_B = H_B * V_B$
Input Soil Parameters				
Assumed increase of soil E with depth	m	30	MPa/m	Dense sand and gravels near surface
Soil poissons ratio	ν	0.35		
Soil density	ρ_o	1.8	t/m^3	
Calculated Parameters				
Cylinder pile outside diameter	D	2.052	m	$D = D_i + 2*t_s/1000$
I for concrete core	I_c	0.837	m^4	$I_c = \pi*D_i^4/64$
I for shell	I_s	0.033	m^4	$I_s = \pi*(D^4 - D_i^4)/64$
Youngs modulus for concrete	E_c	30,550	MPa	E_c =4700*Sqrt(f_c)*1.3: Priestley et al Eq (5.2) Factor 1.3 for probable strength & strain rate increase
Combined shell + Concrete Core EI	EI	32,254	MN m^2	$EI = E_c*I_c + 200{,}000*I_s$
Modified E_p to allow for shell	E_p	37,060	MPa	$E_p = EI/(\pi*D^4/64)$: Pender Eq 3.17
E value of soil at depth D	E_s	61.6	MPa	$E_s = m*D$: Pender Eq 3.23
Modulus ratio	K	602		$K = E_p / E_s$: Pender Eq 3.23
Pile Length / Diameter	L_{Dr}	4.87		$L_{Dr} = L / D$
Short pile length limit	L_r	3.52	m	$L_r = 0.07\ D\ (E_p / E_s)^{0.5}$: $L < L_r$ for short pile
Long pile length limit	L_a	11.05	m	$L_a = 1.3\ D\ (E_p / E_s)^{0.22}$: $L > L_a$ for long pile Pender Eqs 3.35 and 3.27 Assume long piles as clearly not short piles
Depth of maximum moment	L_{Mmax}	4.53	m	$L_{Mmax} = 0.41\ L_a$: Pender Eq 3.29
Moment / Shear Ratio	e	9.20	m	$e = M_B / V_B$
	f	4.483		$f = M_B / (D*V_B)$
Parameter a	a	2.690		a = 0.6*e/D: Pender Eq 3.30
Parameter b	b	0.108		$b = 0.17*f^{-0.3}$: Pender Eq 3.30
Parameter for maximum moment	I_{mh}	5.38		$I_{mh} = a*K^b$: Pender Eq 3.30
Maximum moment in pile	M_{max}	10,008	kN m	$M_{max} = I_{mh}*D*H$: Pender Eq 3.30

Item	Symbol	Value	Units	Formulae / Comments
Flexibility and Stiffness: Long Pile: Linear Increase in E_s With Depth				
Flexibility coefficients:	f_{uHL}	0.00301	m/MN	$f_{uHL} = 3.2\ K^{-0.333} / (E_s * D)$
Pender Eq 3.28	f_{uML}	0.00055	MN^{-1}	$f_{uML} = 5.0\ K^{-0.556} / (E_s * D^2)$
	$f_{\theta ML}$	0.00018	$(m\ MN)^{-1}$	$f_{\theta ML} = 13.6\ K^{-0.778} / (E_s * D^3)$
Stiffness coefficients:	K_{HHL}	775	MN/m	$K_{HHL} = f_{\theta ML} / (f_{uHL} * f_{\theta ML} - f_{uML}^2)$
Pender Eq 3.40	K_{HML}	-2421	MN	$K_{HML} = -f_{uML} / (f_{uHL} * f_{\theta ML} - f_{uML}^2)$
	K_{MML}	13248	MN m	$K_{MML} = f_{uHL} / (f_{uHL} * f_{\theta ML} - f_{uML}^2)$
Pile head horizontal stiffness	K_{HtL}	124	MN/m	$K_{HtL} = (K_{HHL} * K_{MML} - K_{HML}^2) / (K_{MML} - e * K_{HML})$ Pender Eq 3.41
Pile rotational stiffness	$K_{\theta tL}$	4,245	MN m/rad	$K_{\theta tL} = (K_{HHL} * K_{MML} - K_{HML}^2) / (K_{HHL} - K_{HML} / e)$ Pender Eq 3.42
Calculated Deflections				
Deflection at ground level	Δ_g	7.3	mm	$\Delta_g = V_B / (K_{HtL})$
Rotation at ground level	θ_g	2.0	mili rad	$\theta_g = M_B / K_{\theta tL}$
Deflection at top of pier	Δ_B	25	mm	$\Delta_B = \Delta_g + \theta_g * H_{BL}$ Approx as pier shear has inertia component at CoG
Reference				
Pender M J, 1993. *Aseismic Pile Foundation Design*. NZSEE, Vol 26 No 1 pp 49 - 161				

Mangatewai-iti River Bridge

Bridge Analysis: Longitudinal Direction: Sliding Bearings at Abutments

Prepared: J Wood

Edit Date: 18-Aug-17 Print Date: 18-Aug-17

Item	Symbol	Value	Units	Comment / Formula
Structural Inputs				
Weight of superstructure	W_S	8,400	kN	See separate analysis on Page C5-114
Effective weight of Pier C	W_C	599	kN	Cap + 1/3 wt of column, sep analysis, p. C5-114
Effective weight of Pier B	W_B	538	kN	Cap + 1/3 wt of column, sep analysis, p. C5-114
Axial force at base of Column C	N_c	3,051	kN	From analysis on page C5-114
Height of Pier C	H_C	13.2	m	Top of pier above cylinder top
Height of Piers B & D	H_B	9.2	m	Top of pier above cylinder top
Height CoG Pier C	H_{Cc}	12.36	m	Above Pier C cylinder top
Height CoG Piers B & D	H_{Bc}	8.43	m	Above Pier D cylinder top
Column diameter	D_c	1.524	m	As designed - inside pipe liners
Diameter longitudinal bars	d_b	32	mm	
Diameter transverse hoops	d_t	16	mm	As designed
Number of longitudinal bars	N_b	40		As designed
Spacing transverse hoop bars	s_t	80	mm	As designed
Cover to hoops	c_v	40	mm	
Specified concrete 28 day strength	f_c	25	MPa	
Adopted steel yield stress	f_y	300	MPa	Longitudinal & transverse steel (275 Mpa specified)
Elastomeric Bearing Input				
Width of bearings on piers	B_{be}	380	mm	From drawings. Transverse direction
Length of bearings on piers	L_{be}	300	mm	From drawings. Longitudinal direction
Overall thickness of bearing	T_b	119	mm	From drawings.
Thickness of rubber	t_r	92	mm	Assume 8 inner layers at 10 mm thickness
				Top & bottom cover of 6 mm thickness
				9 inner plates of 3 mm tickness
				Assume no dowels
Side cover	s_{co}	10	mm	Skellerup brochure
Bonded area of rubber	A_{br}	0.1008	m^2	Based on 10 mm side covers - not inc in area
				Some design guidelines include side cover
Shear modulus	G_b	0.73	MPa	53 IRHD - Skellerup brochure
Shear stiffness	K_r	0.80	MN/m	$K_r = A_{br}*G_b/(t_r/1000)$
Number of bearings on each pier	N_{be}	8		
Total shear stiffness per pier	K_t	6.4	MN/m	
Pier Cylinder Stiffness Inputs				
Horizontal stiffness at pile top level	K_h	125	MN/m	From analysis on Page C5-117
Rotational stiffness at pile top level	K_θ	4,300	MN m/rad	From analysis on Page C5-117

Item	Sym	Value	Units	Comment / Formula
Earthquake Inputs				
Site Subsoil Category		C		
Zone Factor	Z	0.42		Danneverke
Return Period Factor	R_u	1.8		2,500 year return period
Spectrum corner period	T_c	3.0	s	From BM Fig 5.2
Corner period spectral shape factor	$\Delta_h(3)$	985	mm	From BM Table 5.5
Design corner period displacement	$\Delta(3)$	745	mm	$\Delta(3) = R_u*Z*\Delta_h(3)$
Calculated Structural Parameters				
Cover to longitudinal bars	c_o	56	mm	From cover to hoops
Gross column section area	A_g	1.82	m^2	$A_g = \pi*D_c^2/4$
Area of longitudinal steel	A_s	32,170	mm^2	$A_s = N_b*\pi*d_b^2/4$
Longitudinal steel area ratio	ρ_l	0.0176		$\rho_l = A_s/(10^6*A_g)$
Check minimum required steel area	A_{sm}	24,322	mm^2	$A_{sm} = 4*10^6\ A_g/f_y$: BM Clause 5.6.4(f)
Check maximum permitted steel area	A_{sma}	109,449	mm^2	$A_{sma} = 18*10^6\ A_g/f_y$: BM Clause 5.6.4(f)
Area of transverse reinforcement	A_t	201	mm^2	$A_t = \pi*d_t^2/4$
Column concrete core diameter	D'	1.428	m	$D' = D_c - (2*c_o + d_t)/1000$ Using Priestley el, 1996 & 2007 who define D' as measured on centre-line of hoops. NZS 3101 uses outside of hoops.
Volumetric ratio transverse steel	ρ_s	0.00704		$\rho_s = 4*A_t / (1000*D'*s_t)$ OK: minimum required = 0.005: BM Clause 5.6.4(h)(i)
Strain Limits for Plastic Rotation				
Yield strength transverse reinf.	f_{sy}	300	MPa	
Strain at max stress lateral reinf.	ε_{sut}	0.12		BM Clause 5.3.5(b)
Strain at max stress longitudinal reinf.	ε_{sul}	0.12		BM Clause 5.3.5(a)
Design comp strength plastic hinge	f_{ce}	32.5	MPa	$f_{ce} = 1.3*f_c$: BM Table 5.7
Average confining stress	f_{ld}	1.00	MPa	$f_{ld} = 0.95*f_{sy}*\rho_s/2$: From Priestley et al, 1996
Confined comp strength concrete	f_{cc}	39.0	MPa	$f_{cc} = f_{ce}*(2.254*(1+7.94*f_{ld}/f_{ce})^{1/2} - 2*f_{ld}/f_{ce} - 1.254)$ Priestley et al 1996, Eq (5.6)
Reinforcement limiting strain	ε_{sd}	0.027		$\varepsilon_{sd} = 0.015+6*(\rho_s-0.005) \le 0.5\ \varepsilon_{sul}$: Eq (5-11)
Concrete limiting strain	ε_{cd}	0.0131		$\varepsilon_{cd} = 0.004+(1.4*\rho_s*f_{sy}*\varepsilon_{sut}) / f_{cc}$: Eq (5-12)
Neutral axis depth	c	376	mm	From moment strength analysis
Distance extreme bar to neutral axis	b_{na}	1,076	mm	$b_{na} = D_c*1000 - c - c_o - d_b/2$
Concrete strain from steel strain	ε	0.0095		$\varepsilon = \varepsilon_{sd}*c / b_{na}$ Steel limiting strain governs
Limit state curvature	ϕ_{ls}	0.0253	1/m	$\phi_{ls} = IF(\varepsilon > \varepsilon_{cd}, \varepsilon_{cd}/(c/1000), \varepsilon_{sd}/(b_{na}/1000))$
Plastic curvature	ϕ_p	0.0230	1/m	$\phi_p = \phi_{ls} - \phi_{yy}$
Plastic Hinge Lengths				
Ratio steel ultimate over yield stress	f_u/f_y	1.4		From Pacific Steel test results
Hinge length parameter	k_{lp}	0.08		$k_{lp} = 0.2*(f_u/f_y - 1) \le 0.08$: Eq (5-38)
Dist. to point of contraflexure Pier C	L_C	13.20	m	$L_C = H_C$
Plastic hinge length Pier C	L_{pC}	1.29	m	$L_{pC} = k_{lp}*L_C + L_{sp} \ge 2*L_{sp}$: Eq (5-37)
Distance to contraflexure Piers B & D	L_B	9.20	m	$L_B = H_B$
Plastic hinge length Piers B & D	L_{pB}	0.97	m	$L_p = k_{lp}*L_B + L_{sp} \ge 2*L_{sp}$: Eq (5-33)

Item	Symbol	Value	Units	Comment / Formula
Yield Displacements				
Probable yield strength reinforcement	f_{ye}	330	MPa	$f_{ye} = 1.1*f_y$: BM Table 5.7
Elastic modulus for steel	E_s	200,000	MPa	
Yield strain	ε_y	0.00165		$\varepsilon_y = f_{ye} / E_s$
Yield curvature	ϕ_{yy}	2.33E-03	1/m	$\phi_{yy} = 2.15*\varepsilon_y / D_c$: Eq (5-8)
Strain penetration length	L_{sp}	0.232	m	$L_{sp} = 0.022*f_{ye}*d_b /1000$: Eq (5-510
Coefficient for column fixity	C_1	0.333		See Bridge Manual Commentary C5
Yield displacement Pier C at top	Δ_{yC}	140	mm	$\Delta_{yC} = C_1*\phi_{yy}*(H_C + L_{sp})^2*1000$: Eq (5-10)
Yield displacement Pier C at CoG	Δ_{yCc}	123	mm	$\Delta_{yCc} = C_1*\phi_{yy}*(H_{Cc} + L_{sp})^2*1000$
Yield displacement Piers B & D at top	Δ_{yB}	69	mm	$\Delta_{yB} = C_1*\phi_{yy}*(H_B + L_{sp})^2*1000$: Eq (5-10)
Yield disp. Piers B & D at CoG	Δ_{yBc}	58	mm	$\Delta_{yBc} = C_1*\phi_{yy}*(H_{Bc} + L_{sp})^2*1000$
Ductility Factor Capacities				
Plastic rotation Pier C	θ_{pC}	0.0296	rad	$\theta_{pC} = \phi_p*L_{pC}$
Plastic displacement capacity Pier C	Δ_{pC}	391	mm	$\Delta_{pC} = \theta_{pC}*H_c*1000$
Limit state disp. capacity Pier C	Δ_{lsC}	531	mm	$\Delta_{lsC} = \Delta_{yC} + \Delta_{pC}$: excludes brgs and founds
Ductility capacity Pier C	μ_{lsC}	3.79		$\mu_{lsC} = \Delta_{lsC} / \Delta_{yC}$: based on pier top
Plastic rotation Piers B & D	θ_{pB}	0.0223	rad	$\theta_{pB} = \phi_p*L_{pB}$
Plastic disp. capacity Piers B & D	Δ_{pB}	205	mm	$\Delta_{pB} = \theta_{pB}*H_B*1000$
Plast. disp. capacity Piers B&D at CoG	Δ_{pBc}	188	mm	$\Delta_{pBc} = \theta_{pB}*H_{Bc}*1000$
Limit state disp capacity Piers B & D	Δ_{lsB}	274	mm	$\Delta_{lsB} = \Delta_{yB} + \Delta_{pB}$: excludes brgs and founds
				Critical pier capacity & sets design disp.
Ductility capacity Piers B & D	μ_{lsB}	3.97		$\mu_{lsB} = \Delta_{lsB} / \Delta_{yB}$: based on pier top
Pier Shears at Limit State Displacement *(Iteration reqd as pier shear and inertia forces unknown at this stage)*				
Pier height ratio	R_h	0.697		$R_h = H_B / H_C$
Distance between Pier B Top & CoG	h_{Bco}	0.770	m	$h_{Bco} = H_B - H_{Bc}$
Distance between Pier C Top & CoG	h_{Cco}	0.840	m	$h_{Cco} = H_C - H_{Cc}$
Height correction factor for shear ratio	R_c	0.002		$R_c = (F_{iC}*h_{Cco} - F_{iB}*h_{Bco})/(V_{Bn}*H_C)$
				Assume = 0 for first iteration and then correct after F_{iB}, F_{iC} and V_B are calculated below
Pier shear ratio	R_v	0.699		$R_V = R_h + R_c$
Approx shear in Piers B & D at mom cap	V_{Ba}	857	kN	$V_{Ba} = M_{ac} / H_B$: M_{ac} = trial mom cap: see below
				(Moment capacities are the same for all cols)
Shear in Piers B & D at limit state disp	V_{Bn}	906	kN	Iterate until $V_{Bn} = V_B$ given below
				Can use V_{Ba} to start iteration.
Shear in Pier C at limit state disp	V_{Cn}	634	kN	$V_{Cn} = V_{Bn}*R_v$

Item	Symbol	Value	Units	Comment / Formula
Displacements From Foundations & Bearings *(Iteration required as pier inertia forces unknown at this stage)*				
Pier B top displacement from foundation	Δ_{fB}	24.9	mm	$\Delta_{fB} = V_{Bn}/K_h+((V_{Bn} - F_{iB})*H_B + F_{iB}*H_{Bc})*H_B/K_\theta$
Pier B CoG displacement from foundation	Δ_{fBc}	23.5	mm	$\Delta_{fBc} = V_{Bn}/K_h+((V_{Bn} - F_{iB})*H_B + F_{iB}*H_{Bc})*H_{Bc}/K_\theta$
Pier B displacement in bearings	Δ_{bB}	127.4	mm	$\Delta_{bB} = (V_{Bn} - F_{iB})/K_t$
Shear strain in Pier B bearings	ε_b	1.38		$\varepsilon_b = \Delta_{bB}/t_r > 1.0$ limit. A modification is reqd
Pier C top displacement from foundation	Δ_{fC}	30.4	mm	$\Delta_{fC} = V_{Cn}/K_h+((V_{Cn} - F_{iC})*H_C + F_{iC}*H_{Cc})*H_C/K_\theta$
Pier C CoG displacement from foundation	Δ_{fCc}	28.8	mm	$\Delta_{fCc} = V_{Cn}/K_h+((V_{Cn} - F_{iC})*H_C + F_{iC}*H_{Cc})*H_{Cc}/K_\theta$
Pier C displacement in bearings	Δ_{bC}	80.5	mm	$\Delta_{bC} = (V_{Cn} - F_{iC})/K_t$
				In 1st iteration assume $F_{iB} = 0$ in above expressions
Design limit state disp superstructure	Δ_{tB}	426	mm	$\Delta_{tB} = \Delta_{fB} + \Delta_{bB} + \Delta_{yB} + \Delta_{pB}$
Pier C plastic displacement at top	Δ_{pCd}	175	mm	$\Delta_{pCd} = \Delta_{tB} - \Delta_{fC} - \Delta_{bC} - \Delta_{yC}$
Pier C plastic displacement at CoG	Δ_{pCc}	164	mm	$\Delta_{pCc} = \Delta_{pCd}*H_{Cc}/H_C$
Ductility demand on Pier C at design disp	μ_{dC}	2.25		$\mu_{dc} = (\Delta_{pCd} + \Delta_{yC})/\Delta_{yC}$: based on pier top
Displacements at Mass Locations				
Design disp. of superstructure	Δ_S	426	mm	$\Delta_S = \Delta_{tB}$
Displacement at CoG of Pier B & D	Δ_{Bd}	269	mm	$\Delta_{Bd} = \Delta_{yBc} + \Delta_{pBc} + \Delta_{fBc}$
Displacement at CoG of Pier C	Δ_{Cd}	316	mm	$\Delta_{Cd} = \Delta_{yCc} + \Delta_{pCc} + \Delta_{fCc}$
Sum of weights x displacements	S_{wd}	4,059	kN m	$S_{wd} = (W_S*\Delta_S + 2*W_B*\Delta_{Bd} + W_c*\Delta_{Cd})/1000$
Characteristic design displacement	Δ_d	410	mm	$\Delta_d = (W_S*\Delta_S^2 + 2*W_B*\Delta_{Bd}^2 + W_c*\Delta_{Cd}^2)/(S_{wd}*1000)$: Eq (5-20)
Effective Mass				
Total mass	m_t	1027	t	$m_t = (W_S + 2*W_B + W_c)/9.81$
Effective mass	m_e	1010	t	$m_e = S_{wd}/(\Delta_d*9.81/1000)$: Eq (5-22)
Damping				
Viscous damping Pier C	ξ_C	0.15		$\xi_C = 0.1+0.04*(\mu_{dC} - 1) \le 0.18$: Eq (5-32)
Viscous damping for Piers B & D	ξ_B	0.18		$\xi_B = 0.1+0.04*(\mu_{lsB} - 1) \le 0.18$
				Ductility demand on Pier B & C approx equal to their capacity as disp of these piers is design criterion
Abutment bearing damping ratio	ξ_A	0.25		Assumed for sliding bearings
Damping in pier bearings	ξ_{be}	0.05		BM Clause 5.4.3(g)(vi)
Shear in Pier B bearings	V_{Bb}	815	kN	$V_{Bb} = V_{Bn} - F_{iB}$
Shear in Pier C bearings	V_{Cb}	515	kN	$V_{Cb} = V_{Cn} - F_{iC}$
				(In 1st iteration assume $F_{iB} = F_{iC} = 0$)
System damping including abutments	ξ_{sy}	0.144		$\xi_{sy} = (\xi_A*V_A*\Delta_S+2*\xi_B*V_{Bn}*(\Delta_{yB}+\Delta_{pB})+\xi_C*V_{Cn}*(\Delta_{yC}+\Delta_{pCd})+2*\xi_{be}*V_{Bb}*\Delta_{bB}+\xi_{be}*V_{Cb}*\Delta_{bC})/(V_A*\Delta_S+2*V_{Bn}*(\Delta_{yB}+\Delta_{pB})+V_{Cn}*(\Delta_{yC}+\Delta_{pCd})+2*V_{Bb}*\Delta_{bB}+V_{Cb}*\Delta_{bC})$: Eq (5-23)
				Disp demand on Piers B & D is approxiately equal to their capacity
Damping modifier	R_ξ	0.653		$R_\xi = (0.07/(0.02+\xi_{sy}))^{0.5}$: Eq (5-17)

Item	Symbol	Value	Units	Comment / Formula
Effective Period				
Damping reduced spectrum corner disp	Δ_{cr}	486	mm	$\Delta_{cr} = R_{\xi}*\Delta(3)$
Effective period from design spectrum	T_e	2.53	s	$T_e = 3*\Delta_d / \Delta_{cr}$
Secant stiffness	K_e	6,225	kN/m	$K_e = 4*\pi^2*m_e / T_e^2$: Eq (5-21)
Total base shear	V_T	2,551	kN	$V_T = K_e*\Delta_d$ /1000: Eq (5-19)
Inertia forces				
Inertia force on supestructure	F_{iS}	2,250	kN	$F_{iS} = V_T*W_S*\Delta_S / (S_{wd}*1000)$: Eq (5-39)
Inertia force on Piers B & D	F_{iB}	91	kN	$F_{iB} = V_T*W_B*\Delta_{Bd} / (S_{wd}*1000)$
Inertia force on Pier C	F_{iC}	119	kN	$F_{iC} = V_T*W_C*\Delta_{Cd} / (S_{wd}*1000)$
Base Shears and Moments				
Friction coeff. for abutment bearings	n	0.05		Assumed for sliding teflon bearings BM Cl. 5.3.9(b) gives range as 0.02 to 0.15 A value of 0.02 increases req mom cap 3%
Shear carried by both abutments	V_A	105	kN	$V_A = n*W_S / 4$
Shear in Piers B & D	V_B	906	kN	$V_{BD} = (V_T - V_A) / (2 + R_v)$
Check shear in Piers B & D	V_{Bc}	906	kN	$V_{Bc} = \Delta_{bB}*K_t + F_{iB}$
Shear in Pier C	V_C	634	kN	$V_C = (V_T - V_A)*R_v / (R_v + 2)$
Check shear in Pier C	V_{Cc}	634	kN	$V_{Cc} = \Delta_{bC}*K_t + F_{iC}$
Check shear ratio	R_{vC}	0.699		$R_{vC} = V_C / V_B$
Moment applied to base of Piers B&D	M_B	8,267	kN m	$M_B = (V_B - F_{iB})*H_B + F_{iB}*H_{Bc}$
Check moment applied to base Pier C	M_C	8,267	kN m	$M_C = (V_C - F_{iC})*H_C + F_{iC}*H_{Cc}$
Check P-Δ Moment				
Displacement of cylinder top at Pier C	Δ_{Ct}	5	mm	$\Delta_{Ct} = V_C / K_h$
Displacement of cylinder top at Pier B	Δ_{Bt}	7	mm	$\Delta_{Ct} = V_B / K_h$
P-Δ moment on Pier C	$M_{CP-\Delta}$	1,053	kN m	$M_{CP-\Delta} = (W_S/4*(\Delta_S - \Delta_{Ct}) + W_C*(\Delta_{pCc} + \Delta_{yCc} - \Delta_{Ct}))/1000$ Neglects lower 2/3 length of column
P-Δ moment on Piers B & D	$M_{BP-\Delta}$	1,008	kN m	$M_{BP-\Delta} = (W_S/4*(\Delta_S - \Delta_{Bt}) + W_B*(\Delta_{pBc} + \Delta_{yBc} - \Delta_{Bt}))/1000$
Ratio: $M_{CP-\Delta} / M_C$	M_{rat}	0.13		> 0.1. Increase in moment capacity required < 0.25 so less than maximum limit See BM Clause 5.3.7
Required Moment Capacity				
Required moment capacity	M_{Cr}	8,793	kN m	$M_{Cr} = M_C + M_{cP-D} / 2$
Capacity of section with 40/D32 bars	M_{ac}	7,887	kN m	Need to increase capacity: could use fy = 500 Mpa and reduce number of bars

Reference:

Priestley M J N, Seible F and Calvi G M, 1996. *Seismic Design and Retrofit of Bridges*. John Wiley & Sons Inc

Priestley M J N, Calvi G M and Kowalsky, 2007. *Displacement-Based Seismic Design of Structures*. IUSS Press.

Mangatewai-iti River Bridge

Bridge Analysis:Transverse Direction: Sliding Bearings at Abutments

Prepared: J Wood

Edit Date: 18-Aug-17 Print Date: 18-Aug-17

Item	Symbol	Value	Units	Comment / Formula
Structural Inputs				
Weight of superstructure	W_S	8,400	kN	From separate analysis on Page C5-114
Effective weight of Pier C	W_C	599	kN	Cap + 1/3 wt of column, sep analysis, p. C5-114
Effective weight of Pier B	W_B	538	kN	Cap + 1/3 wt of column, sep analysis, p. C5-114
Axial force at base of column C	N_c	3,051	kN	See separate analysis, Page C5-114
Effective height of Pier C	H_C	14.57	m	Superstructure CoG above Pier C cylinder top
Effective height of Piers B & D	H_B	10.57	m	Superstructure CoG above Pier B cylinder top
Height CoG Pier C	H_{Cc}	12.36	m	Above Pier C cylinder top
Height CoG Piers B & D	H_{Bc}	8.43	m	Above Pier D cylinder top
Column diameter	D_c	1.524	m	As designed. (Ignoring pipe liners.)
Diameter longitudinal bars	d_b	32	mm	As designed
Diameter transverse hoops	d_t	16	mm	As designed
Number of longitudinal bars	N_b	40		As designed
Spacing transverse hoop bars	s_t	80	mm	As designed
Cover to hoops	c_v	40	mm	From drawings
Specified concrete 28 day strength	f_c	25	MPa	
Adopted steel yield stress	f_y	300	MPa	Longitudinal & transverse steel (275 Mpa specified)
Elastomeric Bearing Input				
Width of bearings on piers	B_{be}	380	mm	From drawings. Transverse direction
Length of bearings on piers	L_{be}	300	mm	From drawings. Longitudinal direction
Overall thickness of bearing	T_b	119	mm	From drawings.
Thickness of rubber	t_r	92	mm	Assume 8 inner layers at 10 mm thickness Top & bottom cover of 6 mm thickness 9 inner plates of 3 mm tickness Assume no dowels
Side cover	s_{co}	10	mm	Skellerup brochure
Bonded area of rubber	A_{br}	0.1008	m^2	Based on excluding 10 mm side covers Some guidelines include this cover in area
Shear modulus	G_b	0.73	MPa	53 IRHD - Skellerup brochure
Shear stiffness	K_r	0.80	MN/m	$K_r = A_{br} * G_b/(t_r/1000)$
Number of bearings on each pier	N_{be}	8		
Total shear stiffness per pier	K_t	6.4	MN/m	
Pier Cylinder Stiffness Inputs				
Horizontal stiffness at pile top level	K_h	125	MN/m	From separate analysis on Page C5-117
Rotational stiffness at pile top level	K_θ	4,300	MN m/rad	From separate analysis on Page C5-117

Item	Symbol	Value	Units	Comment / Formula
Earthquake Inputs				
Site Subsoil Category		C		
Zone Factor	Z	0.42		Danneverke
Return Period Factor	R_u	1.8		2,500 year return period
Spectrum corner period	T_c	3.0	s	From BM Fig 5.2
Corner period spectral shape factor	$\Delta_h(3)$	985	mm	From BM Table 5.5
Design corner period displacement	$\Delta(3)$	745	mm	$\Delta(3) = R_u*Z*\Delta_h(3)$
Calculated Structural Parameters				
Cover to longitudinal bars	c_o	56	mm	From cover to hoops
Gross column section area	A_g	1.82	m^2	$A_g = \pi*D_c^2/4$
Area of longitudinal steel	A_s	32,170	mm^2	$A_s = N_b*\pi*d_b^2/4$
Longitudinal steel area ratio	ρ_l	0.0176		$\rho_l = A_s/(10^6*A_g)$
Check minimum required steel area	A_{sm}	24,322	mm^2	$A_{sm} = 4*10^6\ A_g/f_y$: BM Clause 5.6.4(f)
Check maximum permitted steel area	A_{sma}	109,449	mm^2	$A_{sma} = 18*10^6\ A_g/f_y$: BM Clause 5.6.4(f)
Area of transverse reinforcement	A_t	201	mm^2	$A_t = \pi*d_t^2/4$
Column concrete core diameter	D'	1.428	m	$D' = D_c - (2*c_o + d_t)/1000$ Using Priestley el, 1996 & 2007 who define D' as measured on centre-line of hoops. NZS 3101 uses outside of hoops.
Volumetric ratio transverse steel	ρ_s	0.00704		$\rho_s = 4*A_t / (1000*D'*s_t)$ OK: minimum required = 0.005: BM Clause 5.6.4(h)(i)
Strain Limits for Plastic Rotation				
Yield strength transverse reinf.	f_{syf}	300	MPa	
Strain at max stress lateral reinf.	ε_{sut}	0.12		BM Clause 5.3.5(b)
Strain at max stress longitudinal reinf.	ε_{sul}	0.12		BM Clause 5.3.5(a)
Design comp strength plastic hinge	f_{ce}	32.5	MPa	$f_{ce} = 1.3*f_c$: BM Table 5.7
Average confining stress	f_{ld}	1.00	MPa	$f_{ld} = 0.95*f_{syf}*\rho_s/2$: From Priestley et al, 1996
Confined comp strength concrete	f_{cc}	39.0	MPa	$f_{cc} = f_{ce}*(2.254*(1+7.94*f_{ld}/f_{ce})^{1/2} - 2*f_{ld}/f_{ce} - 1.254)$ Priestley et al 1996, Eq 5.6
Reinforcement limiting strain	ε_{sd}	0.027		$\varepsilon_{sd} = 0.015+6*(\rho_s-0.005) \le 0.5\ \varepsilon_{sul}$: Eq (5-11)
Concrete limiting strain	ε_{cd}	0.0131		$\varepsilon_{cd} = 0.004+(1.4*\rho_s*f_{syf}*\varepsilon_{sut}) / f_{cc}$: Eq (5-12)
Neutral axis depth	c	376	mm	From moment strength analysis
Distance extreme bar to neutral axis	b_{na}	1,076	mm	$b_{na} = D_c*1000 - c - c_o - d_b/2$
Concrete strain from steel strain	ε	0.0095		$\varepsilon = \varepsilon_{sd}*c / b_{na}$ Steel limiting strain governs
Limit state curvature	ϕ_{ls}	0.0253	1/m	$\phi_{ls} = IF(\varepsilon > \varepsilon_{cd}, \varepsilon_{cd}/(c/1000), \varepsilon_{sd}/(b_{na}/1000))$
Plastic curvature	ϕ_p	0.0230	1/m	$\phi_p = \phi_{ls} - \phi_{yy}$

Item	Symbol	Value	Units	Comment / Formula
Plastic Hinge Lengths				
Ratio steel ultimate over yield stress	f_u / f_y	1.4		From Pacific Steel test results
Hinge length parameter	k_{lp}	0.08		$k_{lp} = 0.2*(f_u / f_y - 1) \le 0.08$: Eq (5-38)
Distance to pt. of contraflexure Pier C	L_C	14.57	m	$L_C = H_C$
Plastic hinge length Pier C	L_{pC}	1.40	m	$L_{pC} = k_{lp}*L_C + L_{sp} \ge 2*L_{sp}$: Eq (5-37)
Distance to contraflexure Piers B & D	L_B	10.57	m	$L_B = H_B$
Plastic hinge length Piers B & D	L_{pB}	1.08	m	$L_p = k_{lp}*L_B + L_{sp} \ge 2*L_{sp}$: Eq (5-37)
Yield Displacements				
Probable yield strength of reinf.	f_{ye}	330	MPa	$f_{ye} = 1.1*f_y$: Table 5.7
Elastic modulus for steel	E_s	200,000	MPa	
Yield strain	ε_y	0.00165		$\varepsilon_y = f_{ye} / E_s$
Yield curvature	ϕ_{yy}	0.0023	1/m	$\phi_{yy} = 2.15*\varepsilon_y / D_c$: Eq (5-8)
Strain penetration length	L_{sp}	0.232	m	$L_{sp} = 0.022*f_{ye}*d_b /1000$: Eq (5-10)
Coefficient for column fixity	C_1	0.333		See Bridge Manual Commentary C5
Yield disp. Pier C at super CoG	Δ_{yC}	170	mm	$\Delta_{yC} = C_1*\phi_{yy}*(H_C + L_{sp})^2*1000$: Eq (5-10)
Yield displacement Pier C at pier CoG	Δ_{yCc}	123	mm	$\Delta_{yCc} = C_1*\phi_{yy}*(H_{Cc} + L_{sp})^2*1000$
Yield disp Piers B & D at super CoG	Δ_{yB}	91	mm	$\Delta_{yB} = C_1*\phi_{yy}*(H_B + L_{sp})^2*1000$: Eq (5-10)
Yield disp Piers B & D at pier CoG	Δ_{yBc}	58	mm	$\Delta_{yBc} = C_1*\phi_{yy}*(H_{Bc} + L_{sp})^2*1000$
Ductility Factor Capacities				
Plastic rotation Pier C	θ_{pC}	0.0321	rad	$\theta_{pC} = \phi_p*L_{pC}$
Plastic displacement capacity Pier C	Δ_{pC}	397	mm	$\Delta_{pC} = \theta_{pC}*H_{Cc}*1000$: based on ht at CoG of pier
Limit state disp. capacity Pier C	Δ_{lsC}	520	mm	$\Delta_{lsC} = \Delta_{yCc} + \Delta_{pC}$: excludes brgs & foundations
Ductility capacity Pier C	μ_{lsC}	4.23		$\mu_{lsC} = \Delta_{lsC} / \Delta_{yCc}$
Plastic rotation Piers B & D	θ_{pB}	0.0248	rad	$\theta_{pB} = \phi_p*L_{pB}$
Plast disp capacity super at Piers B&D	Δ_{pB}	262	mm	$\Delta_{pB} = \theta_{pB}*H_B*1000$: based on ht of CoG of super
Plast disp cap Piers B & D at pier CoG	Δ_{pBc}	209	mm	$\Delta_{pB} = \theta_{pB}*H_{Bc}*1000$
Limit state disp capacity Piers B & D	Δ_{lsB}	267	mm	$\Delta_{lsB} = \Delta_{yBc} + \Delta_{pBc}$: excludes brgs & foundations Critical pier capacity & sets design disp.
Ductility capacity Piers B & D	μ_{lsB}	4.59		$\mu_{lsB} = \Delta_{lsB} / \Delta_{yBc}$
Pier Shears at Limit State Displacement *(Iteration reqd as pier shear and inertia forces unknown at this stage)*				
Pier height ratio	R_h	0.725		$R_h = H_B / H_C$
Distance between Pier B Top & CoG	h_{Bco}	2.140	m	$h_{Bco} = H_B - H_{Bc}$
Distance between Pier C Top & CoG	h_{Cco}	2.210	m	$h_{Cco} = H_C - H_{Cc}$
Height correction factor for shear ratio	R_c	0.004		$R_c = (F_{iC}*h_{Cco} - F_{iB}*h_{Bco})/(V_{Bn}*H_C)$ Assume = 0 for first iteration and then correct after F_{iB}, F_{iC} and V_B are calculated below
Pier shear ratio	R_v	0.730		$R_V = R_h + R_c$
Approx shear in Piers B & D at mom cap	V_{Ba}	746	kN	$V_{Ba} = M_{ac} / H_B$: M_{ac} = trial mom cap: see below (Moment capacities are the same for all cols)
Shear in Piers B & D at limit state disp	V_{Bn}	751	kN	Iterate until $V_{Bn} = V_B$ given below Can use V_{Ba} to start iteration.
Shear in Pier C at limit state disp	V_{Cn}	548	kN	$V_{Cn} = V_{Bn}*R_v$

Item	Symbol	Value	Units	Comment / Formula
Displacements From Foundations & Bearings *(Iteration required as pier inertia forces unknown at this stage)*				
Pier B superstructure disp from foundation	Δ_{fB}	25.1	mm	$\Delta_{fB} = V_{Bn}/K_h+((V_{Bn} - F_{iB})*H_B + F_{iB}*H_{Bc})*H_B/K_\theta$
Pier B CoG displacement from foundation	Δ_{fBc}	21.3	mm	$\Delta_{fBc} = V_{Bn}/K_h+((V_{Bn} - F_{iB})*H_B + F_{iB}*H_{Bc})*H_{Bc}/K_\theta$
Pier B displacement in bearings	Δ_{bB}	106.0	mm	$\Delta_{bB} = (V_{Bn} - F_{iB})/K_t$
Shear strain in Pier B bearings	ε_b	1.15		$\varepsilon_b = \Delta_{bB}/t_r > 1.0$ limit. A modification should be considered
Pier C superstructure disp from foundation	Δ_{fC}	30.8	mm	$\Delta_{fC} = V_{Cn}/K_h+((V_{Cn} - F_{iC})*H_C + F_{iC}*H_{Cc})*H_C/K_\theta$
Pier C CoG displacement from foundation	Δ_{fCc}	26.8	mm	$\Delta_{fCc} = V_{Cn}/K_h+((V_{Cn} - F_{iC})*H_C + F_{iC}*H_{Cc})*H_{Cc}/K_\theta$
Pier C displacement in bearings	Δ_{bC}	71.2	mm	$\Delta_{bC} = (V_{Cn} - F_{iC})/K_t$ In 1st iteration assume $F_{iB} = 0$ in above expressions
Design limit state disp superstructure	Δ_{tB}	484	mm	$\Delta_{tB} = \Delta_{fB} + \Delta_{bB} + \Delta_{yB} + \Delta_{pB}$
Pier C super plastic displacement	Δ_{pCd}	212	mm	$\Delta_{pCd} = \Delta_{tB} - \Delta_{fC} - \Delta_{bC} - \Delta_{yC}$
Pier C CoG plastic displacement	Δ_{pCc}	180	mm	$\Delta_{pCc} = \Delta_{pCd}*H_{Cc}/H_C$
Ductility demand on Pier C at design disp	μ_{dC}	2.46		$\mu_{dc} = (\Delta_{pCc} + \Delta_{yCc})/\Delta_{yCc}$: based on pier CoG disp
Displacements at Mass Locations				
Design disp. of superstructure	Δ_S	484	mm	$\Delta_S = \Delta_{tB}$
Displacement at CoG of Pier B & D	Δ_{Bd}	288	mm	$\Delta_{Bd} = \Delta_{yBc} + \Delta_{pBc} + \Delta_{fBc}$
Displacement at CoG of Pier C	Δ_{Cd}	329	mm	$\Delta_{Cd} = \Delta_{yCc} + \Delta_{pCc} + \Delta_{fCc}$
Sum of weights x displacements	S_{wd}	4,570	kN m	$S_{wd} = (W_S*\Delta_S + 2*W_B*\Delta_{Bd} + W_c*\Delta_{Cd})/1000$
Characteristic design displacement	Δ_d	464	mm	$\Delta_d = (W_S*\Delta_S^2 + 2*W_B*\Delta_{Bd}^2 + W_c*\Delta_{Cd}^2)/(S_{wd}*1000)$: Eq (5-20)
Effective Mass				
Total mass	m_t	1,027	t	$m_t = (W_S + 2*W_B + W_c)/9.81$
Effective mass	m_e	1,005	t	$m_e = S_{wd}/(\Delta_d*9.81/1000)$: Eq (5-22)
Damping				
Viscous damping Pier C	ξ_C	0.16		$\xi_C = 0.1+0.04*(\mu_{dC} - 1) \le 0.18$: Eq (5-32)
Viscous damping for Piers B & D	ξ_B	0.18		$\xi_B = 0.1+0.04*(\mu_{lsB} - 1) \le 0.18$ Ductility demand on Pier B & C approx equal to their capacity as disp of these piers is design criterion
Abutment bearing damping ratio	ξ_A	0.25		Assumed for sliding bearings
Damping in pier bearings	ξ_{be}	0.05		BM Clause 5.4.3(g)(vi)
Shear in Pier B bearings	V_{Bb}	678	kN	$V_{Bb} = V_{Bn} - F_{iB}$
Shear in Pier C bearings	V_{Cb}	455	kN	$V_{Cb} = V_{Cn} - F_{iC}$ (In 1st iteration assume $F_{iB} = F_{iC} = 0$)
System damping including abutments	ξ_{sy}	0.151		$\xi_{sy} = (\xi_A*V_A*\Delta_S+2*\xi_B*V_{Bn}*(\Delta_{yBc}+\Delta_{pBc})+ \xi_C*V_{Cn}*(\Delta_{yCc}+\Delta_{pCc})+2*\xi_{be}*V_{Bb}*\Delta_{bB}+\xi_{be}*V_{Cb}*\Delta_{bC})/ (V_A*\Delta_S+2*V_{Bn}*(\Delta_{yBc}+\Delta_{pBc})+V_{Cn}*(\Delta_{yCc}+\Delta_{pCc})+ 2*V_{Bb}*\Delta_{bB}+V_{Cb}*\Delta_{bC})$: Eq (5-18) Disp demand on Piers B & D is approxiately equal to their capacity
Damping modifier	R_ξ	0.640		$R_\xi = (0.07/(0.02+\xi_{sy}))^{0.5}$: Eq (5-17)

Item	Symbol	Value	Units	Comment / Formula
Effective Period				
Damping reduced spectrum corner disp	Δ_{cr}	476	mm	$\Delta_{cr} = R_\zeta * \Delta(3)$
Effective period from design spectrum	T_e	2.92	s	$T_e = 3*\Delta_d / \Delta_{cr}$
Secant stiffness	K_e	4,650	kN/m	$K_e = 4*\pi^2*m_e/T_e^2$: Eq (5-21)
Total base shear	V_T	2,156	kN	$V_T = K_e*\Delta_d$ /1000: Eq (5-19)
Inertia forces				
Inertia force on supestructure	F_{iS}	1,916	kN	$F_{iS} = V_T*W_S*\Delta_S/(S_{wd}*1000)$: Eq (5-39)
Inertia force on Piers B & D	F_{iB}	73	kN	$F_{iB} = V_T*W_B*\Delta_{Bd}/(S_{wd}*1000)$
Inertia force on Pier C	F_{iC}	93	kN	$F_{iC} = V_T*W_C*\Delta_{Cd}/(S_{wd}*1000)$
Base Shears and Moments				
Friction coefficient for abutment brgs	n	0.05		Assumed for sliding teflon bearings BM Cl. 5.3.9(b) gives range as 0.02 to 0.15 A value of 0.02 increases reqd mom cap 3%
Shear carried by both abutments	V_A	105	kN	$V_A = n*W_S/4$
Shear in Piers B & D	V_B	751	kN	$V_{BD} = (V_T - V_A)/(2+R_v)$
Check shear in Piers B & D	V_{Bc}	751	kN	$V_{Bc} = \Delta_{bB}*K_t + F_{iB}$
Shear in Pier C	V_C	548	kN	$V_C = (V_T - V_A)*R_v/(R_v+2)$
Check shear in Pier C	V_{Cc}	548	kN	$V_{Cc} = \Delta_{bC}*K_t + F_{iC}$
Check shear ratio	R_{vC}	0.730		$R_{vC} = V_C/V_B$
Moment applied to base of Piers B&D	M_B	7,784	kN m	$M_B = (V_B - F_{iB})*H_B + F_{iB}*H_{Bc}$
Check moment applied to base Pier C	M_C	7,784	kN m	$M_C = (V_C - F_{iC})*H_C + F_{iC}*H_{Cc}$
Check P-Δ Moment				
Displacement of cylinder top at Pier C	Δ_{Ct}	4	mm	$\Delta_{Ct} = V_C / K_h$
Displacement of cylinder top at Pier B	Δ_{Bt}	6	mm	$\Delta_{Ct} = V_B / K_h$
P-Δ moment on Pier C	$M_{CP-\Delta}$	1,185	kN m	$M_{CP-\Delta} = (W_S/4*(\Delta_S - \Delta_{Ct})+W_C*(\Delta_{pCc}+\Delta_{yCc} - \Delta_{Ct}))/1000$
P-Δ moment on Piers B & D	$M_{BP-\Delta}$	1,143	kN m	$M_{BP-\Delta} = (W_S/4*(\Delta_S - \Delta_{Bt})+W_B*(\Delta_{pBc}+\Delta_{yBc} - \Delta_{Bt}))/1000$ The bottom section of the columns are neglected as they only add a small contribution to P-Δ
Ratio: $M_{CP-\Delta} / M_C$	M_{rat}	0.15		> 0.1: increase in moment capacity required
Required Moment Capacity				
Required moment capacity	M_{Cr}	8,376	kN m	$M_{Cr} = M_C + M_{CP-\Delta}/2$
Capacity of section with 40/D32 bars	M_{ac}	7,887	kN m	Need to increase capacity a small amount Moment less critical than in longitudinal direction

References:

Priestley M J N, Seible F and Calvi G M, 1996. *Seismic Design and Retrofit of Bridges*. John Wiley & Sons Inc

Priestley M J N, Calvi G M and Kowalsky, 2007. *Displacement-Based Seismic Design of Structures*. IUSS Press.

Mangatewai-iti River Bridge

Transverse Analysis: Abutment Pile Stiffness: Fixed Head

Prepared: J Wood

Edit Date: 18-Aug-17 Print Date: 18-Aug-17

Description	Symbol	Value	Units	Formulae & Comments
Input Structural Parameters				
Cylinder pile diameter inside shell	D_i	1.372	m	Inside of steel shell
Thickness of steel shell	t_s	6	mm	Design value.
Cylinder pile length	L	11.70	m	At Abutment E
Specified concrete strength	f_c	25	MPa	
Shear applied to abutment	V	2,000	kN	Nominal value to estimate stiffness
Input Soil Parameters				
Assumed inc of soil E with depth	m	15	MPa/m	Medium dense sand and gravels near surface
Soil poissons ratio	ν	0.35		
Soil density	ρ_o	1.8	t/m^3	
Calculated Parameters				
Cylinder pile outside diameter	D	1.384	m	$D = D_i + 2*t_s/1000$
I for concrete core	I_c	0.174	m^4	$I_c = \pi*D_i^4/64$
I for shell	I_s	0.006	m^4	$I_s = \pi*(D^4 - D_i^4)/64$
Youngs modulus for concrete	E_c	30,550	MPa	E_c =4700*Sqrt(f_c)*1.3: Priestley et al Eq (5.2)
				Factor 1.3 for prob strength & strain rate increase
Combined shell + Concrete Core EI	EI	6,547	MN m^2	$EI = E_c*I_c + 200{,}000*I_s$
Modified E_p to allow for shell	E_p	36,351	MPa	$E_p = EI/(\pi*D^4/64)$: Pender Eq 3.17
E value of soil at depth D	E_s	20.8	MPa	$E_s = m*D$
Modulus ratio	K	1,751		$K = E_p / E_s$
Pile Length / Diameter	L_{Dr}	8.45		$L_{Dr} = L / D$
Short pile length limit	L_r	4.05	m	$L_r = 0.07\ D\ (E_p / E_s)^{0.5}$: $L < L_r$ For short pile
Long pile length limit	L_a	9.44	m	$L_a = 1.3\ D\ (E_p / E_s)^{0.22}$: $L > L_a$ For long pile
				Long pile analysis OK
Flexibility and Stiffness: Long Pile: Linear Increase in E_s With Depth				
Flexibility coefficients:	f_{uHL}	0.00926	m/MN	$f_{uHL} = 3.2\ K^{-0.333}/(E_s*D)$
Pender Eq 3.28	f_{uML}	0.00198	MN^{-1}	$f_{uML} = 5.0\ K^{-0.556}/(E_s*D^2)$
	$f_{\theta ML}$	0.00074	$(m\ MN)^{-1}$	$f_{\theta ML} = 13.6\ K^{-0.778}/(E_s*D^3)$
Stiffness coefficients:	K_{HHL}	251	MN/m	$K_{HHL} = f_{\theta ML}/(f_{uHL}*f_{\theta ML} - f_{uML}^2)$
Pender Eq 3.40	K_{HML}	-671	MN	$K_{HML} = -f_{uML}/(f_{uHL}*f_{\theta ML} - f_{uML}^2)$
	K_{MML}	3,141	MN m	$K_{MML} = f_{uHL}/(f_{uHL}*f_{\theta ML} - f_{uML}^2)$
Stiffness Fixed Head				
Flexibility coefficient	f_{FH}	0.0039	m/MN	$f_{FH} = 1.35*K^{-0.333}/(mD^2)$: Pender Eq 3.31
Displacement	u^F	7.8	mm	$u^F = f_{FH}*V$: Pender Eq 3.31
Fixing moment parameter	I_{MF}	1.942		$I_{MF} = 0.37*K^{0.222}$: Pender Eq 3.32
Fixing moment	M^F	5,375	kN m	$M^F = I_{MF}*V*D$: Pender Eq 3.32
Pile horizontal stiffness (single pile)	K_{HHF}	256	MN/m	$K_{HHF} = V/u^F$: small variation from K_{HHL} given above

Reference

Pender M J, 1993. *Aseismic Pile Foundation Design. NZSEE, Vol 26 No 1 pp 49 - 161*

Mangatewai-iti River Bridge

Bridge Analysis: Transverse Direction: Fixed Against Translation at Abutments

Prepared: J Wood

Edit Date: 18-Aug-17 Print Date: 18-Aug-17

Item	Sym	Value	Units	Comment / Formula
Structural Inputs				
Weight of superstructure	W_S	8,400	kN	From separate analysis on Page C5-114
Length of end spans (A-B)	L_{AB}	20.5	m	From drawings
Length of centre spans (B-C)	L_{BC}	21.0	m	Two equal spans - from drawings
Weight of superstructure per unit length	w_{SU}	101.2	kN/m	$w_{SU} = W_S/(2*L_{AB} + 2*L_{BC})$
Effective weight of Pier C	W_C	599	kN	Cap + 1/3 wt of column, sep analysis, p. C5-114
Effective weight of Pier B	W_B	538	kN	Cap + 1/3 wt of column, sep analysis, p. C5-114
Axial force at base of column C	N_c	3,051	kN	From separate analysis on Page C5-114
Effective height of Pier C	H_C	14.57	m	Superstructure CoG above Pier C cylinder top
Effective height of Piers B & D	H_B	10.57	m	Superstructure CoG above Pier B cylinder top
Height CoG Pier C	H_{Cc}	12.36	m	Above Pier C cylinder top
Height CoG Piers B & D	H_{Bc}	8.43	m	Above Pier D cylinder top
Column diameter	D_c	1.524	m	As designed. (Pipe liners neglected)
Diameter longitudinal bars	d_b	32	mm	As designed
Diameter transverse hoops	d_t	16	mm	As designed
Number of longitudinal bars	N_b	40		As designed
Spacing transverse hoop bars	s_t	80	mm	As designed
Cover to hoops	c_v	40	mm	From drawings
Specified concrete 28 day strength	f_c	25	MPa	
Adopted steel yield stress	f_y	300	MPa	Longitudinal & transverse steel (275 Mpa specified)
Elastomeric Bearing Input				
Width of bearings on piers	B_{be}	380	mm	From drawings. Transverse direction
Length of bearings on piers	L_{be}	300	mm	From drawings. Longitudinal direction
Overall thickness of bearing	T_b	119	mm	From drawings.
Thickness of rubber	t_r	92	mm	Assume 8 inner layers at 10 mm thickness Top & bottom cover of 6 mm thickness 9 inner plates of 3 mm tickness Assume no dowels
Side cover	s_{co}	10	mm	Skellerup brochure
Bonded area of rubber	A_{br}	0.1008	m^2	Based on 10 mm side covers
Shear modulus	G_b	0.73	MPa	53 IRHD - Skellerup brochure
Shear stiffness	K_r	0.80	MN/m	$K_r = A_{br}*G_b/(t_r/1000)$
Number of bearings on each pier	N_{be}	8		
Total shear stiffness per pier	K_t	6.4	MN/m	
Foundation Stiffness Inputs				
Horizontal stiffness at pile top level	K_h	125	MN/m	From separate analysis on Page C5-117
Rotational stiffness at pile top level	K_θ	4,300	MN m/r	From separate analysis on Page C5-117
Horizontal stiffness of abutment piles	K_A	500	MN/m	From separate analysis on Page C5-128

Item	Sym	Value	Units	Comment / Formula
Earthquake Inputs				
Site Subsoil Category		C		
Zone Factor	Z	0.42		Danneverke
Return Period Factor	R_u	1.8		2500 year return period
Spectrum corner period	T_c	3.0	s	See BM Fig 5.2
Corner period spectral shape factor	$\Delta_h(3)$	985	mm	From Table 5.5 in BM
Design corner period displacement	$\Delta(3)$	745	mm	$\Delta(3) = R_u*Z*\Delta_h(3)$
Calculated Structural Parameters				
Cover to longitudinal bars	c_o	56	mm	From cover to hoops
Gross column section area	A_g	1.82	m^2	$A_g = \pi*D_c^2/4$
Area of longitudinal steel	A_s	32,170	mm^2	$A_s = N_b*\pi*d_b^2/4$
Longitudinal steel area ratio	ρ_l	0.0176		$\rho_l = A_s/(10^6*A_g)$
Check minimum required steel area	A_{sm}	24,322	mm^2	$A_{sm} = 4*10^6\ A_g/f_y$: BM 5.6.4(f)
Check maximum permitted steel area	A_{sma}	109,449	mm^2	$A_{sma} = 18*10^6\ A_g/f_y$: BM 5.6.4(f)
Area of transverse reinforcement	A_t	201	mm^2	$A_t = \pi*d_t^2/4$
Column concrete core diameter	D'	1.428	m	$D' = D_c - (2*c_o - d_t)/1000$ Using Priestley el, 1996 & 2007 who define D' as measured on centre-line of hoops. NZS 3101 uses outside of hoops.
Volumetric ratio transverse steel	ρ_s	0.00704		$\rho_s = 4*A_t / (1000*D'*s_t)$ OK: minimum required = 0.005 : BM 5.6.4(h)(i)
Strain Limits for Plastic Rotation				
Yield strength transverse reinforcement	f_{syf}	300	MPa	
Strain at max stress lateral reinforcement	ε_{sut}	0.12		BM Clause 5.3.5(b)
Strain at max stress longitudinal reinf.	ε_{sul}	0.12		BM Clause 5.3.5(a)
Design comp strength plastic hinge	f_{ce}	32.5	MPa	$f_{ce} = 1.3*f_c$: BM Table 5.7
Average confining stress	f_{ld}	1.00	MPa	$f_{ld} = 0.95*f_{syf}*\rho_s/2$: From Priestley et al, 1996
Confined comp strength concrete	f_{cc}	39.0	MPa	$f_{cc} = f_{ce}*(2.254*(1+7.94*f_{ld}/f_{ce})^{1/2} - 2*f_{ld}/f_{ce} - 1.254)$ Priestley et al 1996, Eq 5.6
Reinforcement limiting strain	ε_{sd}	0.027		$\varepsilon_{sd} = 0.015+6*(\rho_s-0.005) \le 0.5\ \varepsilon_{sul}$: Eq (5-11)
Concrete limiting strain	ε_{cd}	0.0131		$\varepsilon_{cd} = 0.004+(1.4*\rho_s*f_{syf}*\varepsilon_{sut}) / f_{cc}$: Eq (5-12)
Neutral axis depth	c	376	mm	From moment strength analysis
Distance extreme bar to neutral axis	b_{na}	1,076	mm	$b_{na} = D_c*1000 - c - c_o - d_b/2$
Concrete strain from steel strain	ε	0.0095		$\varepsilon = \varepsilon_{sd}*c / b_{na}$ Steel limiting strain governs
Limit state curvature	ϕ_{ls}	0.0253	1/m	$\phi_{ls} = IF(\varepsilon > \varepsilon_{cd}, \varepsilon_{cd}/(c/1000), \varepsilon_{sd}/(b_{na}/1000))$
Plastic curvature	ϕ_p	0.0230	1/m	$\phi_p = \phi_{ls} - \phi_{yy}$
Plastic Hinge Lengths				
Ratio steel ultimate over yield stress	f_u/f_y	1.4		From Pacific Steel test results
Hinge length parameter	k_{lp}	0.08		$k_{lp} = 0.2*(f_u/f_y - 1) \le 0.08$: Eq (5-38)
Distance to point of contraflexure Pier C	L_C	14.57	m	$L_C = H_C$
Plastic hinge length Pier C	L_{pC}	1.40	m	$L_{pC} = k_{lp}*L_C + L_{sp} \ge 2*L_{sp}$: Eq (5-37)
Distance to contraflexure Piers B & D	L_B	10.57	m	$L_B = H_B$
Plastic hinge length Piers B & D	L_{pB}	1.08	m	$L_p = k_{lp}*L_B + L_{sp} \ge 2*L_{sp}$: Eq (5-37)

Item	Sym	Value	Units	Comment / Formula
Yield Displacements				
Probable yield strength of reinforcement	f_{ye}	330	MPa	$f_{ye} = 1.1*f_y$: Table 5.7
Elastic modulus for steel	E_{sb}	200,000	MPa	
Yield strain	ε_y	0.00165		$\varepsilon_y = f_{ye} / E_{sb}$
Yield curvature	ϕ_{yy}	0.00233	1/m	$\phi_{yy} = 2.15*\varepsilon_y / D_c$: Eq (5-8)
Strain penetration length	L_{sp}	0.232	m	$L_{sp} = 0.022*f_{ye}*d_b /1000$: Eq (5-10)
Coefficient for column fixity	C_1	0.333		See Appendix 5A
Yield displacement Pier C at super CoG	Δ_{yC}	170	mm	$\Delta_{yC} = C_1*\phi_{yy}*(H_C + L_{sp})^2*1000$: Eq (5-10)
Yield displacement Pier C at pier CoG	Δ_{yCc}	123	mm	$\Delta_{yCc} = C_1*\phi_{yy}*(H_{Cc} + L_{sp})^2*1000$
Yield disp Piers B & D at super CoG	Δ_{yB}	91	mm	$\Delta_{yB} = C_1*\phi_{yy}*(H_B + L_{sp})^2*1000$: Eq (5-10)
Yield disp Piers B & D at pier CoG	Δ_{yBc}	58	mm	$\Delta_{yBc} = C_1*\phi_{yy}*(H_{Bc} + L_{sp})^2*1000$
Ductility Factor Capacities				
Plastic rotation Pier C	θ_{pC}	0.0321	rad	$\theta_{pC} = \phi_p*L_{pC}$
Plastic displacement capacity Pier C	Δ_{pC}	397	mm	$\Delta_{pC} = \theta_{pC}*H_{Cc}*1000$: based on ht of CoG of pier
Limit state displacement capacity Pier C	Δ_{lsC}	520	mm	$\Delta_{lsC} = \Delta_{yCc} + \Delta_{pC}$: excludes brgs & foundations
Ductility capacity Pier C	μ_{lsC}	4.23		$\mu_{lsC} = \Delta_{lsC} /\Delta_{yCc}$
Plastic rotation Piers B & D	θ_{pB}	0.0248	rad	$\theta_{pB} = \phi_p*L_{pB}$
Plastic disp capacity Piers B & D	Δ_{pB}	209	mm	$\Delta_{pB} = \theta_{pB}*H_{Bc}*1000$: based on ht of CoG of pier
Limit state disp capacity Piers B & D	Δ_{lsB}	267	mm	$\Delta_{lsB} = \Delta_{yBc} + \Delta_{pB}$: excludes brgs & foundations
Ductility capacity Piers B & D	μ_{lsB}	4.59		$\mu_{lsB} = \Delta_{lsB} /\Delta_{yBc}$
Pier Shears at Limit State Displacement *(Iteration required as pier shear and inertia forces unknown at this stage)*				
Pier height ratio	R_H	0.725		$R_h = H_B / H_C$
Pier B&D dist between CoGs on super & pier	h_{Bco}	2.14	m	$h_{Bco} = H_B - H_{Bc}$
Pier C dist between CoGs on super & pier	h_{Cco}	2.21	m	$h_{Cco} = H_C - H_{Cc}$
Height correction factor for shear ratio	R_C	0.041		$R_c = (F_{iC}*h_{Cco} - F_{iB}*h_{Bco})/(V_{Bn}*H_C)$ Assume = 0 for first iteration and then correct after F_{iB}, F_{iC} and V_B are calculated below
Pier shear ratio	R_V	0.766		$R_V = R_H + R_C$
Approx shear in Piers B & D at mom cap	V_{BA}	746	kN	$V_{Ba} = M_{ac} / H_B$: M_{ac} = trial mom cap: see below (Moment capacities are the same for all cols)
Shear in Piers B & D at limit state disp	V_{Bn}	891	kN	Iterate until $V_{Bn} = V_B$ given below Can use V_{BA} to start iteration.
Shear in Pier C at limit state disp	V_{Cn}	682	kN	$V_{Cn} = V_{Bn}*R_V$
Displacements From Foundations & Bearings *(Iteration required as pier inertia forces unknow at this stage)*				
Pier B super disp from foundation	Δ_{fB}	29.4	mm	$\Delta_{fB} = V_{Bn} /K_h+((V_{Bn} - F_{iB})*H_B + F_{iB}*H_{Bc})*H_B /K_\theta$
Pier B CoG displacement from foundation	Δ_{fBc}	24.9	mm	$\Delta_{fBc} = V_{Bn} /K_h+((V_{Bn} - F_{iB})*H_B + F_{iB}*H_{Bc})*H_{Bc} /K_\theta$
Pier B displacement in bearings	Δ_{bB}	113.1	mm	$\Delta_{bB} = (V_{Bn} - F_{iB})/ K_t$
Shear strain in Pier B bearings	ε_b	1.23		$\varepsilon_b = \Delta_{bB} /t_r > 1.0$ limit. A modification could be made to meet limit
Pier C super disp from foundation	Δ_{fC}	36.1	mm	$\Delta_{fC} = V_{Cn} /K_h+((V_{Cn} - F_{iC})*H_C + F_{iC}*H_{Cc})*H_C /K_\theta$
Pier C CoG displacement from foundation	Δ_{fCc}	31.5	mm	$\Delta_{fCc} = V_{Cn} /K_h+((V_{Cn} - F_{iC})*H_C + F_{iC}*H_{Cc})*H_{Cc} /K_\theta$
Pier C displacement in bearings	Δ_{bC}	44.1	mm	$\Delta_{bC} = (V_{Cn} - F_{iC})/ K_t$
	In 1st iteration assume $F_{iB} = 0.8V_{Bn}$ and $F_{iC} = 0.5V_{Cn}$ in above expressions			

Item	Sym	Value	Units	Comment / Formula		
Superstructure Displacement Profile: Determine by Trial and Error to Agree With Structural Analysis Output						
Displacements at Superstructure CoGs		*Trial Values*		*Struc Analysis Output (see matrix analysis below)*		
Estimated displacement of abutments	Δ_{AS}	3.57	mm	3.57	mm	
Displacement at Piers B & D	Δ_{BS}	195.1	mm	195.1	mm	
Displacement at Pier C	Δ_{CS}	279.0	mm	279.0	mm	
Proportion of shear transferred to abutments	x	0.592		0.592		Trial & error to get $M_p = M_C$
Bending moment at base of piers	M_p	9,057	kN m	Target value = long capacity = 9,060 kN m		
				Moment is sensitive to x value.		
Displacements at Pier CoGs					*Struct Anal Output*	
Displacement at CoG of Pier B & D	Δ_{BG}	83	mm	$\Delta_{BG} = \Delta_{yBc} + \Delta_{pBc} + \Delta_{fBc}$	83	mm
Displacement at CoG of Pier C	Δ_{CG}	179	mm	$\Delta_{CG} = \Delta_{yCc} + \Delta_{pCc} + \Delta_{fCc}$	179	mm
Ductility Demands						
Pier C						
Maximum disp demand on superstructure	Δ_{tC}	279	mm	$\Delta_{tC} = \Delta_{CS}$		
Plastic disp demand of superstructure at Pier C	Δ_{pCd}	28.8	mm	$\Delta_{pCd} = \Delta_{tC} - \Delta_{fC} - \Delta_{bC} - \Delta_{yC}$		
Plastic disp demand at Pier C CoG	Δ_{pCc}	24.4	mm	$\Delta_{pCc} = \Delta_{pCd} * H_{Cc} / H_C$		
Ductility demand on Pier C at design disp	μ_{dC}	1.20		$\mu_{dc} = (\Delta_{pCc} + \Delta_{yCc})/\Delta_{yCc}$: based on pier CoG height		
Piers B & D						
Disp demand on superstructure at Pier B & D	Δ_{tB}	195	mm	$\Delta_{tB} = \Delta_{BS}$		
Plastic disp demand on super at Piers B & D	Δ_{pBd}	0.0	mm	$\Delta_{pCd} = \Delta_{tB} - \Delta_{fB} - \Delta_{bB} - \Delta_{yB} \geq 0$		
Plast disp demand at CoG of Piers B&D CoG	Δ_{pBc}	0.0	mm	$\Delta_{pBc} = \Delta_{pBd} * H_{Bc} / H_B$		
Ductility demand on Piers B and D	μ_{dB}	1.00		$\mu_{dB} = (\Delta_{pBc} + \Delta_{yBc})/\Delta_{yBc}$: based on pier CoG height		
Superstructure Inertia Weights						
Supestructure at each abutment	W_{AS}	1,037	kN	$W_{AS} = w_{SU} * L_{AB}/2$		
Superstructure at Piers B & D	W_{BS}	2,100	kN	$W_{BS} = w_{SU} * (L_{AB} + L_{BC}) /2$		
Superstructure at Pier C	W_{CS}	2,125	kN	$W_{CS} = w_{SU} * L_{BC}$		
Characteristic Design Displacement						
Sum of weights x displacements	S_{WD}	1,616	kN m	$S_{WD} = (2*W_{AS}*\Delta_{AS} + 2*W_{BS}*\Delta_{BS} + W_{CS}*\Delta_{CS} + 2*W_B*\Delta_{BG} + W_C*\Delta_{CG})/1000$		
Characteristic design displacement	Δ_d	218	mm	$\Delta_d = (2*W_{AS}*\Delta_{AS}^2 + 2*W_{BS}*\Delta_{BS}^2 + W_{CS}*\Delta_{CS}^2 + 2*W_B*\Delta_{BG}^2 + W_C*\Delta_{CG}^2)/(S_{WD}*1000)$: Eq (5-20)		
Effective Mass						
Total mass	m_T	1027	t	$m_T = (W_S + 2*W_B + W_c)/9.81$		
Effective mass	m_e	757	t	$m_e = S_{WD}/(\Delta_d*9.81/1000)$: Eq (5-22)		

Item	Sym	Value	Units	Comment / Formula
Damping				
Viscous damping Pier C	ξ_C	0.11		$\xi_C = 0.1+0.04*(\mu_{dC} - 1) \le 0.18$: Eq (5-32)
Viscous damping for Piers B & D	ξ_B	0.10		$\xi_B = 0.1+0.04*(\mu_{dB} - 1) \le 0.18$
Abutment damping ratio	ξ_A	0.05		Assumed for small abutment displacements
Damping in pier bearings	ξ_{be}	0.05		BM Clause 5.4.3(g)(vi)
Shear in Pier B bearings	V_{Bb}	724	kN	$V_{Bb} = V_{Bn} - F_{iB}$
Shear in Pier C bearings	V_{Cb}	282	kN	$V_{Cb} = V_{Cn} - F_{iC}$
				In 1st iteration assume $F_{iB} = F_{iC} = 0$
System damping including abutments	ξ_{sy}	0.078		$\xi_{sy} = (\xi_A*2*V_A*\Delta_{AS}+2*\xi_B*V_{Bn}*(\Delta_{yBc}+\Delta_{pBc})+ \xi_C*V_{Cn}*(\Delta_{yCc}+\Delta_{pCc})+2*\xi_{be}*V_{Bb}*\Delta_{bB}+\xi_{be}*V_{Cb}*\Delta_{bC})/ (2*V_A*\Delta_{AS}+2*V_{Bn}*(\Delta_{yBc}+\Delta_{pBc})+V_{Cn}*(\Delta_{yCc}+\Delta_{pCc})+ 2*V_{Bb}*\Delta_{bB}+V_{Cb}*\Delta_{bC})$: Eq (5-123)
Damping modifier	R_ξ	0.845		$R_\xi = (0.07/(0.02+\xi_{sy}))^{0.5}$: Eq (5-17)
Effective Period				
Damping reduced spectrum corner disp	Δ_{cr}	629	mm	$\Delta_{cr} = R_\xi*\Delta(3)$
Effective period from design spectrum	T_e	1.04	s	$T_e = 3*\Delta_d / \Delta_{cr}$
Secant stiffness	K_e	27,735	kN/m	$K_e = 4*\pi^2*m_e/T_e^2$: Eq (5-21)
Total base shear	V_T	6,038	kN	$V_T = K_e*\Delta_d$ /1000: Eq (5-19)
Inertia forces				
Inertia force on supestructure at abuts	F_{iSA}	13.9	kN	$F_{iS} = V_T*W_{AS}*\Delta_{AS}/(S_{wd}*1000)$: Eq (5-39)
Inertia force on super at Piers B & D	F_{iSB}	1,531	kN	$F_{iSB} = V_T*W_{BS}*\Delta_{BS}/(S_{wd}*1000)$: Eq (5-39)
Inertia force on super at Pier C	F_{iSC}	2,215	kN	$F_{iSC} = V_T*W_{CS}*\Delta_{CS}/(S_{wd}*1000)$: Eq (5-39)
Inertia force on Piers B & D	F_{iB}	167	kN	$F_{iB} = V_T*W_B*\Delta_{BG}/(S_{wd}*1000)$
Inertia force on Pier C	F_{iC}	400	kN	$F_{iC} = V_T*W_C*\Delta_{CG}/(S_{wd}*1000)$
Check sum of inertia forces	F_{iT}	6,038	kN	$F_{iT} = 2*F_{iSA} + 2*F_{iSB} + F_{iSC} + 2*F_{iB} + F_{iC}$
Pier Base Shears				
Shear carried by each abutments	V_A	1,787	kN	$V_A = x*V_T/2$
Shear in Piers B & D	V_B	891	kN	$V_{BD} = (V_T - 2*V_A)/(2+R_v)$
Check shear in Piers B & D	V_{Bc}	891	kN	$V_{Bc} = \Delta_{bB}*K_t + F_{iB}$
Shear in Pier C	V_C	682	kN	$V_C = (V_T - 2*V_A)*R_v/(R_v+2)$
Check shear in Pier C	V_{Cc}	682	kN	$V_{Cc} = \Delta_{bC}*K_t + F_{iC}$
Check shear ratio	R_{vC}	0.766		$R_{vC} = V_C / V_B$
Moment applied to base Piers B & D	M_B	9,057	kN m	$M_B = (V_B - F_{iB})*H_B + F_{iB}*H_{Bc}$
Check moment applied to base Pier C	M_C	9,057	kN m	$M_C = (V_C - F_{iC})*H_C + F_{iC}*H_{Cc}$
Check P - Δ Moment				
Displacement of cylinder top at Pier C	Δ_{CT}	5	mm	$\Delta_{CT} = V_C / K_h$
Displacement of cylinder top at Pier B	Δ_{BT}	7	mm	$\Delta_{CT} = V_B / K_h$
P-Δ moment on Pier C	$M_{CP-\Delta}$	659	kN m	$M_{CP-\Delta} = (W_S/4*(\Delta_{CS} - \Delta_{Ct})+W_C*(\Delta_{pCc}+\Delta_{yCc} - \Delta_{Ct}))/1000$
P-Δ moment on Piers B & D	$M_{BP-\Delta}$	422	kN m	$M_{BP-\Delta} = (W_S/4*(\Delta_{BS} - \Delta_{Bt})+W_B*(\Delta_{pBc}+\Delta_{yBc} - \Delta_{Bt}))/1000$
				The bottom section of the columns is neglected as it is a minor component of P-Δ
Ratio: $M_{CP-\Delta} / M_C$	M_{rat}	0.07		< 0.1: No increase in moment capacity required

Item	Sym	Value	Units	Comment / Formula
Required Moment Capacity				
Required moment capacity	M_{Cr}	9,057	kN m	$M_{Cr} = M_C$
Capacity of section with 40/D32 bars	M_{ac}	7,887	kN m	
Structural Analysis				
Superstructure Inputs				
Transverse MoI	I_T	4.65	m^4	0.3 I_G : cracked deck section at link slabs
Young's modulus superstructure	E_S	28,200	MPa	E_S = 4,700*Sqrt(fc)*1.2: Priestley et al Eq (5.2)
				1.2 factor adjusts for probable strength increase
Pier Inputs				
Stiffness of Pier B & D based on pier CoG	K_{BP}	10,718	kN/m	$K_{BP} = V_B /(\Delta_{BG} /1000)$: includes foundation
Stiffness of Pier C based on pier CoG	K_{CP}	3,814	kN/m	$K_{CP} = V_C /(\Delta_{CG} /1000)$: includes foundation
Model spring between super & Piers B, D CoGs	K_{BE}	6,462	kN/m	$K_{BE} = (V_B - F_{iB})/((\Delta_{tB} - \Delta_{BG})/1000)$
Model spring between super & Pier C CoG	K_{CE}	2,818	kN/m	$K_{CE} = (V_C - F_{iC})/((\Delta_{tC} - \Delta_{CG})/1000)$
Check overall stiffness of Piers B & D	K_B	4,031	kN/m	$K_B = 1/(1/K_{BP} + 1/K_{BE})$
Overall stiffness of Pier C	K_C	1,620	kN/m	$K_C = 1/(1/K_{CP} + 1/K_{CE})$
Check Elastic Stiffness of Piers				
I value of pier column	I_p	0.265	m^4	$I_p = \pi*D_c^4/64$
Assumed reduction factor for cracking	R_{fc}	0.30		
Check elastic stiffness of Piers B & D	K_{BEL}	11,218	kN/m	$K_{BE} = 3*E_S*1000*I_p*R_{fc} /H_{Bc}^3$: (not used)
Check elastic stiffness of Pier C	K_{CEL}	3,559	kN/m	$K_{CE} = 3*E_S*1000*I_p*R_{fc} /H_{Cc}^3$: (not used)
Calculated Stiffness Matrices				
Stiffness coeficient for Beam Span A-B	EI_A	6.4E+06	kN m	$EI_A = 1000*E_S*I_T / L_{AB}$
Stiffness coeficient Beam Span B-C	EI_B	6.2E+06	kN m	$EI_B = 1000* E_S*I_T / L_{BC}$

Stiffness Matrix Beam A-B *(Degree of Freedom Number in First Row & Column)*

	1	2	3	4	6
1	2.6E+07	1.3E+07	1.9E+06	-1.9E+06	0.0
2	1.3E+07	2.6E+07	1.9E+06	-1.9E+06	0.0
3	1.9E+06	1.9E+06	6.8E+05	-1.8E+05	0.0
4	-1.9E+06	-1.9E+06	-1.8E+05	1.9E+05	-3.2E+03
6	0.0	0.0	0.0	-3.2E+03	8.6E+03

1/2 spring stiffness at Piers B, C & D for stiffness coeffs

Full spring used at abutments

Stiffness Matrix Beam B-C *(Degree of Freedom Number in First Row & Column)*

	2	4	5	6	7
2	2.5E+07	1.8E+06	-1.8E+06	0.0	0.0
4	1.8E+06	1.7E+05	-1.7E+05	-3.2E+03	0.0
5	-1.8E+06	-1.7E+05	1.7E+05	0.0	-1.4E+03
6	0.0	-3.2E+03	0.0	8.6E+03	0.0
7	0.0	0.0	-1.4E+03	0.0	3.3E+03

Total Stiffness Matrix *(Degree of Freedom No. in First Row & Column)*

	1	2	3	4	5	6	7
1	2.6E+07	1.3E+07	1.9E+06	-1.9E+06	0.0E+00	0.0E+00	0.0E+00
2	1.3E+07	5.1E+07	1.9E+06	-8.8E+04	-1.8E+06	0.0E+00	0.0E+00
3	1.9E+06	1.9E+06	6.8E+05	-1.8E+05	0.0E+00	0.0E+00	0.0E+00
4	-1.9E+06	-8.8E+04	-1.8E+05	3.6E+05	-1.7E+05	-6.5E+03	0.0E+00
5	0.0E+00	-1.8E+06	0.0E+00	-1.7E+05	1.7E+05	0.0E+00	-1.4E+03
6	0.0E+00	0.0E+00	0.0E+00	-6.5E+03	0.0E+00	1.7E+04	0.0E+00
7	0.0E+00	0.0E+00	0.0E+00	0.0E+00	-1.4E+03	0.0E+00	3.3E+03

Inverted Stiffness Matrix							
	1	***2***	***3***	***4***	***5***	***6***	***7***
1	2.3E-07	1.0E-07	-3.3E-08	3.3E-06	4.3E-06	1.2E-06	1.8E-06
2	1.0E-07	1.2E-07	-2.3E-08	2.1E-06	3.4E-06	8.1E-07	1.4E-06
3	-3.3E-08	-2.3E-08	2.0E-06	1.4E-06	1.1E-06	5.2E-07	4.8E-07
4	3.3E-06	2.1E-06	1.4E-06	6.1E-05	8.3E-05	2.3E-05	3.5E-05
5	4.3E-06	3.4E-06	1.1E-06	8.3E-05	1.2E-04	3.1E-05	5.2E-05
6	1.2E-06	8.1E-07	5.2E-07	2.3E-05	3.1E-05	6.7E-05	1.3E-05
7	1.8E-06	1.4E-06	4.8E-07	3.5E-05	5.2E-05	1.3E-05	3.2E-04

Input Forces from Above		
0	kN m	
0	kN m	
13.9	kN	= F_{iSA}
1531	kN	= F_{iSB}
1108	kN	= F_{iSC} /2
167	kN	= F_{iB}
200	kN	= F_{iC} /2

Rotations		
1	0.0103	rad
2	0.0074	rad

Check Input Forces		
Based on Calculated Displs		
0	kN m	
0	kN m	
13.9	kN	
1531	kN	
1108	kN	
167	kN	
200	kN	

Displacements		
3	0.0036	m
4	0.1951	m
5	0.2790	m
6	0.0831	m
7	0.1789	m

Beam A-B Forces		
1	0.00	kN m
2	-36,357	kN m
3	14	kN
4	2,135	kN
6	84	kN

Beam B-C Forces		
2	36,357	kN m
4	-605	kN
5	1,108	kN
6	84	kN
7	200	kN

Check Force Sums		
3	14	kN
4	1,531	kN
5	1,108	kN
6	167	kN
7	200	kN

Shear in AB		
V_{AB}	-1774	kN

Shear Ratio in AB		
V_R	-0.587	

References:

Priestley M J N, Seible F and Calvi G M, 1996. *Seismic Design and Retrofit of Bridges* . John Wiley & Sons Inc

Priestley M J N, Calvi G M and Kowalsky, 2007. *Displacement-Based Seismic Design of Structures* . IUSS Press.

(This page is intentionally blank)

C6 Site stability, foundations, earthworks and retaining walls

Table C6.1: Unweighted peak ground acceleration coefficients, $C_{0,1000}$, corresponding to a 1000 year return at a subsoil Class A or B rock site and subsoil Class D or E deep or soft soil site, and effective magnitude, M_{eff}, for various return periods for New Zealand towns and cities

Note: For a Class C shallow soil site refer to note 1 at the end of the table.

Town/City	$C_{0,1000}$		Effective magnitudes (M_{eff}) for design return period (years)		Town/City	$C_{0,1000}$		Effective magnitudes (M_{eff}) for design return period (years)	
	Class A/B rock	Class D&E deep/ soft soil	500 – 2500	50 – 250		Class A/B rock	Class D&E deep/ soft soil	500 – 2500	50 – 250
Kaitaia	0.12	0.15	5.75		Whakatane	0.43	0.46	6.1	
Paihia/Russell	0.13	0.16	5.75		Opotiki	0.40	0.44	6.1	
Kaikohe	0.12	0.15	5.75		Ruatoria	0.34	0.41	6.1	
Whangarei	0.13	0.16	5.8		Murupara	0.42	0.41[2]	6.3	
Dargaville	0.13	0.16	5.8		Taupo	0.38	0.42	6.1	
Warkworth	0.13	0.17	5.9		Taumarunui	0.32	0.36	6.0	
Auckland	0.15	0.19	5.9		Turangi	0.36	0.40	6.25	
Manakau City	0.17	0.21	5.9		Gisborne	0.37	0.41	6.4	
Waiuku	0.16	0.20	5.9		Wairoa	0.35	0.41	6.5	
Pukekohe	0.18	0.22	5.9		Waitara	0.27	0.32	6.0	
Thames	0.26	0.30	5.8		New Plymouth	0.28	0.33	6.0	
Paeroa	0.28	0.33	5.8		Inglewood	0.27	0.32	6.1	
Waihi	0.29	0.34	5.9		Stratford	0.27	0.32	6.2	
Huntly	0.23	0.28	5.8		Opunake	0.27	0.32	6.1	
Ngaruawahia	0.23	0.27	5.8		Hawera	0.26	0.32	6.2	
Morrinsville	0.27	0.32	5.8		Patea	0.27	0.34	6.2	
Te Aroha	0.29	0.34	5.9		Whanganui	0.31	0.37	6.0	
Tauranga	0.29	0.34	5.9		Raetihi	0.35	0.37	6.2	
Mount Maunganui	0.29	0.34	5.9		Ohakune	0.35	0.38	6.2	
Hamilton	0.24	0.28	5.9		Waiouru	0.35	0.39	6.25	
Cambridge	0.26	0.32	5.9		Napier	0.41	0.43	6.9	6.2
Te Awamutu	0.24	0.29	5.9		Hastings	0.40	0.43	6.9	6.2
Matamata	0.27	0.34	5.9		Waipawa	0.40	0.44	6.75	6.25
Te Puke	0.30	0.35	6.0		Waipukurau	0.40	0.44	6.75	6.25
Putaruru	0.29	0.34	6.0		Taihape	0.35	0.41	6.3	
Tokoroa	0.31	0.35	6.0		Marton	0.35	0.40	6.25	
Otorohanga	0.25	0.27	5.9		Bulls	0.36	0.41	6.3	
Te Kuiti	0.26	0.27	5.9		Feilding	0.40	0.43	6.7	6.1
Mangakino	0.31	0.36	6.0		Palmerston North	0.42	0.44	6.9	6.1
Rotorua	0.35	0.39	6.0		Dannevirke	0.43	0.46	7.0	6.2
Kawerau	0.41	0.43	6.2		Woodville	0.44	0.46	7.0	6.2

Table C6.1: continued

Town/City	$C_{0,1000}$		Effective magnitudes (M_{eff}) for design return period (years)		Town/City	$C_{0,1000}$		Effective magnitudes (M_{eff}) for design return period (years)	
	Class A/B rock	Class D&E deep/ soft soil	500 – 2500	50 – 250		Class A/B rock	Class D&E deep/ soft soil	500 – 2500	50 – 250
Pahiatua	0.45	0.47	7.1	6.2	Rangiora[3]	0.37	0.38	6.4	
Masterton	0.50	0.45[2]	7.0	6.3	Christchurch[3]	-	-	-	-
Foxton	0.40	0.42	6.7	6.1	Akaroa[3, 4]	-	-	5.8	6.25
Levin	0.43	0.44	6.8	6.1	Ashburton	0.25	0.29	6.1	
Otaki	0.42	0.44	6.8	6.2	Geraldine	0.25	0.28	6.0	
Paraparaumu	0.42	0.44	6.9	6.2	Temuka	0.22	0.24	6.0	
Wellington	0.44	0.45	7.1	6.2	Fairlie	0.32	0.32	6.1	
Porirua	0.43	0.44	7.0	6.2	Mt Cook	0.45	0.48	6.9	6.2
Lower Hutt	0.45	0.45	7.1	6.2	Timaru	0.20	0.23	6.0	
Upper Hutt	0.47	0.45[2]	7.1	6.25	Waimate	0.20	0.24	6.0	
Eastbourne - Point Howard	0.44	0.45	7.1	6.2	Twizel	0.39	0.37[2]	6.1	
					Wanaka	0.39	0.42	6.1	
Wainuiomata	0.47	0.44[2]	7.1	6.2	Cromwell	0.33	0.37	6.25	
Takaka	0.42	0.46	5.8		Alexandra	0.29	0.32	6.3	
Motueka	0.42	0.46	5.9		Arrowtown	0.39	0.42	6.4	
Nelson	0.40	0.43	6.1		Queenstown	0.40	0.42	6.5	
Picton	0.35	0.38	6.6	6.1	Milford Sound	0.62	0.62	7.1	6.1
Blenheim	0.40	0.42	6.75	6.1	Oamaru	0.22	0.24	6.0	
St Arnaud	0.46	0.48	6.9	6.1	Palmerston	0.22	0.25	6.0	
Westport	0.54	0.52[2]	5.7		Mosgiel	0.23	0.26	6.0	
Reefton	0.53	0.56	6.0		Dunedin	0.22	0.25	6.0	
Murchison	0.51	0.54	6.2		Te Anau	0.43	0.42[2]	6.4	
Hanmer Springs	0.55	0.53[2]	7.0	6.5	Riverton	0.26	0.30	6.2	
Kaikoura	0.55	0.53[2]	6.7	6.1	Winton	0.26	0.28	6.2	
Cheviot	0.43	0.42[2]	6.6		Gore	0.26	0.27	6.2	
Greymouth	0.50	0.50	6.5		Mataura	0.24	0.26	6.1	
Hokitika	0.52	0.54	6.75	6.3	Balclutha	0.22	0.24	6.0	
Arthurs Pass	0.65	0.62[2]	7.0	6.3	Invercargill	0.21	0.26	6.1	
Otira	0.65	0.60[2]	7.1	6.4	Bluff	0.20	0.24	6.1	
Darfield[3]	0.40	0.37[2]	6.25		Oban	0.19	0.23	6.1	

Notes:

1. Shallow soil PGAs are determined from the rock values by multiplying by 1.33.
2. The deep soil PGAs are less than the rock values at some high-hazard locations because of nonlinear site-response effects built into the modelling.
3. The Canterbury earthquake region values are to be determined from a new seismic hazard model for the region in 2014.
4. The M_{eff} decreases with return period for Akaroa because its estimated hazard has a larger contribution from the Alpine Fault at low acceleration values which is replaced by contributions from local earthquakes as the PGAs increase.
5. M_{eff} values given in this table may vary slightly from those derived from the maps as they have been assessed conservatively to apply across a range of return periods.

C7 Evaluation of bridges and culverts

In this section

C7.3 Material strengths

C7.3.4 Prestressing steel

The following tables provide prestressing steel strengths and proof loads from historical British standards*, some of which were also declared New Zealand standards or specifications, and NZ Ministry of Works documents†.

Table C7.1: MOW *Bridge manual* (1955)(1) and BS 2691-1:1955 S*teel for prestressed concrete* part 1 Plan hard drawn steel wire(2)

Diameter of wire		Tensile range		Tensile range	
		min	max	min	max
Inch	mm	Tons/in²	Tons/in²	MPa	MPa
0.276	7.0	95	105	1468	1622
0.200	5.1	100	110	1545	1699
0.160	4.1	110	120	1699	1854
0.128	3.3	120	130	1854	2008
0.104	2.6	130	140	2008	2163
0.080	2.0	140	150	2163	2317

Table C7.2(a): BS 2691:1963 S*teel wire for prestressed concrete*(3) (also declared as NZS 1417:1964(4))

Cold drawn and stress relieved wire							
Imperial units			Metric units (original)			Metric units (updated)	
Nominal diameter	Tensile strength		Nominal diameter	Tensile strength		Tensile strength	
	Min.	Max.		Min.	Max.	Min.	Min.
in	Tonf/in²	Tonf/in²	mm	kgf/mm²	kgf/mm²	MPa	MPa
0.276	95	105	7	150	165	1468	1622
0.276	100	110	7	160	175	1545	1699
0.200	100	110	5	160	175	1545	1699
0.200	110	120	5	175	190	1699	1854
0.160	110	120	4	175	190	1699	1854
0.128	110	120	3.25	175	190	1699	1854
0.128	120	130	3.25	190	205	1854	2008
			2.5	190	205	1854	2008

The 0.2% proof stress may be taken as not less than 85% of the minimum specified tensile strength.

* Content in tables C7.1 to C7.6 is reproduced with permission from the quoted British Standards. Permission to reproduce extracts from British Standards is granted by BSI. British Standards can be obtained in PDF or hard copy formats from the BSI online shop: www.bsigroup.com/Shop or by contacting BSI Customer Services for hardcopies only: Tel +44 (0)20 8996 9001, Email: cservices@bsigroup.com.

† Tables C7.7 to C7.9 are reproduced with permission from WSP. The information supplied therein has been superseded by other standards and should therefore not be relied upon for any designs outside of the context of clause 7.3.3 of the *Bridge manual*.

C7.3.3 continued

Table C7.2(b): BS 2691:1963[3] (also declared as NZS 1417:1964[4])

Cold drawn wire							
Imperial units			Metric units (original)			Metric units (updated)	
Nominal diameter	Tensile strength		Nominal diameter	Tensile strength		Tensile strength	
	Min.	Max.		Min.	Max.	Min.	Max.
in	Tonf/in²	Tonf/in²	mm	kgf/mm²	kgf/mm²	MPa	MPa
0.200	100	110	5	160	175	1545	1699
0.200	110	120	5	175	190	1699	1854
0.160	110	120	4	175	190	1699	1854
0.128	110	120	3.25	175	190	1699	1854
0.128	120	130	3.25	190	205	1854	2008
0.104	120	130	3	175	190	1699*	1854
0.080	130	140	2	205	220	2008	2163

The 0.2% proof test may be taken as not less than 75% of the minimum specified tensile strength

Table C7.3: BS 3617:1963 S*tress relieved 7-wire strand for prestressed concrete*[5] (also declared as NZSS 1993:1965[6])

Approx diameter of strand		Minimum breaking load		
in	mm	lbf	kgf	kN (updated)
1/4	6.3	10,000	4,536	44.5
5/16	7.9	15,500	7,031	69.0
3/8	9.5	21,000	9,525	93.4
7/16	11.1	28,000	12,700	124.6
1/2	12.7	37,000	16,783	164.6
0.60	15.2	51,000	23,133	226.9

* There are inconsistencies between the imperial and metric unit tensile strengths for 0.104" strand in BS 2691:1963[3]. Updated metric unit values are conservatively based on the lower strength values (ie the original metric units).

C7.3.3 continued

Table C7.4: BS 2691:1969 *Steel wire for prestressed concrete*[7]

Grade	Nominal diameter	Nominal steel area	Characteristic tensile strength	Maximum tensile strength	Minimum 0.2% proof stress	Max % relaxation after 1000 hours from	
	mm	mm²	MPa	MPa	MPa	70% initial stress	70% initial stress
Normal relaxation	4	12.57	**1720**	1950	1460	5	8.5
	5	19.64	1720	1950	1460	5	8.5
	5	19.64	**1570**	1800	1330	5	8.5
	7	38.48	**1570**	1800	1330	5	8.5
	7	38.48	1470	1700	1250	5	8.5
Low relaxation	4	12.57	**1720**	1950	1550	2	3
	5	19.64	1720	1950	1550	2	3
	5	19.64	**1570**	1800	1410	2	3
	7	38.48	**1570**	1800	1410	2	3
	7	38.48	1470	1700	1320	2	3

The "preferred specified characteristic strengths", as per BS 2691:1969[7] tables 5 and 6 are shown in bold type.

Table C7.5: BS 3617:1971 *Seven-wire steel strand for prestressed concrete*[8]

Grade	Nominal diameter	Nominal steel area	Minimum tensile strength	Minimum 0.2% proof load
	mm	mm²	kN	kN
Normal relaxation	6.4	24.5	44.5	37.9
	7.9	37.4	69.0	58.7
	9.3	52.3	93.5	79.5
	10.9	71.0	125.0	106.3
	12.5	94.2	165.0	140.3
	15.2	138.7	227.0	193.6
Low relaxation	6.4	24.5	44.5	40.0
	7.9	37.4	69.0	62.1
	9.3	52.3	93.5	89.1
	10.9	71.0	125.0	112.5
	12.5	94.2	165.0	148.5
	15.2	138.7	227.0	204.3

C7.3.3 continued

Table C7.6(a): BS 5896:1980 *Specification for high tensile steel wire for the prestressing of concrete*[9]

High tensile steel wire					
	Nominal diameter	Nominal steel area	Nominal tensile strength	Specified characteristic breaking load	Specified characteristic 0.1% proof load*
	mm	mm^2	MPa	kN	kN
Cold-drawn wire	4	12.6	1770	22.3	18.5
	4	12.6	1670	21.0	17.5
	4.5	15.9	1620	25.8	21.4
	5	19.6	1770	34.7	28.8
	5	19.6	1670	32.7	27.2
	6	28.3	1770	50.1	41.6
	6	28.3	1670	47.3	39.3
	7	38.5	1670	64.3	53.4
	7	38.5	1570	60.4	50.1
Cold-drawn wire in mill coil	3	7.07	1860	13.1	10.5
	3	7.07	1770	12.5	10.0
	4	12.6	1770	22.3	17.8
	4	12.6	1720	21.7	17.4
	4	12.6	1670	21.0	16.8
	4.5	15.9	1620	25.8	20.6
	5	19.6	1770	34.7	27.8
	5	19.6	1670	32.7	26.2
	5	19.6	1570	30.8	24.6

* For cold-drawn wire in mill coil the values are specified characteristic load at 1% elongation

C7.3.3 continued

Table C7.6(b): BS 5896:1980[9]

7-wire strand					
	Nominal diameter	Nominal steel area	Nominal tensile strength	Specified characteristic breaking load	Specified characteristic 0.1% proof
	mm	mm^2	MPa	kN	kN
7-wire standard	9.3	52	1770	92	78
	11.0	71	1770	125	106
	12.5	93	1770	164	139
	15.2	139	1670	232	197
7-wire super	8.0	38	1860	70	59
	9.6	55	1860	102	87
	11.3	75	1860	139	118
	12.9	100	1860	186	158
	15.7	150	1770	265	225
7-wire drawn	12.7	112	1860	209	178
	15.2	165	1820	300	255
	18.0	223	1700	380	323

Table C7.7: MWD CDP 802/B (1974) *Design tables*[10] – Table of standard prestressing cables

Standard details							Alternative cable make-up									
Type*	Nominal UTS kN	80% of nominal UTS kN	70% of nominal UTS kN	Min duct size mm	Min dim of conc. at anch. mm	Max cable ecc. in duct mm	7mm wire		8mm wire		12.5mm normal strand		12.5mm super-strand		Macalloy bars	
							Number per cable	Actual UTS kN	Number per cable	Actual UTS kN	Number per cable	Actual UTS kN	Number per cable	Actual UTS kN	Number and size	Actual UTS kN
1	740	590	520	41	250	10	12	762	10	779			4	736	1-32mm	800
2	930	740	650	47	300	10	15	953	12	935	6	1014	5	920	2-25mm*	1000
3	1250	1000	870	56	330	10	20	1270			8	1352	7	1288	1-40mm	1250
4	2000	1600	1400	69	360	13	32	2032			12	2028	11	2024	4-25mm*	2000
5	2750	2200	1930	78	390	13	44	2794					15	2760	4-32mm*	3200
6	3400	2720	2380	85	430	14	54	3429			20	3380	19	3496	2-25mm* + 2-40mm	3500
7	4050	3240	2830	91	460	14	64	4064			24	4056	22	4048		
8	4600	3680	3220	95	500	15	73	4636			27	4563	25	4600		
9	4950	3960	3460	98	540	16	78	4953			30	5070	27	4968		
Notes	a	b	c	d	e	f	g		h		i		j		k	

Notes

a. Nominal U.T.S. is that to be used for design, to permit free use of alternative prestressing systems.
b. 80% of nominal U.T.S. is the maximum prestressing force to be applied temporarily to the cable to overcome friction.
c. 70% of nominal U.T.S. is the maximum prestressing force in the cable at any point after anchoring.
d. Duct size given is the minimum outside diameter to suit all cable make-ups, except those marked*. Where cables are to be threaded into duct after concreting, duct diameter should be 6mm larger.
e. Dimension for thickness of concrete is that sufficient to accommodate a standard stressing end anchorage with 50 mm cover each side. For certain cables and prestressing systems, smaller anchorages may be available for use in thin slabs, etc.
f. The figures given for the maximum eccentricity of the centroid of the cable relative to its enclosing duct are average values for the alternative cable make-ups, and may be used for design, with suitable adjustments made after acceptance of a tender, if the difference is significant.
g. 7 mm wire is assumed to have a characteristic strength of 1650MPa giving 63.5kN per wire.
h. 8 mm wire is assumed to have a characteristic strength of 1550MPa giving 77.9kN per wire.
i. 12.5 mm normal strand is assumed to have a characteristic strength of 169 kN per strand.
j. 12. 5 mm super-strand is assumed to have a characteristic strength of 184 kN per strand.
k. The assumed U.T.S. for Macalloy high strength alloy steel bars are those given by the manufacturer.

* CDP/802 revisions B, C and D provide no definitions of the tendon types 1 to 9 included in tables C7.7 to C7.9. The tendon types are however noted on various MWD drawings.

Table C7.8: MWD CDP 802/C (1982) *Design tables*[11] – Table of standard prestressing cables

Standard details							Alternative cable make-up									
Type	Nominal UTS (a) kN	80% of nominal UTS (b) kN	70% of nominal UTS (c) kN	Min duct size (d) mm	Min dim of conc. at anch. (e) mm	Max cable ecc. in duct (f) mm	7mm wire		8mm wire		12.5mm normal strand		12.5mm super-strand		Macalloy bars	
							Number per cable	Actual UTS kN	Number per cable	Actual UTS kN	Number per cable	Actual UTS kN	Number per cable	Actual UTS kN	Number and size	Actual UTS kN
1	740	590	520	41	250	10	12	772	10	779			4	744	1-32mm	830
2	930	740	650	47	300	10	15	965	12	935	6	984	5	930	2-25mm*	1010
3	1250	1000	870	56	330	10	20	1286			8	1312	7	1302	1-40mm	1300
4	2000	1600	1400	69	360	13	32	2058			12	1968	11	2046	4-25mm*	2020
5	2700	2160	1890	78	390	13	42	2701					15	2790	4-32mm*	3320
6	3450	2760	2415	85	430	14	54	3472			21	3444	19	3534	2-25mm* + 2-40mm	3610
7	3900	3120	2730	91	460	14	61	3922			24	3936	21	3906		
8	4600	3680	3220	95	500	15	73	4694			28	4592	25	4650	) These sizes difficult) to obtain and should	
9	5000	4000	3500	98	540	16	78	5015			31	5084	27	5022	) only be used in excep-) tional circumstances	
															25mm 32mm 40mm	
Area per wire, strand or bar,				mm²			38.5		50.3		93		100		491 804 1257	
Nominal tensile strength,				MPa			1670		1550		1770		1860		1030 1030 1030	
Specified characteristic breaking load,				kN			64.3		77.9		164		186		505 830 1300	
Standard specification							BS 5896:1980		Not covered		BS 5896:1980		BS 5896:1980		BS 4486:1980	

Notes

a. Nominal U.T.S. is that to be used for design, to permit free use of alternative prestressing systems.
b. 80% of nominal U.T.S. is the maximum prestressing force to be applied temporarily to the cable to overcome friction.
c. 70% of nominal U.T.S. is the maximum prestressing force in the cable at any point after anchoring.
d. Duct size given is the minimum outside diameter to suit all cable make-ups, except those marked*. Where cables are to be threaded into duct after concreting, duct diameter 6mm larger should be allowed for detailing.
e. Dimension for thickness of concrete is that sufficient to accommodate a standard stressing end anchorage with 50 mm cover each side. For certain cables and prestressing systems, smaller anchorages may be available for use in thin slabs, etc.
f. The figures given for the maximum eccentricity of the centroid of the cable relative to its enclosing duct are average values for the alternative cable make-ups, and may be used for design, with suitable adjustments made after acceptance of a tender, if the difference is significant.

Table C7.9: MWD CDP 802/D (1990) *Design tables*[12] – Table of standard prestressing tendons for post-tensioning

Tendon type			1	2	3	4	5	6	7	8	9
Standard details	(a) Normal characteristic breaking load (kN)		740	930	1250	2000	2700	3450	3900	4600	5000
	(b) 80% of normal characteristic breaking load (kN)		590	740	1000	1600	2160	2760	3120	3680	4000
	(c) 70% of normal characteristic breaking load (kN)		520	650	870	1400	1890	2415	2730	3220	3500
	(d) Typical duct size (mm)	ID	36	39	51	57	63	75	81	90	90
		OD	41	46	58	64	70	82	88	97	97
	(e) Minimum dimension of concrete at anchorage (mm)		250	300	330	360	390	430	460	500	540
	(f) Maximum tendon eccentricity in duct (mm)		10	10	10	13	13	14	14	15	16
Alternative tendon make-ups	7 wire BS 5896:1980	Number per tendon	12	15	20	32	42	54	61	73	78
		Actual CBL of tendon (kN)	772	965	1286	2058	2701	3472	3922	4694	5015
	12.5mm normal strand BS 5896:1980	Number per tendon		6	8	12		21	24	28	31
		Actual CBL of tendon (kN)		984	1312	1968		3444	3936	4592	5084
	12.9mm super strand BS 5896:1980	Number per tendon	4	5	7	11	15	19	21	25	27
		Actual CBL of tendon (kN)	744	930	1302	2046	2790	3534	3906	4650	5022

Characteristics of one wire, strand or bar (CBL = characteristic breaking load)			
Dia mm	Area mm²	Nominal tensile strength MPa	CBL kN
7	38.5	1670	64.3
12.5	93	1770	164
12.9	100	1860	188
40	1257	1030	1300
32	804	1030	830
25	491	1030	505
36	1018	1230	1252
32	804	1230	989
26.5	552	1230	678
38	1134	*1030 +1080	1175 1230
32	804	*1030 +1080	830 870
29	660	*1030 +1080	680 710
23	415	*1030 +1080	430 450

Macalloy bars BS 4486:1980

Dywidag bars BS 4486:1980

VSL stress-bars AS 1313:1972
* Regular
+ Super

Notes

a. Nominal CBL is that to be used for design, to permit free use of alternative prestressing systems.
b. 80% of nominal CBL is the maximum prestressing force to be applied temporarily to the cable to overcome friction.
c. 70% of nominal CBL is the maximum prestressing force in the tendon at any point after anchoring.
d. Duct size given is the minimum to suit all tendon makeups. Where tendons are to be threaded into duct after concreting, duct diameter 6mm larger should be allowed for in detailing.
e. Dimension for thickness of concrete is that sufficient to accommodate a standard stressing end anchorage with 50 mm cover each side. For certain tendon and prestressing systems, smaller anchorages may be available for use in thin slabs, etc.
f. The figures given for the maximum eccentricity of the centroid of the tendon relative to its enclosing duct are average values for the alternative tendon make-ups, and may be used for design, with suitable adjustments made after acceptance of a tender, if the difference is significant.

C7.3.5 Analysis of test results

a. Introduction

In 7.3.6(a) it is recommended that the characteristic strength of reinforcing steel, where determined by testing, be the 5% percentile strength and determined with 95% confidence. This approach determines the characteristic yield strength which represents the performance of an individual bar.

In practice, reinforcing bars are rarely loaded individually, and the tensile demands are shared. The probability of two independent events with probability P_1 and P_2 occurring simultaneously is $P_1 \times P_2$. For two independent bars, the probability of both bars having strength less than the 5th percentile is 0.25% (ie 5% x 5%). This shows that the total strength of two bars is less variable than the strength of individual bars; the combined characteristic strength of the two bars will therefore be greater than twice the characteristic strength of an individual bar.

As a result, in many cases use of a higher characteristic strength representing the performance of a group of bars may be justified.

b. Background

The distribution of yield strength for a particular grade of reinforcement within a structure is generally accepted to be approximated by a normal distribution. The value of strength which less than 5% of test results would fall below is called the characteristic strength. Figure C7.1 illustrates a standard normal distribution with a mean of zero and a standard deviation of 1; the hatched area represents the 5% probability of falling below the characteristic value.

Figure C7.1: Standard normal distribution

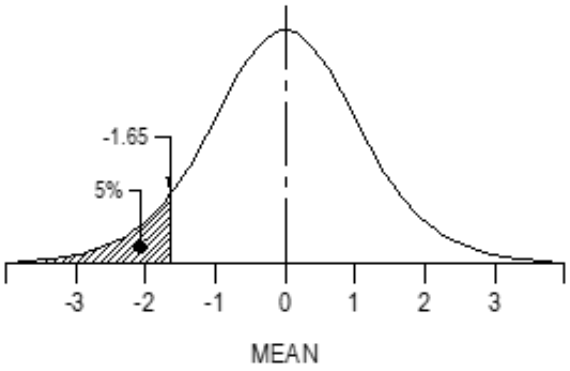

An estimate of the characteristic strength based on a sample of n test results can be represented by:

$F_k = \bar{X} - ks$

Where:

$\bar{X}$ = the mean of the sample $= \frac{1}{n}\sum_{i=1}^{n} X_i$

k = the "tolerance limit factor", which is the number of standard deviations below the mean of the point where the characteristic value lies. This value is sourced from statistical tables. For a normally distributed large population, the value of k is 1.65. When dealing with a sample, the value of k increases as the sample size decreases or the desired level of confidence increases.

C7.3.6 continued

s = the sample standard deviation which is given by:

$$s = \sqrt{\frac{1}{(n-1)}\sum_{i=1}^{n}(X_i - \bar{X})^2}$$

c. Derivation of "characteristic strength" for a group of bars

If X and Y are two independent random variables that are normally distributed the sum of X and Y is also normally distributed with mean and variance as follows:

Mean: $\mu_{(X+Y)} = \mu_X + \mu_Y$

Variance: $\sigma^2{}_{(X+Y)} = \sigma^2{}_X + \sigma^2{}_Y$

Here the symbols μ and σ represent the mean and standard deviation of the entire population. Variance is the square of the standard deviation.

If N bars are resisting tension at a given location in a beam, the probability distribution of the total strength (ie the total yield force) of the group of bars can be defined by:

Mean: $\mu_{Total} = \mu_1 + \mu_2 + \cdots + \mu_N$

Variance: $\sigma^2{}_{Total} = \sigma^2{}_1 + \sigma^2{}_2 + \cdots + \sigma^2{}_N$

If all the bars are taken from the same population $\mu_1 = \mu_2 = \cdots = \mu$ and $\sigma_1 = \sigma_2 = \cdots = \sigma$, therefore:

$\mu_{Total} = N\mu$

$\sigma^2{}_{Total} = N\sigma^2$ and $\sigma_{Total} = \sqrt{N\sigma^2}$

If the population parameters are estimated from tests, the applicable mean is $\bar{X}$ and the standard deviation is s. We therefore have:

$F_{Total} = N\bar{X} - ks_{Total} = N\bar{X} - ks\sqrt{N}$

Where:

F_{Total} = the estimated total characteristic strength (yield force (kN)) of a group of N bars of a particular size resisting tension at a given location in a beam

$\bar{X}$ = the mean value of a series of n representative tests (kN)

s = the sample standard deviation of that series of n tests

k = the "tolerance limit factor" for the specific combination of tolerance limit (eg 5th percentile), sample size (n), confidence limit (eg 95%). This value is sourced from tables such as table 7.2

This equation can be expressed in terms of the characteristic yield strength (stress) of the group (MPa) as follows:

$$f_{Total} = \frac{F_{Total}}{NA_{bar}} = \bar{X}_{stress} - \frac{ks\sqrt{N}}{NA_{bar}} = \bar{X}_{stress} - \frac{ks_{stress}}{\sqrt{N}}$$

C7.3.6 continued

Where:

f_{Total} = the characteristic yield strength (stress) of the group (MPa)

A_{bar} = the cross-sectional area of the reinforcing bar (mm^2)

$\bar{X}_{stress}$ = the mean yield strength (stress) of a series of n tests (MPa)

s_{stress} = the sample standard deviation of yield strength from that series of n tests

d. Application

The application of this approach to specific strength assessments requires the professional judgement of a suitably experienced structural engineer, and must be considered on a case-by-case basis. It is reliant upon a small amount of ductility within the reinforcement, as individual bars will reach yield strength prior to the characteristic strength of the group of bars being reached.

This approach may not be suitable for shear reinforcement where the number of individual bars contributing to shear resistance at a section is likely to be small, and the assumption of independence of the reinforcing bars may not be appropriate.

As described in 7.3.6, in applying this approach the engineer shall also be satisfied that tests have been taken at sufficient locations to represent the whole structure, or the entire group of similar members, as appropriate to the assessment, including making due allowance for any anomalies in the test results.

Where possible, non-destructive sampling (ie hardness testing) should be carried out on the most critical members.

C7.4 Main member capacity and evaluation

C7.4.4 Live loading and analysis – Evaluation loadings based on reference vehicles and axle groups

a. Background for selection of evaluation loadings for normal traffic

The previous *Bridge manual* evaluation loadings based on multiples of HN (normal) loading (from 0.85HN for Class 1 up to 0.95HN for HPMV evaluations and greater than 25m loaded length) were intended to represent the unfactored effects of vehicles conforming with the Land Transport Rule: Vehicle Dimensions and Mass 2016[13]. Evaluations of the maximum load effects of a wide range of conforming vehicles on simply supported and continuous bridge spans have found that evaluation load models based on a multiple of HN loadings would not provide consistent fits to effects of conforming vehicles at all span lengths. Also, adequate representation of hogging moment effects in continuous spans caused by single vehicles (on short spans) or multiple vehicles (loaded lengths greater than 40m) would require longer vehicles or a pair of vehicles.

Alternative forms of evaluation loading models are provided for in AS 5100.7 *Bridge design* part 7 Bridge assessment[14] section 11.3.1. In addition to

i. design traffic load models (such as T44/L44 or SM1600)

the nominated rating vehicles may include:

ii. a specific traffic load configuration for general access vehicles

iii. a specific traffic load configuration for higher mass limit vehicles (conforming HPMV in the New Zealand context)

iv. network specific loading configurations (including cranes, military vehicles).

C7.4.4 continued

Austroads research report AP-R452-14 *Review of AS 5100.7 Rating of existing bridges and the Bridge Assessment Group guidelines*[15] provides the background to the 2017 edition of AS 5100.7[14], assessment practices in Australia and introduces the reference vehicle approach to bridge evaluations, with examples of the vehicle configurations specified by the various state agencies.

In AS 5100.7[14] (section 14) a load rating factor (RF) is calculated for a bridge and a nominated rating vehicle. When used with rating vehicles representing normal traffic ((ii) or (iii) above), the calculation methodology is equivalent to the GROSS factor calculation in section 7.4.6 of the *Bridge manual*.

The new *Bridge manual* evaluation loads for normal traffic adopt the reference vehicle approach from AS 5100.7[14] and nominate the vehicles listed in 7.4.4(c) for HPMV evaluations or 7.4.4(d) for posting (general access vehicles) and 50MAX evaluations. Evaluation outcomes can be stated as percentages of the relevant load effects and 7.4.6 of the *Bridge manual* is therefore unchanged.

b. Analysis methods for reference vehicle load effects

It is expected that structural analysis software will be used to automate the requirements to place vehicles at the most onerous positions for components under consideration and omit axles having a relieving effect at those positions. The requirement to omit axles is important for continuous spans because the reference vehicles are intended to represent the effects of short vehicles in addition to long vehicles, and single rigid vehicles can be more onerous for load effects such as sagging moments in continuous spans.

Software packages with vehicle live load capabilities using influence line or influence surfaces to optimise vehicle positions can generate the required load placements for a predefined set of vehicles automatically with minimal user intervention.

Other software packages may implement moving live loads by stepping multiple vehicles along specified paths at uniform increments with all axle loads present at each step. In this case it is recommended that a larger set of reference vehicles be defined to include parts of vehicles (axle groups, truck, tractor, trailer units). Live load cases can be implemented using one or more of the following approaches:

- a long moving convoy comprising all reference vehicles, relevant parts and axle groups; with spacings sufficient to avoid relieving effects in continuous spans
- multiple single vehicle moving load cases covering all vehicles and relevant parts, with results enveloped to find the maximum effects
- single vehicle moving loads, selected to give the worst effects at the position under consideration. For simply supported spans, the governing vehicle for mid-span bending moment and for end shear force could be pre-selected using the charts provided below as a guide.

c. Selection of reference vehicles for HPMV evaluations

Sagging moment and shear force effects for single HPMV reference vehicles for simply supported span lengths up to 60m are shown in figures C7.2 and C7.3. Hogging moment effects for two equal length continuous spans up to 25m are shown in figure C7.4. Dynamic load factors are excluded, and values are factored by $L^{-1.5}$ (moments) or $L^{-0.5}$ (shear force) to provide a presentable vertical scale. Indicative, unfactored effects, without dynamic load factors, are also shown in table C7.14 and figures C7.10 and C7.11.

C7.4.4 continued

Figures C7.2 and C7.3 show that:

- the short semi-trailer (A224-48t) governs at spans up to 12m for sagging moments or 10m for shear
- the two longer vehicles (B2233-55t and R22T23-61t) suit the longer span lengths
- sagging moments in short spans up to 5m are governed by axle groups within the reference vehicles or individual axle groups in *Bridge manual* table 7.9 (the latter not included in the figures).

For hogging moments, figure C7.4 shows the:

- A224-48t vehicle governs for twin span lengths in the 7.5m-12.5m range and would also suit very short continuous span lengths
- R22T23-61t vehicle governs at span lengths over 12.5m and is also suitable for 4m-7.5m span lengths
- effects of two-vehicle platoons govern for span lengths over 22m (see (f) for guidance).

It should be noted that because of the difference in load factor between axle groups and reference vehicles (see tables 7.3 and 7.6), the cross-over points between axle groups and reference vehicles for factored effects may differ to those shown above and following in (d).

d. Selection of reference vehicles for posting and 50MAX evaluations

Sagging moment and shear force effects for single general access and 50MAX reference vehicles for simply supported span lengths up to 60m are shown in figures C7.5 and C7.6. Hogging moment effects for two equal length continuous spans up to 25m are shown in figure C7.7. Dynamic load factors are excluded, and values are factored as for the HPMV charts to provide a presentable vertical scale. Indicative, unfactored effects, without dynamic load factors, are also shown in table C7.14 and figures C7.10 and C7.11.

Figures C7.5 and C7.6 show that for posting evaluations:

- the front part (tractor) of the A224-45t semi-trailer governs at spans up to 12m for sagging moments or 10m for shear
- the short 5-axle vehicle (A122-32t) covers the 12m-18m range for sagging moments or 10m-15m for shear
- at longer lengths the B1232-46t B-Train governs sagging moments while the R22T22-46t truck-and-trailer governs shear

For 50MAX evaluations:

- the B1233-50t B-Train governs sagging moments for span lengths over 26m
- the R22T23-50t truck-and-trailer governs shear for span lengths over 22m
- general access vehicles govern the shorter span lengths.

Sagging moments in short spans up to 5m are governed by axle groups within the reference vehicles or individual axle groups in *Bridge manual* table 7.9 (the latter not included in the figures).

For hogging moments, figure C7.7 shows that:

- for shorter continuous span lengths up to 5m the A122-32t or A224-45t vehicles may govern
- for 5m-9m span lengths the applicable B-Train (B1232-46t or B1233-50t) is suitable
- the A224-45t vehicle governs posting load effects for twin span lengths of 9m or more

C7.4.4 continued

- for 50MAX the R22T23-50t vehicle governs at span lengths over 15m
- the effects of two-vehicle platoons govern for span lengths over 20m (see (f) for guidance).

The effect of the difference in load factor between axle groups and reference vehicles should be noted as per (c).

Figure C7.2: Sagging moments for single HPMV reference vehicles compared with 0.90HN and 0.95HN load effects

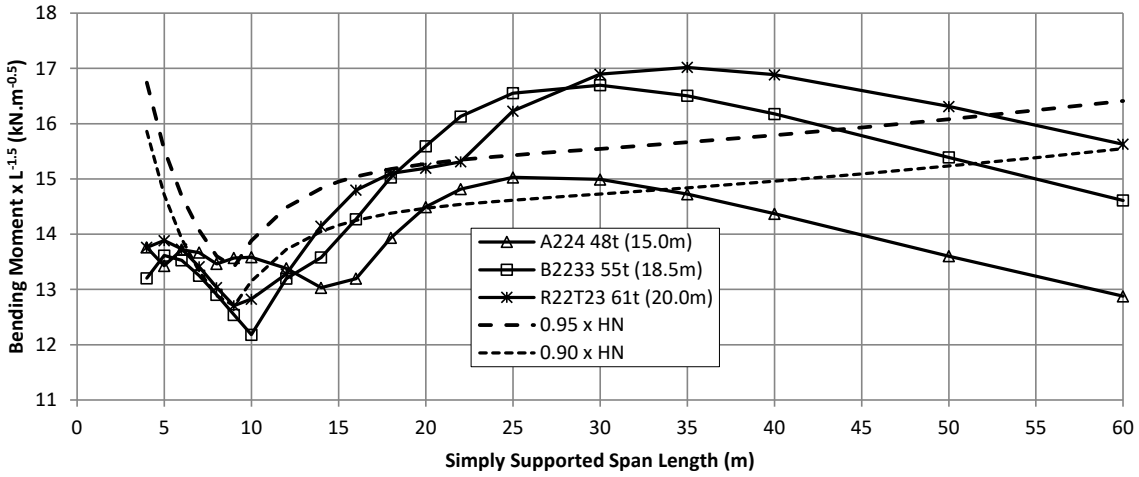

Figure C7.3: End shear forces for single HPMV reference vehicles compared with 0.90HN and 0.95HN load effects

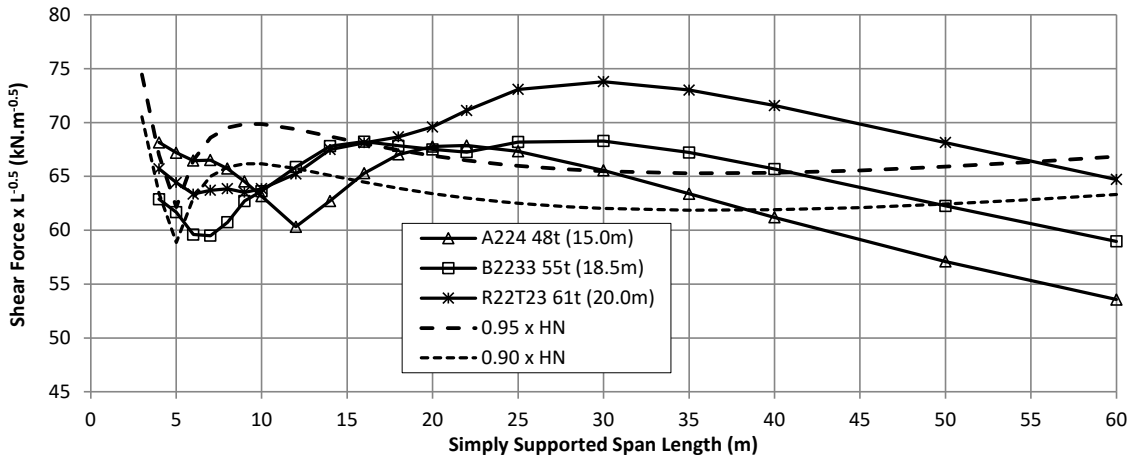

Figure C7.4: Twin span hogging moments for single HPMV reference vehicles compared with 0.90HN and 0.95HN load effects

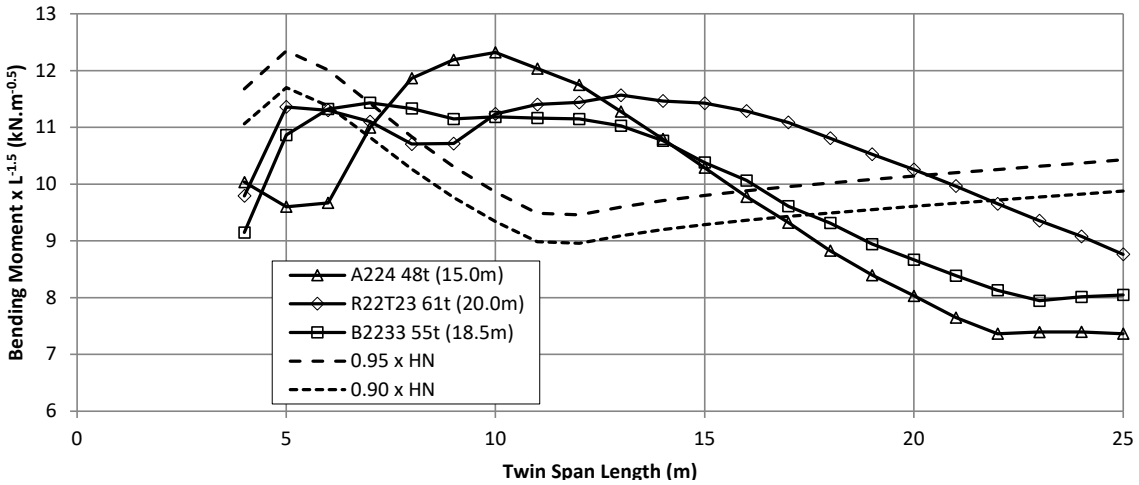

Figure C7.5: Sagging moments for single general access and 50MAX reference vehicles compared with 0.85HN and 0.90HN load effects

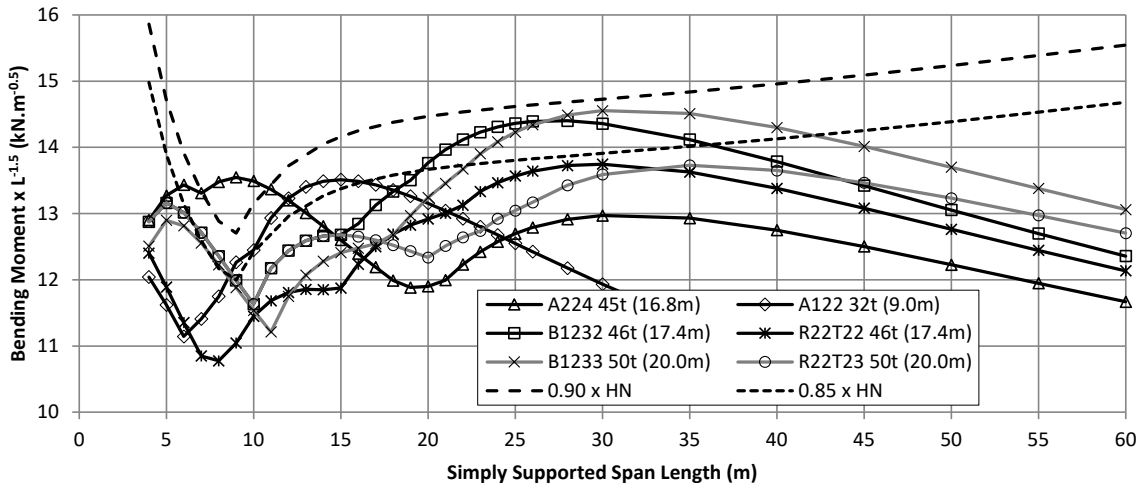

Figure C7.6: End shear forces for single general access and 50MAX reference vehicles compared with 0.85HN and 0.90HN load effects

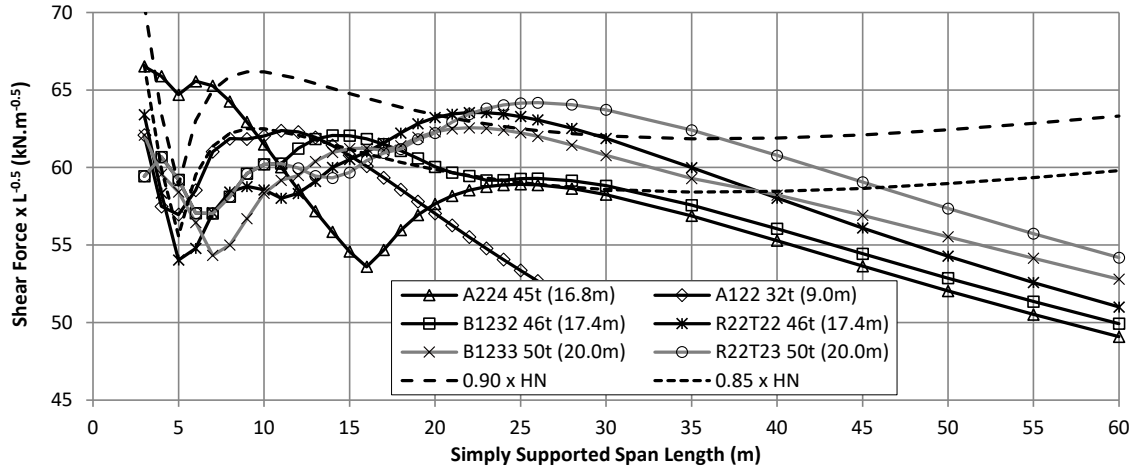

Figure C7.7: Twin span hogging moments for single general access and 50MAX reference vehicles compared with 0.85HN load effects

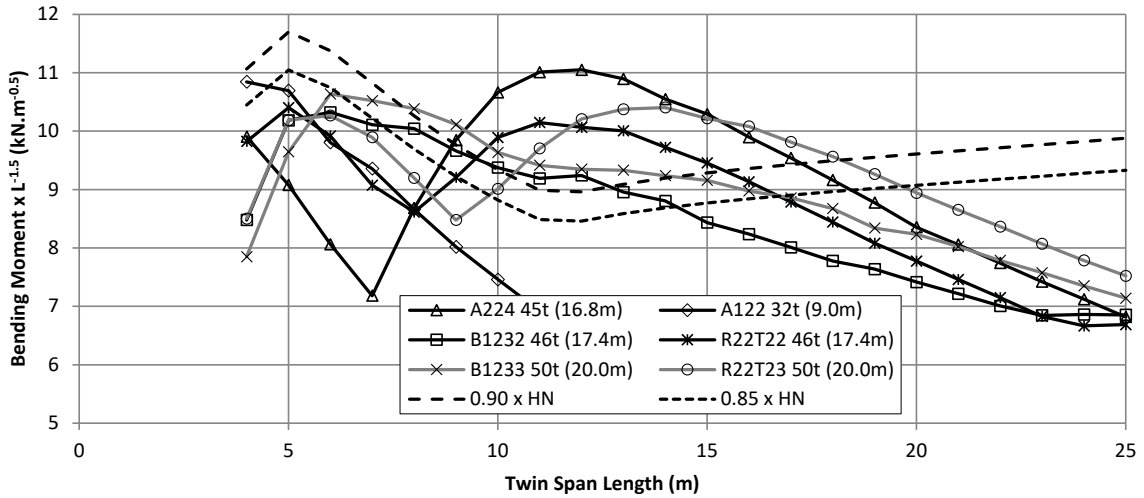

C7.4.4 continued

e. Accompanying lane and multiple vehicle factors

For multiple loaded lanes the new evaluation loadings adopt the accompanying lane approach from AS 5100.2 *Bridge design* part 2 Design loads[16] where the accompanying lane factors (ALF) are applied to the load effects for each load lane (referred to below as the standard approach). If span lengths are long enough to require consideration of multiple vehicles in the same lane, the ALF are also applied to each vehicle in the lane. For example, if the individual lane loadings comprise 2-vehicle platoons and there are three load lanes, the factor on the vehicle having least effect would be 0.8 x 0.4 = 0.32. For three lanes with up to three vehicles per lane the net factors per vehicle would be as shown in table C7.10.

Table C7.10: Net factors for combined accompanying lanes and multiple vehicles

Lane	Net factor for each vehicle		
	Vehicle 1	Vehicle 2	Vehicle 3
1	1.0	0.8	0.4
2	0.8	0.64	0.32
3	0.4	0.32	0.16

The alternative offered in the new evaluation loadings is to adopt the per vehicle ALF as implemented in AS 5100.7[14] clauses 11.3.3 and 11.3.5 where the accompanying lane factors (ALF_i) are applied to the loads for each reference vehicle. Where span lengths are short enough to not require consideration of multiple vehicles in the same lane, the application is equivalent to the standard approach. But where platoon loads are required (see below) the AS 5100.7[14] approach would require the patterns of vehicle loads in each lane to be considered as a whole so that the ALF can be appropriately assigned to each vehicle. For three lanes with up to three vehicles per lane the ALF factors per vehicle could applied following one of two patterns shown in table C7.11.

Table C7.11: Accompanying lane factors assigned to individual reference vehicles in platoons

Lane	Pattern 1 – longitudinal elements			Pattern 2 – transverse elements		
	Vehicle 1	Vehicle 2	Vehicle 3	Vehicle 1	Vehicle 2	Vehicle 3
1	1.0	0.8	0.4	1.0	0.4	0.4
2	0.4	0.4	0.4	0.8	0.4	0.4
3	0.4	0.4	0.4	0.4	0.4	0.4

This alternative scheme results in less total load but may be more complex to implement for the whole bridge. It may be beneficial for assessment of particular elements where a load pattern can be defined according to one of the above arrangements.

f. Guidance for multiple vehicle platoon selections

Consideration of co-existing moving vehicles in the same lane is necessary for evaluation of:

- sagging moment effects on simply supported span lengths greater than 55m
- effects on pier supports with sum of adjacent span lengths greater than 55m
- shear force effects on simply supported span lengths greater than 36m
- hogging moment effects on continuous span lengths greater than 20m.

C7.4.4 continued

The minimum span lengths at which co-existing vehicles begin to govern depend on minimum spacing between vehicles, which is 17.0m for moving vehicles (from AS 5100.7[14] clause 11.3.3(i)). For general access vehicles on continuous spans, hogging moments for platoons may govern for span lengths of 20m or more. For HPMV vehicles that point is about 22m span length.

In general, multiple platoon combinations of the three vehicles in the same lane may be necessary to generate the very worst effects for long and/or continuous spans of varying lengths, but simplifications are possible without significant underestimation of effects. Inspection of the relevant influence lines and adverse lengths should be used to guide vehicle combination selections.

Platoons comprising two vehicles (with 1.0 and 0.8 factors in either order, and either travel direction) should be sufficient in most cases but additional leading and/or trailing vehicles with 0.4 factor should be considered for continuous spans with lengths of 60m or more, or simply supported spans with lengths of 80m or more. For hogging moments, figure C7.8 illustrates the differences between single vehicles and platoons, and span length range where more than 2 vehicles should be considered.

Mixed platoons with two vehicles of different type may be necessary to maximise hogging moments where adjacent continuous span lengths are unequal.

Table C7.12 illustrates the composition of HPMV platoons required to maximise hogging moment effects for a structure with two continuous prismatic spans. Note that reversing the vehicles (travel directions or applied factors) may give a slightly worse effect. For other span length arrangements, it can be observed that the governing vehicle length is around 60% of the span length (for 25m and 30m spans) and for longer spans the heaviest vehicle governs, with spacings increased to maximise effect. The range of span lengths suited to each platoon vehicle combination may vary for different structure configurations.

Table C7.12: HPMV vehicle combinations for maximum 2-span hogging moments

Span length	Vehicle 1	Vehicle 2	Spacing	Comment
10m	1.0 x A224-48t	-	-	Single vehicle (for L<13m)
15m	1.0 x R22T23-61t	-	-	Single vehicle (for 13m-20m)
20m	1.0 x R22T23-61t	-	-	Single vehicle (for L≤22m)
25m	1.0 x A224-48t	0.8 x A224-48t	17m	Min spacing-(for 22m-27m)
30m	1.0 x B2233-55t	0.8 x B2233-55t	17m	Min spacing-(for 27m-33m)
40m	1.0 x R22T23-61t	0.8 x R22T23-61t	19m	Min spacing-(for 33-45m)
50m	1.0 x R22T23-61t	0.8 x R22T23-61t	24m	Vary spacing for L>45m
60m	1.0 x R22T23-61t	0.8 x R22T23-61t	26m	Add 0.4 x A224t-48t, 19m gaps at both ends for L≥60m

Similarly, table C7.13 illustrates the composition of platoons for 50MAX evaluations. For posting evaluations the 50MAX vehicles would be replaced by the A224-45t single vehicle and B1232-46t platoons for the same span length ranges. Figure C7.9 illustrates the span length ranges for hogging moments where the 50MAX vehicles are more onerous than the general access vehicles.

C7.4.4 continued

Table C7.13: 50MAX or general access vehicle combinations for maximum 2-span hogging moments

Span length	Vehicle 1	Vehicle 2	Spacing	Comment
10m	1.0 x A224-45t	-	-	Single vehicle
15m	1.0 x A224-45t	-	-	Single vehicle
20m	1.0 x R22T23-50t	-	-	Single vehicle (for 16m-20m)
	1.0 x A122-32t	0.8 x A122-32t	17m	Min spacing (for 20m-25m)
25m	1.0 x B1232-46t	0.8 x B1232-46t	17m	Min spacing (for 25m-30m)
30m	1.0 x B1232-46t	0.8 x B1232-46t	17m	Min spacing. Also for L>40m GA vehicle but vary spacing
40m	1.0 x B1233-50t	0.8 x B1233-50t	17m	Min spacing (for 32m-40m)
50m	1.0 x B1233-50t	0.8 x B1233-50t	24m	Vary spacing for L>40m
60m	1.0 x B1233-50t	0.8 x B1233-50t	26m	Add 0.4 x A224t-45t, 17m gaps at both ends for L≥60m

Figure C7.8: Twin span hogging moments for HPMV platoons compared with single HPMV vehicles

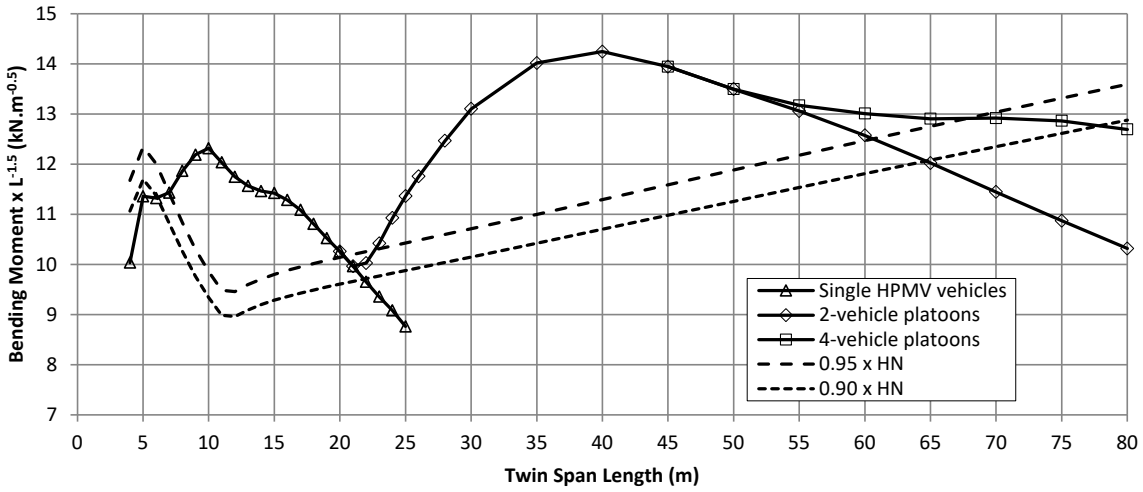

Figure C7.9: Twin span hogging moments for general access and 50MAX platoons compared with single vehicles

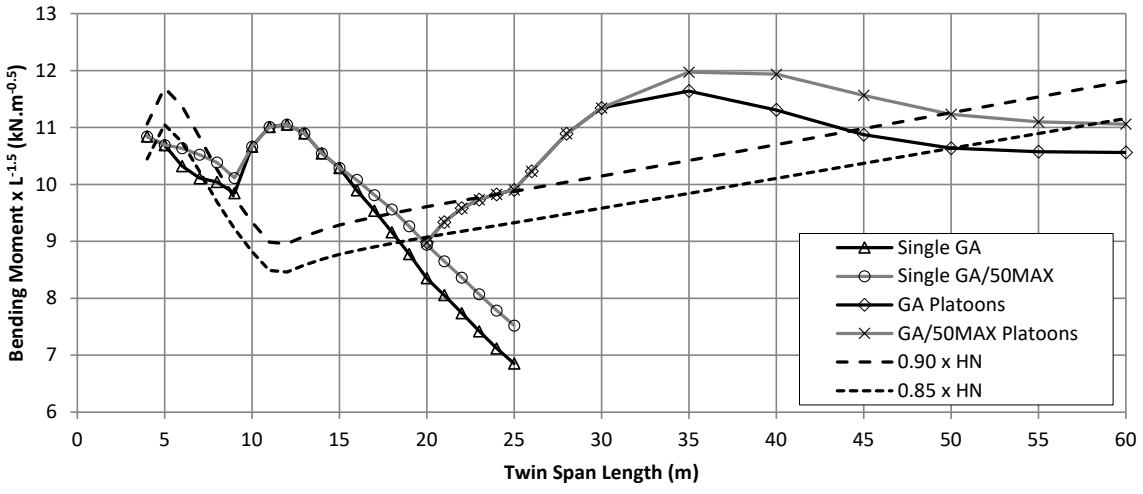

Table C7.14: Simply supported moment and shear effects from general access, 50MAX and HPMV axle groups and reference vehicles – unfactored, one lane of loading, without impact

Span (m)	General Access				50MAX				HPMV			
	Moment (kNm)	Vehicle	Shear (kN)	Vehicle	Moment (kNm)	Vehicle	Shear (kN)	Vehicle	Moment (kNm)	Vehicle	Shear (kN)	Vehicle
2	47	Axle groups	110	Axle groups	As for General Access		As for General Access		47	Axle groups	115	Axle groups
3	75		120						77		125	
4	110		135	A224-45t (tractor)					115		140	A224-48t
5	150		145						160		155	
6	200	A224-45t (tractor)	165						205	A224-48t	165	
7	250		175						255		180	
8	305		185						305		190	
9	370		190						370		195	
10	430		200	A122-32t					430		205	
11	490		210						495		220	B2233-55t
12	555		220						560		230	
13	630	A122-32t	225						640	R22T23-61t	245	
14	710		235	B1232-46t					745		255	
15	785		245						845		265	
16	865		250						950		275	
17	945		255	R22T22-46t					1,055		285	R22T23-61t
18	1,025		265						1,155		295	
19	1,120	B1232-46t	275						1,275	B2233-55t	305	
20	1,235		285						1,395		315	
21	1,345		295						1,530		325	
22	1,460		300				300	R22T23-50t	1,665		335	
23	1,570		305				310		1,800		350	
24	1,685		315				315		1,935		360	
25	1,800		320				325		2,070		370	
26	1,910		325				330		2,205		375	
27	2,025		330		2,025	B1233-50t	335		2,340		385	
28	2,135		335		2,150		340		2,480	R22T23-61t	395	
29	2,250		340		2,270		345		2,630		400	
30	2,360		340		2,395		350		2,780		405	
31	2,475		345		2,515		355		2,930		415	
32	2,585		350		2,640		360		3,080		420	
33	2,700		350		2,760		365		3,230		425	
34	2,815		355		2,885		370		3,380		430	
35	2,925		360		3,005		370		3,525		435	
36	3,040		365		3,130		375		3,675		440	
37	3,150		370		3,250		380		3,825		445	
38	3,265		375		3,375		385		3,975		450	
39	3,375		380		3,500		390		4,125		450	
40	3,490		385		3,620		395		4,275		455	
45	4,055		415	Platoons	4,235		420	Platoons	5,025		485	Platoons
50	4,620		445		4,845		455		5,770		520	
55	5,390	Platoons	480		5,530	Platoons	485		6,520		555	
60	6,250		505		6,430		515		7,390	Platoons	595	
65	7,120		530		7,350		545		8,410		630	
70	8,010		550		8,280		570		9,465		665	
75	8,955		575		9,225		590		10,665		690	
80	10,025		595		10,265		615		11,955		715	
85	11,180		615		11,435		635		13,320		740	
90	12,345		635		12,625		655		14,740		765	
95	13,515		655		13,875		680		16,205		790	
100	14,680		675		15,125		700		17,720		815	

Notes for table C7.14:

a. This table is provided as a guide to expected effects on single spans.

b. The table provides maximum moments and shears for one lane of loading without dynamic load factor on simply supported spans. Loading includes axle groups (table 7.9), reference vehicles and platoons of vehicles.

c. Load effects in structural members shall be determined independently using the loadings specified in *Bridge manual* section 7.4.4 and shall not rely on table C7.14.

d. Note that because of the difference in load factor between axle groups and reference vehicles (see tables 7.3 and 7.6), the cross-over points between axle groups and reference vehicles for factored effects may differ to those shown in the table.

Figure C7.10: Simply supported moment effects for general access, 50MAX and HPMV reference vehicles and axle groups – unfactored, without impact

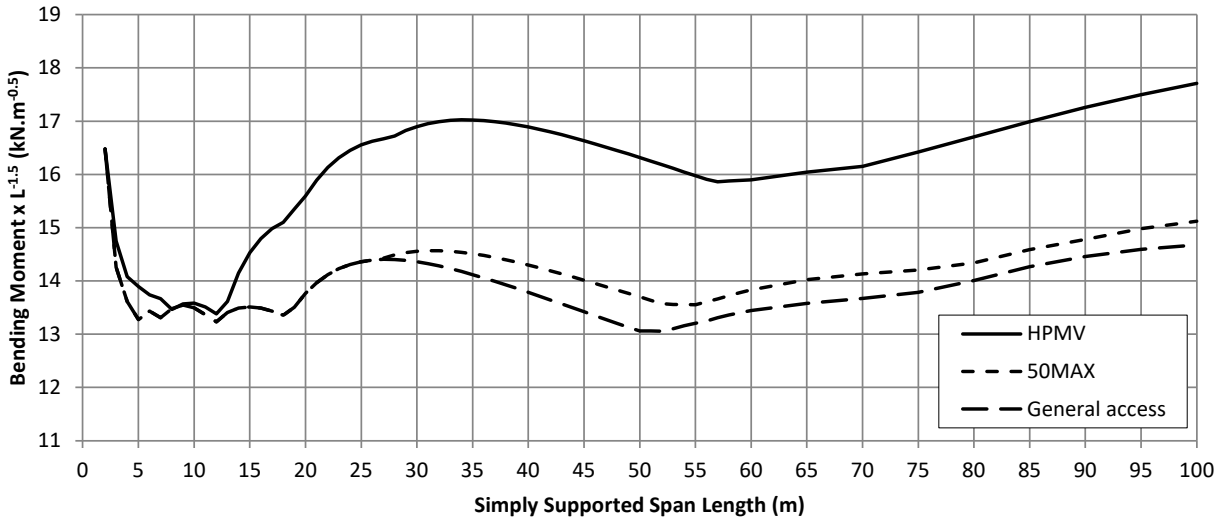

Figure C7.11: Simply supported shear effects for general access, 50MAX and HPMV reference vehicles and axle groups – unfactored, without impact

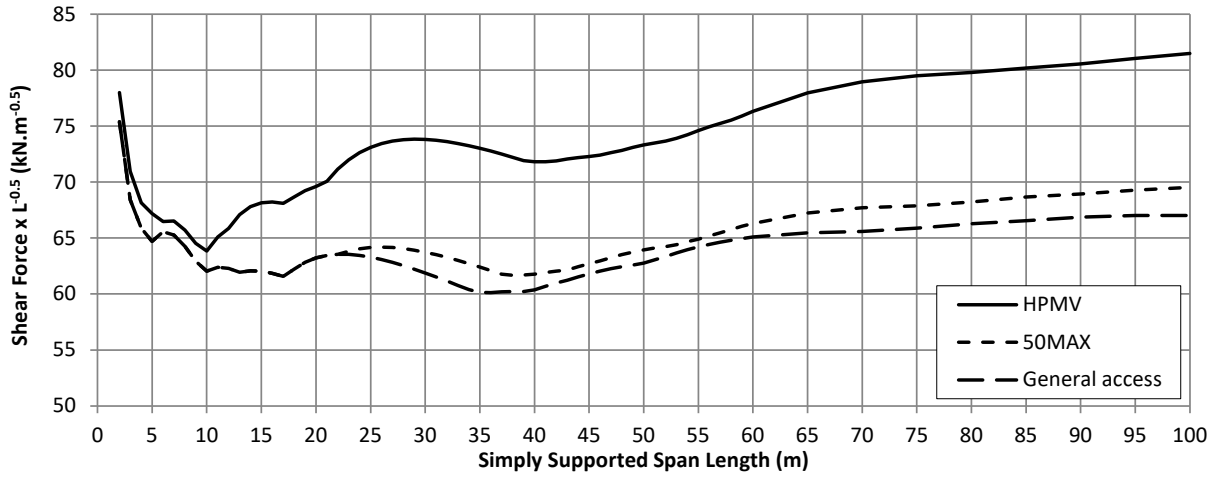

References for C7

(1) Ministry of Works (1955) *Bridge manual*. Wellington. Superseded

(2) British Standards Institution BS 2691-1:1955 *Steel for prestressed concrete*. Part 1 Plan hard drawn steel wire. Withdrawn.

(3) British Standards Institution BS 2691:1963 *Steel wire for prestressed concrete*. Withdrawn.

(4) Standards New Zealand NZS 1417:1964 *Steel wire for prestressed concrete*. Withdrawn.

(5) British Standards Institution BS 3617:1963 *Stress relieved 7-wire strand for prestressed concrete*. Withdrawn.

(6) Standards New Zealand NZSS 1993:1965 *Stress relieved 7-wire strand for prestressed concrete*. Withdrawn.

(7) British Standards Institution BS 2691:1969 *Steel wire for prestressed concrete*. Superseded, withdrawn.

(8) British Standards Institution BS 3617:1971 *Seven-wire steel strand for prestressed concrete*. Superseded, withdrawn.

(9) British Standards Institution BS 5896:1980 *Specification for high tensile steel wire for the prestressing of concrete*. Superseded, withdrawn.

(10) Ministry of Works and Development CDP 802/B (1974) *Design tables*. Wellington. Superseded.

(11) Ministry of Works and Development CDP 802/C (1982) *Design tables*. Wellington. Superseded.

(12) Ministry of Works and Development CDP 802/D (1990) *Design tables*. Wellington. Superseded.

(13) Ministry of Transport (2016) Land Transport Rule: Vehicle Dimensions and Mass 2016. Wellington.

(14) Standards Australia AS 5100.7:2017 *Bridge design*. Part 7 Bridge assessment.

(15) Lake N, Ngo H and Kotze R (2014) *Review of AS 5100.7 Rating of existing bridges and the Bridge Assessment Group guidelines*. Research report AP-R452-14, Austroads, Sydney, NSW, Australia.

(16) Standards Australia AS 5100.2:2017 *Bridge design*. Part 2 Design loads.